Scientific Validation of the IEC Specification for the Assessment and Characterization of Wave Resources using SWAN

Steffanie Piché

Thesis submitted to the University of Ottawa
in partial Fulfillment of the requirements for the
Doctorate in Civil Engineering

Academic Advisors: Dr. Ioan Nistor and Dr. Andrew Cornett

Department of Civil Engineering
University of Ottawa

Acknowledgements

First, I would like to thank my supervisors Dr. Ioan Nistor and Dr. Andrew Cornett for their help and guidance during this thesis. It has been a long haul, but I am happy that we have finally reached the end.

I would like to express all my thanks and love to my family and friends who have helped me over the past years. To my husband, Nick who put up with all my excited rants about wave energy, to my parents and sister who helped encourage me throughout. A big thank you to Dr. Mathieu Toupin who shared an office with me during my thesis, for providing encouragement and the occasional much needed distractions.

A final thanks to the coastal team at CBCL for allowing me to continue progressing on my thesis while working, and for cheering me on as I completed my journey.

Abstract

The research conducted in this study sought to appraise and validate the IEC-TC-114 technical specification for wave energy resource assessment in terms of its methodologies, requirements, and sources of error. This assessment was conducted through the pilot application of the IEC-TS to a project site located on the west coast of Vancouver Island in British Columbia. The objectives of this research were to (1) establish a firm scientific rational for the technical specification, (2) suggest improvements for future iterations of the technical specification, (3) conduct a sensitivity analysis to determine sources or error and uncertainty within the specification, (4) develop a user guidance , and (5) to complete an assessment of the wave energy resource for all three classes of assessment at the pilot project site. At the time of this research there has been limited assessment and validation of the technical specification and its applicability to real world studies. This study is also limited in its scope to a singular site within Canada and so specific observations made may not be applicable to all locations.

It was observed over the course of this study that the IEC-TS could be applied to the assessment of wave energy with reasonable computational effort. Additionally, the IEC-TS is overall relatively easy to understand and apply, with the only exception to this being the validation procedure which lacked clarity. However, it was noted that in many cases the IEC-TS would not provide defined requirements, but only recommendations which would allow researchers to potentially disregard the recommendations provided within. While this is likely due to the fact that different sites may have different requirements, it does call into question the need for a standard if it is not going to have strict requirements to ensure that all resource assessments are completed using state of the art knowledge and procedures.

List of Figure

List of Tables

Symbols and Units

$c_{g,i}$	Group velocity of the i^{th} discrete frequency	[m/s]
d	Directionality coefficient	
f_i	i^{th} discrete frequency	[Hz]
h	Water depth	[m]
H_{m0}	Spectrally estimated spectral wave height	[m]
J	Omni–directional wave power	[W/m]
$J_{\theta Jmax}$	Maximum directionally resolved wave power	[W/m]
k_i	Wave number associated with the i^{th} discrete frequency	[m^{-1}]
m_n	Spectral moment of n^{th} order	[m^2s^{-n}]
n	Order of the spectral moment	
S_i	Variance density over the i^{th} discrete frequency	[m^2/Hz]
S_{ij}	Variance density over the i^{th} discrete frequency and j^{th} discrete direction	[m^2/Hz.rad]
T_e	Spectrally defined energy period (equivalent to T_{-10})	[s]
δ	Factor ensuring that only positive components are summer	
Δf_i	Frequency width of the variance density of the i^{th} discrete frequency	[Hz]
$\Delta \theta_j$	Angular width of the variance density of the j^{th} discrete direction	[rad]
ε_0	Spectral width	
ρ	Reference sea water density	[kg/m^3]
θ	Direction of resolution of wave power	[deg]
θ_{Jmax}	Direction of maximum directionally resolved wave power	[deg]

List of Abbreviations

2D	Two-dimensional
3D	Three-dimensional
CHS	Canadian Hydrographic Service
IEC	International Electro-technical Commission
OBS	Oscillating Body Systems
OTD	Overtopping Devices
OWC	Oscillating Water Column
SI	Scatter Index
TC	Technical Committee
TS	Technical Specification
WAB	Wave Activated Body
WCWI	West Coast Wave Initiative
WEC	Wave Energy Converter
WWIII	Wave Watch-III

1 Introduction

1.1 Study Significance

Wind-generated waves have the potential to become a large source of renewable energy for coastal communities. Due to the ever-growing demand for clean, renewable energy sources, research in this field has expanded, with development occurring in new technologies and regulations. The accurate estimation of the wave energy resource and the wave climate is critical for the development and deployment of these projects. This is performed through the selection of potential project locations, equipment, and infrastructure development, and to accurately predict the scale of power that will be generated by the wave energy converters (WEC). Technical Committee 114 of the International Electro-technical Commission (IEC-114) has been working to develop a set of standards for the growing field of wave energy that will regulate the estimation of the wave climate and resource at potential project sites. This technical specification prescribes methodologies and procedures for objectively and reliably determining the wave energy resource within a region of interest. The application of recognized international standards to the field of wave energy will lead to greater certainty in the quality and accuracy of the resource assessments, helping to increase stakeholder confidence in the projects, and reducing the overall risk. The proposed methods are to be applied through numerical modelling of the wave and wind climate with validation from field measurements. This technical specification (TS) has only just begun being applied to real world case studies and so it is not yet known whether the proposed methodology can be applied successfully or will lead to the desired level of accuracy and reliability.

The current research applied the TS to a pilot project site located on the west coast of Vancouver Island, British Columbia, Canada. This region has been the location of multiple wave energy resource assessments allowing for validation of this project against both field measurements (provided by the West Coast Wave Initiative) and previous research. No wave energy developments have been deployed within this region, though it does have significant wave energy potential. This study is intended to benefit the Canadian and global marine energy sector through the development and dissemination of the technical specification.

1.2 Thesis Objectives

The purpose of this research was the pilot application of the IEC technical specification (TS) to perform a scientific assessment and validation for the assessment and characterization of the wave energy resource. The main objectives of this thesis are:

1. To establish a firm scientific rational for the technical specification;
2. To develop suggestions for improvement of future iterations of the specification;
3. To conduct a thorough sensitivity analysis to determine sources of error and uncertainty within the specification;
4. Develop a user guidance;
5. To complete a wave energy resource assessment at the pilot site as per the requirements of the specification.

1.3 Thesis Limitations

The main limitation of the current research is that it is restricted to a single site along the west coast of Vancouver Island. Therefore, observations made within this thesis may not be applicable to all wave energy resource assessments. Additional limitations in the study are as follows:

1. Limitations in data availability such as high-resolution bathymetry at the study site;
2. Limitations in wave boundary conditions

It is noted that the limitations listed here are likely to be the same limitations experienced by those conducting wave energy resource assessments as availability of data is a known issue within the coastal field.

1.4 Thesis Novelty

At the time of this research, wave energy standards existed only in draft form with minimal application in real world case studies (Cornett, et al., 2014; Piché, Cornett, et al., 2015; Piché, Cornett, et al., 2015; Ramos and Ringwood, 2016; and Ramos et al., 2016). This research intends to evaluate and assess the performance of the draft specification by applying its methodologies and recommendations to a pilot project along the west coast of Canada. Observations from this study will then be used to inform future iterations of the technical specification, to provide guidance to users of the technical specification, and to promote its use within Canada and internationally through conferences and scientific articles.

1.5 Thesis Outline

This thesis has been organized into 11 chapters; a general description of the different chapters is presented below.

Chapter 1 – An introduction to the research topic and the projects scope, main objectives. This section includes the contributions this research provides to the field of wave energy.

Chapter 2 – An introduction to the field of wave energy. Including a history of wave energy, the theory behind wave energy, and an explanation on the different types of wave energy converters.

Chapter 3 – A review of the International Electro–Technical Commissions specification for wave energy resource assessments. This section contains information on the specification requirements and validation criteria.

Chapter 4 – A detailed literature review into the wave energy resources assessments that have been conducted along the west coast of Canada and touching upon those conducted across the world in different wave climates. This section also examines the current research that has been conducted on the IEC specification for wave energy resources assessments, sensitivity analyses which have been conducted in the field of wave modelling, and research relating to the interaction and siting of wave energy converters.

Chapter 5 – This section includes information on the project study location, including the wave and wind climate.

Chapter 6– An introduction into the background of the SWAN model, its applications to the field of wave modeling and its implementation. This includes the governing equations and formulations that were used as part of this thesis.

Chapter 7 – An explanation of the measurements obtained for this study and a detailed description of the numerical setup and domains of the different models used during this thesis.

Chapter 8 – The results of the validation of the IEC specification for wave energy completed through conducting a sensitivity analysis for key parameters used within the numerical model. This section also examines the uncertainty and long–term variability within the model as required by the specification and the criteria required to validate the numerical model.

Chapter 9 – This section presents a comprehensive comparison between the numerical and measured results for the validation sites, and a comparison between the three assessment phases.

Chapter 10 – Critical analysis of the potential issues within the IEC specification and user guidance containing recommendations and suggestions for future users of the IEC specification.

Chapter 11 – Summary of the project results and conclusions, including recommendations for future research within the field.

2 Wave Energy

2.1 A History of Wave Energy

While research into wave energy has become more common within recent years it is not a novel concept. Patents concerning wave energy devices have dated since the late 18th century, with the first patent being registered in 1799 by Girard [Szabó et al., 2008], for a device consisting of a ship attached along the shore, with the waves driving pumps and other machinery [NREL, 2009]. Unfortunately, until the oil crisis of the 1970s, wave energy was not regarded as a viable source of energy, and as reliance on oil and petroleum as a source of fuel and energy continued, research into wave energy converters was reduced in the 1980s [Falnes, 2007]. However, with current concerns over climate change and our reliance on fossil fuels, research into renewable energy resources is again at the forefront.

The use of waves as a means of renewable energy has a number of advantages and disadvantages. While the potential for wave energy is high along many coastlines, which may result in the generation of significant power [Drew *et al.*, 2009], the conditions in which these devices must operate can sometimes be extreme. This means that the WECs must be robust enough to withstand these extreme conditions or must be capable of avoiding them entirely [Drew *et al.,* 2009; Carter, 2005]. Additionally, the WEC converters must be designed with consideration for the corrosive environment the devices must operate under, which can damage exposed mechanisms [Clement *et al.*, 2002]. This may offset the potential advantages of the WEC which can include the protection of the coastline through the dissipation of the wave energy [Carter, 2005] and the ability to provide energy to remote communities which currently rely on expensive diesel generators.

2.2 Wave Energy Theory

The availability and concentration of potential wave energy is dependent on location, with the potential energy increasing along the coastlines farthest from the equator. This is due to the increased fetch of these waves which allow for the propagation of larger ocean waves.

Ocean waves can be classified as either swell or wind sea. Swells are long period waves which have been propagated from a storm; these waves are capable of propagating long distances across the ocean with minimal energy loss [Falnes, 2007]. Wind sea waves are a result of localized wind forces acting upon the water body, the direction and scale of the wind waves can change significantly based on the local conditions. The long period swell are the reason that wave energy is highest at the poles.

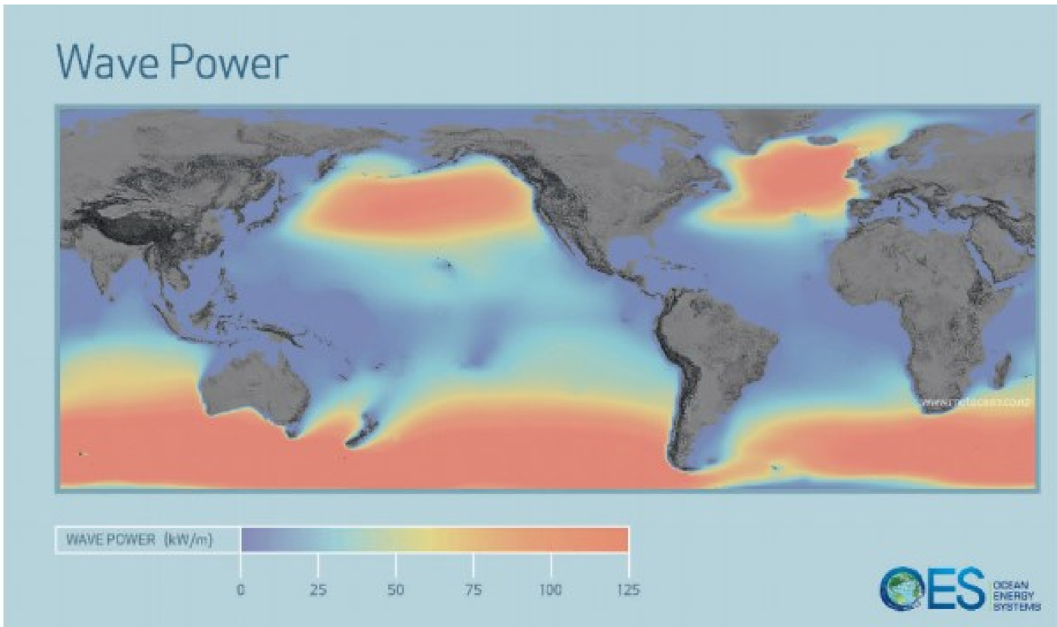

Figure 2.1 – Global Resource Assessment [Huckerby *et al.*, 2011]

The location of the wave energy converter (WEC) along the coastline is also important when trying to maximize the capture of wave energy. Convex bathymetries, such as headlands, will act to concentrate the energy, while bays will cause the energy to diffuse, resulting in lower available wave energy for the WEC [Carter, 2005]. Additionally, wave breaking results in a decrease in wave energy, meaning that devices located on the shoreline, or in very shallow water may not be able to capture as much wave energy as those located in deeper water. Due to the variations in bathymetry, wave fetch, and climate in different locations WECs need to be designed for specific site conditions in order to take advantage of the available energy at these locations [Ivanova *et al.*, 2005] which requires a good understanding of the wave climate and potential energy resource.

The wave power (J) can be approximated by the significant wave height (H_s) and the peak energy period (T_p) based on the following equation, as per Hagerman and Bedard (2003):

$$J \cong 0.42 H_s^2 T_p \qquad [2.1]$$

The factor 0.42 was found to be exact for any sea state that is well represented by a two-parameter Bretschneider spectrum; however, this factor could range from 0.3 to 0.5 depending on the amount of energy in the sea and swell and the shape of the wave energy spectrum [Hagerman *et al.*, 2003].

McCormick (1978) presented a different set of equations to calculate the wave power, based on the theory that in deep water, a random sea could be considered as numerous linear waves of varying heights and periods, as per Pierson (1952). Based on this theory, McCormick provided the following equation:

$$J_{ij} = \frac{\rho g^2}{16} \frac{H_{ij}^2}{\omega_i} I_j i_j \qquad [2.2]$$

where i represents the wave and j the wave direction, ω_i is the circular wave frequency, ρ is the density of sea water, and I_j is the projection of the wave energy conversion array length, L, on the wave crest. Using equation 2.2 the total wave power being transmitted in the j^{th} direction can be obtained with:

$$J_j = \frac{\rho g^2}{16} L \sum_{i=1}^{m} \frac{H_{ij}^2}{\omega_i} \cos(\theta_j)\, i_j \qquad [2.3]$$

while, the total wave power being transmitted can be calculated with:

$$J_x = \sum_{j=1}^{m} J_j \cos(\theta_j)\, i \; = \; \frac{\rho g^2}{16} L \sum_{j=1}^{m} \sum_{j=1}^{n} \frac{H_{ij}^2}{w_i} \cos(\theta_j)\, i \qquad [2.4]$$

where θ is the angle of incidence. McCormick (1978) found that this equation was valuable for site investigations into wave energy resources at specific locations, where m was the number of waves studied in each of the n directions. The accuracy of this equation is increased as the number of waves and directions studied is increased.

A more complicated method of determining the wave power is using wave energy spectra. Falnes (2007) determined that the amount of stored energy per unit area on the ocean surface could be calculated based on the waves' energy spectrum, where the average energy associated with the wave could be calculated using:

$$E = \rho g H_{m0}^2/16 = \rho g \int_0^\infty S(f)df \qquad [2.5]$$

where H_{m0} is the significant wave height for the sea state and the integrand *S(f)* is the wave spectrum in m^2/Hz. *S(f)* is used to quantitatively describe how different wave frequencies, *f*, contribute the wave energy.

According to Falnes (2007) to determine the approximate wave energy spectrum for a particular site, wave measurements would need to be taken and transformed using Fourier analysis. To obtain long-term statistics, it was recommended that the wave measurements and analyses would have to be repeated every 3 hours. For cases of fully developed seas, Falnes determine that the semi-empirical Pierson-Moskowitz (PM) spectrum matched the experimentally obtained spectra reasonably well, based on the following formulation:

$$S(f) = (A/f^5)exp(-B/f^4) \qquad [2.6]$$

where $A = BH^2{}_{m0}/4 = 0.0005$ m^2HZ^4 and $B = (5/4)_p{}^4 = 0.74g^4/(2\pi U)^4$ where f_p is the peak frequency (where *S* has its maximum) and where *U* is the mean speed taken at a level of 19.5m [Falnes, 2007]. Falnes (2007) also defined the spectral moment of order *j* as

$$m_j = \int_0^\infty f^j S(f)df \qquad [2.7]$$

For sinusoidal waves with period $T = 1/f$, the wave energy would be transported with an energy velocity equal to that of the group velocity, c_g [Falnes, 2007]. Therefore, the wave-power level (defined by Falnes as the transport of energy per unit width of the progressing wave front) is equal to c_gE or $c_g\rho gH^2/8$. Based on this, the wave power could be expressed as a function of the wave spectrum for deep water waves using:

$$J = \rho g \int_0^\infty c_g(f)S(f)\,df = \rho g^2 m_{-1}/4\pi = \rho g^2\, T_J H_{m0}^2/64\pi \qquad [2.8]$$

For real waves which are composed of wave elements propagating in different directions, equation 2.5 can be generalized as [Falnes, 2007]:

$$E = \rho g H_{m0}^2/16 = \rho g \int_0^{\infty} \int_{\beta 1}^{\beta 2} s(f,\beta) df d\beta \qquad [2.9]$$

2.3 Wave Energy Converters

An understanding of the wave climate and locale is meaningless without the appropriate means of operating and harvesting the energy in that climate. Wave energy converters (WEC) are technology currently under development that convert the potential/kinetic wave energy into power for consumption by the local communities. When conducting a wave energy resource assessment, it is necessary to have a good understanding of the types of devices being developed and deployed to understand what information is necessary by the developers for the creation and site placement of the WEC.

There are a number of different operational modes and classifications which can be used to categorize wave energy converters (WEC). They can be categorized based on their directional characteristics (which describes the direction in which the WEC exploit the waves and includes point absorbers, attenuators, and terminators), their working/operating principles (oscillating water column (OWC), oscillating body systems (OBS) also known as wave activated body (WAB), and overtopping devices (OTD)) or their location (shoreline, nearshore, and offshore). Both the directional characteristics and their working principles reflect how the WECs convert the available potential and kinetic energy into usable electricity [Carter, 2005]. Table 2.1 shows the relationship between the principal locations of the WEC, its operating principle, and its directional characteristics.

Table 2.1 – Operating Principles for Location and Directional Characteristics [Harris *et al.,* 2004]

Principle Location	***Directional Characteristic***		
	Point Absorber	Terminator	Attenuator
Shoreline		OWC, OTD	
Nearshore	OBS/WAB	OWC, OTD, OBS/WAB	OBS/WAB
Offshore	OBS/WAB	OWC, OTD, OBS/WAB	OBS/WAB

This section will focus on the description of different wave energy converters based on their operating principles, though a brief explanation of the different directional characteristics is also included.

2.3.1.1 Directional Characteristics

Point absorbers are relatively small devices with respect to the incident wavelength and are capable of extracting energy from waves larger than the WEC itself [Carter, 2005]. These WEC can be designed for either long or short wave periods and are able to operate under most wave states using active control; however, the diameter of the point absorber should be less than 1/6 of the incoming wavelength otherwise the device will begin to counteract itself [Holmberg *et al.*, 2011]. Point absorbers are typically floating buoys located on the ocean's surface which are attached to fixed systems such as large inertial bodies or to a damper, through wired or rigid connections [Holmberg *et al.*, 2011]. These devices are capable of energy extraction from any direction and are designed for operation at near or offshore sites in most sea states. The energy generation is through the relative displacement between the float and the fixed system below.

Wave terminators have their main axis perpendicular to the incident wave direction. These waves function by effectively terminating the wave action by creating waves which have the exact opposite phase as the incident waves [Carter, 2005]. Terminator style devices consist of a variety of operating principles, permitting them to extract energy using a number of different methods, and to operate in most locations.

Wave attenuators have their main axis parallel to the incident wave direction [Drew *et al.,* 2009]. They operate by attenuating the amplitude of the wave and extracting the energy due to the relative motion of the system as the wave passes under it [Harris *et al.,* 2004]. The majority of attenuators tend to be constructed with long multi-segmented structures where the length of each segment is typically smaller than ¼ of the wavelength [Holmberg *et al.*, 2011]. These devices tend to be designed for operation at near or offshore sites.

2.3.1.2 Oscillating Water Columns

Oscillating water columns (OWCs) use the wave action to expand and compress the air located above a water column, causing the rotation of an air turbine or generator which leads to the generation of electrical energy. These structures typically consist of a partially submerged, hollow structure designed to be open to the ocean below the water level [Carter, 2005]. As the waves approach the system the water is forced into the hollow chamber resulting in an increase in pressure on the interior air column. This additional pressure is dissipated by the air exiting through the turbine or generator. As the wave passes and the water level recedes, air is then forced back into the hollow chamber due to the pressure imbalance.

The size of the air chamber will have an influence on the optimal operational wave frequency and amplitude; therefore these devices can be optimized to operate in almost any wave climate. These devices can be deployed as either fixed structures built along the coastline, or as floating structures in either the nearshore or offshore region and are considered to be wave terminators.

An example of an OWC installation is the Mutriku wave plant commissioned by the Spanish utility Ente Vasca de la Energia (EVE) in the Basque Country of Spain with construction commencing in 2009 [Tethys, 2017]. This device is an addition to an existing harbour at the Mutriku harbour. It contains 16 air chamber which are 4.5m wide, 3.1m deep and 10m high. At the top of the chamber is a 0.75m diameter hole which leads to a wells turbine and an 18.5kW electrical generator. The site officially opened in July 2011 and as of April 2017 has supplied the grid with over 1.3 GWh of electricity.

Figure 2.2 – Mutriku Wave Plant [Ente Vasco De La Energia, 2013]

2.3.1.3 Oscillating Body Systems/ Wave Activated Bodies

Oscillating body systems (OBS), also known as wave activated bodies (WAB), operate by using the heaving, pitching, or rolling motion of the device to generate energy. These devices' function based on the oscillatory motion of one part of the system in reference to a fixed point. There are a number of different forms of OBS based on their type of motion and the level of submergence, including heaving buoys, heaving systems, and pitching devices [Falcão, 2010].

Single-body heaving buoys are considered the simplest OBS, and are a typical example of a point absorber, where the buoy reacts relative to a fixed frame of reference such as the seabed or bottom of the structure. Two-body heaving systems are more complicated and are used in scenarios where the site is too deep for a single-body system to be practical. In this system the energy is converted from the motion of two oscillating bodies moving relative to each other.

Submerged heaving systems are point absorbers which are placed below the ocean surface, allowing them to use the pressure difference between the wave crest and trough to generate energy [Drew *et al.*, 2009]. This system comprises of a seabed fixed air-filled cylinder and a mobile upper cylinder. As the wave crest passes over the system, the water pressure above the system compresses the air within the fixed cylinder, causing the upper cylinder to descend [Drew *et al.,* 2009]. Pitching systems rely on the relative rotation, pitch, of the system as opposed to its vertical movement as described for the previous systems.

Finally, bottom-hinged systems operate use relative pitch motion, and function based on the concept of an inverted pendulum hinged at the seabed. This system is positioned perpendicular to the prominent wave direction and functions as a wave terminator [Drew *et al.,* 2009].

The Pelamis is a well-known example of an OBS which was developed by Pelamis Wave Power (PWP), see Figure 2.3. The full-scale prototype P1 was the tested at the EMEC wave test site in 2004 and became the world’s first offshore wave power converter to successfully generate energy. Based on the findings of the EMEC testing, completed from 2004 - 2007, a second-generation device was created. Unfortunately, the Pelamis went into administration in 2014 and most of the devices have been dismantled.

Figure 2.3 – Pelamis wave power converter, now decommissioned [EMEC]

2.3.1.4 Overtopping

The final operating principle being discussed is overtopping systems. This method of wave energy conversion functions by capturing the wave crests and having them propagate into a reservoir via a ramp, where they are stored at higher water elevations when compared to the sea level. Energy is then generated by the potential energy of the reservoir as it passes through low-head turbines [Falcão, 2010]. In order to maximize the amount of water propagated into the reservoir, many devices use a narrowing channel, designed to concentrate the waves, and increase their wave heights.

An example of an overtopping device is the Wave Dragon, see Figure 2.4 which was developed in Denmark. This device underwent testing in Nissum Bredning, a fjord in the northern part of

Denmark in 2003, where it was tested continuously until 2005. The device was developed at full scale for the wave climate within the fjord. Another pilot project is planned using a full-scale prototype in Milla Fjord, Wales

Figure 2.4 – Wave Dragon Prototype testing [Wave Dragon, 2009]

3 IEC Technical Specification

The goal of this research was to validate IEC project number 62600–101 TS: Marine energy – Wave, tidal and other water current converters – Part 101: Wave energy resource assessment and characterization which was developed by subcommittee 114 of the IEC (IEC-TC-114). Within this technical specification a set of procedures and requirements are outlined for the proper assessment and characterization of the wave energy climate at the users' site of interest.

3.1 Introduction

The IEC–TS proposed by IEC–TC–114 outlines procedures for data collection, numerical model development and validation, data analysis and reporting. Its purpose is to propose a standardized methodology for the assessment of the wave energy resource in a manner consistent with the current best practises and in a manner that will be useful for WEC developers to determine ideal locations for deployment based on the wave climate. In order to accomplish this standardization, the IEC–TS recommends three classes (or stages) of resource assessment based on the users' required level of accuracy and reliability:

1. Class 1 – Reconnaissance
2. Class 2 – Feasibility
3. Class 3 – Design

Each class of assessment is intended to address a specific need in the wave energy resource assessment process. Class 1 – Reconnaissance is intended for use as an initial assessment of the wave energy resource within a large region in order to highlight potential areas of high energy which may be used for future development. This class of assessment is intended to be of lower accuracy, with minimal effort and computational cost. The second class of assessment is feasibility, this class of assessment entails more effort than the reconnaissance class and is therefore intended to provide a more accurate and reliable estimation of the wave energy resource. It can be used as a refinement of the reconnaissance class assessment to examine the resources at known sites of interest. The final class of assessment is design, this stage is intended to give a highly accurate and reliably estimation of the wave energy resource at a specific site of interest within a smaller region then used in the previous classes. This class of assessment has the highest computational cost, modeling, and data requirements.

The framework proposed by the IEC-TS for the numerical modeling of the wave energy resource can be divided into seven steps, as shown in Figure 3.1. The initial step of the assessment is study planning, this step requires the user to determine their region of interest and to select which class of assessment is best suited to their requirements (reconnaissance, feasibility, or design). The next step is the collection and analysis of all data required for the setup of the numerical model. This will include wind, wave, and bathymetric measurements, but may also entail measurements on regional currents, tidal flows, and ice within the study domain. Step three is the setup of the numerical model; the exact requirements for the model setup is determined by the class of resource assessment being undertaken, these requirements are discussed in Section 2.2 at greater length. After the setup of the model and the initial computations the model needs to be validated against the measured wave climate within the domain (step four), the validation requirements are dependent on the class of assessment and are described in Section 2.3. Should the desired level of validation not be achieved then the model must be modified and revalidated until it is within the required levels of accuracy (step five). Once the validation is sufficient the user will progress to steps six and seven, which requires the hindcasting of the wave climate over a 10-year period and the reporting of the modeled results as per the IEC–TS requirements, respectively. Reporting the results requires the calculation of the resource assessment uncertainty.

The IEC–TS recommends that the uncertainty be assessed in terms of the total uncertainty, which considers three distinct categories: the field measurement uncertainty, the modeling uncertainty, and the uncertainty due to the long-term variability. The IEC–TS recommends that the uncertainty be calculated based on the procedures within the ISO information publication "Guide to the expression of uncertainty in measurement".

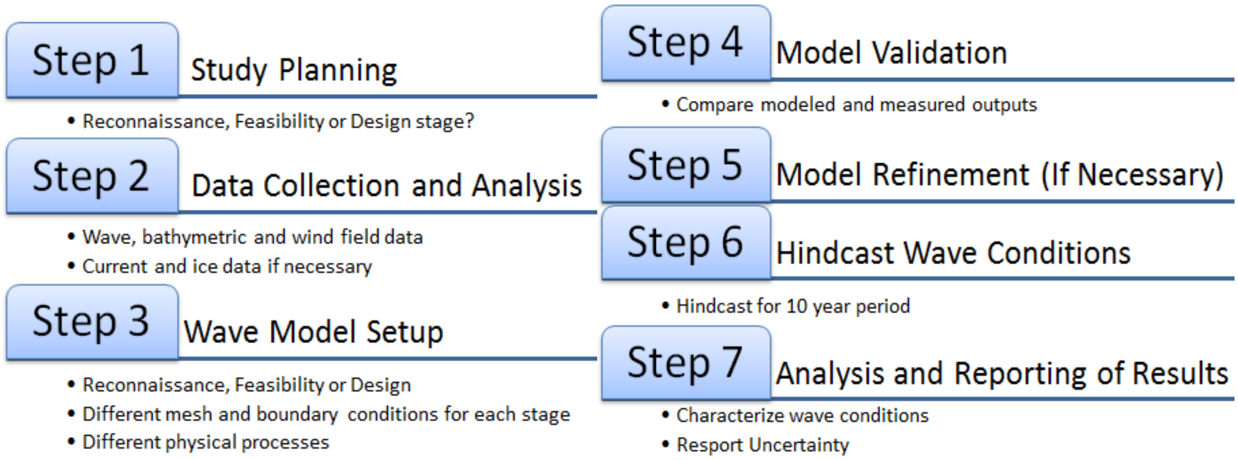

Figure 3.1 – Simplified Wave Energy Resource Assessment Procedure

An alternative to modeling the wave energy resource is also proposed within the IEC–TS for the assessment of the wave energy resource at discrete locations as opposed to a larger region. The proposed method is referred to as the Measure–Correlate–Predict (MCP) method. The purpose of this method is for the prediction of the wave climate at a single location or for the development of boundary conditions for numerical modeling. It requires the measurement of the wave climate at the site of interest for a limited time period, and then the correlation of the measured wave climate to long–term wave measurements at a reference location. This correlation function can then be used to predict the wave climate at the site of interest for the duration of the study period. There are obvious limitations to this method as it can only be applied when the wave climate at both locations is strongly correlated, and it may result in the exclusion of large wave events if the two sites are not adjacent. However, it is presented as an alternative method to the numerical modeling of the wave energy across a larger region. An investigation into this methodology was not considered within the scope of this research as it was not the focus of the IEC-TS.

3.2 Specification Requirements

The IEC–TS outlines the requirements for the measured data required to force and develop the numerical model, including the bathymetry, wave characteristics, and the wind velocity. These requirements are shown in Table 3.1, Table 3.2, Table 3.3, and Table 3.4. The bathymetric requirements assume that the user has access to existing bathymetry at sufficient resolution for the reconnaissance stage assessment and can use this as the basis for determining the required resolution at the feasibility and design stages. Additional requirements provided by the IEC–TS include the type of boundary conditions required for the different classes of assessment, and the physical processes required for consideration in each class.

Table 3.1 – IEC–TS Specified Wind Resolution

	Reconnaissance	Feasibility	Design
Minimum Temporal Resolution	3hr	3hr	1hr
Minimum Spatial Resolution	100km	50km	25km

Table 3.2 – IEC–TS Specified Numerical Resolution

	Reconnaissance	Feasibility	Design
Minimum Temporal Resolution	3hr	3hr	1hr
Minimum Spatial Resolution	5km	500m	50m
Minimum Number of Wave Component Frequencies	25	25	25
Minimum Number of Directions	24	36	48

Table 3.3 – IEC–TS Specified Bathymetric Resolution

	Reconnaissance	Feasibility	Design
Maximum Percentage Difference Adjacent Bathymetry Points in Water Depth Less than 200m	10%	5%	2%
Maximum Horizontal Spacing in Water Depth Over 200m	5km	2km	1km
Maximum Horizontal Spacing in Water Depth Less than 200m	500m	100m	25m
Maximum Horizontal Spacing in Water Depth Less than 20m	100m	50m	10m

There are three different types of boundary conditions considered by the IEC–TS, they are the parametric, hybrid, and spectral boundaries. Parametric boundary conditions are defined in terms of the significant wave height, peak period, dominant wave direction and an assumed directional spreading factor. This condition is considered acceptable for use only in the reconnaissance class assessment. The hybrid boundary is defined by a one–dimensional wave spectrum with a parametric directional parameter, this boundary is not used in this study but is considered acceptable for either the reconnaissance or feasibility class assessment. The final boundary type is the fully directional wave spectrum, which is the wave energy spectrum defined across both frequency and direction. This type of boundary condition is recommended at all stages of assessment but is the only type of condition considered acceptable for the design class.

Each class of assessment requires the inclusion of different physical processes such as whitecapping, wave breaking etc. It is required that all physical processes be included for all stages of assessment apart from depth–induced wave breaking and bottom friction which are recommended for the reconnaissance class assessment, but not required as shown in Table 3.4. Additional conditions such as tides, wave-current interactions, diffraction, and the effect of sea ice should also be considered if applicable. The user can exclude a physical process if it is shown through sensitivity analysis that there is minimal impact on the predicted wave climate.

Table 3.4 – IEC-TS Specified Physical Processes (R – Required, A – Acceptable for Consideration)

	Reconnaissance	Feasibility	Design
Wind-Wave Growth	R	R	R
Whitecapping	R	R	R
Quadruplet Interactions	R	R	R
Wave Breaking	A	R	R
Bottom Friction	A	R	R
Triad Interactions	R	R	R
Refraction	R	R	R

3.3 Validation Criteria

Validation of the numerical model with measured wave data is required for each class of assessment based on the criteria provided by the IEC-TS. The TS requires the validation of the model for the spectral estimate of the significant wave height, the wave energy period, and the omni–directional wave power for all classes of assessment. At the feasibility and design classes further validation is required against the spectral width, the direction of maximum wave power, and the directionality coefficient. The IEC–TS provides the following equations for the calculation of these parameters to ensure that there is consistency in their estimation:

Spectral estimate of significant wave height, $H_{m0}=4\sqrt{m_0}$ [3.1]

Omni–directional wave power, $J= \rho g \Sigma cg, \Delta f i \Delta \theta j i j$ [3.2]

Energy Period, $Te= \frac{m_{-1}}{m_0}$ [3.3]

Directional wave energy, $J\theta= \rho g \Sigma c_{g,} \Delta f_i \Delta \theta_j \cos(\theta - \theta_j)\delta$

$$\begin{cases} \delta = 1, cos(\theta - \theta_j) \geq 0 \\ \delta = 0, cos(\theta - \theta_j) < 0 \end{cases}$$ [3.4]

Direction of maximum wave energy, θ_{Jmax} = direction of max J_θ [3.5]

Spectral width, $\varepsilon 0 = \sqrt{\frac{m_0 m_{-2}}{m_{-1}^2} - 1}$ [3.6]

Directionality coefficient, $d= \frac{J\theta jmax}{J}$ [3.7]

where m_n is the spectral moment of order n, c_g is the group velocity, and S_{ij} is the variance density over frequency and direction. Throughout the current research the directionality coefficient was adjusted to have consistent directional bin sizes between the different tests, as the maximum power is dependent on the directional bin size. Therefore, the directionality coefficient and maximum directionally resolved wave power were scaled for 1° directional bins.

The validation procedure outlined in the IEC–TS, Figure 3.2, requires the calculation of the weighted mean systematic and random errors which are based on the bias and standard deviation of the different wave states. This process requires the calculation of the normalized error between the measured and the modeled parameters within each cell of an omni-directional H_{m0}-T_e scatter table (in the case of the characteristic direction, no normalization is applied. For each cell the product of the proportional frequency of occurrence (*F*) and the mean incident wave power (*J*) will be used to calculate the weighting factor (*w)*:

$$w_{ij} = J_{ij}F_{ij} \quad [3.8]$$

Which is then normalized by the sum of all the weighted factors. The weighted mean systematic error $b(e_p)$ is calculated as the sum of the product of the normalized weighting matric and the systematic error matrix (the mean bias in each cell), while the weighted mean random error $\sigma(e_p)$ is calculated using the product of the normalized weighting matrix and the random error matrix (the standard deviation of the errors in each cell).

The maximum acceptable systematic and random errors for the different validation parameters for each class of assessment are shown in Table 3.5. This procedure and the maximum acceptable validation criteria have not yet been tested in real world applications at the time of the IEC–TS development, this means that an assessment of this procedure and criteria is necessary to ensure that the criteria reflect what is currently considered achievable through numerical modeling.

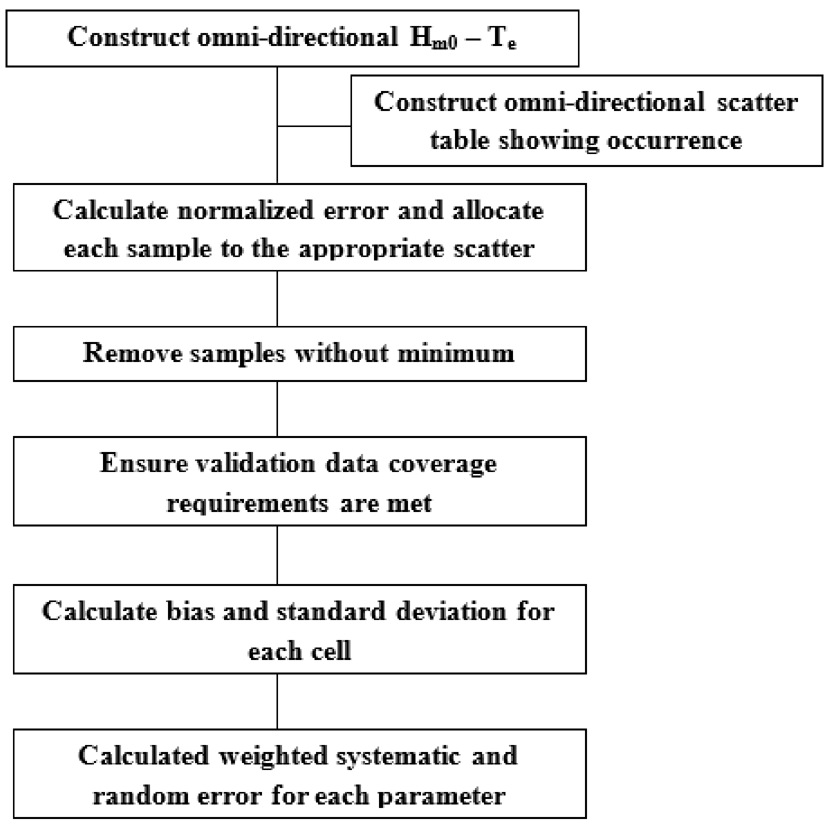

Figure 3.2 – IEC–TS Specification Validation Procedure

Table 3.5 – Minimum Validation Criteria Required by the IEC–TS

	Class 1: Reconnaissance	*Class 2: Feasibility*	*Class 3: Design*
Validation data coverage requirements			
Minimum number of validation data points to represent cell	3	5	5
Minimum coverage by validation data	90%	90%	95%
Max acceptable weighted mean systematic error, $\boldsymbol{b(e_p)}$			
Significant wave height, H_{mo}	10%	5%	2%
Energy period, T_e	10%	5%	2%
Omni-directional wave power, J	25%	12%	5%
Direction of max. directionally resolved wave power θ_{Jmax}	-	10°	5°
Spectral width, ε_o	-	12%	5%
Directionality coefficient, d	-	12%	5%
Max acceptable weighted mean random error, $\boldsymbol{\sigma(e_p)}$			
Significant wave height, H_{mo}	15%	10%	7%
Energy period, T_e	15%	10%	7%
Omni-directional wave power, J	35%	25%	20%
Direction of max. directionally resolved wave power θ_{Jmax}	-	15°	10°
Spectral width, ε_o	-	25%	15%
Directionality coefficient, d	-	25%	15%

3.4 Classification of Sensitivity

3.4.1 IEC Technical Specification Classification of Sensitivity

To determine the sensitivity that the different components of the numerical model have on the resource assessment objectively, a set of recommended thresholds must be considered. The TS provides a basic procedure for the classification of the sensitivity as well as recommended sensitivity thresholds, as shown in Table 3.6. This sensitivity is determined by running the model including and excluding the process under investigation, then examining the effect of this process on a single sea state with reference to the wave power and the significant wave height. If the difference between the measured wave heights and power are higher than a set sensitivity threshold the sea state is considered to be sensitive to the parameter. As with the validation criteria, no real world case studies have been completed to determine whether these threshold differences are reasonable. Similar to the recommended sensitivity thresholds, the TS also provides a condition of insensitivity, whereupon the model is considered to be completely insensitive to a particular process should the percentage of sample sea states defined as having a significant effect on the wave power and wave height be less than the threshold shown in Table 3.7.

Table 3.6 – IEC-TS Recommended Sensitivity Thresholds

	Threshold Percentage Difference	
	Wave Power	Significant Wave Height
Class 1 - Reconnaissance	20%	10%
Class 2 – Feasibility	12%	6%
Class 3 - Design	6%	3%

Table 3.7 – IEC-TS Recommended Condition of Insensitivity

	Maximum Percentage of Sea States Where There is a Significant Effect
Class 1 - Reconnaissance	5%
Class 2 – Feasibility	2%
Class 3 - Design	1%

This sensitivity calculation is not required for every sea state, but rather for a set of sample sea states. These representative sea states should be randomly selected from all the cells in a scatter table, defined by the significant wave height and energy period. An additional condition is that the set of sample sea states should contain at least one sample from each cell in the scatter table with a relative frequency of occurrence greater than 0.1%, which may require that additional sea states be selected. Appropriate values must be selected for the model component being investigated.

The disadvantage of this classification is that it only considers the sensitivity with regards to the wave power and significant wave height, ignoring the impact the different processes may have on the wave direction or energy period, which are both important to developers of WECs. In addition, the random selection of these wave states has the possibility of under or overestimating the sensitivity of the resource assessment. Additionally, no recommendation is made for the percentage of points that should be selected.

3.5 Reporting Requirements

The TS requires that certain information be reported so that developers and those interested in the resource within the region will be able to find all relevant information with ease. Each class of assessment has different requirements for reporting as discussed further in this section. Correct reporting of the results is essential as will allow the comparison of the wave climate with the capabilities of different WEC to determine an optimal deployment location.

In general terms, after completion of the resource assessment, documentation indicating the methodologies used for the assessment and a summary of the results must be completed, including [IEC, 2014]:

- Class and purpose of the resource assessment;
- Intended resolution and level of uncertainty;
- Description of the study region;
- Summary of the raw data used in the assessment, including sources;
- Description of modeling methods;
- Description of MCP methods (if applicable);

- Preparation of model inputs;
- Model calibration and the data used for calibration;
- Model validation procedure and results;
- Analysis of the model results;
- Estimation of the long-term wave resource;
- Presentation of results;
- Underlying assumptions;
- Assessment of the total uncertainty;
- Discussion of limitation/ factors not considered.

In addition to the reporting of the results, all data must be stored in a geo-referenced digital database for future reference.

The TS requires that maps be prepared and included within the report to illustrate the spatial variability of the key wave resource parameters within the study region. The required parameters are shown in Table 3.8.

In addition to the requirements indicated in Table 3.8, the IEC-TS also requires the:

- Annual scatter table, showing the proportional frequency of occurrence of the sea states;
- Graphical and/ or tabular presentation of the annual variation of the long-term monthly mean values of the significant wave height, the energy period, the omni-directional wave power, and the maximum directionally resolved wave power;
- Annual wave rose depicting the maximum directionally resolved wave power and the direction.

Additional figures such as the annual and monthly cumulative distributions are recommended to further illustrate the wave resource at the site of interest.

Table 3.8 – Wave Parameters for Archiving and Mapping (• - Required, o – Recommended)

Parameter	*Units*	*Assessment Class*		
		Class 1	*Class 2*	*Class 3*
Mean Water Depth	m	•	•	•
Annual Mean Omni-Directional Wave Power	kW/m	•	•	•
Extent of Successful Model Validation		•	•	•
Monthly Variability of Omni-Directional Wave Power	kW/m		o	o
Annual Mean Significant Wave Height	m	o	o	o
Monthly Variability of Significant Wave Height	m		o	o
Annual Mean Energy Period	s	o	o	o
Monthly Variability of Energy Period	s		o	o
Annual Spectral Width	-		o	o
Monthly Variability of Spectral Width	-			o
Annual Mean of Maximum Directionally Resolved Wave Power	kW/m		o	o
Monthly Variability of Maximum Directionally Resolved Wave Power	kW/m			o
Annual Mean Direction of Maximum Wave Power	deg		o	o
Monthly Variability of Annual Mean Direction of Maximum Wave Power	deg			o
Annual Mean Directionality Coefficient	-		o	o
Monthly Variability of Annual Mean Directionality Coefficient	-			o

4 Literature Review

Wave energy assessments and modeling are ongoing high-interest topics for research globally and within Canada. This chapter examines the current literature with respect to wave modeling for WEC design. This includes research involving the modeling of wave energy with a focus on western Canada and the IEC-TS. It also includes literature on the sensitivity of the resource assessment to model parameters, the impact of currents on wave energy, WEC array interactions and WEC site selection considerations.

4.1 Direct Measurements

Direct measurements obtained by wave buoys can be used as a point of validation for analytical or numerical models. However, with sufficient measurement locations and duration this data can be used to directly determine seasonal trends and wave characteristics within a region. The equations that are used to determine the wave characteristic from these wave buoys can also be used to obtain the wave characteristics from spectral models.

Lenee-Bluhm *et al.* (2011) characterized the wave energy resource off the coasts of Washington, Oregon, and Northern California using archived spectral records from ten wave buoys operated along the coast. This was completed by calculating six IEC parameters from each measured spectra. From this they were able to observe seasonal and depth trends, and to create bivariate distributions of the energy and occurrence for the measured sites. While this method does reveal the suitability of the measured locations and the nearby regions, it is limited in its ability to characterize the surrounding regions and can obscure much of the variability present in the resource assessment.

4.2 Numerical Models

The most common method of determining the wave energy resource and wave climate is through numerical modeling. There are a number of commercially available numerical models which are used to conduct these assessments.

4.2.1 Western Canada Resource Assessments

There have been a number of studies examining the wave energy resource along the west coast of Vancouver Island, British Columbia corresponding to the same region of the current research. This allows for the comparison between the wave energy resources observed in these previous studies with that found by the current work.

Robertson *et al.* [2014a] focused their study along the south–western coast of Vancouver Island, extending the model down into the United States and into the Strait of Juan de Fuca, as shown in Figure 4.1. This study was run for a hindcast period of 2005 to 2012 using the SWAN model to determine the long–term wave climate based on the requirements set out by the IEC–TS.

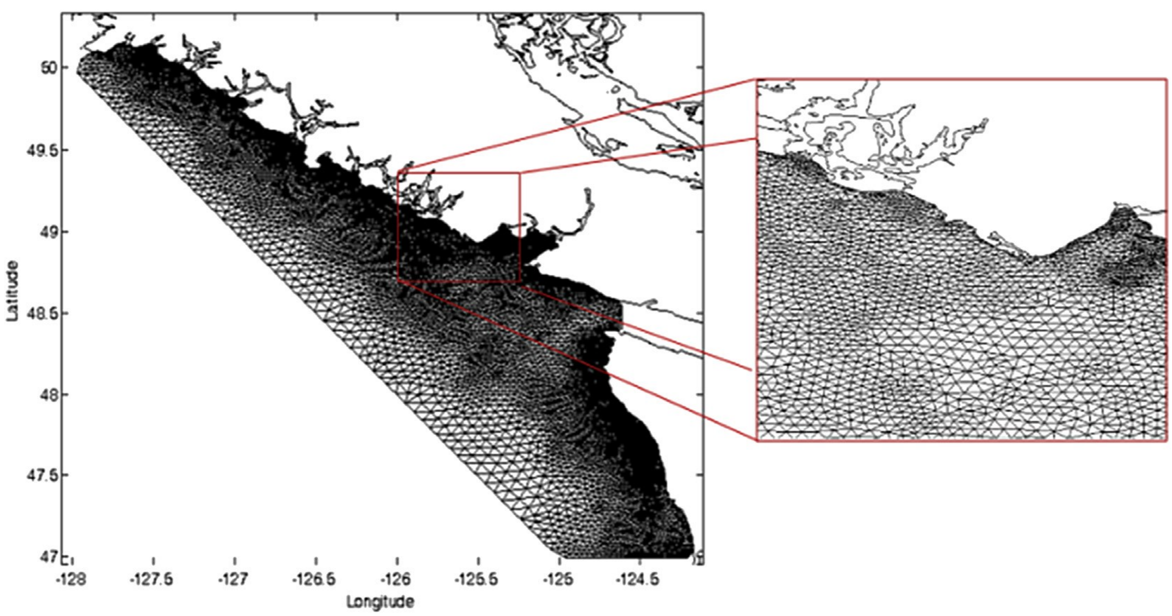

Figure 4.1 – Model Domain and Mesh for the West Coast of Vancouver Island [Robertson *et al.*, 2014a]

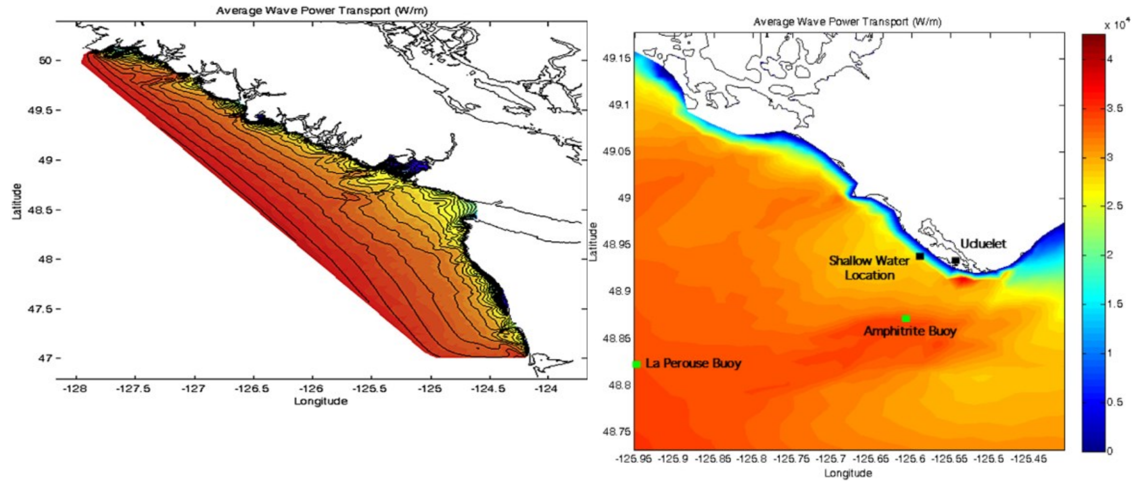

Figure 4.2 – Annual Mean Modeled Wave Power Transport (W/m) for 2010 [Robertson *et al.*, 2014a]

Robertson *et al.* [2014a] observed in their study that the near shore mean energy transport located at Amphitrite Bank (which is the site of the Beverley directional wave buoy) was 34.5kW/m, while the mean energy transport was 27.8kW/m in shallower water, as shown in Figure 4.2.

Cornett and Zhang [2008] also completed a resource assessment within the same region, focusing their model on the west coast of Vancouver Island for a hindcast period of 2002–2007. During the course of this study they discovered that the annual mean power varied significantly in shallower water, along the 20m isobath, with the power ranging from 17kW/m up to 37kW/m, but that in deeper water at the 50m isobath the annual mean power became more consistent, ranging from 35 kW/m to 38kW/m, as shown in Figure 4.3.

When comparing the results of these two studies at the Amphitrite and shallow water locations it was found that the resource estimated by Cornett and Zhang typically exceeded those obtained by Robertson *et al.* in the active winter months, while being in better agreement over the calmer summer period. Robertson *et al.* was also able to validate their modeled wave power from the Amphitrite Bank location with wave energy measurements obtained from April – October 2010, finding that the mean measured and modeled power transport differed by only 0.1kW/m.

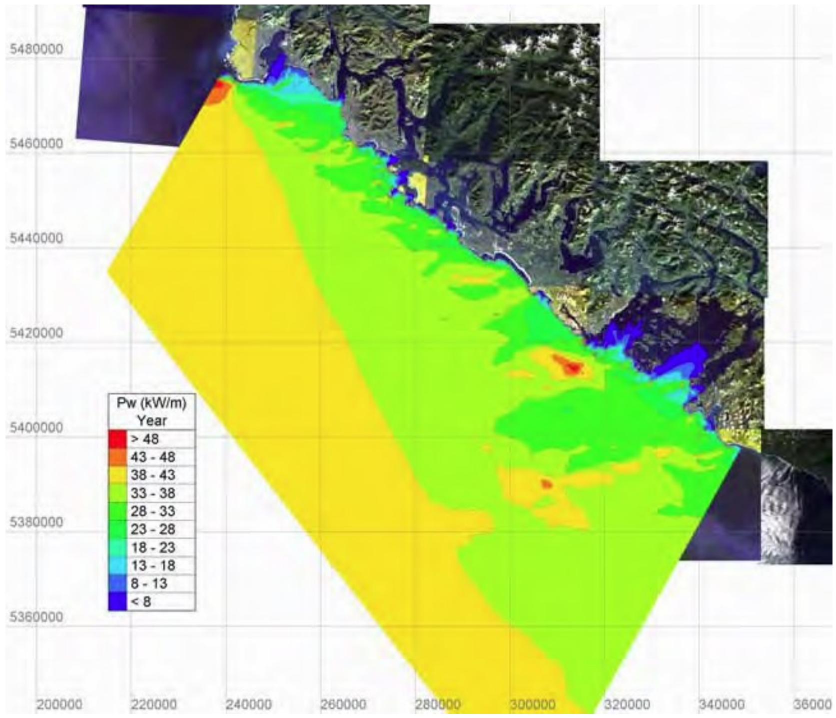

Figure 4.3 – Annual Mean Modeled Wave Power Transport (kW/m) during a Typical Year [Cornett and Zhang, 2008]

Robertson *et al.* [2014b] expanded on the domain shown in Figure 4.1 by extending the domain up towards Bella Bella in Northern British Columbia, and by extending it further into the Strait of Juan de Fuca. This study was completed for a hindcast period of 2004 to 2013 and was used as a means of examining potential wave farm sites along the coastline. In the course of this study, it was discovered that there was significant variation in the monthly directional wave energy at Amphitrite Bank, with values ranging from 6 to 50kW/m with directionality coefficients varying from 0.75 to 0.84. This indicates that the energy is fairly concentrated along the direction of wave energy transport, but that the average wave energy may not be a good indication of the available resource due to its high variability.

The final study being examined in the literature review for this region was conducted by Hiles *et al*. [2013]. This study was completed in a small region off the west coast of Vancouver Island near Hot Springs Cove, see Figure 4.4. This study was completed for a hindcast period of 2005 to 2013 using the REF/DIF– model. At the reference location shown in the figure they found a large seasonal variation in both wave height and power, which was also observed in the previously mentioned studies by Robertson. At this reference location the average yearly omni–directional wave power was found to be 31kW/m, which is slightly below the range of wave powers observed by Cornett and Zhang along the same 50m isobath.

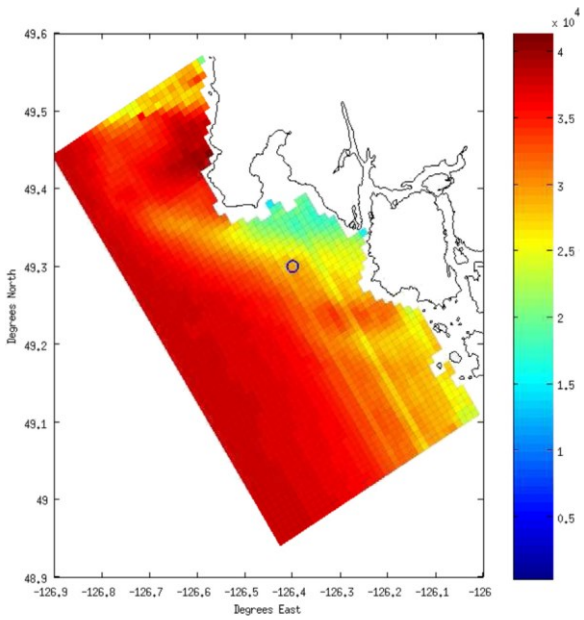

Figure 4.4 – Model Domain and Annual Mean Wave Power (W/m) for Hot Springs Cove [Hiles *et al*., 2013]

All the studies in this location indicate the potential for the western coast of Canada to rival the current established wave testing sites such as EMEC (24kW/m) [Folley, Elsaesser. & Whittaker, 2009] and WaveHub (18 – 20kW/m) [Smith, Haverson, Smith, Cornish, & Baldock, 2011]. Though the highly seasonal range of potential energy may limit the actual extractable wave energy within this region due to the operational ranges of WECs.

4.2.2 Global Resource Assessments

There are a significant number of resource assessments being conducted annually globally, as it is not possible to examine all resource assessments being done this section will highlight a few studies which have been completed within the past 10 years to illustrate the global observations of the wave climate which may need to be considered when applying the IEC–TS.

One study being examined is that performed by Liberti, Carillo, & Sannino [2013], who developed a high resolution WAM model in order to study the wave energy distribution within the Mediterranean Sea over a 10-year hindcast period (2001–2010), Figure 4.5. The researchers found that the most productive regions within the Mediterranean Sea have average power values of up to 12kW/m, which is significantly lower than that seen in common testing sites such as EMEC. However, they note that the average energy values are not indicative of the range of power available at the site stating that the power of the most energetic, though less frequent sea state may be an order magnitude greater than that of the most common sea state. This may impact the actual available potential power at a site as WECs are designed to operate within a specific range of wave states. This also highlights the importance of the seasonal variability on the potential wave power and revenue obtained from the operation of a WEC.

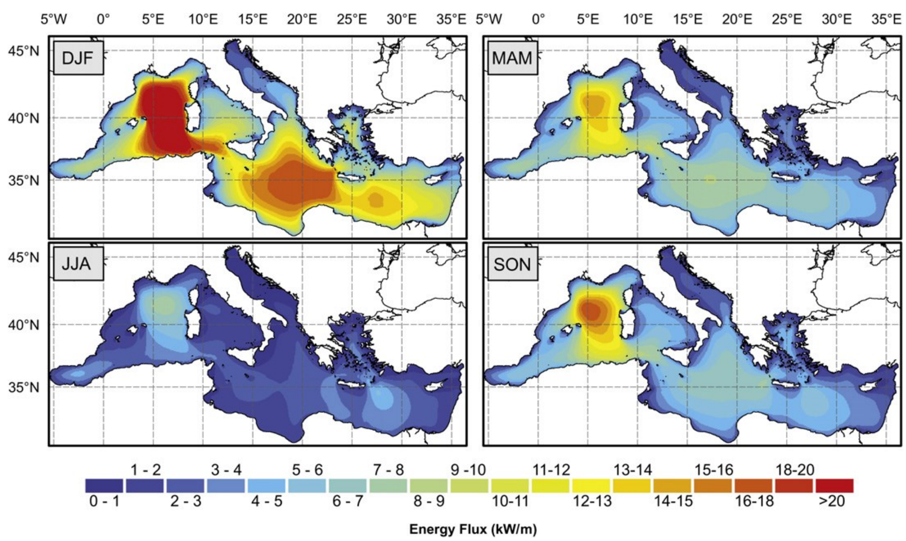

Figure 4.5 – Model Domain and Seasonal Variability for the Mediterranean Sea [Liberti, Carillo, Sannino, 2013]

Stopa *et al.* [2013] examined the nearshore wave energy resource along the Hawaiian Island chain using a coupled Wave Watch 3 (WW3) and SWAN model for a 10-year hindcast period from 2000 to 2009, shown in Figure 4.6. Similar to the study completed by Liberti *et al.* the researchers noted that the presence of strong seasonal variability within the wave resource; they stressed that consistency in the wave energy resource is a key concern for the placement of wave energy devices and that proximity to population centers is also ideal. In this study they determined that the northwestern swells typically produce 35kW/m of wave power, with the power reaching up to 50 kW/m 10% of the time. However, due to the need for consistent wave power, the regions providing a constant power of 12kW/m, as a result of the trade winds, may be more economically viable for the potential development of wave energy farms.

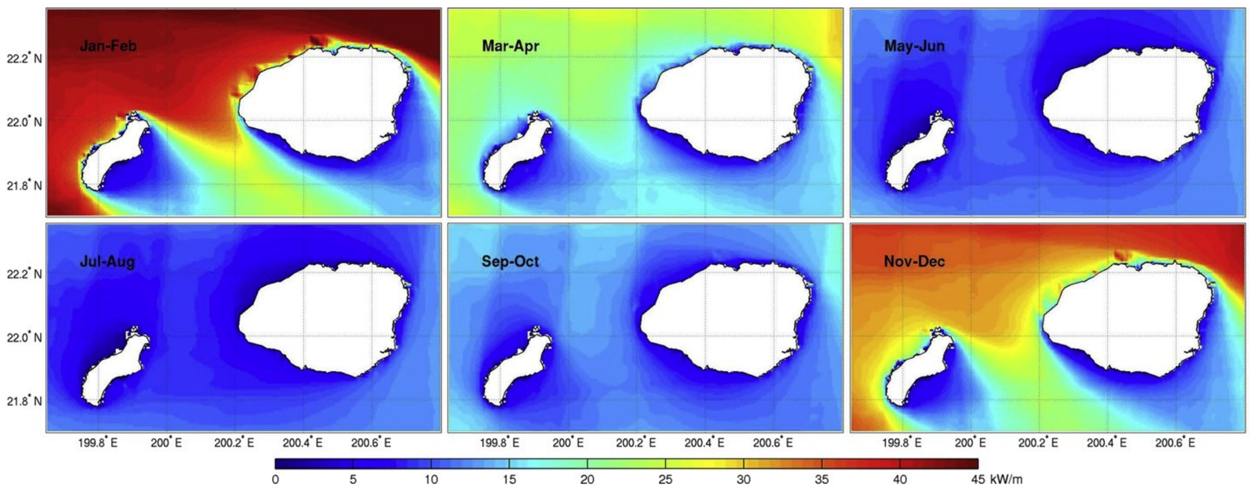

Figure 4.6 –Seasonal Variability for the Hawaiian Islands [Stopa *et al.*, 2013]

4.3 IEC Technical Specification Validation

At the time of this research there was only one other study beyond the current work that attempted to validate the IEC–TS for wave energy resource assessments, which was published by Ramos and Ringwood in 2016 and by Ramos *et al.*, also in 2016. This study looked at the application of the IEC–TS along the Irish west coast near the Belmullet Wave Energy Test Site located offshore of Annagh Head, see Figure 4.7 for the three model domains. The purpose of this study was to provide recommendations to IEC Technical Committee 114 for the IEC–TS and to compare the three different classes of resource assessment in terms of their uncertainty and required level of effort.

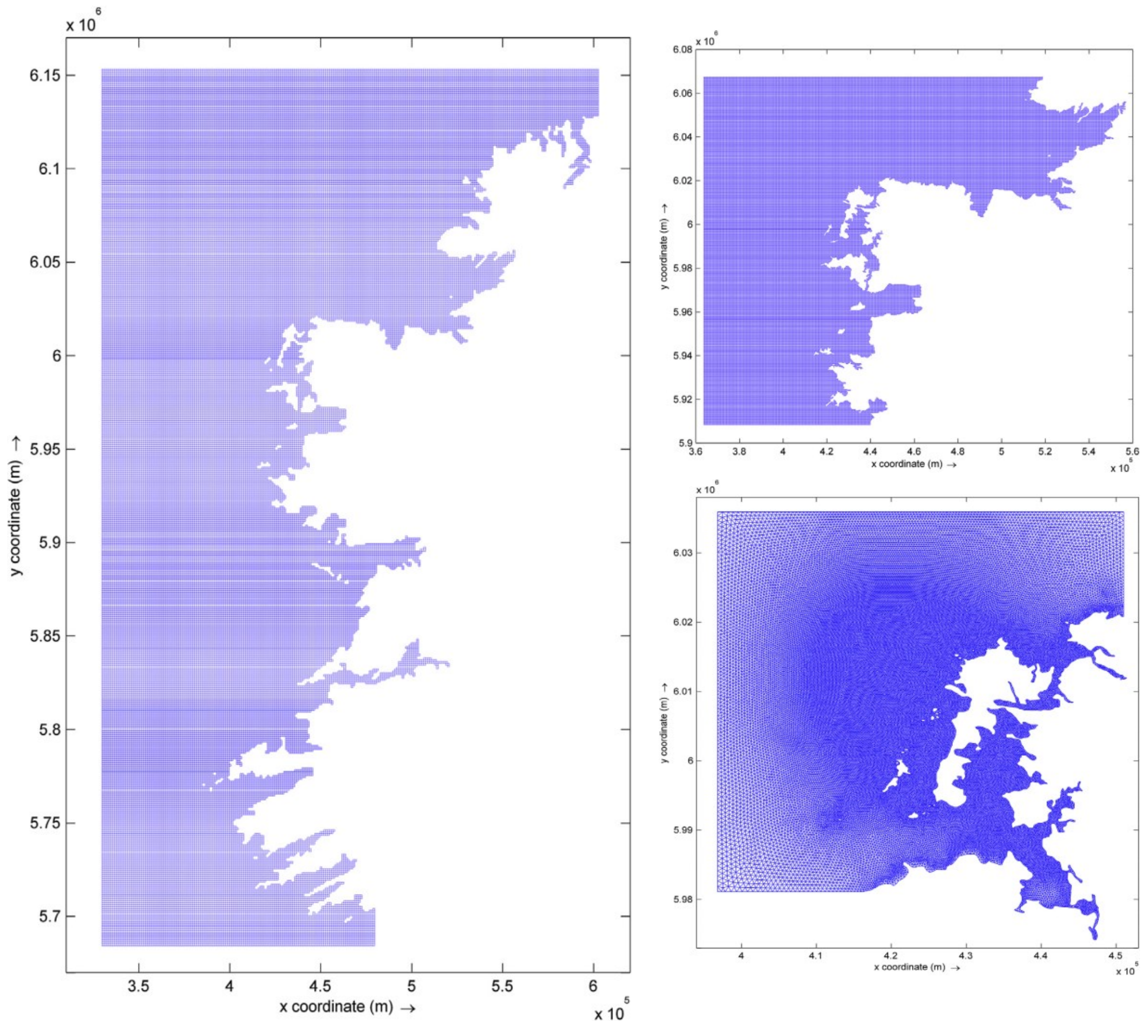

Figure 4.7 – Model Domain A) Reconnaissance; B) Feasibility; and C) Design [Ramos and Ringwood, 2016]

This case study was conducted using the SWAN model and was run for a period of 10 years from 2005 to 2014, with a validation period of 1 year (2014). Model validation was completed using hourly wave data obtained through two wave buoys located within the Belmullet test site. In completing this research, they determined that the model validation improved with refinement of the mesh, but that the mean systematic error for the wave height and power were not in line with the required validation criteria provided by the IEC–TS, whereas the more traditional validation methods of RMSE, Correlation Coefficient, and Scatter Index provided better agreement. When comparing the resource assessments with each other they determined that the reconnaissance (or M1) model seemed to underestimate the wave resource in comparison with the feasibility (MII), and design (MIII) models, while MII and MIII provided more similar results, as shown in Figure 4.8 for the intra-annual wave resource. When comparing the models from a computational standpoint they observed that the MIII model had significantly higher costs as a result of the higher mesh resolution, they observed similar computational costs for the MI and MII models.

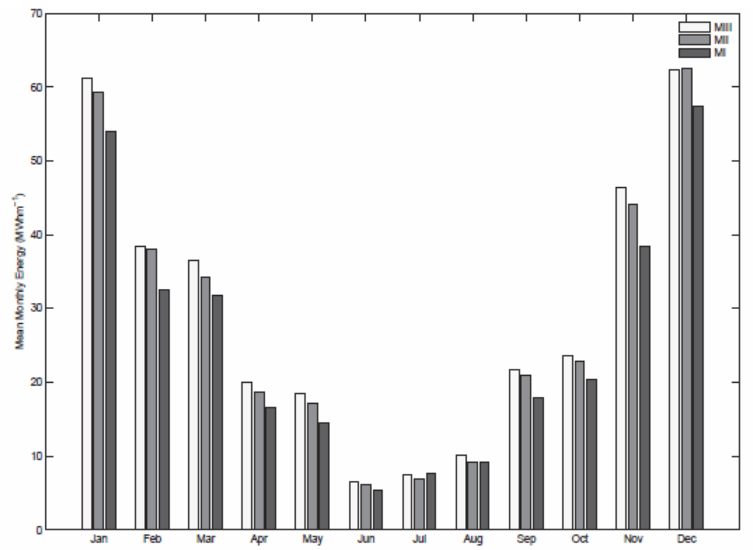

Figure 4.8 – Mean Monthly Wave Power [Ramos and Ringwood, 2016]

As a result of their research Ringwood and Ramos proposed the inclusion of the intra–annual variability of the wave energy for future iterations of the IEC–TS. They also noted that the wave boundary conditions had a larger impact on the modeled wave energy resource when compared to the mesh resolution. This was noted in the comparison between the feasibility and design class assessment, which were both set up using spectral boundaries, as they had similar resource assessments despite the vastly different mesh resolutions and computational effort between the two classes.

4.4 IEC Technical Specification for Wave Energy Resources

Since the publication of the IEC-TS for wave energy resource assessment studies have begun using its methodology to complete their assessments. As the IEC-TS is still fairly new there have been limited studies looking at its application, some of which are discussed below.

Lokuliyana et al. [2020] conducted a resource assessment study on Sri Lankan wave energy based on the Class 1 standards. This study was completed using the SWAN model to conduct a comprehensive resource assessment for the whole Sri Lankan region which was categorized as a moderate wave energy resource with a small frequency bandwidth and narrow directionality. The researchers noted that the next steps of the study would include conducting Class 2 and Class 3 resource assessments; however, they noted several concerns such as the availability of higher resolution bathymetry and wind data, and additional buoy measurements for model validation. They also noted in their research that IEC-TS should also include minimum model validation requirements for additional periods such as mean wave period or peak period as they are more commonly available as measured parameters.

García-Medina *et al.* [2021] conducted a wave resource assessment for the southern coast of Alaska based on a 32-year hindcast closely following the IEC-TS recommendations. This study was completed using the SWAN model extending 2,836,000km^2 around Alaska. The model was configured to be a Class 2 resource assessment and used the IEC-TS to calculate the main wave climate parameters. The researchers calculated the mean systematic and mean random errors but did not consider them for model validation as they found that the requirements were very strict. They noted that the traditional error statistics suggested that model performance was comparable to or exceeded the performance of similar modelling studies but that the model was not always able to meet the Class 2 maximum errors.

4.5 Sensitivity of Resource Assessment

The sensitivity of the resource assessment to model parameters, many of which have also been examined in the context of this research, has been examined by numerous researchers. By comparing the observations of these studies with the current research it is possible to determine whether the sensitivity of the model is site specific or is notable only under specific conditions.

Dykes *et al.* [2003] completed their research in the Mississippi Bight to evaluate and build confidence in the SWAN model results. For this study they examined the impact of the model frequency range (using a cutoff at 1Hz and at 0.35Hz), the impact of the whitecapping empirical parameter for the dissipation function (which has a default of 1), and the impact of the inclusion/exclusion of bottom friction.

Dykes *et al.* [2003] observed that the increases in the wave height as a result of extending the frequency cutoff to 1Hz for the calculation of the bulk parameters was small, but that there was a significant impact on the mean wave period as by definition the mean wave period is weighted by the frequency. It should be noted that this cutoff was applied only to the calculation of the bulk parameters after the SWAN model was run and that the frequency range within the SWAN model was not modified. The dissipation parameter for the whitecapping processes was compared for a default value of 1 and for a value of 2. Dykes *et al.* noted that both the significant wave height and mean period had better agreement with a dissipation parameter of 2, additionally it was noted that using a value of 2 resulted in less high frequency energy and better agreement at lower frequencies. Finally, the authors determined that there was a significant drop in the wave heights when including the bottom friction parameter, indicating that the model was being overly dissipative for a buoy in 13.4m water depth.

Yang *et al.* [2017] presented a model test bed to benchmark, test, and evaluate modeling methodologies using the wave energy resource parameters suggested by the IEC-TS using WaveWatch III (with the ST2 physics package) and SWAN run in both stationary and non-stationary model. This was completed through application of the models to the Oregon coastline. The authors completed a sensitivity analysis for the different physics packages provided for the WWIII model and for the spectral resolution. By varying the number of frequency bins from 29 to 50, and the number of directional bins from 24 to 36 bins Yang *et al.* observed no improvements in the model skill for both the WWIII and SWAN models. They believe this may be a result of the large water depth (128 m) and the absence of any bathymetric features at the point of interest.

The final sensitivity assessed in this literature review was completed by Van Vledder and Akpinar [2015] who compared the impact of different wind fields on the performance of the SWAN model for the Black Sea. Their study used seven different wind fields from different sources with varying temporal coverage, temporal resolution, and spatial resolutions. By comparing the performance of the model using these different wind fields they observed that the quality of the wind data did have an impact on the wave models performance.

Van Vledder and Akpinar [2015] also examined the impact of the spatial and temporal resolution of the wind field on the model performance. The impact of the different spatial resolutions on the wave model was completed using the CFSR wind data with resolutions of 2.5°, 1.5°, 1°, 0.5°, and 0.25°, while the original CFSR wind resolution was 0.3125°. It was observed that when the wind resolution was refined, the accuracy of the significant wave height and the spectral period was increased. The impact of the temporal resolution of the wind fields was assessed using wind fields with the same spatial resolution, but different temporal resolutions. This was completed with the CFSR wind field by increasing the time step from 1hr up to 2, 3, 4, and 6hrs. The researchers observed that the finer temporal resolution did not generally improve the performance of the wave model significantly, with the only improvement being seen in the bias of the spectral period.

4.6 Wave-Current Interaction

While not generally considered in wave energy resource assessments, local currents and tides have an impact on the local wave climate, with potential impacts on the wave direction, and on the wave height and period. As the power is a function of the wave height, this means that the presence of currents and tides can have a direct impact on the amount of power available at a potential WEC site and on how the devices interact with the wave climate.

Guillou [2017] examined the impacts that currents have on waves and the wave power resource at a study site in the Fromveur Strait, off western Brittany using the SWAN model. During this study Guillou observed that during high tide, the northeastern tidal currents induced a change of direction of the incoming waves towards the south in the southern and southeastern region of the study site. While it was observed at low tide that the waves were refracted from the west towards the north-east by the southwestern currents, causing a reduction in the significant wave height. The influence of the tide on the significant wave height is shown in Figure 4.9.

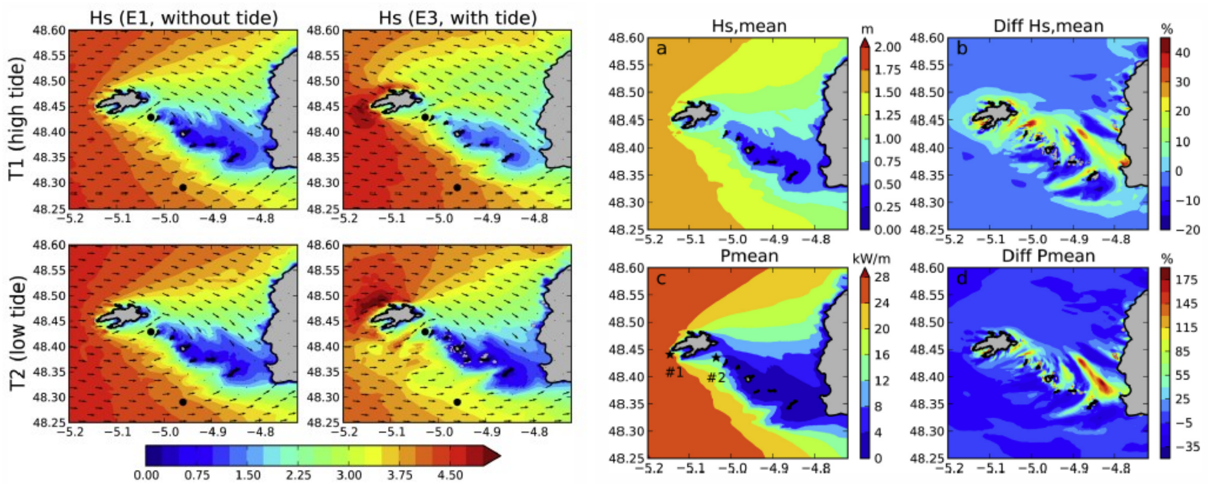

Figure 4.9 – Significant Wave Heights without and with Tides (Left); and the Averaged Significant Wave Height and Power without Tides (E1) with the Relative Difference between configurations E3 and E1 (Right) [Guillou, 2017]

Guillou [2017] also investigated the effect of the tidal currents on the wave power resource at the site of interest, where it was shown that the inclusion of tidal-currents had an impact on the available wave power. Guillou associated these differences with the theoretical formulations of the wave height and power, as the significant wave height is calculated from the square root of the total wave energy and the wave power is defined as the evolution of the wave energy transport by the group velocity and tidal currents.

Liang *et al.* [2017] characterized how the wave-current interaction would impact the wave energy available for conversion by a WEC using MIKE21 DW along the Qingdao Coast. From this research they observed that the coupling of the tides to the wave model modified the wave power, as shown in Figure 4.10. From these differences Liang *et al.* noted that the inclusion of the tides resulted in the average wave power increasing along the nearshore areas, with the maximum wave power increasing also in the offshore area.

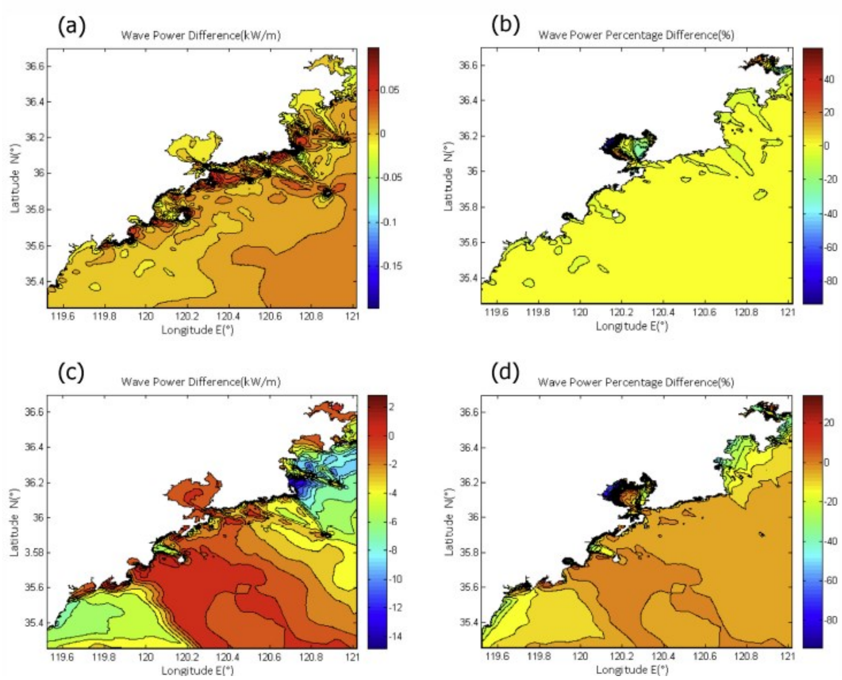

Figure 4.10 – Difference and Percent Difference of the Average Wave Power (A, B) and the Maximum Wave Power (C, D) Between the Coupled and Uncoupled Wave and Tidal Model [Liang *et al.,* 2017]

Beya *et al.* [2021] examined the impact of tidal currents on wave energy resource by comparing the results of two nearly identical SWAN models for the west coast of Canada. From this study they noted that the inclusion of the tidal currents increased the accuracy of the wave resource characterization by improving the models' ability to simulate the wave periods. This improvement was consistent at all buoy locations. They also noted that the peakedness of the wave spectrum was the parameters most sensitive to tidal currents, resulting in reduced wave peakedness at every location. They noted that the wave height and power were also consistently decreased with the tidal currents but that the impact of the currents on the wave characteristics did not follow a consistent pattern making it difficult to interpret.

Finally, Saruwatari *et al.* [2013] examined the changes that would occur in the wave climate when considering the currents using SWAN to model the Orkney Islands. From this study they observed that when the waves were subjected to strong currents in the same direction as the wave propagation the wave amplitude was decreased, but the wave length increased, while during ebb the opposing currents increased the wave height and shortened the wave length. When considering the wave power with the tides, they observed that during the flood tide the wave power was reduced in key locations by the tidal current, while at high tide the wave power in the southern region was increased, and during the ebb tide the wave power was significantly increased in the channels where the tidal currents were flowing.

4.7 Array Interaction

While prototype testing and most theoretical assessments of WEC technology is based on the placement of single devices, the intended future of wave energy is the creation of wave farms containing large arrays of devices. While the wave energy resource assessment may be important in determining where areas of high power are, they do not account for the impact that large arrays may have on the resource, and how this may impact the other devices within the array. There is significant research on both the interactions of the array devices and the factors which may influence the array layouts, however this section will focus on the impact these arrays have on the surrounding resource.

Venugopal *et al.* [2017] applied Mike21 SW and WAMIT to assess the wave energy extraction of an array at a proposed development site in the Orkney Islands, Scotland. This was done by assessing two generic types of WEC (a surface attenuator in deep water and an oscillating wave surge converter in shallow water). From this application they observed that the mean significant wave height was decreased downwave of the arrays, as shown in Figure 4.11. In addition to impacting the wave climate downwave of the array the presence of the devices impacted the wave climate within the array and the neighbouring arrays.

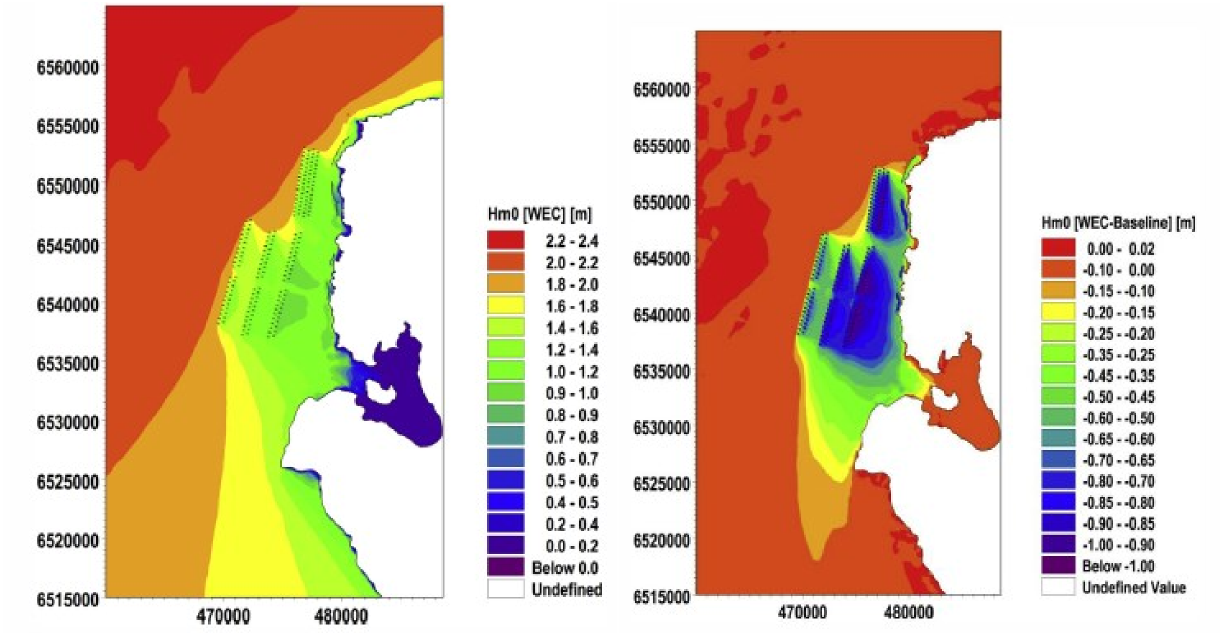

Figure 4.11 – Mean Significant Wave Height (Left) and Absolute Difference of Mean Significant Wave Height (Right) [Venugopal *et al.*, 2017]

Jones *et al.* [2014] assessed the impacts that an array of WECs have on hydrodynamics and sediment transport within Monterey Bay and Santa Cruz, California. The WEC array was simulated in SWAN as discrete obstructions, with the subsequent wave fields then being passed to the SNL-EFDC model, this array consisted of 200 individual devices arranged in a honeycomb shape. For the average wave climate test, Jones *et al.* observed that the devices caused the wave heights to be reduced behind the devices due to the absorption of the wave energy by the devices, as shown in Figure 4.12. The simulation of these devices was based on 100% energy extraction which is not realistic, therefore the researchers proposed this as a worst-case scenario in terms of the impact the WEC array would have on the wave climate.

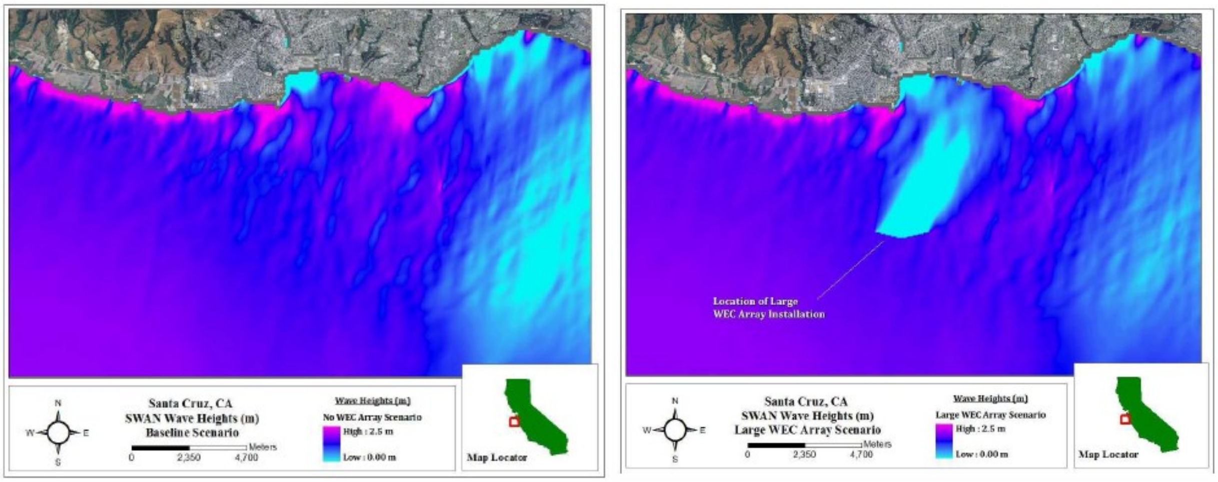

Figure 4.12 – Modeled Wave Heights Before (Left) and After (Right) Installation of a WEC Array for Incoming Wave Height of 1.7m and Peak Period of 12.5s [Jones *et al.*, 2014]

4.8 Site Selection

The wave energy resource assessment is a valuable tool for assessing the wave climate within a region. However, simply seeking the site with the highest yearly mean power is not necessarily ideal as there are a number of important factors to consider in terms of the site location: such as the seasonal variability, distance from the shoreline, proximity to grid-connections and communities, extreme events, ship activity, and environmental impact to name a few. Additionally, there are device specific constraints such as its operational range and orientation with respect to the oncoming waves (for directional WEC). Some researchers work to develop tools and procedures for optimizing the amount of extractable energy at potential wave energy sites to determine suitable sites, while other researchers consider site selection from an operational and maintenance perspective.

Carballo *et al.* [2014] worked to develop a tool which would allow for the computation of a characterization matrix using Matlab at any coastal location, allowing developers to obtain information required to select a site for wave energy development. This procedure focused on optimizing the extractable power available for a WEC. By specifying the type of WEC the energy output per unit of power installed could be computed. However, this tool does not consider the installation of arrays of devices which can have an impact on the surrounding wave climate and will have an impact on the extractable wave energy.

Gray *et al.* [2017] characterized sites in terms of accessibility for marine operations combined with power generation using a Monte Carlo-based operation and maintenance simulation tool. This tool considered the failure rates of the devices, maintenance parameters, and the local weather. To assess the effectiveness of this tool Gray *et al.* compared two different sites located within the UK (Site A located in the North and Site B located at Wave Hub). With these two sites they observed that overall, the significant wave height and energy period are lower at site B, but the wind speed is higher. The implication being that site A will have higher potential energy. Due to the higher wave conditions, they determined that they would need to wait slightly longer for favourable weather conditions for maintenance and installation at site A which would incur slightly higher costs; however, this is offset by the higher potential revenue. This type of analysis requires comprehensive knowledge on the amount of time required for installation and maintenance, the potential failure rates of the devices, and the wave climate to name a few, which can make it difficult to get an accurate assessment of the potential revenue and risks associated with different potential wave sites.

A study published by Kim *et al.* [2012] examined the issue of site selection for western Vancouver Island, British Columbia to develop a decision-supported tool to aide in siting WEC arrays that would be compatible with other ocean users and marine habitats. This process requires the quantification of the harvestable wave energy and an assessment of the economic value of the WEC facility, which considers the annual revenue as a product of the price of electricity and the harvestable wave energy, and the cost of acquiring, installing, operating, and maintaining the facility. This process also requires the identification of compatibility with existing marine use, using a spatial compatibility analysis which shows where existing users occur. In the application of this method to the west coast of Vancouver Island they noted that the fishing and recreational industries have large contributions to the local communities, shown in Figure 4.13, which means that siting a WEC facility near or offshore could affect these communities.

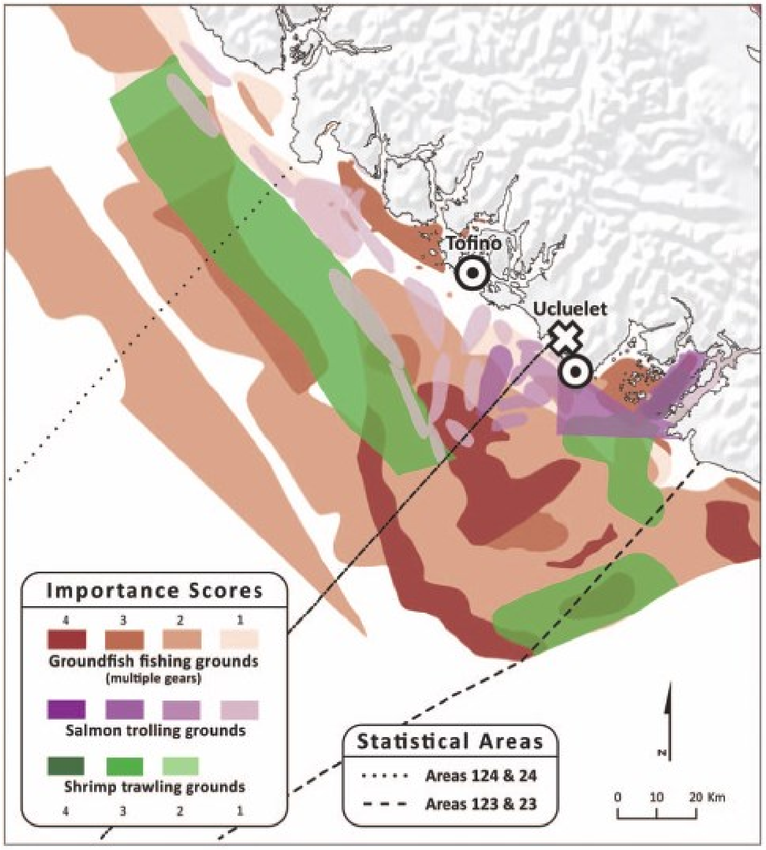

Figure 4.13 – Department of Fisheries and Oceans Canada Fishing Grounds. Grounds are shaded by their Importance: High Values Indicate Greater Importance [Kim *et al.*, 2012]

Kim *et al.* [2012] then found that the wave conditions become stronger nearshore and that there was significant seasonal variation in the wave height, with the annual mean being power greater than 10kW/m in most areas, as shown in Figure 4.14. By overlapping the harvestable wave power with existing marine users, they were then able to determine which sites may be most compatible for development, as demonstrated in Figure 4.15.

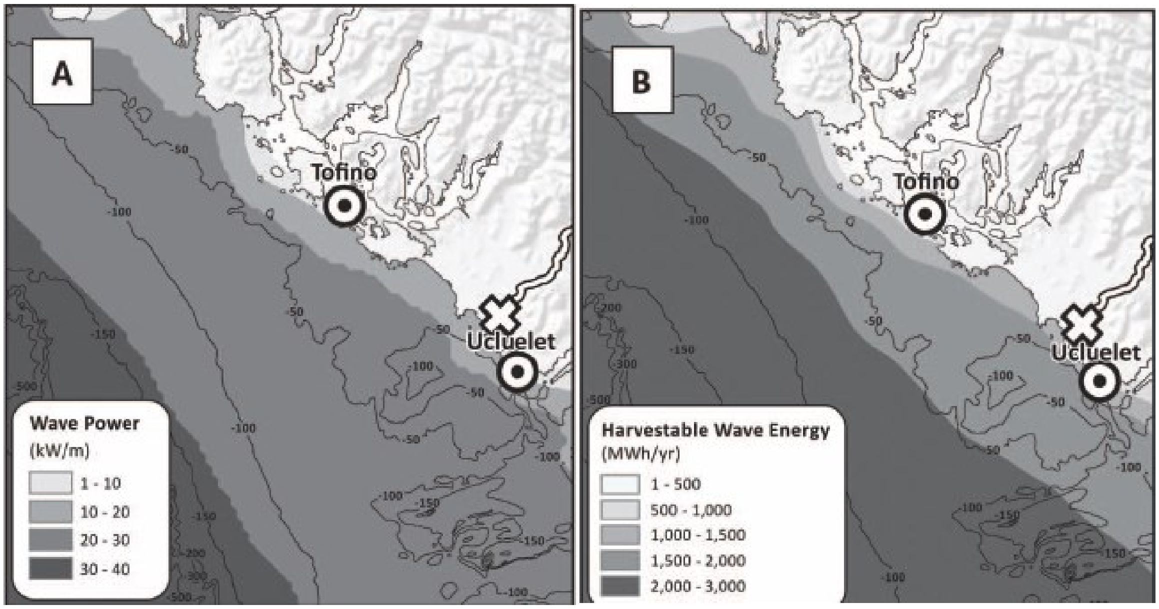

Figure 4.14 – A) Potential Wave Power (kW/m); and B) Harvested Wave Energy (MWh/yr) for a Pelamis WEC with 750 kW power rate [Kim *et al.,* 2012]

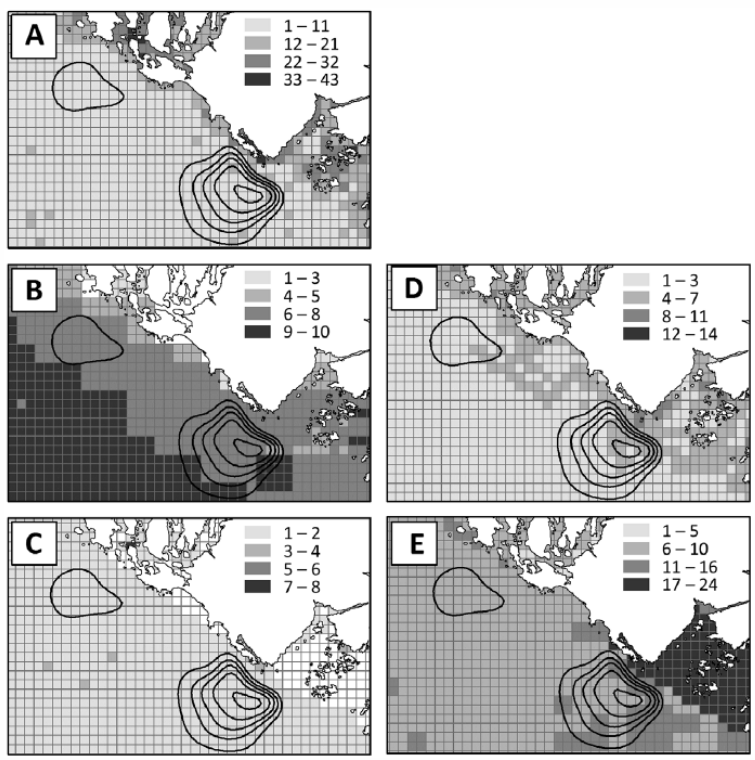

Figure 4.15 – Overlap between Areas of Positive Annual Net Value over the Lifespan of the WEC (Black Contour Lines) and Five Categories of Existing Users A) Ecological Characteristics; B) Shipping and Transport; C) Tenures and Offshore Energy; D) Tourism and Recreation; and E) Commercial Fisheries [Kim *et al.,* 2012]

Finally, Xu *et al.* [2020] proposed a new approach for site identification which includes device-agnostic performance constraints and economic considerations to identify development sites over coastal regions. This site selection process consists of a screening process to determine the extractable wave resource and an economic evaluation to determine locations for near-term wave development. The extractable wave resource was screened both for frequency and frequency-direction, while the economic evaluation used the Net Revenue Index (NRI), see Figure 4.16. For the west coast of Canada if fully developed the resource hot spot have a potential annual wave energy delivery of ~67,000GWh, while the economic hot spots have a potential annual wave energy delivery of 21,00 GWh. By intersecting the economic and energy hot spots there is a potential 336km² zone with an average wave energy flux of 35kW/m.

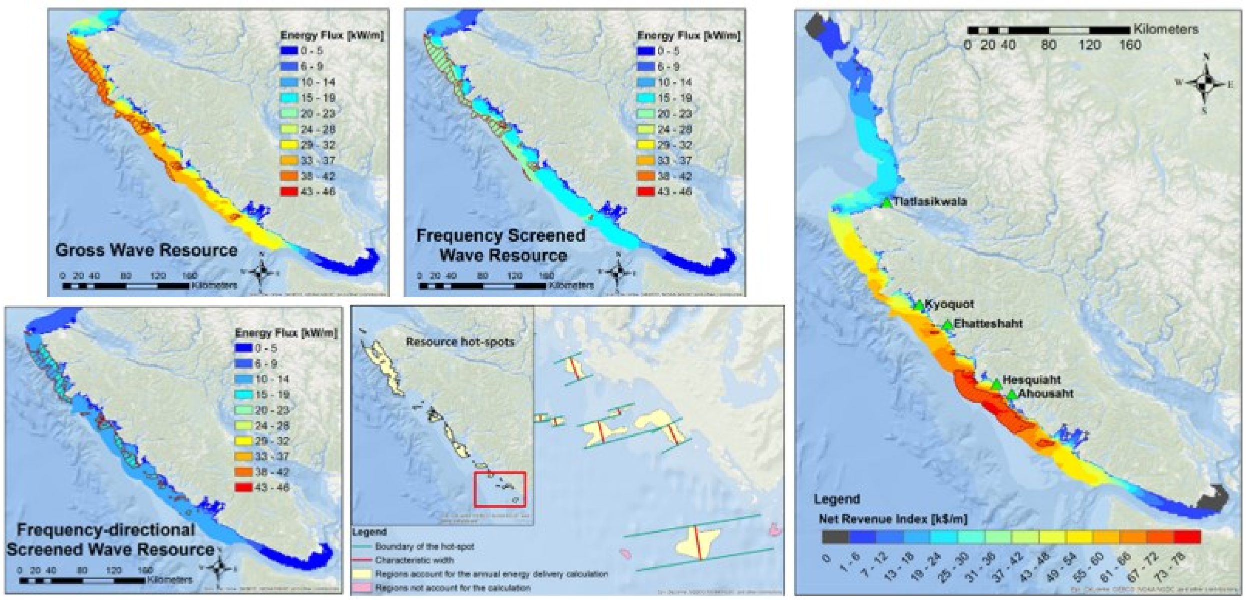

Figure 4.16 – Energy Flux, Net Revenue Index and Resource Hot-Spots for the West Coast of Canada. Sites with Energy Flux or NRI in Excess of 90th Percentile are Shown in the Red-Dashed Region [Xu *et al.*, 2020]

4.9 Summary

This literature review highlights the range of topics that must be considered when conducting a resource assessment or determining the viability of a site for WEC development. The Canadian assessments show the need for a modelling framework as similar models were noted to have different modelled resources. While newer studies completed using the IEC-TS framework indicated the difficulties encountered in its usage such as data availability or strict validation criteria. Other studies highlight topics that are not directly considered within the IEC-TS such as the impact of currents on the potential wave energy resource, the impact of wave arrays on the available wave energy resource, and the actual viability of wave energy development through proper site selection.

All together this shows the complexity of the field and the need for continuous research to help grow the fields collective understanding. It also highlights that the IEC-TS will need to be a living document as new research and development may change our understanding of how to properly conduct a wave energy resource assessment.

5 Study Location

The study location selected for the pilot wave energy resource assessment is along the south–western coast of Vancouver Island, British Columbia, Canada, with a focus on the coastal community of Ucluelet. The study region is located predominately on the continental shelf, which extends roughly 70km off the coastline, see Figure 5.1. The Vancouver Island coastline is characterized by a significant number of inlets, straits, sounds, and narrows which are believed to affect the localized wave climate [Thomson, 1981].

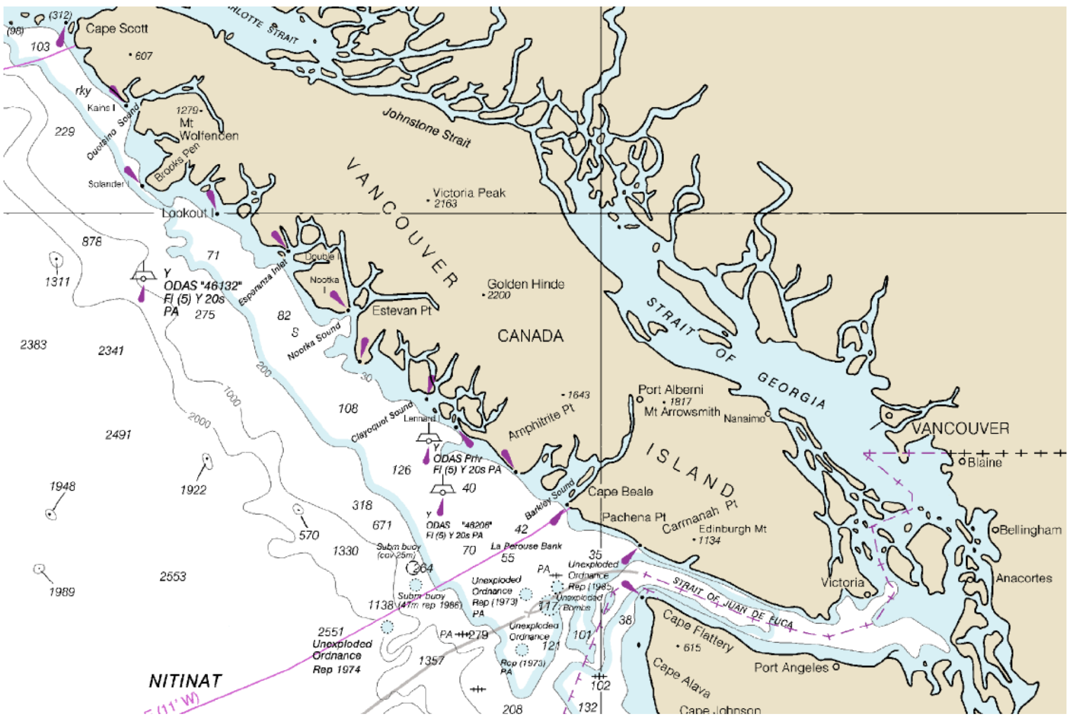

Figure 5.1 – Nautical Chart for Vancouver Island, British Columbia [NOAA]

The prevailing regional wind conditions in this area are predominantly controlled by the location and intensity of two semi–permanent atmospheric pressure cells, the Aleutian Low and North Pacific High [Thomson, 1981]. The combination of these pressure cells means that the winds are predominantly from the southeast and southwest from late fall to early spring, while May through September the winds are predominantly northwestern. Any deviations from these wind conditions are caused by transitional weather systems [Thomson, 1981].

The western coast of Vancouver Island has a very energetic wave climate, causing it to be a viable source of wave energy for communities located along the coastline. The wave climate along the coastline is highly variable in accordance to the oceanic winds, with the direction of the wave swell corresponding to the localized wind direction and the sea typically coming from the northwest or southwest based on the time of year. Wave sea and swell in the offshore regions tend to be highest in the fall and winter when the duration, strength, and fetch of the wind is highest. During the summer, when the wind comes from the northwest the wave heights are much lower due to the limited fetch. The roughest season occurs from October to March when the sea can be expected to exceed wave heights of 1.5m 30% of the time along the coast and swells exceed 1.5m approximately 25%. This contrasts sharply to the calm summer season when the seas and swells exceed 1.5m only 15% and 10% of the time, respectively [Thomson, 1981].

6 SWAN Model

6.1 Introduction

The SWAN model is a third-generation wave model developed by Delft University for the modeling of wave parameters in coastal regions, lakes, and estuaries based on regional wind, bathymetric, and current conditions. SWAN was selected for use in this thesis due to its wide commercial use which would allow for the findings of this study to be applicable to industry.

Third-generation wave models can calculate explicit representations of the source terms and the step-by-step evolution of the wave spectrum without assumptions of the spectral shape [Mackay and Hassan, 2012]. This section describes the SWAN formulation and equations which were obtained from the SWAN user and technical manuals [2013] to explain the different key parameters in the SWAN model.

6.2 SWAN Model Description

The basic principle of the SWAN model is the spectral action balance equation which calculates the transfer, dissipation, and input of energy into the wave spectra. This section gives the equations governing each of these different wave interactions.

6.2.1 Spectral Action Balance

The SWAN numerical model uses the spectral action balance equation to show the evolution of the action density, $N = E/\sigma$, in space, and the distribution of the wave energy over frequency and direction [Mei, 1983; Komen *et al.* 1994]:

$$\frac{\partial N}{\partial t} + \nabla_{\bar{x}} \cdot \left[\left(\bar{c}_g + \bar{U}\right)N\right] + \frac{\partial c_\sigma N}{\partial \sigma} + \frac{\partial c_\theta N}{\partial \theta} = \frac{S_{tot}}{\sigma} \qquad [6.1]$$

where the wave propagation velocities within a Cartesian framework and in the spectral space are obtained from [Whiteham, 1974; Mei, 1983]:

$$\frac{d\bar{x}}{dt} = \left(c_x, c_y\right) = \bar{c}_g + \bar{u} = \frac{1}{2}\left(1 + \frac{2\left|\bar{k}\right|d}{\sinh\left(2\left|\bar{k}\right|d\right)}\right)\frac{\sigma\bar{k}}{\left|\bar{k}\right|^2} + \bar{u} \qquad [6.2]$$

$$\frac{d\sigma}{dt} = c_\sigma = \frac{\partial\sigma}{\partial d}\left(\frac{\partial d}{\partial t} + \bar{u}\cdot\nabla_{\bar{x}} d\right) - c_g \bar{k}\frac{\partial\bar{u}}{\partial s} \quad [6.3]$$

$$\frac{d\theta}{dt} = c_\theta = -\frac{1}{k}\left(\frac{\partial\sigma}{\partial d}\frac{\partial d}{\partial m} + \bar{k}\cdot\frac{\partial\bar{u}}{\partial m}\right) \quad [6.4]$$

where c_x, and c_y are the propagation velocities of the wave energy in space, and c_σ and c_θ are the propagation in spectral space. In these equations d is the water depth, s is the space co–ordinate in the wave propagation direction and m is the co–ordinate perpendicular to s, c_g is the group velocity, and k is the wave number.

In equation 6.1 the left–hand side of the equation controls the kinematics while the right-hand side controls the energy sources and sinks. This equation can be modified for either Cartesian or spherical co–ordinates depending on the model. The current study uses spherical coordinates, however the solution for both are presented below:

$$\frac{\partial N}{\partial t} + \frac{\partial c_x N}{\partial x} + \frac{\partial c_y N}{\partial y} + \frac{\partial c_\sigma N}{\partial \sigma} + \frac{\partial c_\theta N}{\partial \theta} = \frac{S_{tot}}{\sigma} \quad [6.5]$$

and,

$$\frac{\partial \tilde{N}}{\partial t} + \frac{\partial c_\lambda \tilde{N}}{\partial \lambda} + \frac{\partial c_\varphi \tilde{N}}{\partial \varphi} + \frac{\partial c_\sigma \tilde{N}}{\partial \sigma} + \frac{\partial \tilde{c}_\theta \tilde{N}}{\partial \theta} = \frac{S_{tot}}{\sigma} \quad [6.6]$$

with $\tilde{N}$ being the action density with respect to the longitude λ and latitude φ. For spherical co–ordinates the propagation velocities become:

$$dx = R\cos\varphi d\lambda \quad [6.7]$$

$$dy = Rd\varphi \quad [6.8]$$

$$d\lambda = c_\lambda = \frac{1}{R\cos\varphi}\left[\frac{1}{2}\left(1 + \frac{2|\bar{k}|d}{\sinh(2|\bar{k}|d)}\right)\frac{\sigma\bar{k}\cos\theta}{|\bar{k}|^2} + u_\lambda\right] \quad [6.9]$$

$$\frac{d\varphi}{dt} = c_\varphi = \frac{1}{R}\left[\frac{1}{2}\left(1 + \frac{2|\bar{k}|d}{\sinh(2|\bar{k}|d)}\right)\frac{\sigma\bar{k}\cos\theta}{|\bar{k}|^2} + u_\varphi\right] \quad [6.10]$$

where R is the radius of the earth.

6.2.1 Sources and Sinks

In equation 6.1 S_{tot} represents the model sources and sinks:

$$S_{tot} = S_{in} + S_{nl3} + S_{nl4} + S_{ds,w} + S_{ds,b} + S_{ds,br} \qquad [6.11]$$

These represent the dissipation and input of energy into the system through physical processes such as wind, or wave breaking, and the shifting of energy due to wave interaction.

6.2.1.1 Wind Input – S_{in}

The model wind input represents the growth of the waves due to wind pressure. This transfer of energy is described using a resonance mechanism [Phillips, 1957] and a feed-back mechanism [Miles, 1957]. The resonance mechanism represents the waves resonance with wind-induced pressure fluctuations. If the harmonic pressure waves remain in phase with the free surface waves, then the wind energy is transferred from the pressure wave to the surface wave. This mechanism contributes to the initial stage of wave growth and varies linearly with time. The feed-back mechanism is a result of the initial resonance mechanism which has distorted the wind profile just above the water surface. This distortion results in increased pressure on the wind ward side of the wave crest and less pressure on the lee side, allowing the transfer of energy into the waves. This energy transfer is proportional to the energy of the surface wave, so the wave grows exponentially. These mechanisms are represented within the SWAN model by:

$$S_{in}(\sigma,\theta) = A + BE(\sigma,\theta) \qquad [6.12]$$

where A is the linear growth and BE represents the exponential growth. The wind input for the saturation–based model used in this study is based on Yan (1987):

$$\beta_{fit} = D\left(\frac{u_*}{c}\right)^2 \cos(\theta-\alpha) + E\left(\frac{u_*}{c}\right)\cos(\theta-\alpha) + F\cos(\theta-\alpha) + H \qquad [6.13]$$

where β_{fit} replaces B in equation 6.12, and $\frac{u_*}{c} \approx 0.036$. The parameters D, E, F, and H are 4.0x10^{-2}, 5.52x10^{-3}, 5.2x10^{-5}, and –3.02x10^{-4}, respectively.

6.2.1.2 *Triad Wave Interactions* – S_{nl3}

Triad wave interactions are a shallow water three-wave interaction that result in the transfer of energy across the wave spectrum. Triad wave interactions are important for steep waves, which is why they are considered a shallow water process (as shallower water results in the shoaling of waves). This interaction transfers energy to higher frequencies, resulting in higher harmonics [Beji and Battkes, 1993]. This energy transfer can be done over a relatively short distance but can result in a dramatic change in the shape of the wave spectra, potentially transforming single peaked spectra into multi-peaked spectra. The SWAN model triad interactions use the Lumped Triad Approximation (LTA) of Eldeberky (1996) for each spectral direction:

$$S_{nl3}(\sigma,\theta) = S_{nl3}^{-}(\sigma,\theta) + S_{nl3}^{+}(\sigma,\theta) \qquad [6.14]$$

where

$$S_{nl3}^{+}(\sigma,\theta) = \max\left[0, \alpha_{EB} 2\pi c c_g J^2 |\sin\beta| \{E^2(\sigma/2,\theta) - 2E(\sigma/2,\theta)E(\sigma,\theta)\}\right] \qquad [6.15]$$

and,

$$S_{nl3}^{-}(\sigma,\theta) = -2S_{nl3}^{+}(2\sigma,\theta) \qquad [6.16]$$

In these equations α_{EB} is a tunable proportionality coefficient with a default model value of 0.1, and β is approximated using:

$$\beta = -\frac{\pi}{2} + \frac{\pi}{2}\tanh\left(\frac{0.2}{Ur}\right) \qquad [6.17]$$

with the Ursell number being:

$$Ur = \frac{g}{8\sqrt{2}\pi^2}\frac{H_S T_{m01}^2}{d^2} \qquad [6.18]$$

with H_s being the significant wave height, and T_{m01} being the mean wave period. It should be noted that triad interactions are only calculated for when the Ursell number is between 0 and 1. Finally, the interaction coefficient J (from equation 6.15 is [Madsen and Sorensen, 1993]:

$$J = \frac{k_{\sigma/2}^2\left(gd+2c_{\sigma/2}^2\right)}{k_\sigma d\left(gs+\frac{2}{15}gd^3k_\sigma^2-\frac{2}{5}\sigma^2 d^2\right)} \quad [6.19]$$

6.2.1.3 *Quadruplet Wave Interactions* – S_{nl4}

Quadruplet wave interactions are dominant in deep water. This interaction transfers the wave energy from the spectral peak to lower frequencies (resulting in the peak frequency being lowered), and to higher frequencies (where the energy is then dissipated by whitecapping). The method used in the current study is the Discrete Interaction Approximation (DIA) method which is considered a relatively crude approximation of the Boltzmann integral [Hasselmann *et al.*, 1985 and adapted by Tolman]. With the DIA method two quadruplet wave number configurations are considered with the frequencies:

$$\sigma_1 = \sigma_2 = \sigma,\ \sigma_3 = \sigma(1+\lambda) = \sigma^+,\ \sigma_4 = \sigma(1-\lambda) = \sigma^- \quad [6.20]$$

where λ has a default value of 0.25. The wave numbers with frequency σ_3 and σ_4 lie at an angle of $\theta_3 = -11.48°$ and $\theta_4 = 33.56°$ with respect to the angle of the wave numbers with frequencies σ_1 and σ_2. The second quadruplet is a mirror image to the first.

Within this approximation the source term is given by:

$$S_{nl4}(\sigma,\theta) = S_{nl4}^*(\sigma,\theta) + S_{nl4}^{**}(\sigma,\theta) \quad [6.21]$$

where S_{nl4}^* refers to the first quadruplet and S_{nl4}^{**} refers to the second quadruplet, the expressions for these two expressions are identical except for the direction. This method exchanges the wave variance at all three wave number vectors involved in the quadruplet wave number configuration. The rate of change of the wave variance due to quadruplet interactions is given as:

$$\begin{pmatrix}\delta S_{nl4}^*(\sigma,\theta)\\ \delta S_{nl4}^*(\sigma,\theta)\\ \delta S_{nl4}^*(\sigma,\theta)\end{pmatrix} = \begin{pmatrix}2\\-1\\-1\end{pmatrix} C_{nl4}(2\pi)^2 g^{-4}\left(\frac{\sigma}{2\pi}\right)^{11} \times$$

$$\left[E^2(\sigma,\theta)\left\{\frac{E(\sigma^+,\theta^+)}{(1+\lambda)^4} + \frac{E(\sigma^-,\theta^-)}{(1-\lambda)^4}\right\} - 2\frac{E(\sigma,\theta)E(\sigma^+,\theta^+)E(\sigma^-,\theta^-)}{(1-\lambda^2)^4}\right] \quad [6.22]$$

where C_{nl4} is equal to $3x10^7$. In equation 6.22 the wave variance densities at the frequency–direction bins $E(\sigma^+,\theta^+)$ and $E(\sigma^-,\theta^-)$ are obtained through the bi–linear interpolation of the four surrounding frequency–direction bins. Likewise, the rate of change of the variance density is distributed between the four surrounding bins using the same weights used in the interpolation.

6.2.1.4 *Whitecapping Dissipation* – $S_{ds,w}$

Whitecapping is the breaking of the wave crests due to wind forcing; within the SWAN model it is controlled by the wave steepness. This is the largest source of energy dissipation within deep water. The whitecapping equations used in the current research is based on the saturation–based model proposed by Van der Westhuysen *et al.* (2007a) and Van der Westhuysen (2007b) which was adapted from the equations of Alves and Banner (2003):

$$S_{ds.w}(\sigma,\theta) = f_{br}(\sigma)S_{ds,break} + [1 - f_{br}(\sigma)]S_{ds,non-break} \quad [6.23]$$

in which $S_{ds,break}$ is the contribution to the dissipation through wave breaking:

$$S_{ds,break}(\sigma,\theta) = -C'_{ds}\left(\frac{B(k)}{B_r}\right)^{p/2}(\tanh(kh))^{(2-p_o)/4}\sqrt{gk}E(\sigma,\theta) \quad [6.24]$$

where the density function $B(k)$ is the azimuthal–integrated spectral saturation which is calculated using:

$$B(k) = \int_0^{2\pi} c_g k^3 E\,(\sigma,\theta)d\theta \quad [6.25]$$

and B_r is equal to $1.75x10^{-3}$ which is the threshold saturation level. C'_{ds} is the proportionality coefficient which is equal to $5x10^{-5}$. In cases where $B(k) > B_r$ the waves are breaking and the exponent p is equal to p_0 which is equal to:

$$p_0(\sigma) = 3 + \tanh\left[w(\frac{u_*}{C} - 0.1)\right] \quad [6.26]$$

In cases where there is no breaking p is equal to 0. To achieve a smooth transition an equation provided by Alves and Banner (2003) is used:

$$p = \frac{p_0}{2} + \frac{p_0}{2}\tanh\left[10\left(\sqrt{\frac{B(k)}{B_r}}\right) - 1\right] \qquad [6.27]$$

From equation 6.23 $S_{ds,non-breaking}$ is the dissipation caused by other means than breaking such as turbulence and is given by the whitecapping formula [Hasselmann, 1974]:

$$S_{ds,w}(\sigma,\theta) = -\Gamma\tilde{\sigma}\frac{k}{\tilde{k}}E(\sigma,\theta) \qquad [6.28]$$

where $\tilde{\sigma}$ and $\tilde{k}$ are the mean frequency and the mean wave number, respectively, while Γ is a steepness dependent parameter:

$$\Gamma = \Gamma_{KJ} = C_{ds}\left((1-\delta) + \delta\frac{k}{\tilde{k}}\right)\left(\frac{\tilde{s}}{\tilde{s}_{PM}}\right)^p \qquad [6.29]$$

where,

$$\tilde{s}_{PM} = \sqrt{3.02 \times 10^{-3}} \qquad [6.30]$$

$$\tilde{s} = \tilde{k}\sqrt{E_{tot}} \qquad [6.31]$$

and,

$$\tilde{\sigma} = \left(E_{tot}^{-1}\int_0^{2\pi}\int_0^{\infty}\frac{1}{\sigma}E(\sigma,\theta)d\sigma d\theta\right)^{-1} \qquad [6.32]$$

$$\tilde{k} = \left(E_{tot}^{-1}\int_0^{2\pi}\int_0^{\infty}\frac{1}{\sqrt{k}}E(\sigma,\theta)d\sigma d\theta\right)^{-2} \qquad [6.33]$$

$$E_{tot} = \int_0^{2\pi}\int_0^{\infty}E(\sigma,\theta)d\sigma d\theta \qquad [6.34]$$

From equation 6.23:

$$f_{br}(\sigma) = \frac{1}{2} + \frac{1}{2}\tanh\left[10\left(\sqrt{\frac{B(k)}{B_r}}\right) - 1\right] \qquad [6.35]$$

6.2.1.5 *Dissipation due to Bottom Friction* – $S_{ds,b}$

Wave dissipation as a result of bottom friction is considered important in shallow water. This is a result of the interaction of the orbital movement of the water particles (induced by the surface waves) with the sea floor. The dissipation due to bottom friction used in this research was determined using the empirical model of JONSWAP [Hasselmann *et al.,* 1973] which can be expressed as:

$$S_{ds,b} = -C_b \frac{\sigma^2}{g^2(\sinh kd)^2} E(\sigma,\theta) \qquad [6.36]$$

where, C_b is equal to 0.038m^2/s^3 for swell conditions and 0.067m^2/s^3 for wind sea conditions.

6.2.1.6 *Dissipation due to Depth–Induced Wave Breaking* – $S_{ds,br}$

Similar to dissipation due to bottom friction, dissipation as a result of depth-induced wave breaking is also a shallow water process. As the surface waves propagate into shallower water, shoaling results in an increase in wave height. Once a critical ratio of wave height over water depth is exceeded the waves will begin to break, resulting in a rapid dissipation of the wave energy. In extreme shallow water this process becomes dominant over all others.

The energy dissipation due to depth–induced breaking is modeled in SWAN using the bore–based model of Battjes and Janssen (1978) including the expression presented by Elderberky and Battjes (1995) to include the spectral directions, this equation is:

$$S_{ds,br}(\sigma,\theta) = \frac{D_{tot}}{E_{tot}} E(\sigma,\theta) \qquad [6.37]$$

where D_{tot} is the mean rate of energy dissipation per unit horizontal area caused by wave breaking:

$$D_{tot} = \alpha_{BJ} Q_b \tilde{\sigma} \frac{H_{max}^2}{8\pi} \qquad [6.38]$$

where α_{BJ} is equal to 1 and the fraction of wave breaking Q_b is:

$$Q_b = \begin{cases} 0, & for\ \beta \leq 0.2 \\ Q_0 - \beta^2 \dfrac{Q_0 - {exp(Q_0-1)}/{\beta^2}}{\beta^2 - {exp(Q_0-1)}/{\beta^2}}, & for\ 0.2 > \beta < 1 \\ 1, & for\ \beta \geq 1 \end{cases} \qquad [6.39]$$

where $\beta = H_{rms}/H_{max}$ for $\beta \leq 0.5$, $Q_0 = 0$ and for $0.5 < \beta \leq 1$, $Q_0 = (2\beta - 1)^2$. H_{max} is the maximum wave height which is determined by $H_{max} = \gamma d$, where γ is the breaker parameter.

7 Methodology

The pilot application of the IEC–TS for wave energy resource assessments was conducted in the western coast of Canada near the coastal community of Ucluelet, British Columbia. This project involved the comparison of the modeled wave energy and wave climate to measured observations within the study region. This was completed for all classes of assessment based on the recommendations proposed within the IEC–TS. In addition to the comparison of the baseline modeled and observed wave resources a large–scale sensitivity analysis was conducted to determine the largest sources of error and uncertainty within the resource assessment procedure and requirements. This section describes the measurements obtained for the validation and comparison of the model, and the baseline model used for the three different classes of assessment.

7.1 Measurements

The validation of the numerical model was completed through the comparison of the modeled wave climate with measured observations obtained from wave buoys located within the model domain. The main validation source was from a directional wave buoy deployed by the West Coast Wave Initiative [Buckham, 2013], which is a research effort led by the University of Victoria, at the "Beverley" Buoy Station (Latitude: 48°52.82', Longitude: 125°3.08'), located in approximately 45m water depth, 6km offshore from the town of Ucluelet. Two secondary wave buoys were also used for comparison; the first buoy is located at Neah Bay (deployed by NOAA), and the second buoy is at La Perouse (deployed by Environment Canada). A full description of the instrumentation and deployment periods can be seen in Table 7.1, while the locations of the buoys in reference to the reconnaissance and feasibility model domains can be seen in Figure 7.1.

Table 7.1 – Deployment Period for Wave Instrumentation

Site	Location	Platform/Payload	Deployment	Sampling Interval (hrs)
Beverley	48° 56.23' 125° 33.37'	Axys Watchmate	2009 - 2014	3
La Perouse	48° 50.10' 125° 59.88'	3m Discus /AE	1988 - 2018	1
Neah Bay	48° 29.64' 124° 43.68'	3m Discus /AMPS	2004 - 2018	0.5 - 1

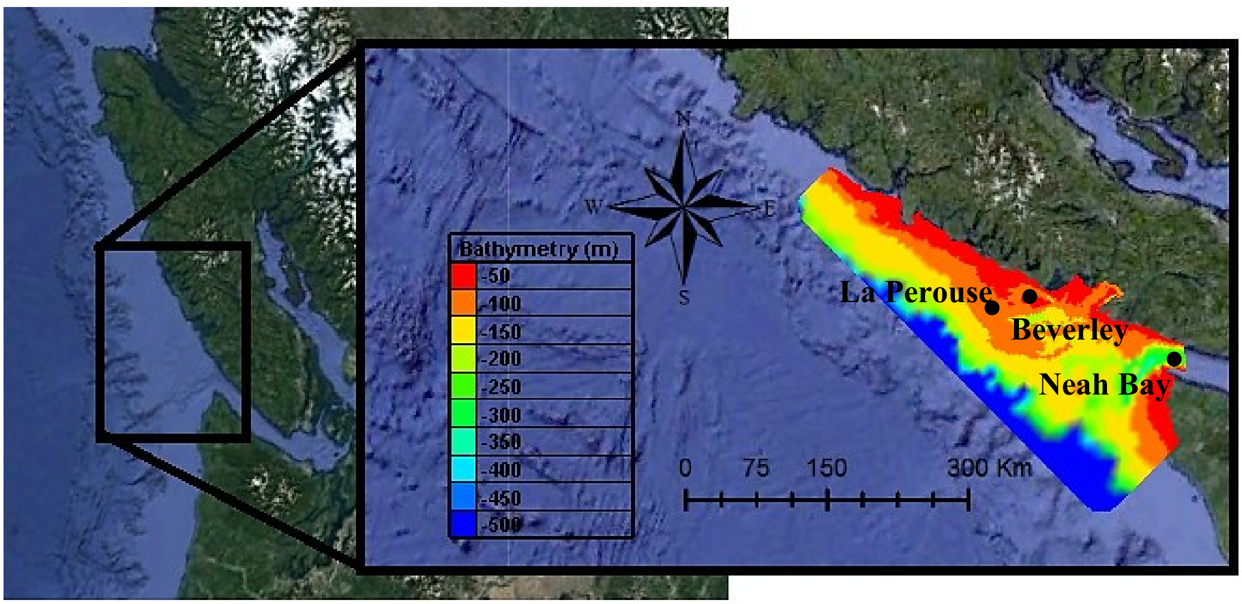

Figure 7.1 – Study Domain and Buoy Locations for Reconnaissance and Feasibility Class Assessments

The deployment of the Beverley Buoy commenced in 2009 and is still ongoing; however, the buoy was not consistently operational during its deployment period resulting in large gaps in the measured wave spectrums. The longest continuous measurement campaign used in this research from the Beverley Buoy is from 2013–2014. This buoy is a fully–directional wave buoy that obtains the wave spectrum at its location, allowing for the wave parameters to be calculated using the same formulations as provided by the IEC–TS for direct comparison with all required model parameters.

The buoys deployed at Neah Bay and La Perouse were operational starting in 2004 and 1988, respectively, and are still active to this date. The measurements obtained by these buoys are not the full set of wave parameters required for validation of the numerical model, as such they were used as secondary validation points to ensure that the modeled wave heights were accurate across multiple locations within the domain. Due to the size of the study domain for the design class assessment both the Neah Bay and La Perouse were outside the boundaries, therefore these buoys were only used for the reconnaissance and feasibility classes.

The bathymetric data used for this project was consolidated by the National Research Council of Canada (NRC) through the combination of bathymetric charts and datasets, see Figure 7.2 obtained from the following three sources:

1. Digital hydrographic dataset purchased from the Canadian Hydrographic Service (CHS);
2. Digital and paper nautical charts purchased from the CHS;
3. Digital dataset obtained from a GIS databased maintained by the Government of British Columbia.

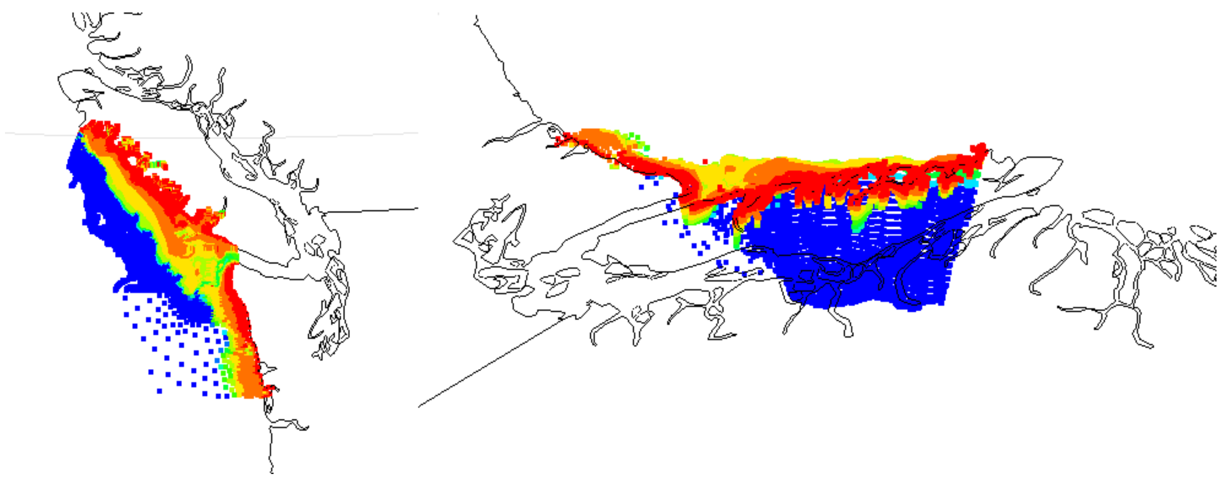

Figure 7.2 – Bathymetric Dataset for SWAN Model Development

7.2 Wave Propagation Models

The project required the development of three different core SWAN models based on the requirements set out for each stage of the assessment by the IEC–TS. These models were used for the prediction of the temporal and spatial variation in the wave climate over a period of 10 years (2005 to 2014). All the SWAN models feature an unstructured grid (developed using Blue Kenue [CHC–Canadian Hydraulics Centre, 2011]) and were run in non–stationary mode in one–month periods. Due to the availability of bathymetric datasets, mentioned in Chapter 7.1, all of the models utilized the same bathymetry despite recommendations to increase the bathymetry resolution for the increasing assessment stages.

7.2.1 Boundary Conditions

The model boundary conditions for all classes of assessment were derived from the WaveWatch–III (WW3) global wave hindcast database, created by the Marine Modeling Branch of the National Oceanographic and Atmospheric Administration (NOAA–MMB) [NOAA; Tolman, 2014]. This is a state-of-the-art hindcast which provides parametric, partitioned, and spectral modeled wave data at high resolution globally.

NOAA provides validation for the WaveWatch-III model, as shown in Figure 7.3 and Figure 7.4. From this validation it was noted that the wave model could have significantly different accuracy in terms of the significant wave heights, wind speed and peak period when compared to NOAA buoys. It was also noted that WaveWatch-III nodes located farther offshore tended to have greater accuracy than those located in close proximity to the shoreline. The model is less able to consistently represent the peak period. The accuracy of the WaveWatch-III model will directly impact the accuracy of the current model as the WW3 model is being used to force the boundary conditions and the wind within the model.

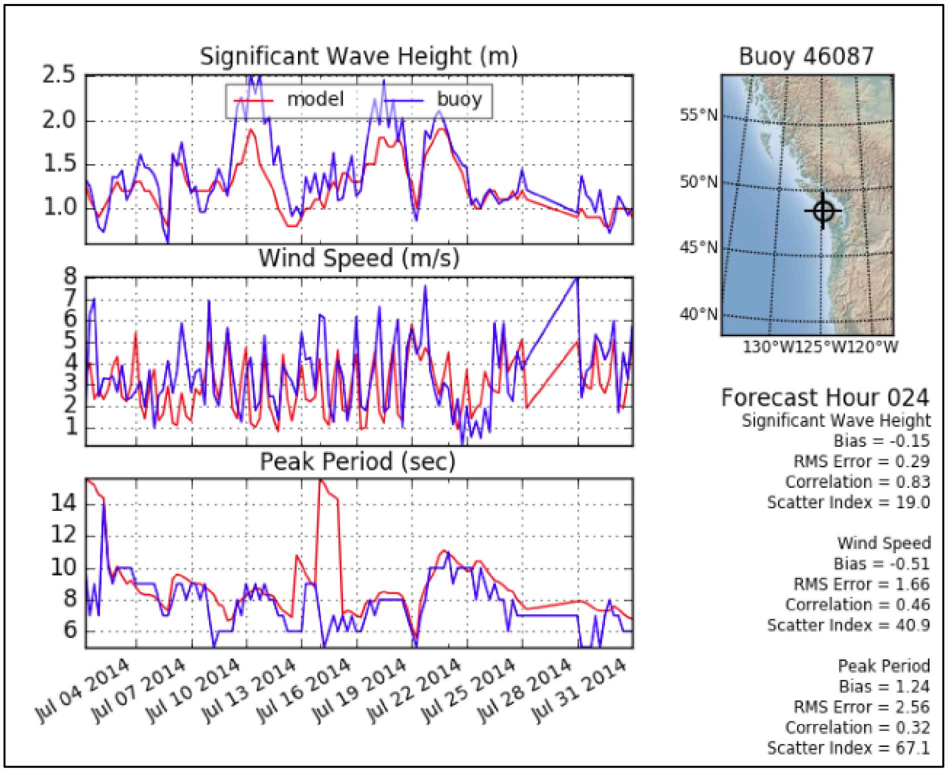

Figure 7.3 – Wave Watch-III Validation for Neah Bay July 2014 (NOAA)

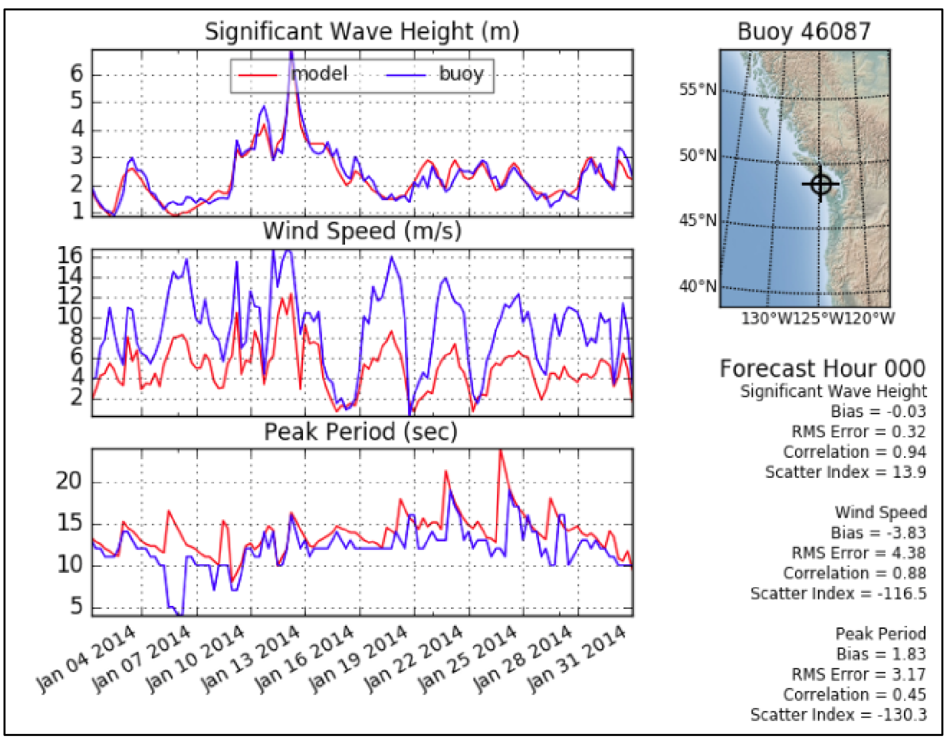

Figure 7.4 – Wave Watch III-Validation for Neah Bay January 2014 (NOAA)

For the reconnaissance class assessment this hindcast was used to force the model along its lateral and offshore boundary in three locations, as shown in Figure 7.5. These boundary conditions were forced using parametrized waves which were defined in terms of their significant wave height, peak wave period, and dominant wave direction. An assumed constant directional spreading factor based on the $\cos^S(\theta - \theta_o)$ formulation was also provided. This was interpolated across the boundary by the SWAN model and was used to develop a JONSWAP spectrum within the model to represent the waves coming in across the entire boundary. Due to the simplified nature of the parametrized waves, which are only able represent to a single wave propagating along the boundary at each location), this boundary condition is only considered acceptable for use at the reconnaissance class assessment. As per the IEC-TS boundary conditions were forced at three-hour time intervals. The advantages of this form of boundary condition are its ease of use, and the fact that the parameterized values are easy to obtain from global hindcast models and most locations.

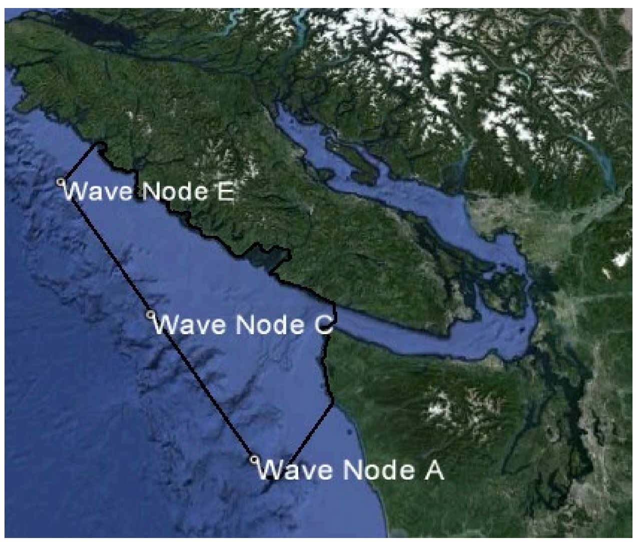

Figure 7.5 – Class 1– Reconnaissance and Class 2 – Feasibility Boundary Condition Locations

The boundary conditions at the feasibility class assessment were defined at the same locations used for the reconnaissance class, Figure 7.5. However, due to the requirements of the IEC–TS the feasibility class boundary conditions were not parametric, but rather 2D wave spectra developed from the partitioned wave states made available by WW3. The partitioned wave states represent the waves at each point as a group of waves (as opposed to the single wave used for the parametric conditions). These waves have distinct wave heights, periods and directions allowing the differentiation between swell and sea waves, allowing for the construction of more realistic boundary conditions. Wave spectra were constructed for each individual wave state using a directional spreading factor based on the cos2s formulation and a JONSWAP spectral shape with an assumed gamma value of 1 for wind sea states and 5 for swell. The individual wave spectra for each partitioned wave state were than combined, resulting in a realistic representation of the wave climate at each location. As per the IEC-TS boundary conditions were forced at three-hour time intervals.

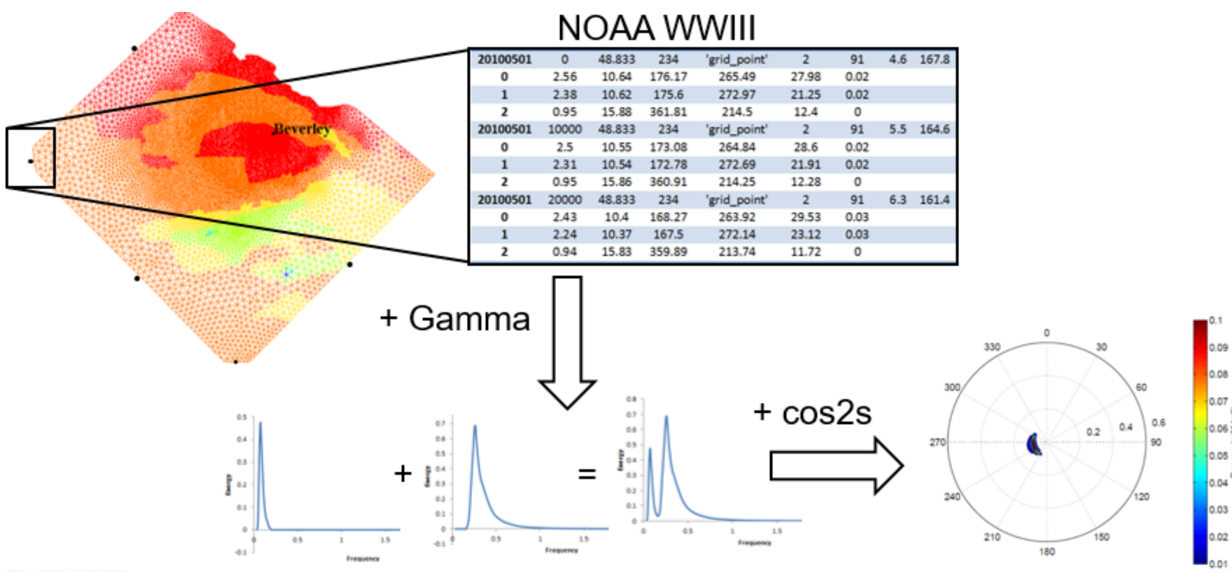

Figure 7.6 – Converting Partitioned NOAA WaveWatch-III Data to Wave Spectra

The boundary conditions for the design class assessment were applied at five locations along the boundary, see Figure 7.7, and were represented using 2D wave spectra. Unlike the feasibility class assessment WW3 an assumed JONSWAP factor was not used, instead the wave spectra obtained from WW3 at Node B was partitioned into its respective sea states and JONSWAP gamma factors were calibrated for each of the different sea states based on their wave height and energy period. These calibrated factors were then applied to the partitioned wave data at all other boundary locations within the domain. While not exact, this method provided a more accurate estimation of the wave climate at the location of interest when compared to the feasibility method. However, it is significantly more computationally expensive. The directional spread of the wave states was based on the cos2s formulation as with the feasibility class assessment. The boundary conditions for this class of assessment were forced at one-hour intervals, as per the IEC-TS, between 2010 and 2014; however, prior to 2010 the partitioned wave data was only provided at three-hour intervals and so the temporal resolution was decreased accordingly.

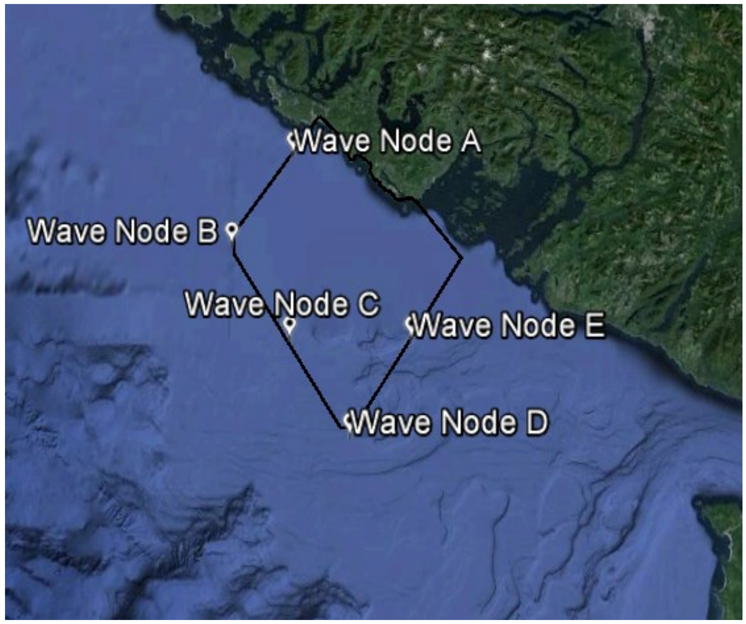

Figure 7.7 – Class 3 – Design Boundary Condition Locations

7.2.2 Wind Conditions

The model wind conditions for all classes of assessment were also obtained from the WaveWatch–III (WW3) global wave hindcast database [NOAA; Tolman, 2014]. The reconnaissance class model used a spatially constant wind field across the domain that varied at three-hour time intervals. This spatial resolution was selected due to the relatively low wind resolution required by the IEC–TS for this stage of assessment when compared to the scale of the model domain. For the feasibility class assessment, the model wind resolution was specified on a 40km by 60km rectangular grid, see Figure 7.8. For both the reconnaissance and feasibility class assessments the wind was provided at three-hour time intervals as per the IEC-TS requirements.

Figure 7.8 – Class 2 – Feasibility Class Wind Grid

Finally, for the design class assessment the wind was specified using a 22km rectangular grid, see Figure 7.9, resulting in a total of nine wind nodes in accordance with the recommendations by the IEC–TS. All model inputs were specified at one hour time intervals from 2010 to 2014, however, prior to 2010 the partitioned wave data from WW3 was only available at three-hour time scales, and so the temporal resolution had to be decreased for this time period.

Figure 7.9 – Class 3 – Design Wind Resolution

7.2.3 Reconnaissance

The mesh used for the reconnaissance class assessment, shown in Figure 7.10, was developed to cover a span of 280km along the Pacific coastline of Vancouver Island, extending up to approximately 90km offshore. This model contains roughly 4,300 nodes with a resolution of 1,500m at the location of interest (the main validation site Beverley Buoy) which is within the bounds set by the IEC–TS.

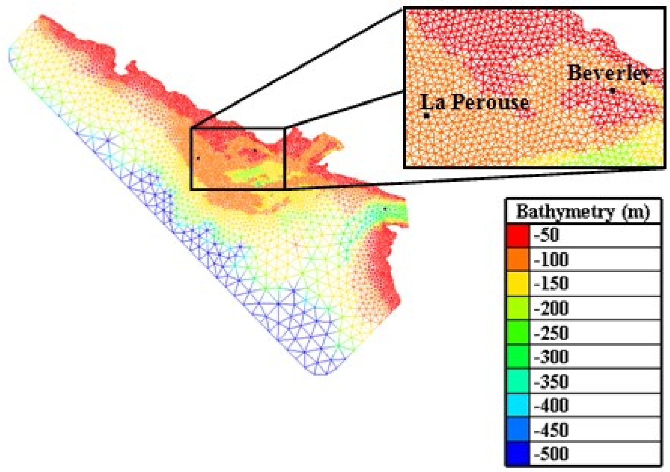

Figure 7.10 – Class 1– Reconnaissance SWAN Model

The wave spectra within the SWAN model were resolved using the minimum suggested resolution of the IEC–TS with 25 frequency bins (ranging up to 2Hz) and 24 directional bins. The frequency bins were calculated based on a logarithmic distribution while the directional bins were defined at constant intervals. All model inputs were specified at three-hour intervals as per the IEC–TS. For the baseline reconnaissance class resource assessment, the bottom friction and depth–induced wave breaking parameters were not included as they are not requirements for this class. All other physical parameters were included as required.

7.2.4 Feasibility

The feasibility class assessment used a similar model domain as for the reconnaissance class assessment; however, in order to comply with the requirements set out by the IEC–TS the feasibility class uses a denser mesh resolution, resulting in approximately 16,000 nodes with a resolution of 500m at the site of interest (Beverley Buoy), this finer mesh resolution is depicted in Figure 7.11.

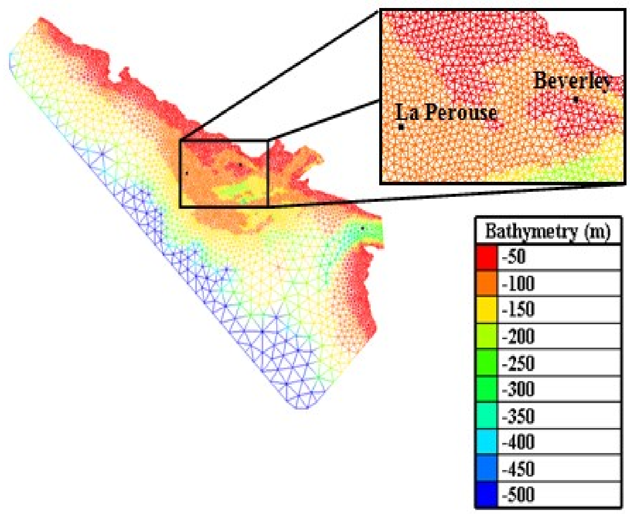

Figure 7.11 – Class 2 – Feasibility SWAN Model

The wave spectra within the SWAN model were resolved at higher resolution than required by the IEC–TS with 41 frequency bins (ranging up to 2Hz) and 36 directional bins. The frequency bins were calculated based on a logarithmic distribution, while the directional bins were distribution linearly. All physical processes were considered for this class of assessment as required by the IEC–TS.

7.2.5 Design

The design class resource assessment was conducted over a smaller region than both the feasibility and reconnaissance class assessments as recommended by the IEC–TS, with dimensions of 45km x40km. This model used a higher resolution mesh, resulting in approximately 45,000 nodes and a 50m grid located in a 3.5km radius around the site of interest, see Figure 7.12.

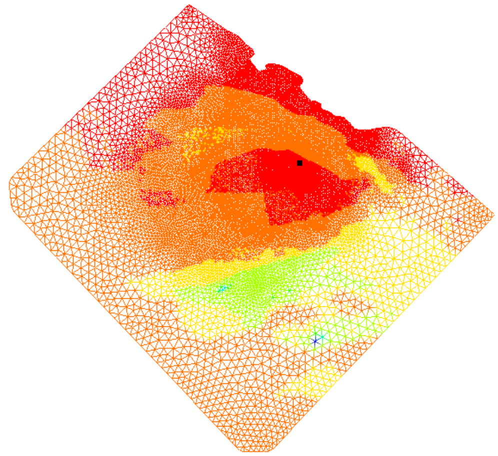

Figure 7.12 – Class 3 – Design SWAN Model

Within the SWAN model the directional wave spectra was defined using 41 frequency bins (ranging up to 2Hz) with 48 directional bins. As with the other classes of assessment, the frequency bins were varied based on a logarithmic distribution, while the directional bins were constant in size. As per the IEC–TS all physical processes were considered at this class of assessment.

8 Validation of the IEC Specification

The validation of the IEC–TS was completed through a one-year (2013 – 2014) sensitivity analysis for key parameters to determine the uncertainty within the IEC–TS and to examine whether its requirements are too stringent or lenient. This sensitivity analysis was conducted on a number of parameters to determine their impact, including: the model physical processes, the mesh resolution, the spectral resolution, the wind resolution, and the model boundary conditions. Parameters which may be specific to the model software such as coefficients or formulations were not analysed as they would not be relevant to all users of the IEC-TS, it was assumed that the users would use best judgement or the default model values.

Analysis was completed by comparing the monthly and yearly mean values with those obtained at the Beverley Buoy site for the same period, and by performing a statistical analysis on the results with commonly used statistical parameters such as the normalized mean bias, coefficient of determination, scatter index, and Cv(RMSE) based on the formulation provided below, and using the IEC–TS specified validation criteria: the systematic error and random error. It should be noted that the scatter index has two different definitions, one is calculated with the standard deviation as shown in equation 8.3, another is calculated using the root mean square error, and is analogous to the normalized root mean square error, equation 8.4, both methods can be found in literature.

$$Normalized\ Mean\ Bias\ (NB) = \frac{\sum_{i=1}^{N}(M_i - O_i)}{\sum_{i=1}^{N} O_i}\ x\ 100 = \left(\frac{\bar{M}}{\bar{O}} - 1\right) x\ 100 \qquad [8.1]$$

$$Coefficient\ of\ Determination\ (R^2) = \left(\frac{\sum_{i=1}^{N}(M_i - \bar{M})(O_i - \bar{O})}{\left\{\sum_{i=1}^{N}(M_i - \bar{M})^2 \sum_{i=1}^{N}(O_i - \bar{O})^2\right\}^{1/2}}\right)^2 \qquad [8.2]$$

$$Scatter\ Index\ (SI) = \frac{STD_{error}}{\bar{O}} \qquad [8.3]$$

$$Normalized\ Root\ Mean\ Square\ (CvRMSE) = \frac{RMSE_{error}}{\bar{O}} \qquad [8.4]$$

where M_i and O_i are values at modeled and observed times i, N is number of time samples, and $\bar{M} = \frac{1}{N}\sum_{i=i}^{N} M_i$, while $\bar{O} = \frac{1}{N}\sum_{i=i}^{N} O_i$.

The root mean square error in equation 8.4 is calculated using:

$$RMSE = \sqrt{\frac{\sum_{i=1}^{N}(O_i - M_i)^2}{N}} \quad [8.5]$$

and the standard deviation in equation 8.3 is calculated using:

$$STD = \sqrt{\frac{\sum_{i=1}^{N}(error_i - \mu)^2}{N}} \quad [8.6]$$

which is the standard deviation of the differences between the modeled and observed values.

8.1 Baseline Validation

This section shows the baseline comparison between the numerical and measured wave resource assessment for the period of March 2013 to April 2014. It should be noted that the results from October 29th to November 13th, 2013, were not included in the assessment due to errors with the NOAA WW3 wind.

When examining the baseline statistics presented in Table 8.1 it was observed that the reconnaissance class assessment had the lowest accuracy of the three classes, though it did still have reasonable R^2 values for the wave height and wave power. However, the normalized errors and the biases are quite large, which was expected as this class of assessment was not intended to be extremely accurate.

Table 8.1 – Baseline Reconnaissance Class Statistics for 2013-2014

A) Wave Height

Reconnaissance		R^2	NB (%)	CvRMSE (%)	SI (%)
	Baseline	0.74	21.84	44.26	38.50

B) Wave Power

Reconnaissance		R^2	NB (%)	CvRMSE (%)	SI (%)
	Baseline	0.71	55.75	133.72	121.57

C) Energy Period

Reconnaissance		R^2	NB (%)	CvRMSE (%)	SI (%)
	Baseline	0.37	15.13	32.39	28.65

Table 8.2 – Baseline, Feasibility, and Design Class Statistics for 2013-2014

A) Wave Height

Feasibility	R^2	NB (%)	CvRMSE (%)	SI (%)	*Design*	R^2	NB (%)	CvRMSE (%)	SI (%)
Baseline	0.88	0.26	21.34	21.34	Baseline	0.86	6.65	24.37	23.44

B) Wave Power

Feasibility	R^2	NB (%)	CvRMSE (%)	SI (%)	*Design*	R^2	NB (%)	CvRMSE (%)	SI (%)
Baseline	0.80	37.40	116.35	110.2	Baseline	0.78	32.12	105.64	100.32

C) Wave Energy Period

Feasibility	R^2	NB (%)	CvRMSE (%)	SI (%)	*Design*	R^2	NB (%)	CvRMSE (%)	SI (%)
Baseline	0.49	19.75	26.85	18.19	Baseline	0.63	12.36	18.67	13.99

D) Spectral Width

Feasibility	R^2	NB (%)	CvRMSE (%)	SI (%)	*Design*	R^2	NB (%)	CvRMSE (%)	SI (%)
Baseline	0.32	-13.4	32.66	29.79	Baseline	0.38	-3.41	27.43	27.22

E) Direction

Feasibility	R^2	NB (%)	CvRMSE (%)	SI (%)	*Design*	R^2	NB (%)	CvRMSE (%)	SI (%)
Baseline	0.33	1.96	54.22	54.4	Baseline	0.26	109.6	58.07	58.00

F) Directionality Coefficient

Feasibility	R^2	NB (%)	CvRMSE (%)	SI (%)	*Design*	R^2	NB (%)	CvRMSE (%)	SI (%)
Baseline	0.27	46.67	57.29	33.24	Baseline	0.28	36.40	48.53	32.10

When examining the baseline feasibility and design class assessments, shown in Table 7.2, it became apparent that the feasibility class provided marginally better statistics for the modeled wave height and wave direction. This was also noted for the R^2 value for the wave power.

However, the design class assessment showed significant improvement in the modeling of the energy period, and spectral width, and moderate improvement for the directionality coefficient. As expected, both the feasibility and design class assessments provided better accuracy than the reconnaissance class assessment. Based on the similarities between both the feasibility and design class assessments, it appears that the additional effort and computational cost of the design class model did not translate into better results as intended by the IEC-TS. This may be the result of a number of factors, including the fact that the same bathymetry was used for all three model. It may also indicate that the boundary conditions were not sufficiently accurate for the design class assessment. This observation would need to be corroborated with additional studies to determine whether it is necessary to have both a feasibility and design class assessment procedure prescribed by the TS.

The monthly R^2 values were examined for all three classes of assessment, shown in Table 8.3, in order to examine how precise the assessments were across the year. The intent behind this comparison was to examine the measured R^2 values for each month to determine if there was high variability in the modeled predictions. It was expected that the reconnaissance class would have the highest variability on a month-to-month basis, while the feasibility and design classes should be more precise as per the IEC-TS. This comparison was only completed using the R^2 value which is a measure of the models' ability to follow the trend of the measured data.

When examining the R^2 values for the reconnaissance class assessment it is very clear that the model lacks precision, with the values fluctuating significantly monthly. The wave heights ranged from 0.34 up to 0.86, the power ranged from 0.03 to 0.81, and the energy period ranged from 0.07 to 0.60. A wide range of R^2 values were expected for this class of assessment, as the model was not intended to be overly precise or accurate. A clear trend in the R^2 values was also observed, with the months of May, August and July have the lowest accuracy for all three parameters. However, when looking at the time-histories of these summer months, Figure 8.1, it can be seen that the absolute error is within the same margin for the winter and summer months, but the model was less able to represent the general trend of the waves. This may be due to a number of factors such as errors within the boundary or wind conditions.

When examining the R^2 values for the feasibility and design class assessments, the values tend to generally be more consistent across the months. Similar to the reconnaissance class assessment certain trends are apparent, for example neither the reconnaissance nor feasibility class assessments had high R^2 for the month of the July, as both models shared the same boundary locations this could be a result of inaccuracies in the boundary conditions for this month. It should be noted that wave energy levels in this region tend to be low in the northern hemisphere summer, and the poor validation performance observed for July 2013 could well be related to the absence of energetic wave conditions. Furthermore, performance errors in low-energy months have less influence on overall yearly performance results than do errors in high-energy months and are therefore less critical.

Table 8.3 - Monthly Model R^2 Values for the Reconnaissance (R); Feasibility (F); and Design (D) Stages of Assessment for May 2013 to April 2014

		May	*June*	*July*	*Aug*	*Sept*	*Oct*	*Nov*	*Dec*	*Jan*	*Feb*	*Mar*	*Apr*
	R	0.54	0.66	0.34	0.54	0.86	0.83	0.66	0.62	0.74	0.68	0.58	0.61
Wave	*F*	0.82	0.86	0.73	0.75	0.91	0.89	0.85	0.84	0.80	0.89	0.77	0.82
Height	*D*	0.77	0.82	0.76	0.58	0.89	0.87	0.86	0.82	0.76	0.88	0.72	0.77
	R	0.21	0.67	0.03	0.24	0.81	0.78	0.71	0.65	0.74	0.71	0.50	0.73
Power	*F*	0.75	0.87	0.25	0.57	0.87	0.77	0.86	0.79	0.72	0.85	0.61	0.78
	D	0.70	0.84	0.67	0.39	0.82	0.78	0.83	0.75	0.71	0.81	0.62	0.81
	R	0.33	0.33	0.07	0.54	0.18	0.45	0.26	0.60	0.60	0.56	0.43	0.57
Energy Period	*F*	0.43	0.47	0.14	0.59	0.51	0.51	0.43	0.57	0.67	0.74	0.48	0.64
	D	0.44	0.61	0.29	0.66	0.57	0.68	0.26	0.57	0.67	0.67	0.46	0.64
Direc.	*F*	0.32	0.39	0.07	0.47	0.46	0.42	0.28	0.30	0.26	0.30	0.40	0.28
	D	0.41	0.42	0.16	0.42	0.45	0.50	0.20	0.07	0.20	0.16	0.31	0.23
Spect.	*F*	0.12	0.15	0.11	0.11	0.29	0.16	0.36	0.20	0.38	0.59	0.31	0.25
Width	*D*	0.24	0.37	0.39	0.19	0.18	0.19	0.40	0.16	0.34	0.57	0.28	0.22
Direc. Coeff.	*F*	0.15	0.16	0.02	0.49	0.26	0.29	0.32	0.16	0.26	0.46	0.31	0.49
	D	0.22	0.29	0.40	0.37	0.20	0.33	0.24	0.15	0.22	0.32	0.21	0.43

The last model validation that was completed for the baseline resource assessments was the calculation of the systematic and random errors as required by the IEC-TS, shown in Figure 8.2. These figures show the errors for the required validation parameters at each stage of assessment, compared with the maximum allowable errors. At first glance it is readily apparent that the omni-directional wave power exceeds the maximum validation criteria by a significant amount for all three classes of assessment. When examining this parameter closer it was noted that the while the error for each individual wave state fell within the required validation criteria, the summation of the error across all the wave states resulted in a much higher value. Additionally, it was noted that the highest errors occurred in relatively calm wave states, with low wave heights and energy periods. When examining the other systematic and random errors it was noted that the models had excessive errors for certain parameters but fell within the required validation criteria for others. While the direction and spectral width always had sufficiently low errors (and the wave power had excessively high errors) the validation of the other parameters varied for each class of assessment. However, while the reconnaissance and feasibility assessments were generally able to come within or near the maximum validation criteria (except for the wave power), the design class assessment generally had errors above the maximum value. This may indicate that the criteria is too stringent for this stage of assessment, or it may indicate that this model was not able to perform adequately. Similar observations were made in the study by Ramos and Ringwood [2016] and Ramos *et al.,* [2016], who noted that the TS requirements may be excessive for certain classes of assessment. Finally, it was noted that the calculated mean random errors (which is based on the standard deviation) were generally larger than the mean systematic errors (based on the bias), which is in line with the expectations provided by the TS.

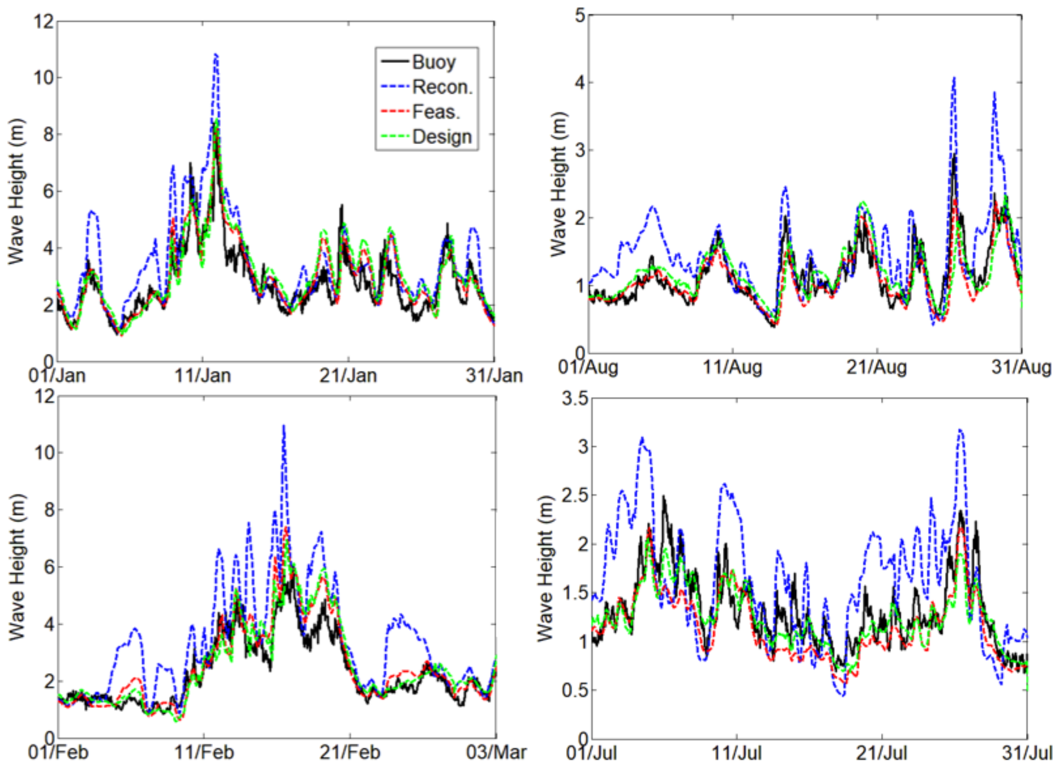

Figure 8.1 – Time-Histories of Monthly Baseline Summer and Winter Wave Heights for all Classes of Assessment

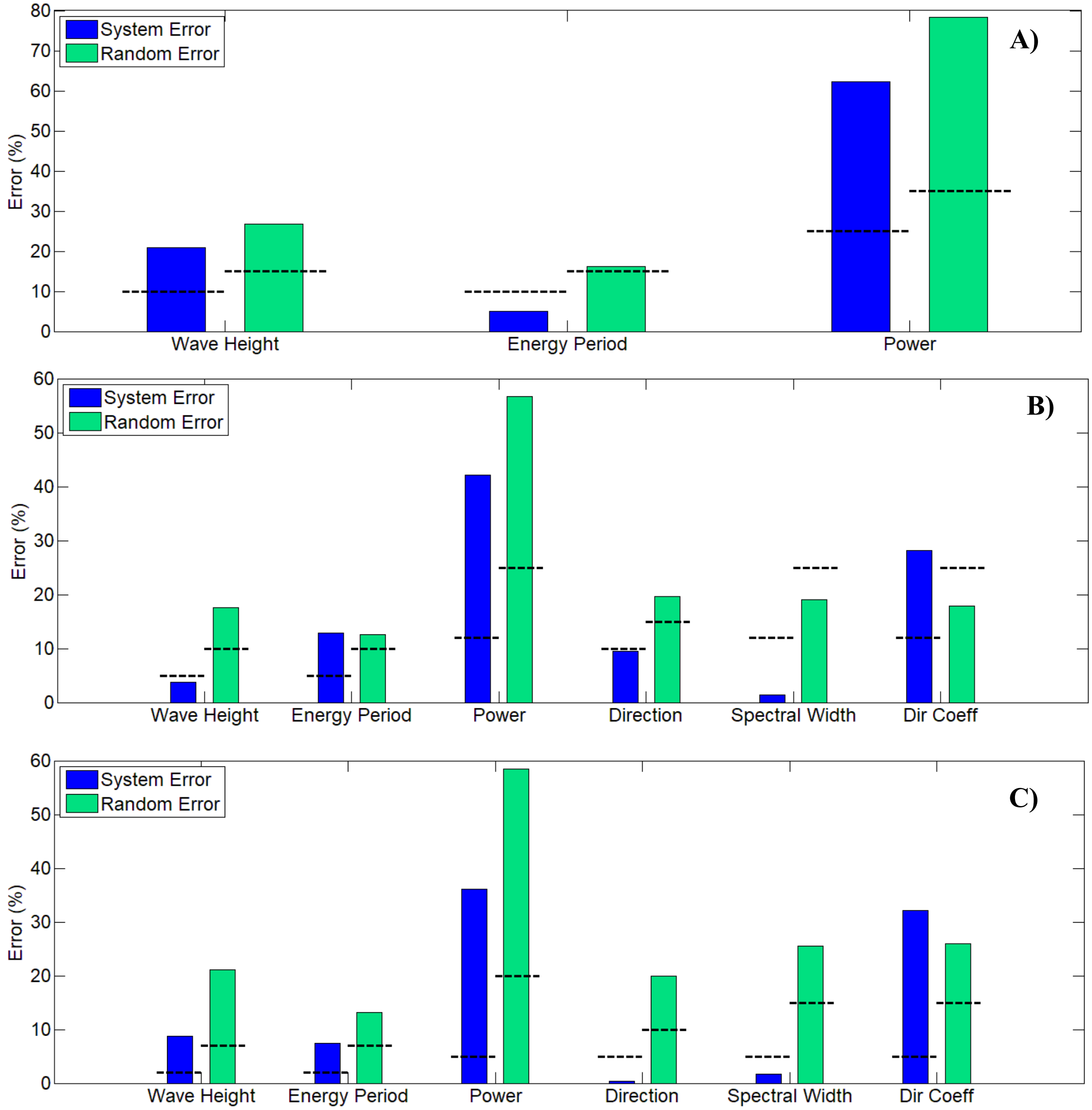

Figure 8.2 – Systematic and Random Errors for May 2013 to April 2014 for A) Reconnaissance; B) Feasibility; and C) Design Class Assessment (Direction Error is in Deg.)

8.2 Influence of Model Processes

As discussed in Section 2.1, not all physical processes are required for consideration for each class of assessment. The physical processes that were assessed during this stage of validation were (as shown in Table 8.4):

- Bottom friction,
- Depth–induced wave breaking,
- Non–linear wave–wave triad interactions, and
- Whitecapping.

Within this study, non–linear wave–wave quadruplet interactions and wind–wave growth were not examined as the exclusion of these parameters resulted in no generated wave spectra. Each of these parameters was defined previously in Chapter 6. This analysis was completed for both the reconnaissance and feasibility classes. As the observations were consistent for both stages it is assumed that they would hold true for the design class assessment as well.

Table 8.4 – SWAN Model Physical Process Sensitivity Analysis Runs

Run Number	Bottom Friction	Wave Breaking	Triad	Whitecapping
Recon_Baseline	OFF	OFF	ON	ON
Recon_Process_1	ON	OFF	ON	ON
Recon_Process_2	OFF	ON	ON	ON
Recon_Process_3	OFF	OFF	OFF	ON
Recon_Process_4	OFF	OFF	ON	OFF
Feas_Baseline	ON	ON	ON	ON
Feas _Process_1	OFF	ON	ON	ON
Feas _Process_2	ON	OFF	ON	ON
Feas _Process_3	ON	ON	OFF	ON
Feas _Process_4	ON	ON	ON	OFF

8.2.1 Time-History

When examining the averaged time–histories for the different physical processes, Figure 8.3, it was noted that the resource assessment was not sensitive to the use of triad wave interaction and wave breaking, while some sensitivity was observed for the use of bottom friction. The most sensitive parameters appeared to be the use of whitecapping, where the difference between its inclusion and exclusion could result in variations of up to 2m in wave height. These observations were consistent between the reconnaissance and feasibility class assessments and seem to indicate that the resource assessment at the pilot project site was not as sensitive to shallow water processes (such as depth-induced wave breaking). This may be a result of the water depth at the project site, and it may be more important at different study locations.

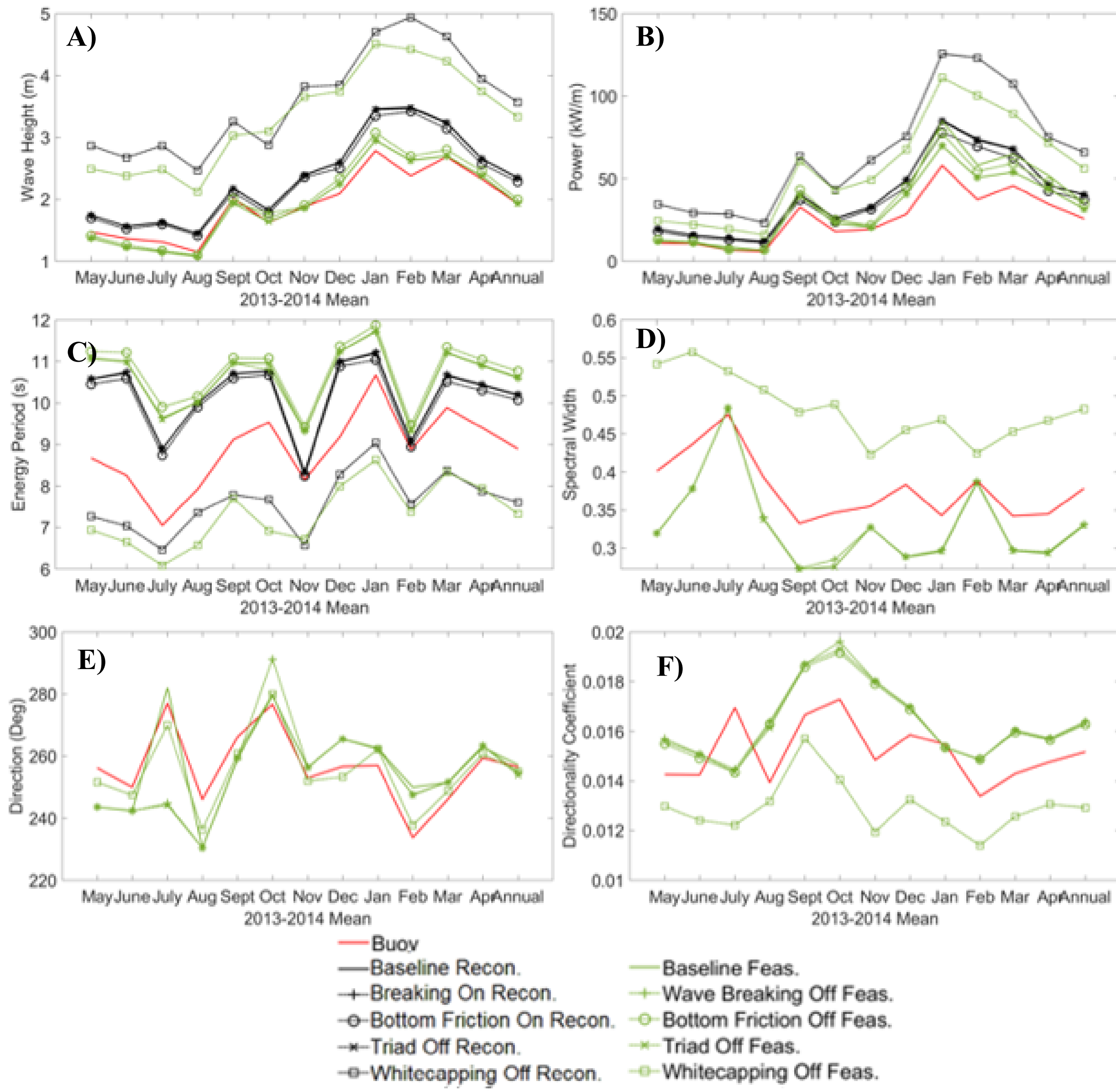

Figure 8.3 – Influence of Model Processes on A) Wave Height; B) Wave Power; C) Energy Period; D) Spectral Width; E) Direction; F) Directionality Coefficient

8.2.2 Baseline Statistics

The statistical analysis of the modeled wave resource using standard statistical parameters is shown for all the modeled wave parameters in Table 8.5. As with the time-series presented in the previous section it was observed that the exclusion of the whitecapping process resulted in a marked change to accuracy of the model. Additionally, for the reconnaissance class assessment the inclusion of the bottom friction process had some impact on the accuracy of the model, while both the wave breaking, and triad wave processes had minimal impact. A similar trend was observed for the feasibility class assessment, except for the wave power, where there was a wider range of values noted.

8.2.3 IEC Errors

The systematic and random errors for the reconnaissance and feasibility class assessments are shown in Figure 8.4 and Figure 8.5. Observations made from these errors are similar to those made for the time series in Figure 8.3 and the statistics in Table 8.5, which is that the exclusion of the whitecapping parameter introduces large error into the resource assessment. Similarly, it was noted that the inclusion of the bottom friction processes resulted in increased accuracy, while the triad and wave breaking processes had minimal impact. The exception to this appears to be with the directionality coefficient, where the wave breaking processes has minimal impact and the bottom friction and triad processes both increase the model systematic error and decrease its random error.

What is interesting to note in both assessments is that the exclusion of whitecapping has a larger impact on the systematic error (bias) then the random error (standard deviation) and in the case of the energy period and the directionality coefficient the random error is improved by the exclusion of the whitecapping parameter. Additionally, the direction does not appear to be impacted significantly by any of the parameters, which could be due to the fact that these parameters all have an impact on the amount of energy and its frequency within the wave spectrum, but not on its direction.

Table 8.5 – Statistics for the Impact of Model Processes on A) Wave Height; B) Wave Power; C) Energy Period; D) Spectral Width; E) Direction; F) Directionality Coefficient

A) Wave Height

		R^2	NB (%)	CvRMSE (%)	SI (%)
Reconnaissance	Breaking	0.74	21.47	43.55	37.90
	Bottom Friction	0.72	18.32	42.12	37.94
	Triad	0.74	21.64	43.96	38.27
	Whitecap	0.77	84.90	95.51	43.74

		R^2	NB (%)	CvRMSE (%)	S (%)
Feasibility	Breaking	0.88	0.97	21.48	21.47
	Bottom Friction	0.88	3.61	23.33	23.06
	Triad	0.88	0.35	21.38	21.38
	Whitecap	0.78	71.90	79.67	34.33

B) Wave Power

		R^2	NB (%)	CvRMSE (%)	SI (%)
Reconnaissance	Breaking	0.72	54.91	131.20	119.17
	Bottom Friction	0.70	43.47	119.11	110.91
	Triad	0.71	55.34	132.64	120.56
	Whitecap	0.72	153.5	249.20	196.34

		R^2	NB (%)	CvRMSE (%)	SI (%)
Feasibility	Breaking	0.80	23.59	89.87	86.73
	Bottom Friction	0.80	34.34	107.46	101.84
	Triad	0.80	22.88	89.67	86.71
	Whitecap	0.79	117.0	188.29	147.57

C) Wave Energy Period

		R^2	NB (%)	CvRMSE (%)	SI (%)
Reconnaissance	Breaking	0.37	15.29	32.47	28.65
	Bottom Friction	0.37	13.82	31.55	28.37
	Triad	0.37	15.24	32.44	28.64
	Whitecap	0.47	-14.24	22.97	18.02

		R^2	NB (%)	CvRMSE (%)	SI (%)
Feasibility	Breaking	0.49	19.54	26.69	18.18
	Bottom Friction	0.48	21.44	28.36	18.56
	Triad	0.50	19.67	26.72	18.09
	Whitecap	0.48	-17.61	23.61	15.73

D) Spectral Width

		R^2	NB (%)	CvRMSE (%)	SI (%)
Feasibility	Breaking	0.32	-12.99	32.23	29.50
	Bottom Friction	0.30	-14.05	33.23	30.11
	Triad	0.32	-13.37	32.59	29.73
	Whitecap	0.32	27.84	37.48	25.10

E) Direction

		R^2	NB (%)	CvRMSE (%)	SI (%)
Feasibility	Breaking	0.28	-22.13	50.51	50.93
	Bottom Friction	0.27	-16.33	51.49	52.27
	Triad	0.29	-15.27	51.60	52.35
	Whitecap	0.42	-48.50	53.82	53.88

F) Directionality Coefficient

		R^2	NB (%)	CvRMSE (%)	SI (%)
Feasibility	Breaking	0.24	8.04	30.38	29.30
	Bottom Friction	0.27	7.22	29.37	28.47
	Triad	0.27	7.56	29.38	28.39
	Whitecap	0.33	-14.23	29.32	25.64

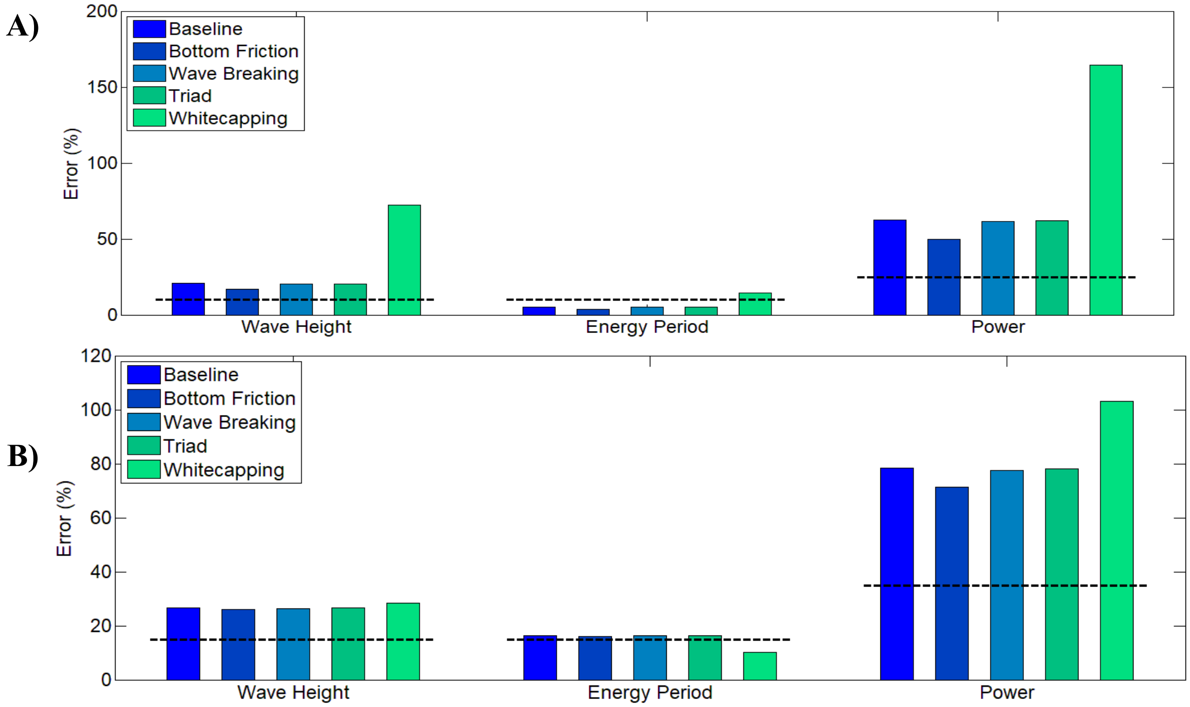

Figure 8.4 – Systematic and Random Errors for the Reconnaissance Class A) Systematic Errors; and B) Random Errors

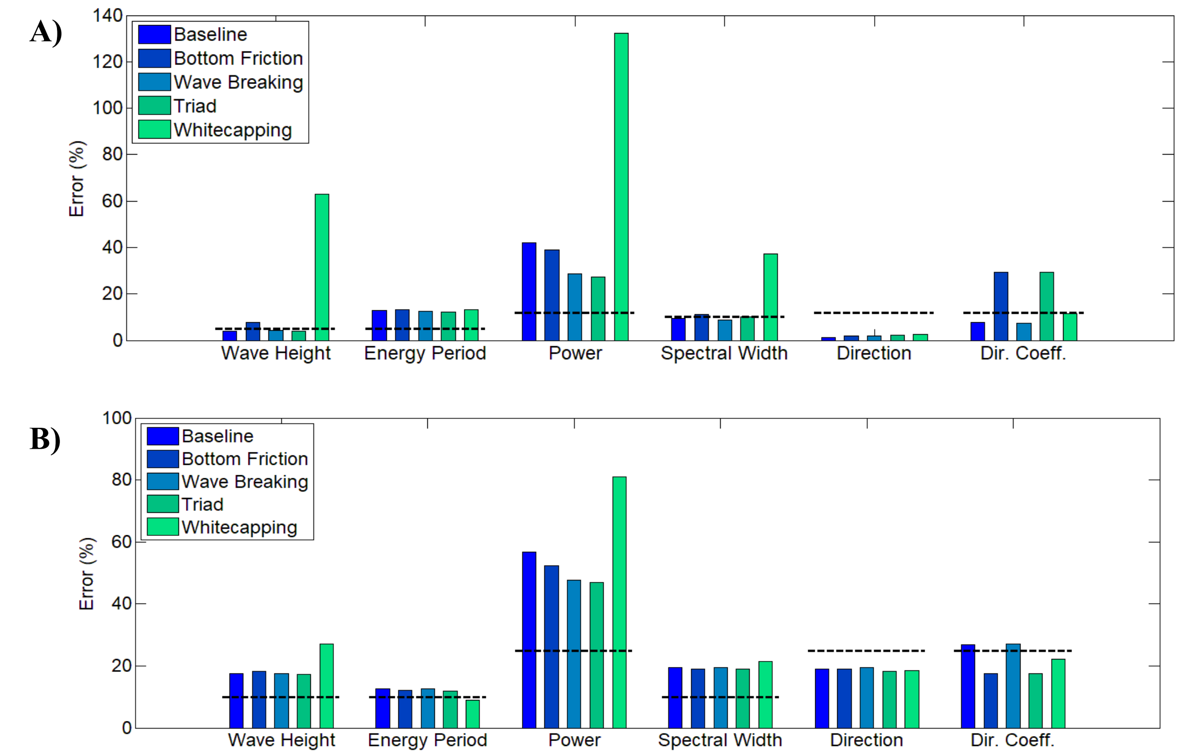

Figure 8.5 – Systematic and Random Errors for the Feasibility Class A) Systematic Errors; and B) Random Errors (Direction Error is in Deg.)

8.2.4 Domain Comparison

To assess the impact that these parameters may have at shallower locations, the results were also compared across the entire model domain. This would give an indication as to whether the observations made in Figure 8.6 hold for the entire domain, or whether the localized bathymetry had an impact on the model sensitivity.

The difference between the wave heights when including or excluding each of the physical parameters (based on Table 8.4) is shown in Figure 8.6 for the 12th of January 2014, as this day exhibited particularly large waves. From this figure it was noted that there is a significant difference in the modeled wave heights for both the reconnaissance and feasibility class assessments when removing the impact of whitecapping on the resource assessment, which is consistent with the previous observations made. The impact of the whitecapping parameter decreases as the waves approach the nearshore region, particularly in the case of the feasibility class assessment. When looking at the impact of the bottom friction (including bottom friction for the reconnaissance assessment and excluding it for the feasibility assessment) on wave height this parameter is only important within the nearshore region. However, its impact even close to the shoreline is fairly minimal, with differences ranging from 0.15m to 0.3m for the feasibility class assessment, and differences of approximately 0.05m for the reconnaissance class assessment. The depth-induced wave breaking parameter (including depth-induced wave breaking for the reconnaissance assessment, and excluding it for the feasibility assessment), shows some locations immediately along the nearshore boundary when significant variations are found However, this parameter has minimal effect elsewhere in the model domain. Finally, for the case of excluding wave-wave nonlinear triad interactions, there are a few nearshore regions within the model domain where there is significant impact on the wave height; however, this is believed to be the result of the model mesh and not indicative of the actual impact. The remainder of the model domain sees no impact for the inclusion/exclusion of this physical process.

This comparison highlights the importance of the whitecapping parameter on the results of the resource assessment and indicates that for most resource assessments the depth-induced wave breaking, bottom friction, and triad non-linear wave interaction processes are not necessary unless the site of interest is located in very shallow water.

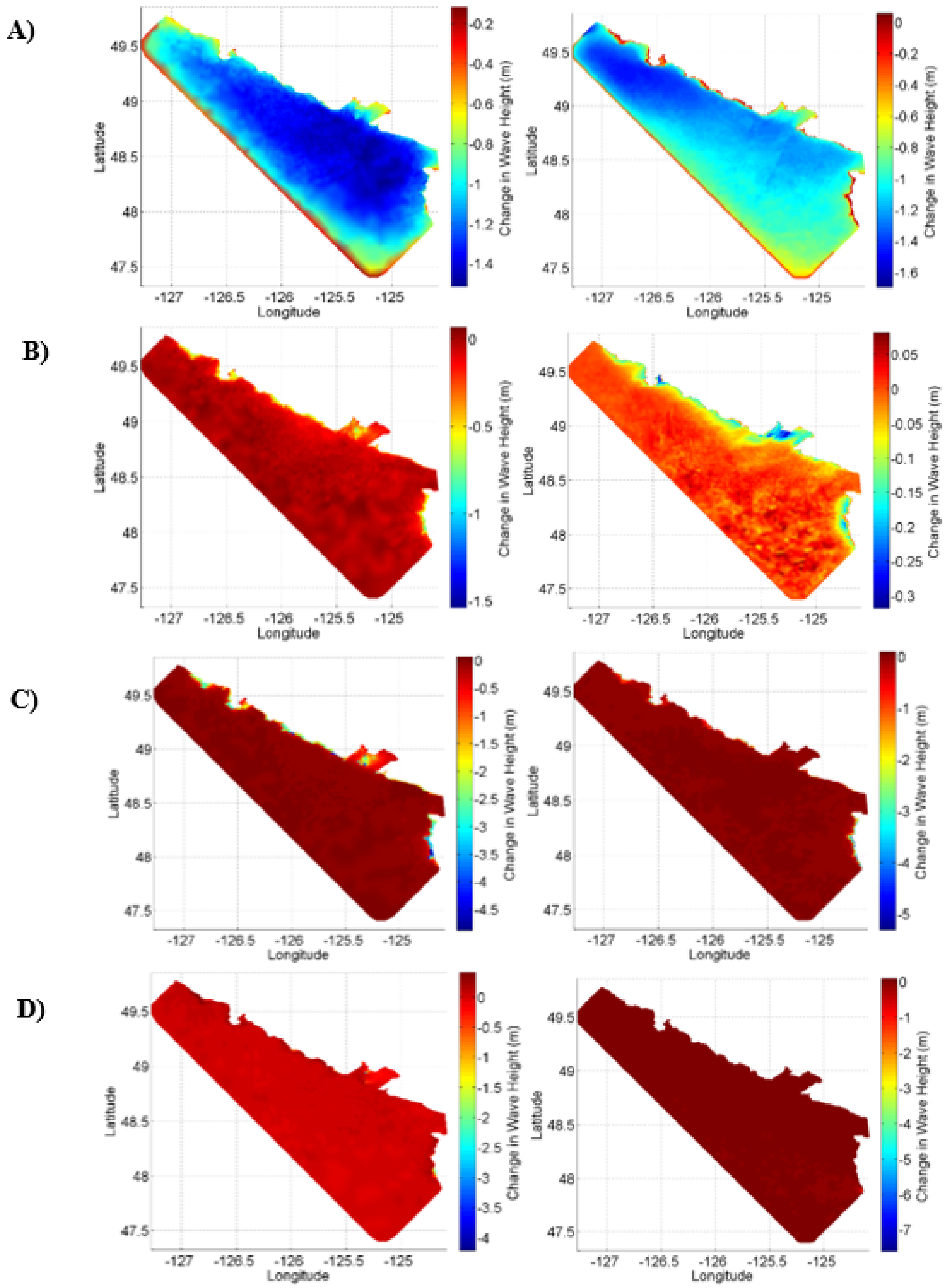

Figure 8.6 – Domain Comparison for the Sensitivity of the Resource Assessment to Physical Processes on January 12th 2014 00:00 for A) Whitecapping; B) Bottom Friction; C) Depth-Induced Wave Breaking; and D) Triad Non-Linear Interactions for both the *Reconnaissance* (Left Side) and *Feasibility* Stage (Right Side)

8.2.5 Model Sensitivity

To determine whether the model is sensitive to the inclusion or exclusion of these physical processes the model sensitivity was assessed based on the recommendations provided by the IEC-TS. The results of this sensitivity assessment were also compared to the statistical analysis to determine whether the IEC-TS requirements are representative of the actual impact that these parameters have on the resource assessment.

This assessment was completed by selecting three time periods for each wave state, with the average error for those three periods being used as the basis to determine whether there was a significant impact on this wave state. The wave states selected for this assessment are shown in Appendix B. The results of the sensitivity assessment are shown in Table 8.6. For the reconnaissance class assessment, the model was deemed to be not sensitive to all model processes except for whitecapping, which is supported by both the statistics and the time histories. This differs slightly for the feasibility class assessment where the model also showed sensitivity to both the wave breaking and bottom friction processes for the wave height, and for all processes for the wave power. The model was found to be sensitive to the wave breaking by 0.02% over the threshold. This is caused by a lowering of the sensitivity threshold from the reconnaissance assessment, and not due to an increase of the error within the model.

Chapter 8.7.4 recommends a new criteria for assessing the sensitivity of the parameters, which is also presented in Table 8.6 which indicates that the models are only sensitive to the whitecapping parameter for the wave height for both stages of assessment, but is still sensitive to all the parameters for the feasibility class assessment wave power. These sensitivity observations are in line with the statistics and time-histories of the reconnaissance and feasibility class assessments.

Table 8.6 - Sensitivity of Model to Physical Processes for Reconnaissance and Feasibility Class Assessments for A) IEC-TS Recommendation; and B) New Recommendation

		Wave Breaking	Bottom Friction	Triads	Whitecapping
Reconnaissance	Wave Height	A) Not Sensitive B) Not Sensitive	A) Not Sensitive B) Not Sensitive	A) Not Sensitive B) Not Sensitive	A) Sensitive B) Sensitive
	Power	A) Not Sensitive B) Not Sensitive	A) Not Sensitive B) Not Sensitive	A) Not Sensitive B) Not Sensitive	A) Sensitive B) Sensitive
Feasibility	Wave Height	A) Sensitive[1] B) Not Sensitive	A) Sensitive B) Not Sensitive	A) Not Sensitive B) Not Sensitive	A) Sensitive B) Sensitive
	Power	A) Sensitive B) Sensitive	A) Sensitive B) Sensitive	A) Sensitive B) Sensitive	A) Sensitive B) Sensitive

[1]Value is sensitive in 2.02% of cells which is marginally above the maximum threshold of 2%

8.3 Influence of Mesh Resolution

An analysis of the impact of model mesh resolution on the wave resource and climate was completed for all classes of assessment based on the range of recommended model resolutions provided by the IEC-TS. The mesh resolutions selected for this sensitivity analysis are shown in Table 8.7.

Table 8.7 – Mesh Resolution Sensitivity Analysis Runs

Run Number	Nominal Size (m)	Node Count
Recon_1000	1,000	5,892
Recon_Baseline	1,500	4,323
Recon_2500	2,500	1,558
Recon_4000	4,000	801
Feas_100	100	106,626
Feas_300	300	23,092
Feas_Baseline	500	16,105
Design_Baseline	50	45,000
Design_100	100	16,000

8.3.1 Time-History

The monthly and annual average wave climates for all three classes of assessment are shown in Figure 8.7. From this figure an unusual trend for the reconnaissance class assessment was observed; it appears that the lower mesh resolution resulted in the modeled parameters being closer to the measured values obtained at the Beverley Buoy site. When examining these time histories, it is apparent that the reconnaissance class assessment is sensitive to the model mesh resolution, most likely as a result of the large range of acceptable mesh resolutions for this class. Supporting this conclusion is the fact that resource assessment appears to become less sensitive for the feasibility class assessment, where the differences in mesh resolution are smaller, and for the design class assessment where the sensitivity of the model appears to be minimal.

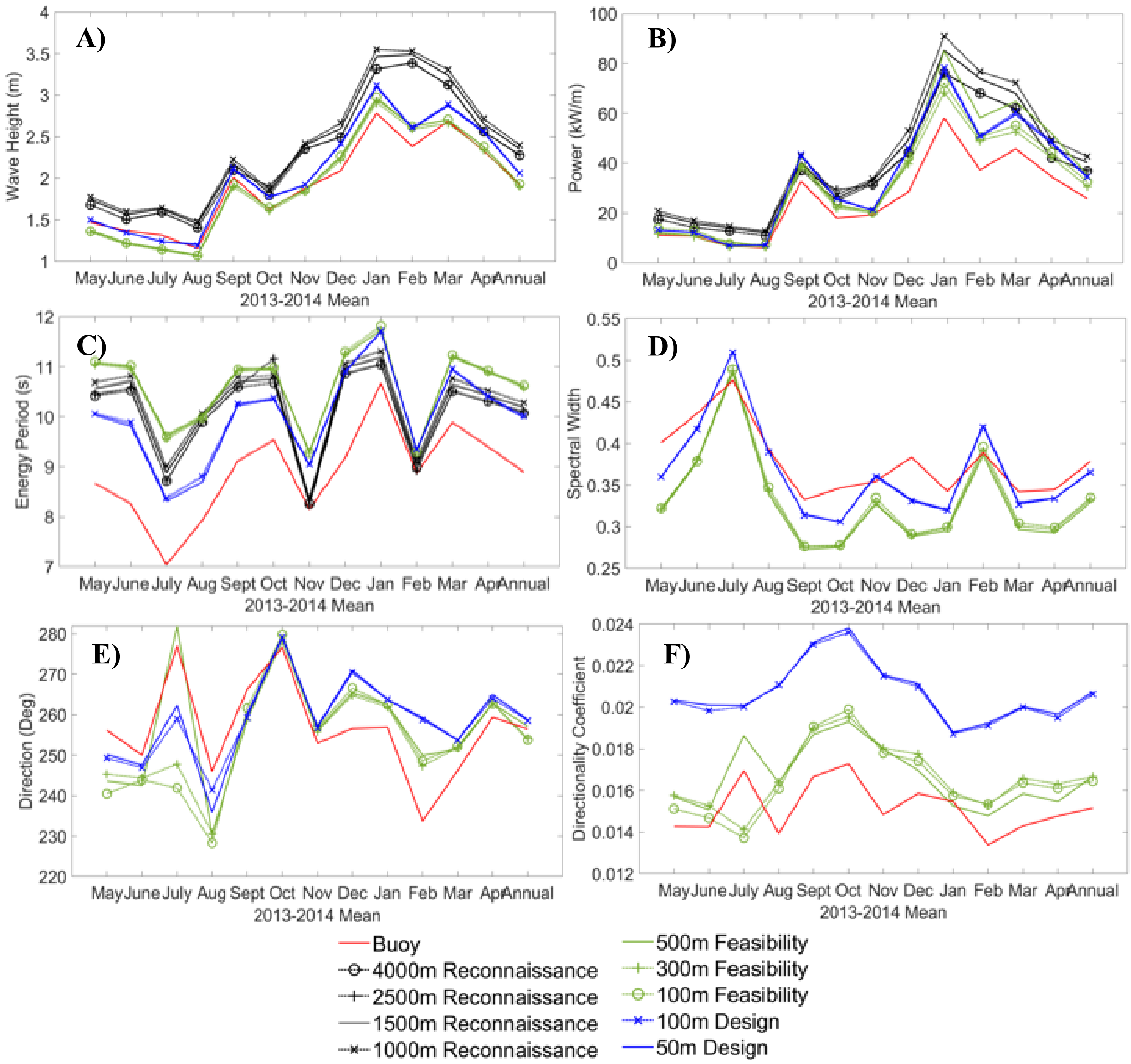

Figure 8.7 – Influence of Mesh Resolution on A) Wave Height; B) Wave Power; C) Energy Period; D) Spectral Width; E) Direction; F) Directionality Coefficient

8.3.2 Baseline Statistics

A statistical analysis of the resource assessment was completed for all three classes of assessment, shown in Table 8.8. When examining the statistics for the reconnaissance class assessment it becomes clear that while the lower mesh resolutions may have lower biases, they are marginally less able to represent the actual trend of the wave height and wave power as represented by the R^2 value. The errors and the scatter indexes for the wave height and the energy period tend to be relatively close, while for the wave power the error and scatter index are higher for the higher resolution mesh.

For the feasibility class assessment slight variations in the R^2 values were observed, but the model biases, errors, and scatter index were relatively close for all parameters, except for the wave power and wave direction. For the wave power it appears that the 300m mesh had the greater accuracy, while for the direction the baseline model performed the best.

Finally, for the design class assessment, it was observed that there was some influence on the model mesh resolution on the biases of the wave direction (and energy period, though this impact was observed to be relatively small), with marginal differences in the errors or the R^2 values.

The observations made from these statistics appear to indicate that the wave power and direction are most impacted by the mesh resolution for the higher-class models, and all the parameters were influenced for the reconnaissance class assessment likely due to the range of acceptable resolutions tested. The direct impact of the mesh resolution can be difficult to obtain as it is also impacted by other factors such as bathymetry, and the layout of the mesh itself. However, these results do show that for both the reconnaissance and feasibility class assessments care must be made in the construction of the mesh as it may have a large impact on the results.

Table 8.8 – Statistics for the Impact of Mesh Resolution on A) Wave Height; B) Wave Power; C) Energy Period; D) Spectral Width; E) Direction; F) Directionality Coefficient

A) Wave Height

Stage	Mesh	R^2	NB (%)	CvRMSE (%)	SI (%)
Reconnaissance	1,000	0.75	24.21	45.64	38.70
Reconnaissance	2,500	0.73	18.13	41.92	37.81
Reconnaissance	4,000	0.72	17.62	42.37	38.54
Feasibility	100	0.86	0.36	23.34	23.35
Feasibility	300	0.88	-1.22	21.39	21.36
Design	100	0.86	7.14	24.65	23.60

B) Wave Power

Stage	Mesh	R^2	NB (%)	CvRMSE (%)	SI (%)
Reconnaissance	1,000	0.72	65.04	145.33	129.99
Reconnaissance	2,500	0.70	42.99	116.51	108.30
Reconnaissance	4,000	0.70	41.98	117.93	110.22
Feasibility	100	0.76	26.98	101.87	98.25
Feasibility	300	0.79	19.26	88.34	86.23
Design	100	0.78	35.04	108.92	103.14

C) Wave Energy Period

Stage	Mesh	R^2	NB (%)	CvRMSE (%)	SI (%)
Reconnaissance	1,000	0.36	16.24	33.22	28.99
Reconnaissance	2,500	0.36	14.22	31.75	28.39
Reconnaissance	4,000	0.38	13.78	31.14	27.93
Feasibility	100	0.48	19.85	27.29	18.72
Feasibility	300	0.49	19.40	26.74	18.40
Design	100	0.63	12.82	18.95	13.96

D) Spectral Width

Stage	Mesh	R^2	NB (%)	CvRMSE (%)	SI (%)
Feasibility	100	0.29	-12.01	33.60	31.38
Feasibility	300	0.31	-12.60	32.67	30.15
Design	100	0.38	-3.71	27.34	27.09

E) Direction

Stage	Mesh	R^2	NB (%)	CvRMSE (%)	SI (%)
Feasibility	100	0.25	-17.71	51.63	52.27
Feasibility	300	0.30	-5.75	51.82	52.63
Design	100	0.27	82.53	56.05	56.00

F) Directionality Coefficient

Stage	Mesh	R^2	NB (%)	CvRMSE (%)	SI (%)
Feasibility	100	0.24	8.34	31.10	29.97
Feasibility	300	0.28	9.80	30.15	28.52
Design	100	0.29	35.69	47.70	31.65

8.3.3 IEC Errors

The systematic and random errors for all three classes of assessment are shown in Figure 8.8 and Figure 8.9. From Figure 8.8, which shows the results of the reconnaissance class assessment, the observations made previously still hold. Decreases in the mesh resolution generally result in improvements for both errors. However, it was noted that the errors for both the 2500m and the 4000m mesh were fairly consistent, with the only variation being the random error for the wave power. It was also noted that the systematic error appeared to be influenced more by changes in the mesh resolution. This is supported by the statistics which show that the bias was heavily impacted by changes in mesh resolution. However, the impact on the wave power for the 4000m is not something that appears in the standard statistical values, though the similarity between the 2500m and 4000m mesh does.

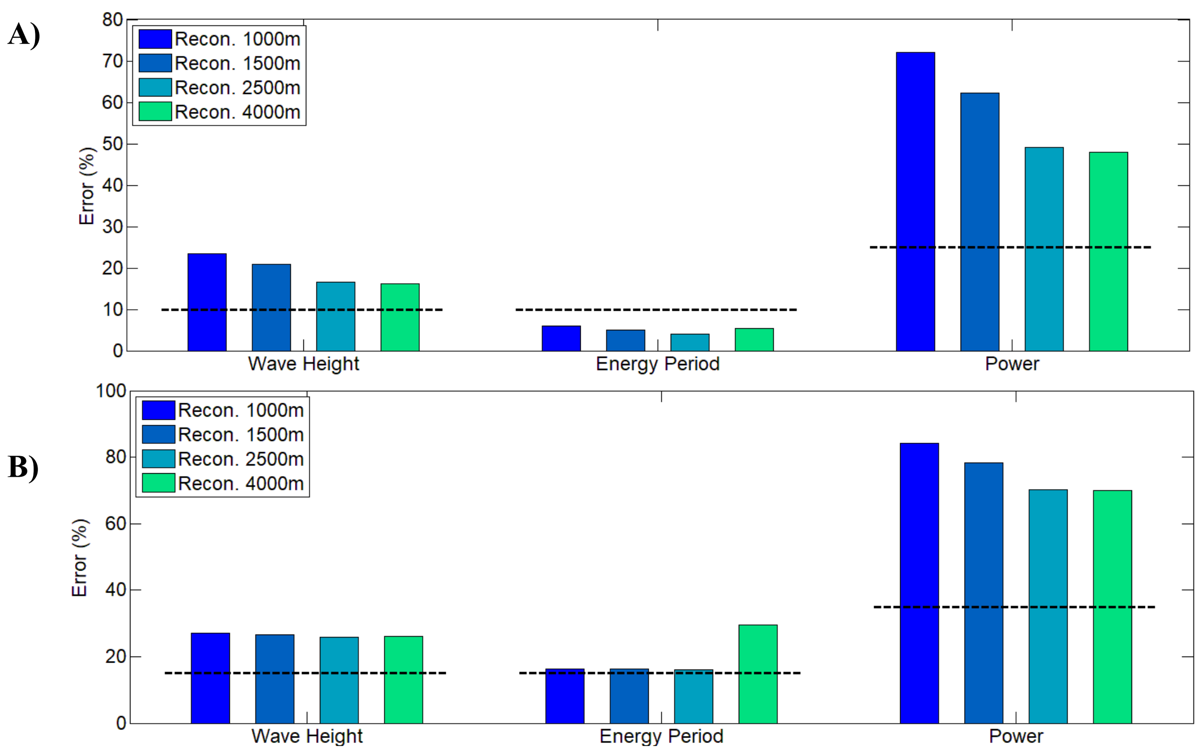

Figure 8.8 – Systematic and Random Errors for the Reconnaissance Model Mesh Resolution A) Systematic Errors; and B) Random Errors

For the feasibility class assessment, shown in Figure 8.9, the systematic and random errors fluctuate based on the specific parameter. For example, the 300m resolution mesh provides the lowest systematic error for the wave height and wave power, while providing the highest systematic error for the direction and directionality coefficient. For the random error large ranges in values are only truly noted for the wave power, in which the 300m resolution provides the lowest error. Similar to the reconnaissance class assessment the systematic error is more heavily influenced by the mesh resolution than the random error.

Finally, for the design error it was noted in the general statistics that only the wave direction bias was sensitive to changes in the mesh resolution. However, for the systematic error there does seem to be some impact from the mesh resolution for all parameter, with the largest difference occurring for the directionality coefficient. Differences in the random error are much smaller though they are still generally present. For this model it appears that the 50m mesh performs better for the wave height and power, while the 100m mesh performs better for all the other parameters. However, the differences between the mesh resolutions for both the systematic and random errors is generally quite small, indicating that at the model was not very sensitive to this parameter.

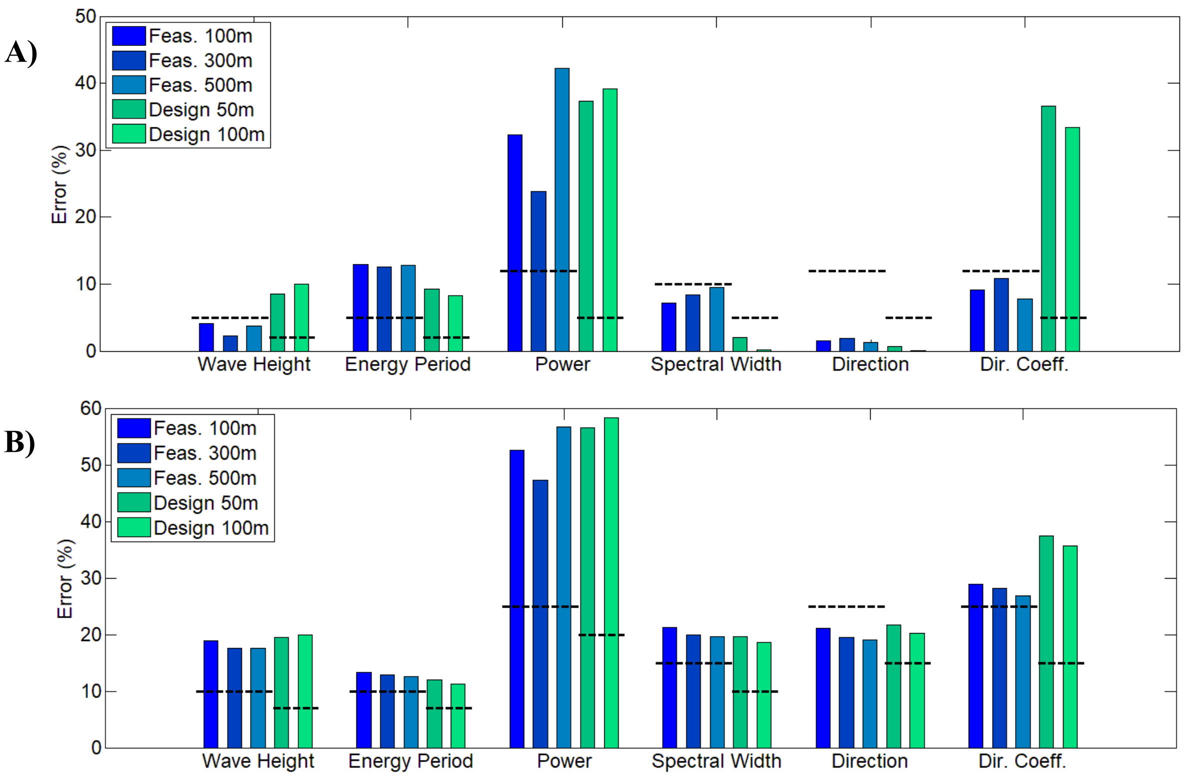

Figure 8.9 – Systematic and Random Errors for the Feasibility and Design Model Mesh Resolution A) Systematic Errors; and B) Random Errors (Direction Error is in Deg.)

8.3.4 Model Sensitivity

The sensitivity criteria proposed by the IEC-TS was not intended for testing model resolutions, but rather for examining whether a model process should be included within the model. However, model resolutions such as the mesh, wind, or spectra are important parameters, and it is necessary to determine if the model is sensitive to changes within these parameters. As a result, it was applied to the mesh resolution by comparing the different meshes against the baseline mesh in order to determine if there were any significant differences between the use of the baseline mesh or the sensitivity meshes.

When examining the results of the sensitivity analysis for the reconnaissance class assessment, shown in Table 8.9, it was observed that increasing the resolution from the baseline scenario to 1,000m did not have a significant impact on the model, whereas decreasing the mesh resolution to 2,5000m the model became sensitive for the wave power. Surprisingly, the model was again considered not sensitive to a further decrease in resolution to 4,000m. When comparing these results to the IEC-TS errors and the statistics it is a bit surprising that neither the 1,000m nor 4,000m were also sensitive as there is a similarly large difference between the 2,500 and 4,000m IEC-TS errors and there is a notable difference for the 1,000m resolution as well. When using the newly developed criteria the sensitivity remains relatively similar.

For the feasibility assessment the model was sensitive to increases in the model resolution for wave power, and for larger increases in resolution for the wave height was well. When using the new criteria for sensitivity the model becomes sensitive to all increases in model resolution for both the wave height and power. This is generally supported by the IEC-TS errors as there was a large range of errors for both the modelled wave height and power.

Finally, for the design class assessment, the model was determined to be sensitive to a decrease in the resolution from 50m to 100m when using the IEC sensitivity characterization thresholds. This is due to the low threshold recommended for the design class assessment, as it would not be considered sensitive when using the reconnaissance or feasibility class thresholds. This is also not supported by the statistics or the IEC-TS errors which do not show large variations between the values. When considering the new recommendation, the design class assessment would not be considered sensitive to the decrease in mesh resolution, which is in line with observations made previously.

Table 8.9 - Sensitivity of Model to Mesh Resolution for all Classes of Resource Assessment Compared to the Baseline Resolution for A) IEC TS Recommendation; and B) New Recommendation

		1000m	**2500m**	**4000m**
Reconnaissance	Wave Height	A) Not Sensitive B) Not Sensitive	A) Not Sensitive B) Partially Sensitive	A) Not Sensitive B) Not Sensitive
	Power	A) Not Sensitive B) Not Sensitive	A) Sensitive B) Sensitive	A) Not Sensitive B) Not Sensitive
		100m	**300m**	
Feasibility	Wave Height	A) Sensitive B) Sensitive	A) Not Sensitive B) Sensitive	
	Power	A) Sensitive B) Sensitive	A) Sensitive B) Sensitive	
		100m		
Design	Wave Height	A) Sensitive B) Not Sensitive		
	Power	A) Sensitive B) Not Sensitive		

[1]Value is sensitive in 2.19% of cells which is above the maximum threshold of 2%

The results shown in Table 8.9 are based on a comparison to the baseline mesh resolution, which does not indicate how sensitive the model is to incremental increases or decreases in mesh resolution. In the case of the reconnaissance class assessment, the model was not sensitive to increases in mesh resolution from 1,500 to 1,000m, but was sensitive to decreases to in resolution from 1,500m to 2,500m. The model was not found to be sensitive to decreases in resolution from 2,500m to 4,000m, which is consistent with observations made from the IEC-TS errors. For the feasibility class assessment, the model is sensitive to changes in mesh resolution from 500m to 100m, but it is also sensitive to increases in resolution from 300m to 100m.

8.4 Influence of Boundary Conditions

The IEC-TS gives recommendations for the use of boundary conditions when running the numerical model, mentioning three different types of boundary conditions that are typically available to the user (parametric, hybrid, and spectral). The IEC-TS comments on when it is considered acceptable to use each type of boundary and restricts the use of certain types to specific classes of assessment. To assess the impact that different boundary conditions can have on the resource assessment a comparison was made between the parametric and spectral boundaries for both the reconnaissance and feasibility class assessments, see Table 8.10. This was completed by comparing the baseline models with a secondary model forced using the other boundary condition, spectral for the reconnaissance assessment as per Section 6.3.2, and parametric for the feasibility assessment.

Table 8.10 – Boundary Condition Sensitivity Analysis Runs

Run Number	Spectrum Type	Wave Input Format
Recon_Baseline	JONSWAP	Parameterized
Recon_Boundary	JONSWAP	2D Spectral
Feas_Baseline	JONSWAP	2D Spectral
Feas _ Boundary	JONSWAP	Parameterized

8.4.1 Time-History

The average monthly and yearly time histories of the wave resource assessments are shown in Figure 8.10. From this figure it was observed that the parametric and spectral boundary conditions provided similar wave height and wave power values during the fall and winter months for the reconnaissance class assessment, but that during the summer and late spring the parametric boundary conditions tended to over predict these values. When considering the energy period, the parametric boundary over predicted the parameter throughout the year for the reconnaissance class assessment.

For the feasibility class assessment, the results showed that there was a large difference between the model results for the two different boundary conditions. In general, the spectral boundary conditions provided more accurate assessments throughout the year and in the yearly average. This is especially notable in the modeled spectral width which is not well represented when using parametric boundary conditions.

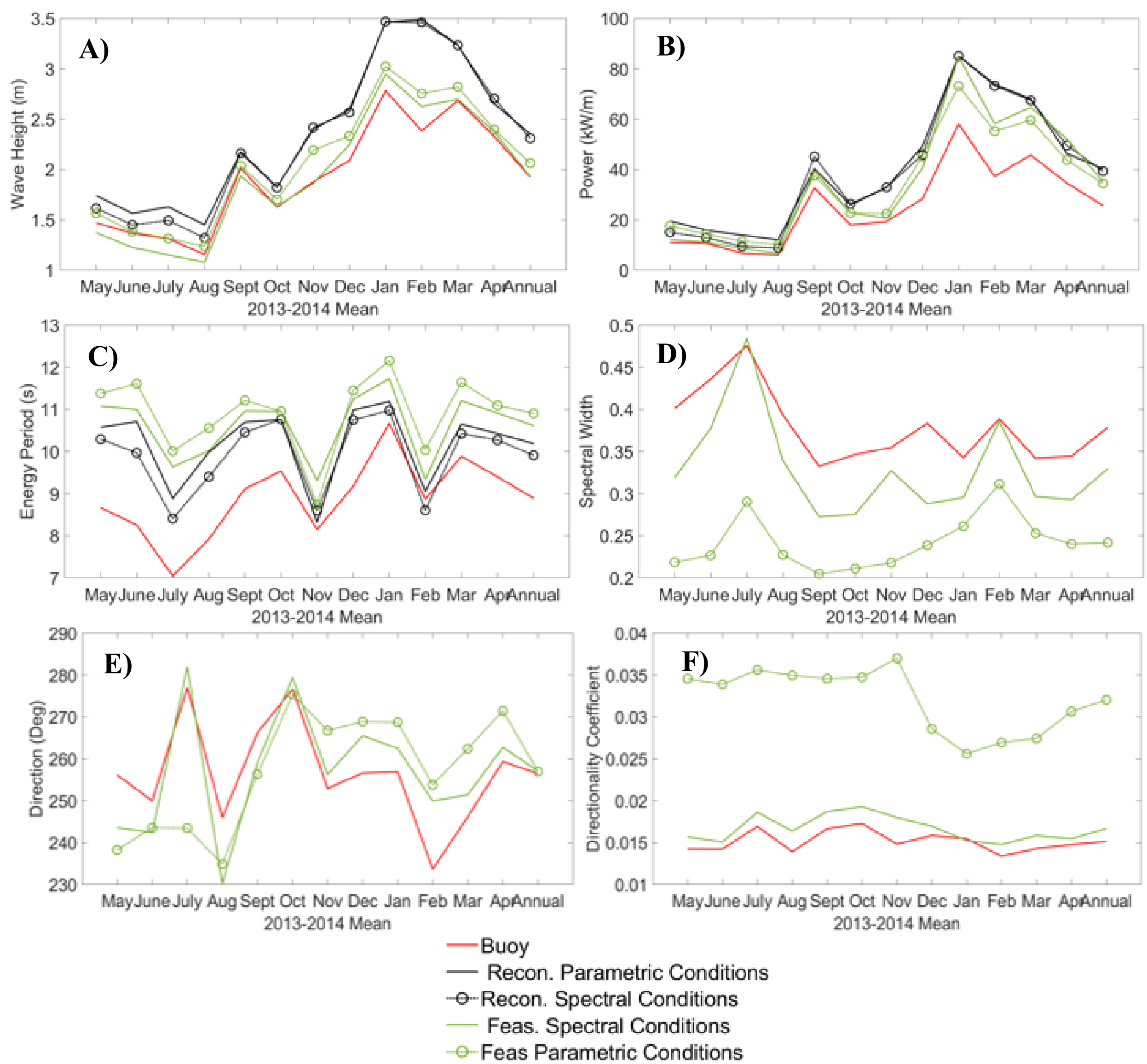

Figure 8.10 – Influence of Boundary Conditions on A) Wave Height; B) Wave Power; C) Energy Period; D) Spectral Width; E) Direction; F) Directionality Coefficient

8.4.2 Baseline Statistics

The baseline statistics for the different boundary conditions are shown in Table 8.11. From this table it was found that for the reconnaissance class assessment the use of the spectral boundary condition resulted in an increase in the R^2 value and bias for all parameters. This was especially notable for the energy period. The root mean error and the scatter index typically decreased as well except for the wave power where there was a slight increase. Overall, the greatest strength of the spectral boundary condition is its ability to allow the parameters to follow the trend of the measured data more accurately.

For the feasibility class assessment, the use of the parametric boundary condition resulted in greater inaccuracy in the modeled parameters, except for the wave power where the error, bias, and scatter index are better with the parametric boundary condition. This agrees with the observations made in the time-histories and supports the recommendation by the IEC-TS that parametric boundary conditions should not be used for this class of assessment.

8.4.3 IEC Errors

Figure 8.11 and Figure 8.12 show the systematic and random errors for the reconnaissance and feasibility class assessments. For the reconnaissance class assessment using spectral boundary conditions resulted in lower errors for the wave power for both the systematic and random error, as well as lower random errors for the energy period. The wave height showed similar error values for both types of boundary conditions.

For the feasibility class assessment spectral boundary conditions were found to provide lower errors in almost all parameters, the exception being the random error for spectral width. This was surprising as the baseline statistics and time-histories tend to show that the spectral boundary condition was more accurate for this parameter than the parametric boundary conditions. However, both random errors for the spectral width do fall outside of the acceptable error range regardless of the boundary condition selected. Additionally, the systematic error for the wave power was found to be similar, which is unsurprisingly as there is not a large difference in the model bias between the spectral and parametric boundary conditions.

Table 8.11 – Statistics for the Impact of Boundary Conditions on A) Wave Height; B) Wave Power; C) Energy Period; D) Spectral Width; E) Direction; F) Directionality Coefficient

A) Wave Height

		R^2	NB (%)	CvRMSE (%)	SI (%)
Reconnaissance	2D Spectra	0.79	19.47	42.42	37.70
Feasibility	Param	0.85	6.18	23.73	22.92

B) Wave Power

		R^2	NB (%)	CvRMSE (%)	SI (%)
Reconnaissance	2D Spectra	0.77	51.81	135.38	125.09
Feasibility	Param	0.78	34.42	92.60	85.98

C) Wave Energy Period

		R^2	NB (%)	CvRMSE (%)	SI (%)
Reconnaissance	2D Spectra	0.51	11.81	24.12	21.03
Feasibility	Param	0.30	23.59	36.81	28.26

D) Spectral Width

		R^2	NB (%)	CvRMSE (%)	SI (%)
Feasibility	Param.	0.07	-35.56	48.39	32.82

E) Direction

		R^2	NB (%)	CvRMSE (%)	SI (%)
Feasibility	Param	0.17	13.67	50.22	50.40

F) Directionality Coefficient

		R^2	NB (%)	CvRMSE (%)	SI (%)
Feasibility	Param.	0.04	110.8	134.89	76.96

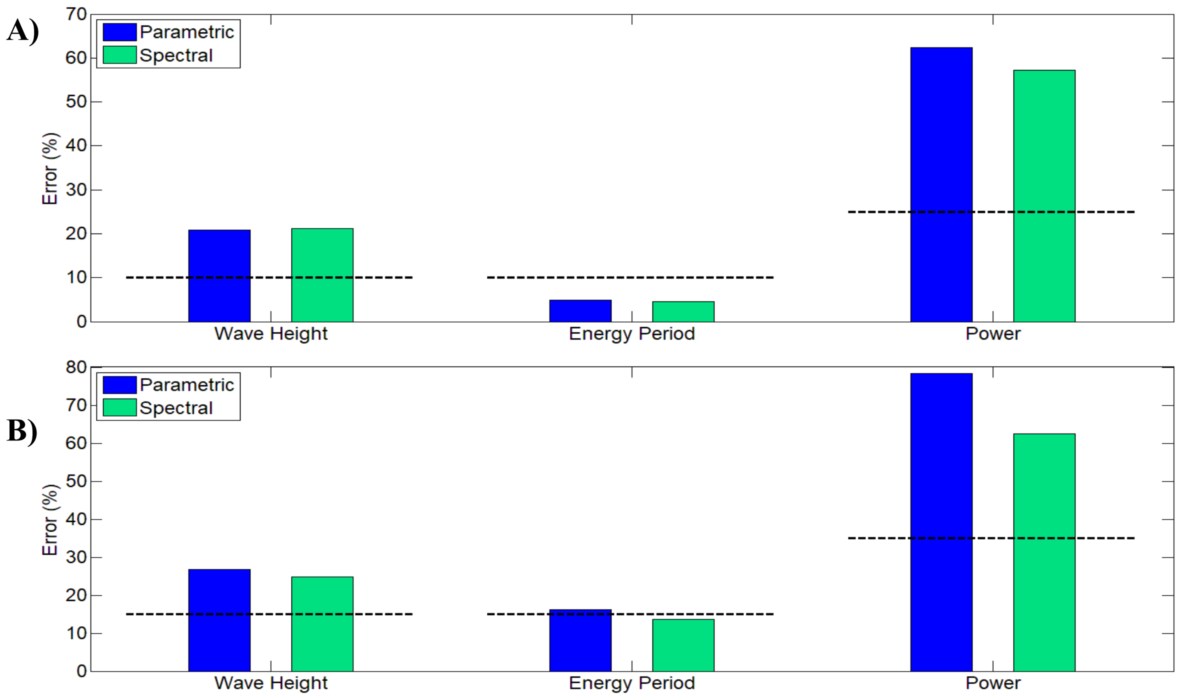

Figure 8.11 – Systematic and Random Errors for the Reconnaissance Model Boundary Conditions A) Systematic Errors; and B) Random Errors

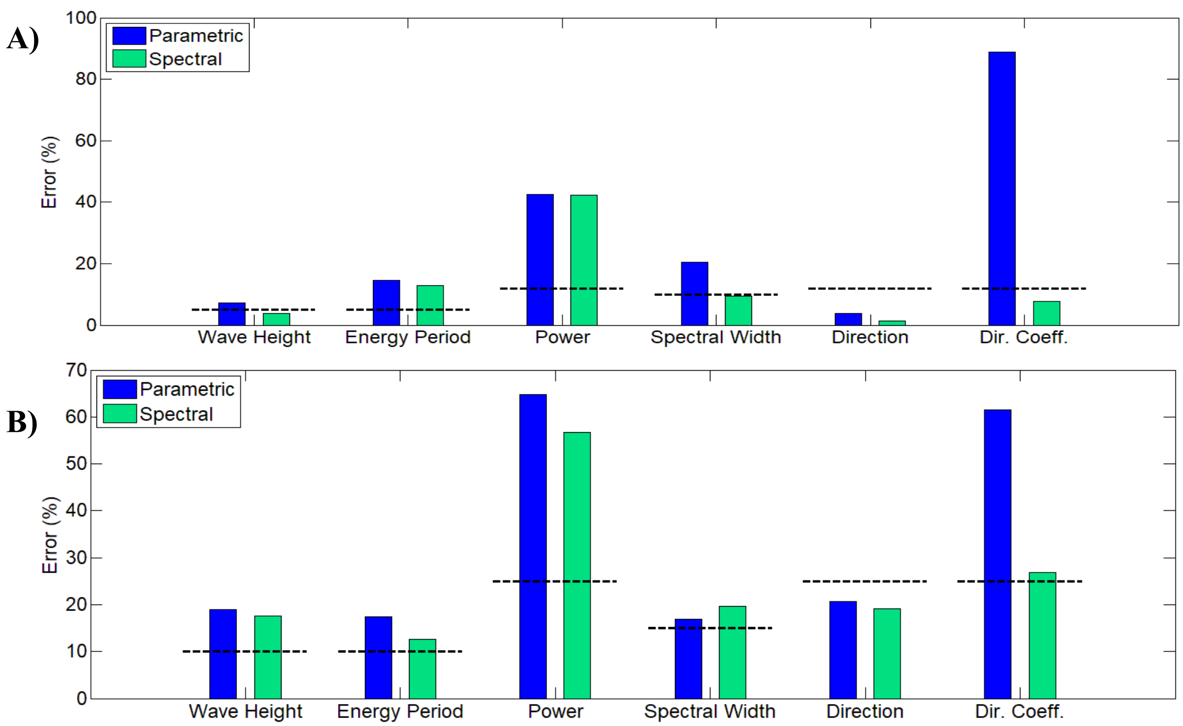

Figure 8.12 – Systematic and Random Errors for the Feasibility Model Boundary Conditions A) Systematic Errors; and B) Random Errors (Direction Error is in Deg.)

8.4.4 Model Sensitivity

Both the reconnaissance and feasibility class assessment models were found to be sensitive to changes in the boundary conditions, Table 8.12. This is generally supported by the statistics presented in Table 8.11 and in the IEC-TS errors for the feasibility class, though the wave power was not found to have a significant difference in the bias and systematic error. For the reconnaissance class assessment, the statistics and IEC-TS errors only showed significant differences in the wave power, so it is surprising that the wave height was also considered sensitive to changes in the boundary condition.

Table 8.12 - Sensitivity of Model to Boundary Condition for the Reconnaissance and Feasibility Class Assessments for A) IEC TS Recommendation; and B) New Recommendation

		Spectral
Reconnaissance	Wave Height	A) Sensitive B) Sensitive
	Power	A) Sensitive B) Sensitive
		Parametric
Feasibility	Wave Height	A) Sensitive B) Sensitive
	Power	A) Sensitive B) Sensitive

8.5 Influence of Spectral Resolution

The model spectral resolution is defined by the number of directions and frequencies used in the SWAN model for its computations. The number of directions and frequencies are defined using 'bins' which represent a spread of values, with more bins resulting in higher resolution in terms of the directions and frequencies. To assess the sensitivity of the model parameters to this resolution all classes of assessment were run using varying frequency and directional resolutions as shown in Table 8.13. Due to the number of tests conducted for this analysis the results were separated based on the class of assessment. Note that the frequency resolution does not much the IEC specification at the feasibility and design stages as it was increased in anticipation of changes in later IEC iterations.

Table 8.13 – Spectral Resolution Sensitivity Analysis Runs

Run Number	Directional Resolution	Frequency Resolution
Recon_Baseline	24	25
Recon_Dir_Res_1	36	25
Recon_Dir_Res_2	48	25
Recon_Dir_Res_3	72	25
Recon_Dir_Res_4	120	25
Recon_Freq_Res_1	24	41
Recon_Freq_Res_2	24	57
Recon_Freq_Res_3	24	73
Recon_Freq_Res_4	24	89
Feas_Baseline	36	41
Feas_Dir_Res_1	24	41
Feas_Dir_Res_2	48	41
Feas_Dir_Res_3	72	41
Feas_Dir_Res_4	120	41
Feas_Freq_Res_1	36	25
Feas_Freq_Res_2	36	57
Feas_Freq_Res_3	36	73
Feas_Freq_Res_4	36	89
Design_Baseline	48	41
Design _Dir_Res_1	36	41
Design _Dir_Res_2	72	41
Design _Freq_Res_1	48	25
Design _Freq_Res_2	48	57

8.5.1 Reconnaissance Time-History

The baseline resolution used by the reconnaissance class assessment was a frequency resolution of 25 bins and a directional resolution of 24 bins (direction discretized in 15° increments). To assess the sensitivity of the resource to these two parameters the model resolution was increased incrementally up to 89 frequency bins and 120 directional bins (3° increments). These increases were done independent of each other, the combined impact of increasing both the frequency and directional resolution was not assessed.

Figure 8.13 shows the average monthly and yearly time–histories for the wave parameters. From this figure it was noted that increases in the spectral resolution (for both frequency and direction) have an impact on the resource assessment. For the wave height and wave power increases in the frequency resolution was observed to have a larger impact on the resource assessment than increases in the directional resolution, while the opposite was observed for the energy period.

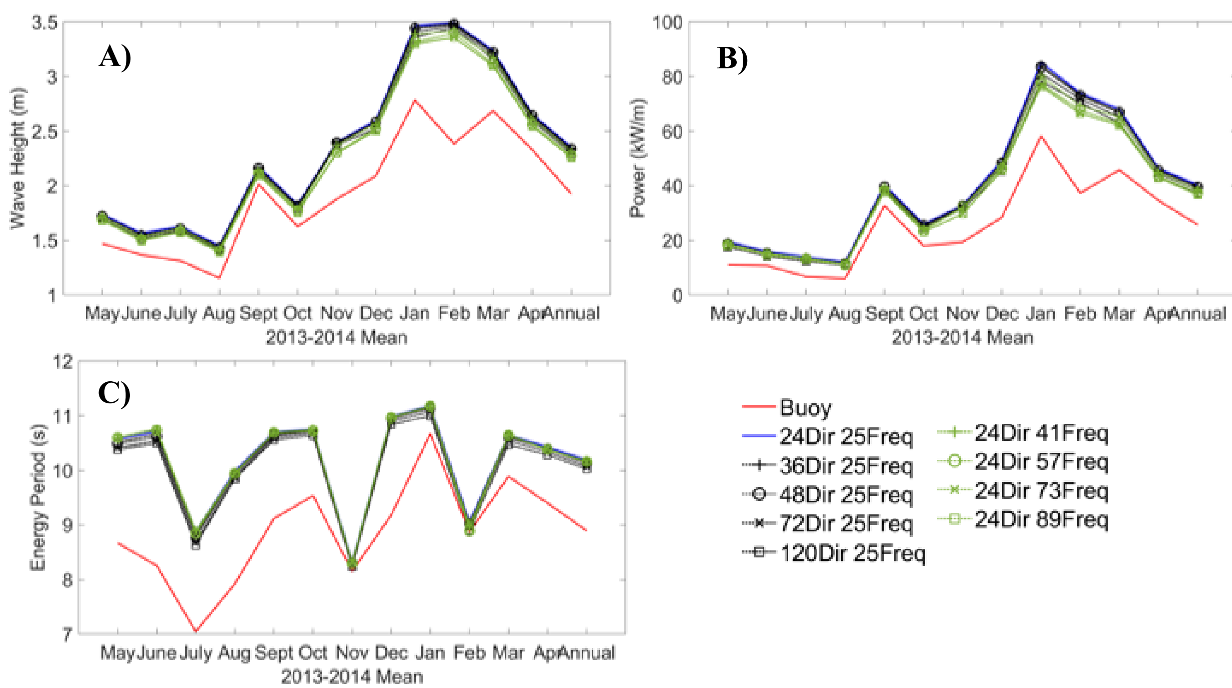

Figure 8.13 – Influence of Spectral Resolution on the Reconnaissance Class Assessment for A) Wave Height; B) Wave Power; C) Energy Period

8.5.2 Reconnaissance Baseline Statistics

When examining the baseline statistics, shown in Table 8.14, it was observed that changes in the frequency and directional resolution had the greatest influence on the wave power and the wave height. This was mainly observed in the model bias for the wave height, and in all parameters except the R^2 value for the wave power. Minimal changes were observed for the energy period, where only a slight improvement was observed. The R^2 values did not change overly for any of the models, indicating that the overall trends haven't changed by modifying the resolutions. Additionally, it was noted that increasing the frequency resolution from the baseline value of 25 bins up to 57 to bins resulted in the greatest improvement, beyond that resolution there was less improvement seen, while computational costs increased. For the directional resolution the largest improvement was observed when increasing the resolution from 48 bins up to 72 bins or 120 bins.

Table 8.14 – Statistics for the Impact of Spectral Resolution on the Reconnaissance Class Assessment for A) Wave Height; B) Wave Power; C) Energy Period

A) Wave Height

		R^2	NB (%)	CvRMSE (%)	SI (%)			R^2	NB (%)	CvRMSE (%)	SI (%)
Directional	36	0.74	21.27	43.66	38.14	*Frequency*	41	0.74	19.67	42.61	37.81
	48	0.74	20.90	43.67	38.35		57	0.76	17.86	39.44	35.17
	72	0.74	19.96	42.97	38.06		73	0.75	17.07	39.30	35.40
	120	0.74	18.83	42.21	37.78		89	0.75	16.89	39.23	35.41

B) Wave Power

		R^2	NB (%)	CvRMSE (%)	SI (%)			R^2	NB (%)	CvRMSE (%)	SI (%)
Directional	36	0.71	53.51	130.51	119.05	*Frequency*	41	0.72	48.75	112.84	112.78
	48	0.71	52.37	129.85	118.84		57	0.74	44.58	113.26	104.13
	72	0.71	48.74	124.91	115.03		73	0.73	42.52	111.83	103.46
	120	0.71	44.41	119.62	111.09		89	0.73	41.76	110.96	102.82

C) Wave Energy Period

		R^2	NB (%)	CvRMSE (%)	SI (%)			R^2	NB (%)	CvRMSE (%)	SI (%)
Directional	36	0.37	14.70	31.97	28.40	*Frequency*	41	0.37	15.03	32.63	29.97
	48	0.38	14.49	31.64	28.13		57	0.36	14.79	32.67	29.14
	72	0.38	13.86	31.15	27.90		73	0.36	14.97	32.69	29.07
	120	0.38	13.26	30.82	27.83		89	0.36	14.83	32.69	29.14

8.5.3 Reconnaissance IEC Errors

The systematic and random errors for the directional and frequency resolution, Figure 8.14 and Figure 8.15 respectively, show similar trends. Increases in the bin resolution result in smaller systematic errors for wave power, minimal changes to the energy period errors, and some changes in the wave height errors, primarily for changes in frequency resolution. For the random error most of the improvement occurs for the wave power, however similar trends are observed as with the systematic error. Additionally, these figures confirm that increases in the frequency resolution have a larger impact on the error for both the wave height and power when compared to the directional resolution.

A)

B)

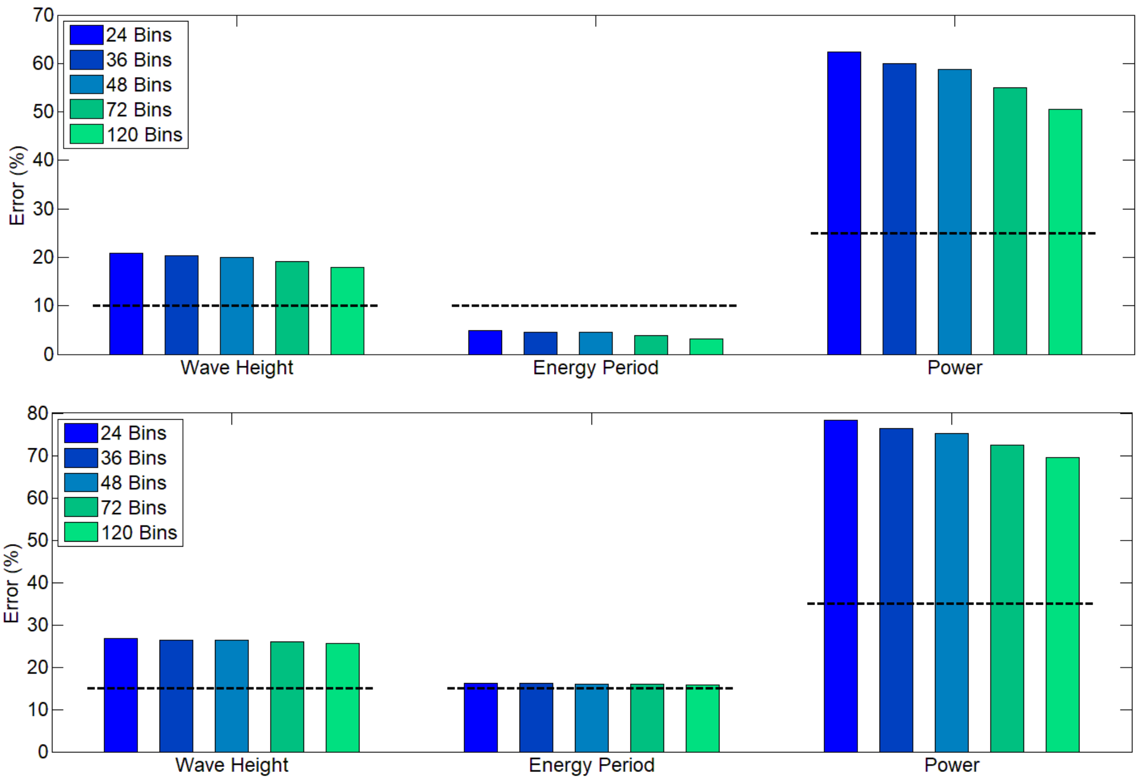

Figure 8.14 – Systematic and Random Errors for the Reconnaissance Class Directional Resolution A) Systematic Errors; and B) Random Errors

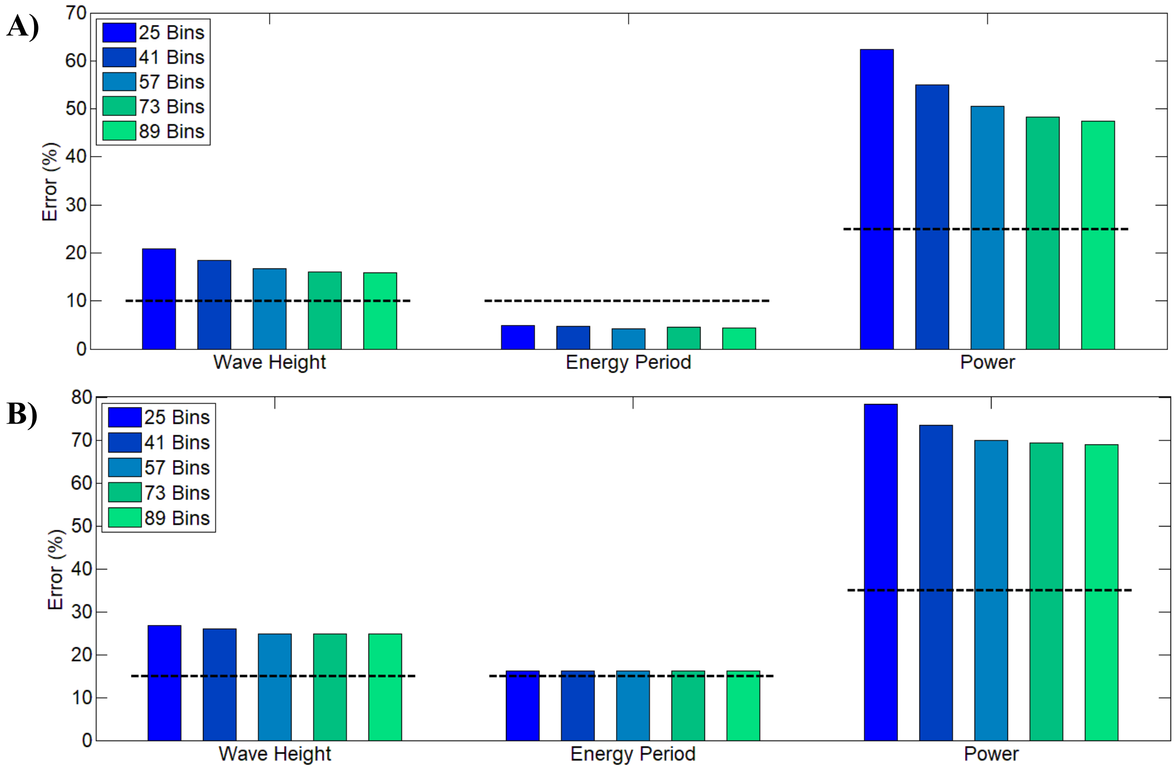

Figure 8.15 – Systematic and Random Errors for the Reconnaissance Class Frequency Resolution A) Systematic Errors; and B) Random Errors

8.5.4 Feasibility Time-History

The baseline resolution used by the feasibility class assessment was a frequency resolution of 41 bins and a directional resolution of 36 bins (direction discretized in 10° increments). To assess the sensitivity of the resource to these two parameters the model resolution was increased incrementally up to 89 frequency bins and 120 directional bins (3° increments), while lower resolutions of 25 frequency bins and 24 directional bins were also examined. These changes were done independent of each other, the combined impact of increasing both the frequency and directional resolution was not assessed.

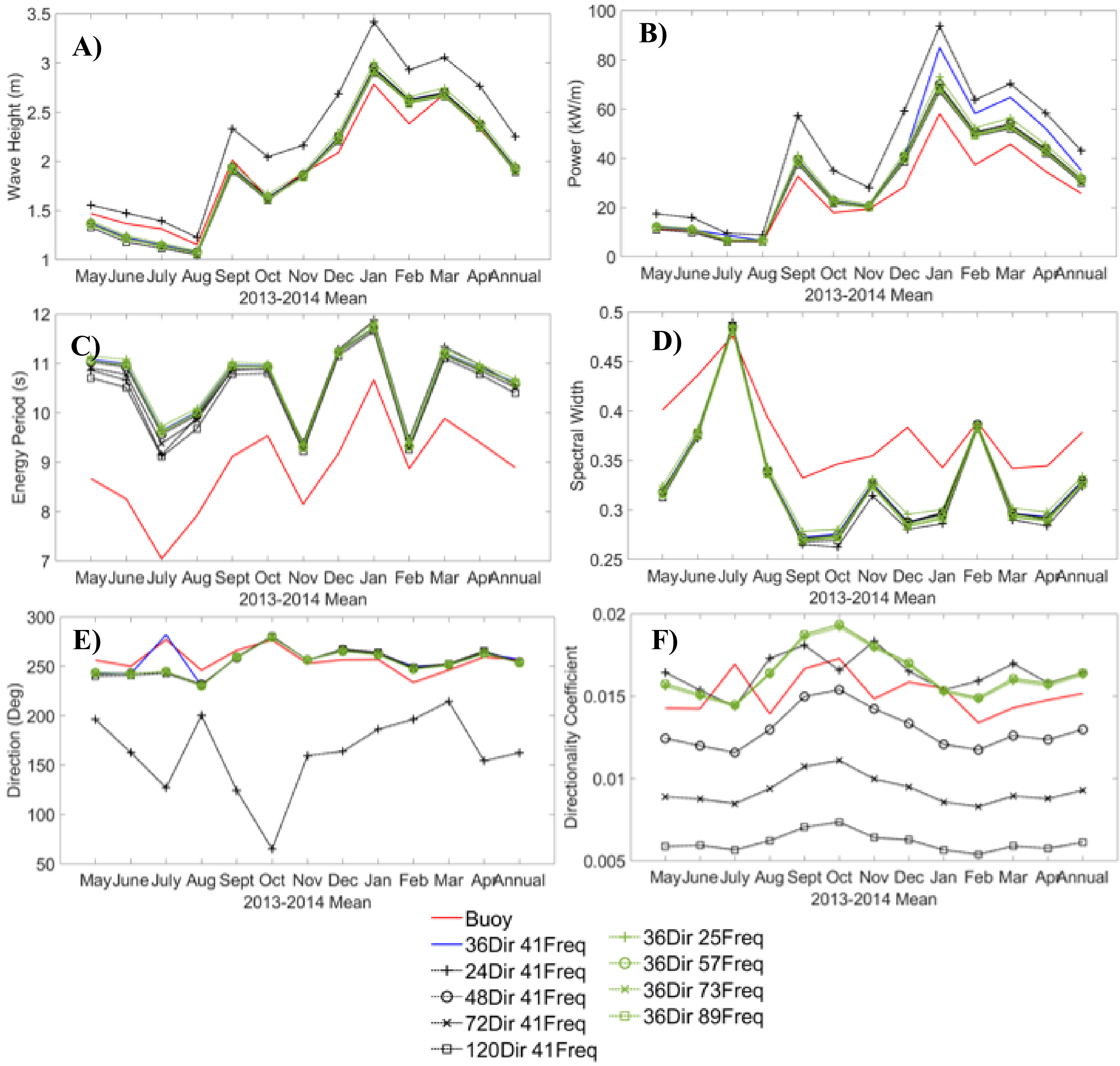

Figure 8.16 – Influence of Spectral Resolution on the Feasibility Class Assessment for A) Wave Height; B) Wave Power; C) Energy Period; D) Spectral Width; E) Direction; F) Directionality Coefficient

When examining the time-histories, Figure 8.16, the main observation was that the use of a 15° directional resolution (24 directional bins) resulted in significant differences in the modeled resources for the wave height, power, and direction. At the time of this analysis the recommended resolution for this class of assessment was 24 bins which means that there is the potential introduction of significant variation in the modeled resource assessment. When looking at the other parameters it appears that the resource assessment is most sensitive to the directional resolution for most of the parameters, but that it is most sensitive to the frequency resolution for the wave power (when excluding the 24 directional resolution scenario).

Excluding the outlier of the 24-bin directional resolution only the energy period and directionality coefficient show and sensitivity to the selection of the resolutions. The energy period shows sensitivity to the directional resolution in the summer months, and the directionality coefficient shows a wide range of values based on the directional resolution.

8.5.5 Feasibility Baseline Statistics

When looking at the baseline statistical parameters, Table 8.15, it was noted that the use of 24 directional resolution bins introduces a significant amount of error into the resource assessment. For this class of resource assessment increases to the directional resolution tended to have a greater impact than increases in the frequency resolution. However, when examining the statistics closely they do not show a significant amount of improvement when increasing the resolution beyond that of the original model, again except for the wave power and directionality coefficient. The model does show that the directional resolution cannot be decreased. The overall conclusion from this analysis is that the baseline resolutions provide a good compromise between accuracy and computational efficiency.

Table 8.15 – Statistics for the Impact of Spectral Resolution on the Feasibility Class Assessment for A) Wave Height; B) Wave Power; C) Energy Period; D) Spectral Width; E) Direction; F) Directionality Coefficient

A) Wave Height

Directional	R^2	NB (%)	CvRMSE (%)	SI (%)	*Frequency*	R^2	NB (%)	CvRMSE (%)	SI (%)
24	0.86	17.13	33.23	28.48	25	0.88	1.96	22.05	21.97
48	0.88	0.20	21.45	21.45	57	0.88	-0.38	21.14	21.15
72	0.88	-0.33	21.36	21.36	73	0.88	-0.75	21.06	21.05
120	0.88	-1.64	21.06	21.00	89	0.88	-1.13	20.96	20.94

B) Wave Power

Directional	R^2	NB (%)	CvRMSE (%)	SI (%)	*Frequency*	R^2	NB (%)	CvRMSE (%)	SI (%)
24	0.79	68.02	152.80	136.85	25	0.80	27.93	96.81	92.71
48	0.80	22.71	90.07	87.17	57	0.80	21.13	87.73	85.17
72	0.80	21.09	88.45	85.91	73	0.80	20.15	86.67	84.31
120	0.81	17.12	84.08	82.33	89	0.80	19.36	85.77	83.57

C) Wave Energy Period

Directional	R^2	NB (%)	CvRMSE (%)	SI (%)	*Frequency*	R^2	NB (%)	CvRMSE (%)	SI (%)
24	0.54	19.02	25.43	16.89	25	0.50	20.53	27.36	18.09
48	0.50	19.41	26.47	18.01	57	0.50	19.62	26.75	18.18
72	0.52	18.61	25.58	17.56	73	0.50	19.53	26.67	18.16
120	0.55	17.23	24.10	16.85	89	0.50	19.55	26.66	18.14

D) Spectral Width

Directional	R^2	NB (%)	CvRMSE (%)	SI (%)	*Frequency*	R^2	NB (%)	CvRMSE (%)	SI (%)
24	0.34	-14.77	32.81	29.30	25	0.33	-12.18	31.68	29.25
48	0.32	-13.49	32.64	29.72	57	0.32	-13.79	32.89	29.87
72	0.33	-13.71	32.49	29.46	73	0.32	-14.20	33.08	29.88
120	0.35	-14.01	32.23	29.03	89	0.32	-14.43	33.20	29.91

E) Direction

Directional	R^2	NB (%)	CvRMSE (%)	SI (%)	*Frequency*	R^2	NB (%)	CvRMSE (%)	SI (%)
24	0.20	41.85	52.78	77.06	25	0.30	-17.02	51.57	52.29
48	0.29	-19.11	51.13	51.70	57	0.30	-15.34	51.49	52.26
72	0.28	-22.45	50.66	51.17	73	0.30	-15.9	51.37	52.15
120	0.27	-22.71	50.04	50.54	89	0.29	-15.28	51.56	52.33

F) Directionality Coefficient

Directional	R^2	NB (%)	CvRMSE (%)	SI (%)	*Frequency*	R^2	NB (%)	CvRMSE (%)	SI (%)
24	0.06	260.6	271.83	77.34	25	0.27	7.23	29.39	28.49
48	0.27	184.9	194.73	61.11	57	0.27	8.04	29.52	28.41
72	0.25	103.9	113.17	44.74	73	0.27	8.17	29.60	28.46
120	0.21	34.80	48.69	31.06	89	0.27	8.24	29.61	28.45

8.5.6 Feasibility IEC Errors

The systematic and random errors for the directional and feasibility resolution are shown in Figure 8.17 and Figure 8.18, respectively. For the direction resolution the response of the model to the lowered resolution to 24 directional bins is very clear. This results in a large increase in error for the systematic errors for the wave height, power, and direction, as well as a large increase in error for the random error in direction. When looking at the systematic error there is a reduction in error for increased resolution for the power, while the opposite is true for the directional resolution. Energy Period, wave height, spectral width, and direction are not largely impacted. The random error appears to have similar trends though they are much less impacted by changes in the resolution. These trends tend to agree relatively well with the trends observed in the statistics and the time-histories.

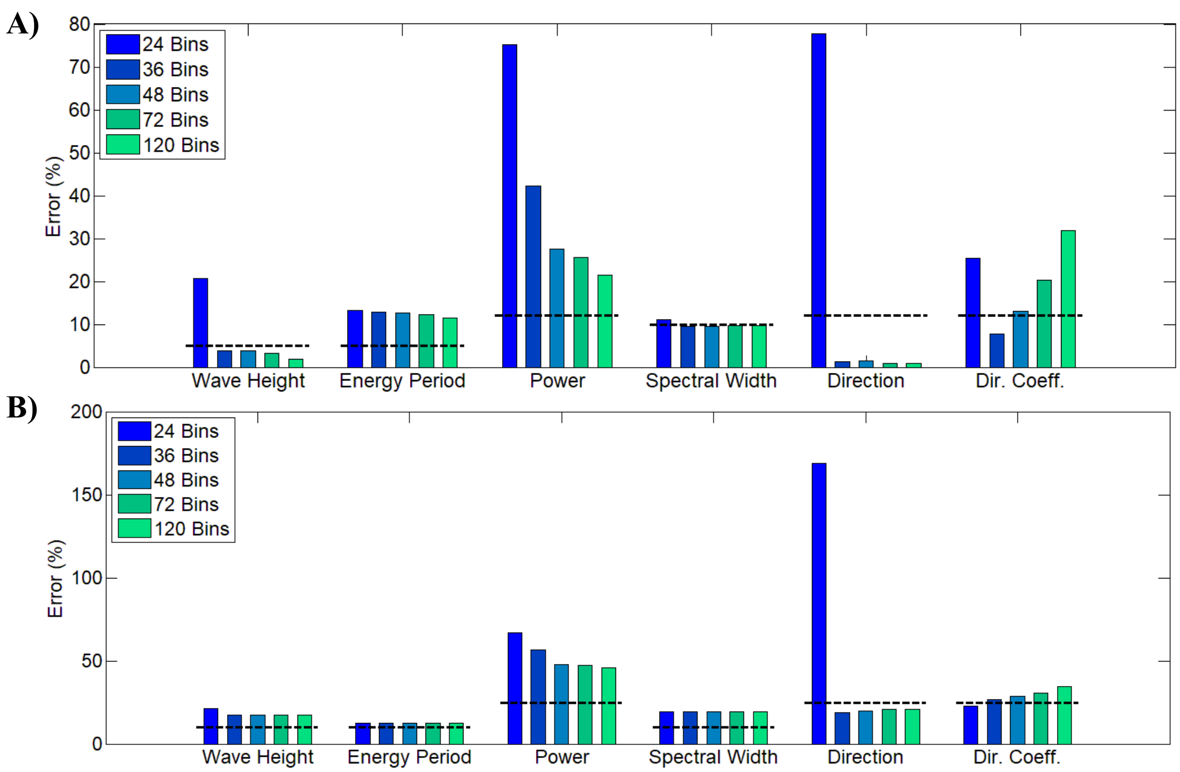

Figure 8.17 – Systematic and Random Errors for the Feasibility Class Directional Resolution A) Systematic Errors; and B) Random Errors (Direction Error is in Deg.)

For the frequency resolution it was observed that increases in the bin resolution decreased the systematic error for the wave height, and power. But increased the systematic error for the spectral width and to a much lesser degree the directionality coefficient. No difference is really seen in the direction or the energy period for all but the lowest resolution. For the random error the resolution appears to have very little influence on the error except in the case of power. The trends in power do appear to be a bit unusual, with the baseline frequency bins having a larger systematic error. This does not seem to be consistent with the statistics determined in the previous section which show that the lowest frequency scenario is the one with the highest errors.

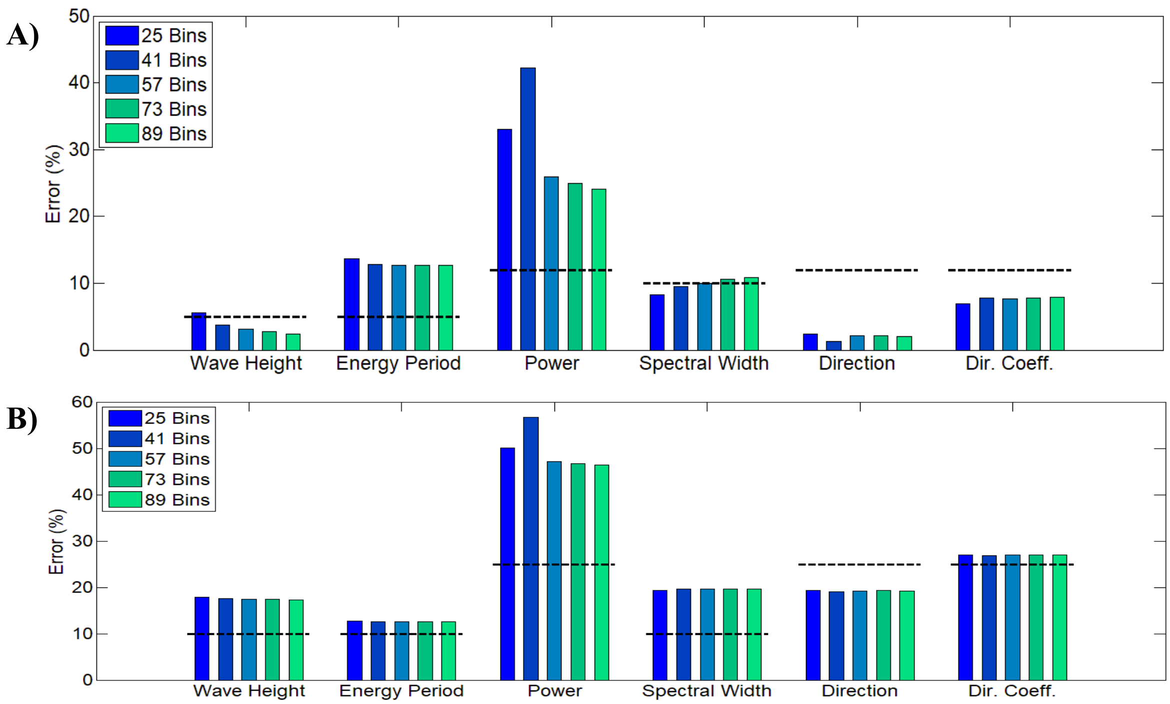

Figure 8.18 – Systematic and Random Errors for the Feasibility Class Frequency Resolution A) Systematic Errors; and B) Random Errors (Direction Error is in Deg.)

8.5.7 Design Time-History

Finally, the baseline resolution used by the design class assessment was a frequency resolution of 41 bins and a directional resolution of 48 bins (direction discretized in 7.5° increments). To assess the sensitivity of the resource to these two parameters the model resolution was increased incrementally from 25 to 57 frequency bins and from 36 to 72 directional bins (10° resolution up to 5° resolution). Due to the resolution of the model a smaller range of values were tested due to the computational cost. These changes were performed independently of each other, the combined impact of increasing both the frequency and directional resolution was not assessed.

When examining the results in Figure 8.19, it was observed that there was some sensitivity in the modeled resource, primarily for the direction and directionality coefficient where sensitivity was noted for both the directional resolution and frequency resolution. Some sensitivity was also noted in the winter and spring months for the frequency resolution in the wave height and power. In general, it appeared that increasing the resolution beyond the baseline values used did not result in significant improvement to the resources assessment. Overall, when averaged over the year, the parameters were all fairly consistent regardless of the resolution selected.

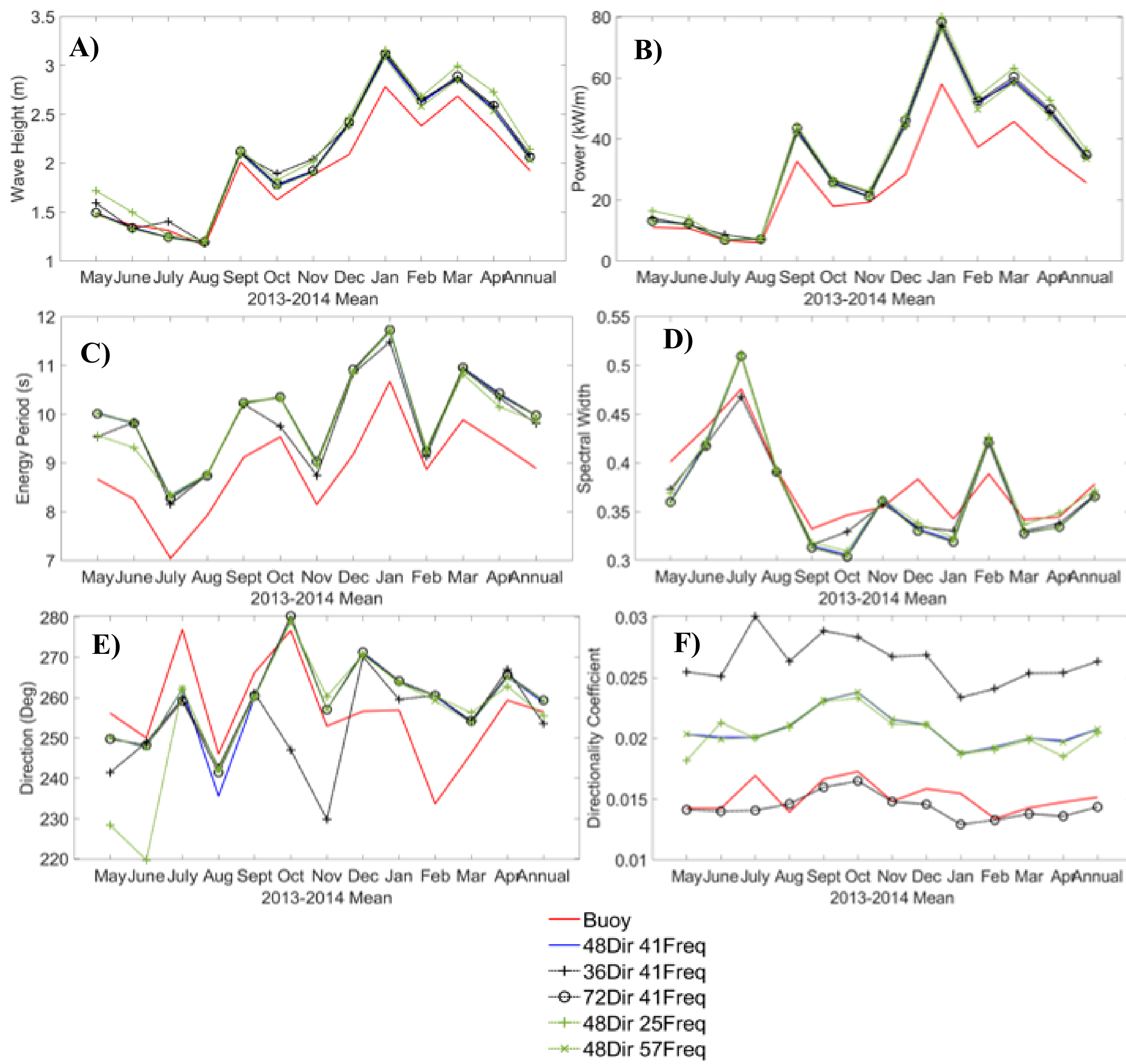

Figure 8.19 – Influence of Spectral Resolution on the Design Class Assessment for A) Wave Height; B) Wave Power; C) Energy Period; D) Spectral Width; E) Direction; F) Directionality Coefficient

8.5.8 Design Baseline Statistics

When examining the baseline statistical parameters, shown in Table 8.16, it was observed that the directional resolution did not have a significant impact on the resource assessment except in the case of the direction and directionality coefficient, and some slight variation in the R^2 value for the energy period. Beyond those parameters, changes in the bias were typically under 3%, while for the root means square error and scatter index it was observed that there were slightly lower values, especially for the wave power. For the frequency resolution, it was observed that reducing the resolution to 25 bins tended to introduce error into the model, while increasing the resolution to 57 bins had minimal impact.

8.5.9 Design IEC Errors

The systematic and random errors are presented for the design class of assessment in Figure 8.20 and Figure 8.21 for the directional resolution and frequency resolution, respectively. For the directional resolution the errors were relatively similar for the systematic error except for the directionality coefficient which exhibited increasing errors as the resolution increased. For the random error a bit more variation was observed in the errors, with 48 directional bins typically providing the lowest error values. Unlike previous estimates it appears that the random error shows more sensitivity to the model parameter than the systematic error.

For the frequency resolution the 25-bin resolution does appear to have an influence on the systematic error and random errors. Though in the case of the directionality coefficient and the energy period it does appear that the error is lower for the systematic error. The difference between the 41 and 57 bin resolutions is only notable in the case of the wave height and power for the systematic error. Again, the systematic error does appear to be less sensitive to variations of the frequency resolution.

Table 8.16 – Statistics for the Impact of Spectral Resolution on the Design Class Assessment for A) Wave Height; B) Wave Power; C) Energy Period; D) Spectral Width; E) Direction; F) Directionality Coefficient

A) Wave Height

Directional	R^2	NB (%)	CvRMSE (%)	SI (%)	*Frequency*	R^2	NB (%)	CvRMSE (%)	SI (%)
36	0.83	7.84	26.50	25.32	25	0.83	10.38	28.49	26.53
72	0.84	6.30	26.77	26.02	57	0.86	5.78	23.92	23.21

B) Wave Power

Directional	R^2	NB (%)	CvRMSE (%)	SI (%)	*Frequency*	R^2	NB (%)	CvRMSE (%)	SI (%)
36	0.78	32.92	103.71	98.35	25	0.77	40.64	114.34	106.87
72	0.78	34.40	109.27	103.72	57	0.78	30.98	102.91	98.15

C) Wave Energy Period

Directional	R^2	NB (%)	CvRMSE (%)	SI (%)	*Frequency*	R^2	NB (%)	CvRMSE (%)	SI (%)
36	0.51	9.67	19.72	17.18	25	0.52	10.21	19.96	17.15
72	0.52	11.51	20.78	17.30	57	0.63	12.31	18.65	14.00

D) Spectral Width

Directional	R^2	NB (%)	CvRMSE (%)	SI (%)	*Frequency*	R^2	NB (%)	CvRMSE (%)	SI (%)
36	0.35	-4.00	27.50	27.21	25	0.37	-1.46	17.80	17.74
72	0.35	-4.54	29.02	28.67	57	0.37	-3.61	27.70	27.47

E) Direction

Directional	R^2	NB (%)	CvRMSE (%)	SI (%)	*Frequency*	R^2	NB (%)	CvRMSE (%)	SI (%)
36	0.22	-102.2	62.69	62.64	25	0.21	74.68	62.33	62.28
72	0.24	-72.30	53.16	53.13	57	0.27	110.1	56.38	56.27

F) Directionality Coefficient

Directional	R^2	NB (%)	CvRMSE (%)	SI (%)	*Frequency*	R^2	NB (%)	CvRMSE (%)	SI (%)
36	0.21	29.17	45.74	35.24	25	0.23	33.42	48.00	34.45
72	0.27	-29.71	40.26	27.17	57	0.28	36.46	48.52	32.01

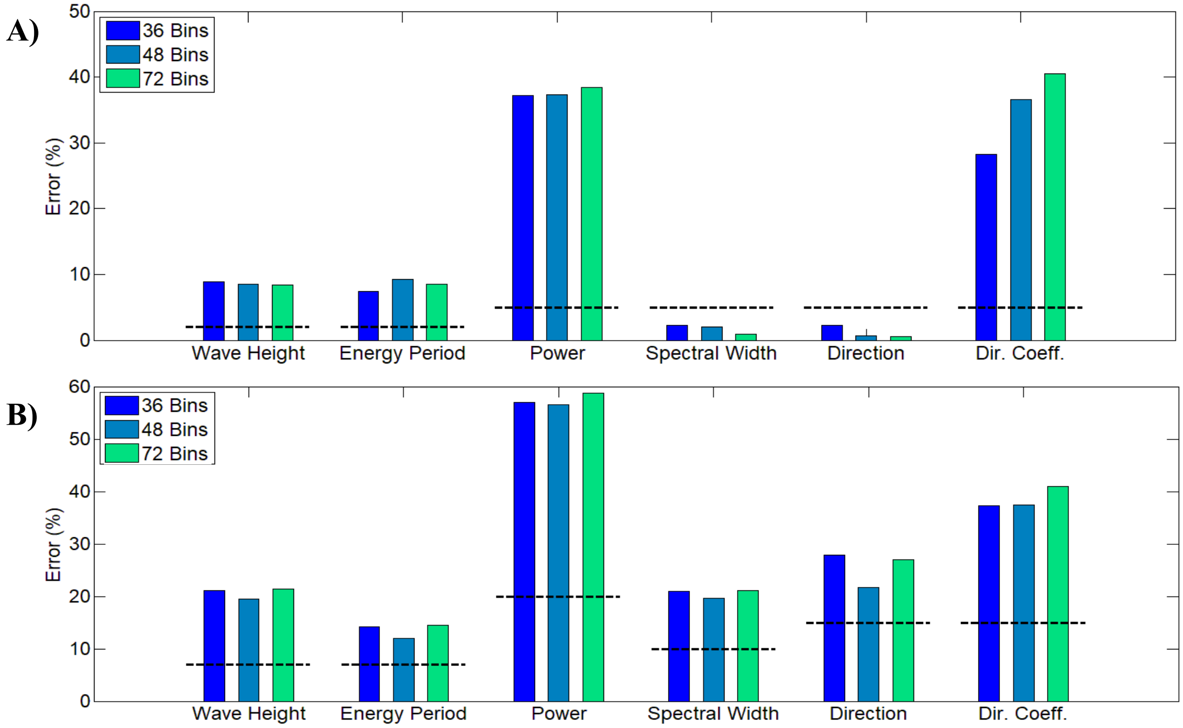

Figure 8.20 – Systematic and Random Errors for the Design Class Directional Resolution A) Systematic Errors; and B) Random Errors (Direction Error is in Deg.)

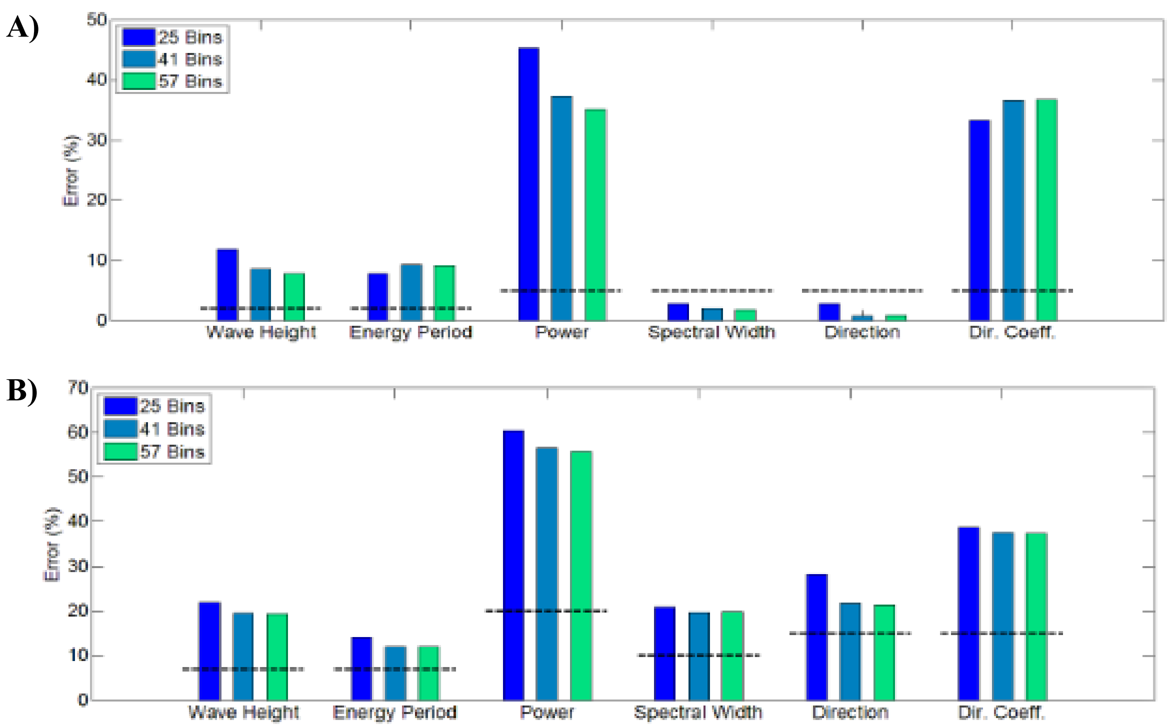

Figure 8.21 – Systematic and Random Errors for the Design Class Frequency Resolution A) Systematic Errors; and B) Random Errors (Direction Error is in Deg.)

8.5.10 Model Sensitivity

This section shows the sensitivity of the modeled wave height and power to changes in the spectral resolution. Table 8.17 shows the model sensitivity to the frequency resolution, relative to the baseline resolution, while Table 8.18 shows the model sensitivity to the directional resolution, relative to the baseline resolution. In addition to these comparisons with the baseline model the sensitivity to incremental changes in the resolution was also examined, these results are shown in, Table 8.19 and Table 8.20. These two tables only show the results for the reconnaissance and feasibility class assessments as it was not necessary for the design class.

The model sensitivity to the frequency resolution, Table 8.17, indicates that the reconnaissance class model was sensitive to all changes in resolution with respect to the baseline model, except for the 41-bin resolution for the wave heights, based on the IEC-TS sensitivity characterization. When using the new recommendation for sensitivity characterization the modeled wave height was observed to become more sensitive to changes in the frequency resolution as the resolution increased, as did the wave power. For the feasibility class assessment, the model was not found to be sensitive to increases or decreases in the resolution for the wave height or the wave power. Finally, for the design class assessment, it was observed that the model was sensitive to all changes in the spectral resolution, based on both the existing IEC characterization, but was not sensitive to increases based on the proposed methodology.

The model sensitivity to the directional resolution, Table 8.18, indicates that the reconnaissance class model was sensitive only to increases in the resolution up to 72 bins for power, and 120 bins for both the wave power and height. This tends to agree with the observations previously made that indicated that the reconnaissance class model was more sensitive to the frequency resolution rather than the directional resolution. For both the feasibility and design class assessments the models were found to be sensitive to decreases in the resolution for both methods of characterization. Some differences in results were observed for the 48-bin feasibility assessment and 72 bin design assessment which were found to be sensitive with the IEC-TS characterization but not with the new recommendation. Similar to the reconnaissance class assessment, these general observations due tend to agree with the trends observed previously.

Table 8.17 – Sensitivity of Model to Frequency Resolution for all Classes of Resource Assessment when compared to the Baseline Model for A) IEC TS Recommendation; and B) New Recommendation

		41	57	73	89
Reconnaissance	Wave Height	A) Not Sensitive B) Not Sensitive	A) Sensitive B) Not Sensitive	A) Sensitive B) Partially Sensitive	A) Sensitive B) Sensitive
	Power	A) Sensitive[1] B) Not Sensitive	A) Sensitive B) Partially Sensitive	A) Sensitive B) Sensitive	A) Sensitive B) Sensitive
		25	**57**	**73**	**89**
Feasibility	Wave Height	A) Not Sensitive B) Not Sensitive	A) Not Sensitive B) Not Sensitive	A) Not Sensitive B) Not Sensitive	A) Not Sensitive B) Not Sensitive
	Power	A) Sensitive B) Not Sensitive	A) Sensitive B) Sensitive	A) Sensitive B) Sensitive	A) Sensitive B) Sensitive
		25	**57**		
Design	Wave Height	A) Sensitive B) Sensitive	A) Sensitive B) Not Sensitive		
	Power	A) Sensitive B) Sensitive	A) Sensitive B) Not Sensitive		

[1]Parameter is sensitive in 5.14% of the cells which is marginally above the maximum threshold of 5%

Table 8.19 shows the sensitivity of the model to incremental increases in the frequency resolution for the reconnaissance and feasibility class assessments. From this table, it was observed that the reconnaissance class was not sensitive to these small incremental changes in resolution. While the feasibility model was not sensitive for the wave height. In the case of the wave power, it was observed that the feasibility was not sensitive to changes in resolution with the potential exception of going from 41 to 57 bins. For this comparison the sensitivity of the model was dependent on the criteria used for assessment.

Table 8.18 – Sensitivity of Model to Directional Resolution for all Classes of Resource Assessment when compared to the Baseline Model for A) IEC TS Recommendation; and B) New Recommendation

		36	48	72	120
Reconnaissance	Wave Height	A) Not Sensitive B) Not Sensitive	A) Not Sensitive B) Not Sensitive	A) Not Sensitive B) Not Sensitive	A) Sensitive B) Sensitive
	Power	A) Not Sensitive B) Not Sensitive	A) Not Sensitive B) Not Sensitive	A) Sensitive B) Partially Sensitive	A) Sensitive B) Sensitive
		24	**48**	**72**	**120**
Feasibility	Wave Height	A) Sensitive B) Sensitive	A) Not Sensitive B) Not Sensitive	A) Not Sensitive B) Not Sensitive	A) Sensitive B) Sensitive
	Power	A) Sensitive B) Sensitive	A Sensitive B) Not Sensitive	A) Sensitive B) Sensitive	A) Sensitive B) Sensitive
		36	**72**		
Design	Wave Height	A) Sensitive B) Sensitive	A) Sensitive[2] B) Not Sensitive		
	Power	A) Sensitive B) Sensitive	A) Sensitive B) Not Sensitive		

[2] Parameter is sensitive in 1.16% of the cells which is marginally above the maximum threshold of 1%

Table 8.20 shows the sensitivity of the model to incremental increases in the directional resolution for the reconnaissance and feasibility class assessments. These results show that the reconnaissance class assessment model was not sensitive to incremental increases in the model. For the feasibility class assessment, the model was found to be sensitive to changes in resolution from 24 bins to 36 bins which was represented fairly well in the statistics and time-histories. However, model sensitivity was also noted when increasing the resolution from 72 bins to 120 bins when using the IEC-TS characterization method. This is supported by observations made in the IEC-TS errors and the baseline statistics; however, this variation was considered within the bounds of acceptability when using the newly recommended characterization criteria.

Table 8.19 – Sensitivity of Model to Frequency Resolution for Reconnaissance and Feasibility Classes of Resource Assessment for Incremental Increases in Resolution for A) IEC TS Recommendation; and B) New Recommendation

		25 to 41	41 to 57	57 to 73	73 to 89
Reconnaissance	Wave Height	A) Not Sensitive B) Not Sensitive	A) Not Sensitive B) Not Sensitive	A) Not Sensitive B) Not Sensitive	A) Not Sensitive B) Not Sensitive
	Power	A) Not Sensitive B) Not Sensitive	A) Not Sensitive B) Not Sensitive	A) Not Sensitive B) Not Sensitive	A) Not Sensitive B) Not Sensitive
		25 to 41	41 to 57	57 to 73	73 to 89
Feasibility	Wave Height	A) Not Sensitive B) Not Sensitive	A) Not Sensitive B) Not Sensitive	A) Not Sensitive B) Not Sensitive	A) Not Sensitive B) Not Sensitive
	Power	A) Sensitive B) Not Sensitive	A) Sensitive B) Sensitive	A) Not Sensitive B) Not Sensitive	A) Not Sensitive B) Not Sensitive

[1]Parameter is sensitive in 5.43% of the cells which is marginally above the maximum threshold of 5%

Table 8.20 – Sensitivity of Model to Directional Resolution for Reconnaissance and Feasibility Classes of Resource Assessment for Incremental Increases in Resolution for A) IEC TS Recommendation; and B) New Recommendation

		24 to 36	36 to 48	48 to 72	72 to 120
Reconnaissance	Wave Height	A) Not Sensitive B) Not Sensitive	A) Not Sensitive B) Not Sensitive	A) Not Sensitive B) Not Sensitive	A)Not Sensitive B) Not Sensitive
	Power	A) Not Sensitive B) Not Sensitive	A) Not Sensitive B) Not Sensitive	A) Not Sensitive B) Not Sensitive	A)Not Sensitive B) Not Sensitive
		24 to 36	36 to 48	48 to 72	72 to 120
Feasibility	Wave Height	A) Sensitive B) Sensitive	A) Not Sensitive B) Not Sensitive	A) Not Sensitive B) Not Sensitive	A) Sensitive B) Not Sensitive
	Power	A) Sensitive B) Sensitive	A) Not Sensitive B) Not Sensitive	A) Not Sensitive B) Not Sensitive	A) Sensitive B) Not Sensitive

8.6 Influence of Wind Resolution

The impact of wind resolution on the modeled resource was examined for both the reconnaissance and design class assessments. The resolution selected for this analysis are shown in Table 8.21.

Table 8.21 – Wind Resolution Sensitivity Analysis Runs

Run Number	Wind Input Type (km)	Temporal Resolution (hrs)
Recon_Baseline	Constant	3
Recon_Wind_1	N/A	3
Recon_Wind_2	40 x 60 grid	3
Design_Baseline	25 x 25 grid	1
Design_Wind_1	50 x 50 grid	1

8.6.1 Time-History

For the reconnaissance class assessment, the modeled time-histories, Figure 8.22, show that the selected wind resolution has an impact on the modeled resource. It was found that a constant wind, which was the baseline scenario, resulted in over estimations of the wave height and power, and the best estimate of the energy period, while the scenario with no wind was found to have the opposite results. This would indicate that a varying wind resolution might be the best compromise, which was confirmed by the model results. The difference in the modeled wave height and power does seem to be impacted by the season, as the variation was larger in the winter months. This is not surprising as the winds in the region tend to be higher in the winter months and so using a constant wind would potentially result in a more significant over estimation of the wind across the domain. These observations support that the reconnaissance class assessment is potentially sensitive to the wind resolution. The results of this analysis are site specific as they are based on the variability of the wind across the domain. In locations such as this, it is apparent that a fine wind mesh is necessary, however in locations with a uniform wind this may not be necessary.

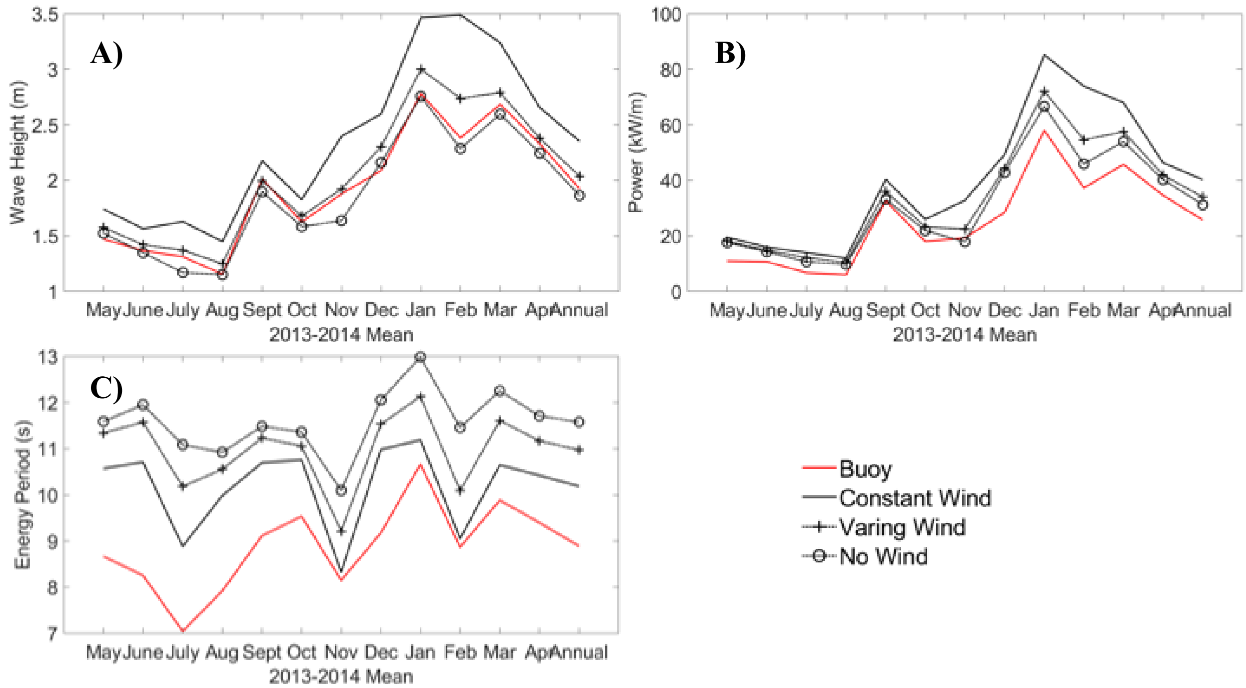

Figure 8.22 – Influence of Wind Resolution on the Reconnaissance Class Assessment for A) Wave Height; B) Wave Power; C) Energy Period

The average monthly and yearly time-histories for the design class assessment, shown in Figure 8.23, indicate that there is minimal sensitivity to the wind resolution in all assessment parameters. The largest impact was found during the summer months around June and July, however even this is minimal. This is a result of the relatively small domain of the design class assessment. Over a smaller domain such as this it is less likely to have large variations in the wind speed and direction; additionally, the model fetch is much smaller, meaning that there is not a large area for the wind-waves to build up over the domain. These considerations mean that the impact of the higher resolution wind mesh is negligible. Similar to the reconnaissance class assessment, the results of this analysis could vary based on location, as highly localized wind variations or a larger region may necessitate a finer wind mesh resolution.

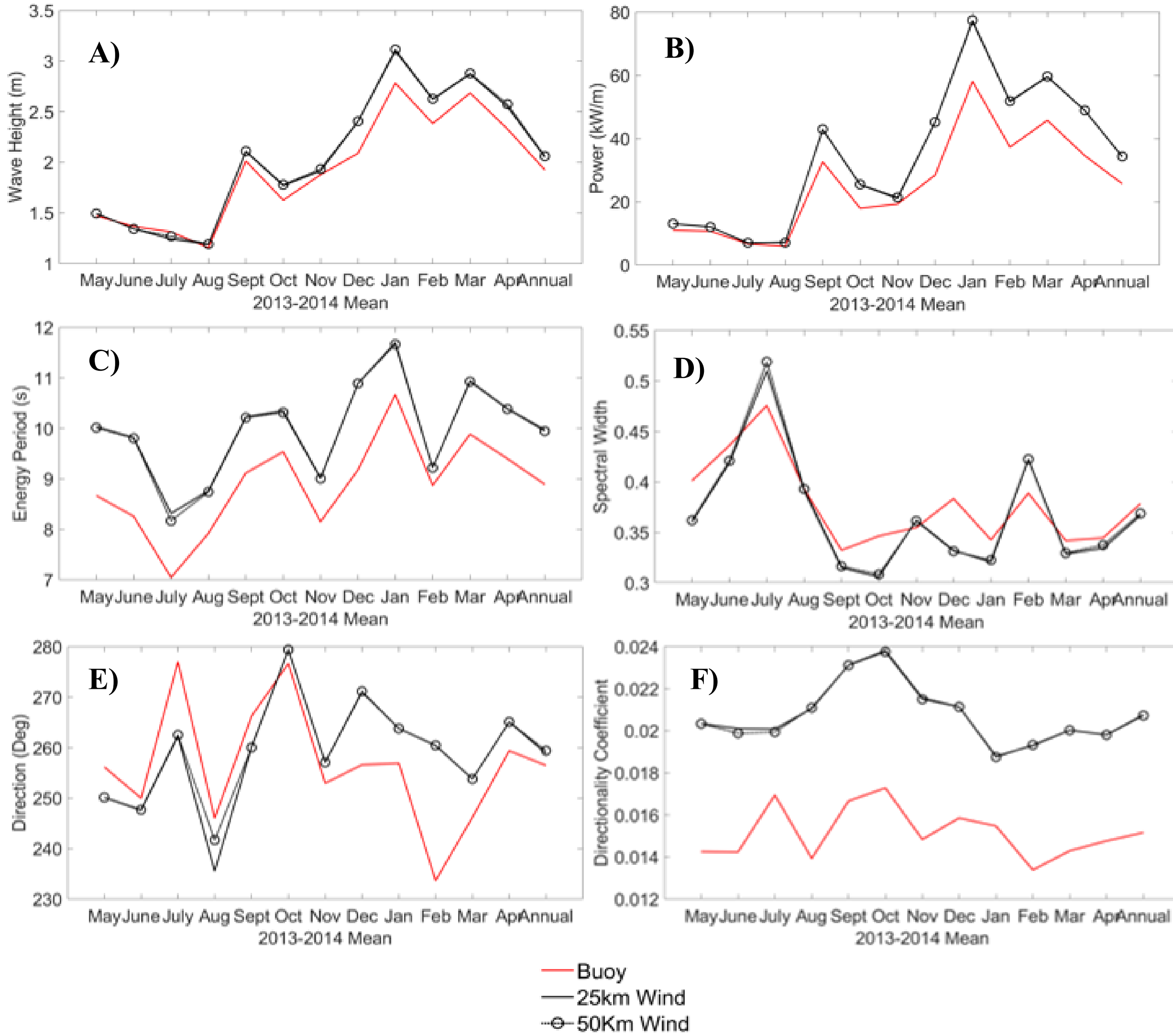

Figure 8.23 – Influence of Wind Resolution on the Design Class Assessment for A) Wave Height; B) Wave Power; C) Energy Period; D) Spectral Width; E) Direction; F) Directionality Coefficient

8.6.2 Baseline Statistics

The baseline statistics for the wind resolutions are shown in Table 8.22. When looking at the statistics for the reconnaissance class assessment it was observed that both no wind and variable wind resulted in better estimations of the wave height and wave power when compared to the constant wind. For the wave energy period the opposite was true, with the constant wind providing the best estimate This confirms that the wind selected to represent the conditions across the domain overestimated the scale of the wind, and that the use of a variable wind mesh would be better able to capture the localized wind patterns. The fact that the using no wind also resulted in a more accurate assessment can be used as an indication that overall, the wind speed across the domain was not significant with respect to the wave resource.

In the case of the design class assessment, very little was observed in the statistics for any of the resource parameters, with the largest differences occurring for the wave direction. This confirms that there was little variation in the wind field across this smaller domain, and, as such, there was little impact from the wind resolution on the resource assessment.

Table 8.22 – Statistics for the Impact of the Wind Resolution on A) Wave Height; B) Wave Power; C) Energy Period; D) Spectral Width; E) Direction; F) Directionality Coefficient

A) Wave Height

		R^2	NB (%)	CvRMSE (%)	SI (%)
Reconnaissance	No Wind	0.77	-2.68	26.09	25.95
Reconnaissance	40 x 60	0.84	5.89	24.05	23.32
Design	50 x 50	0.86	6.96	24.53	23.52

B) Wave Power

		R^2	NB (%)	CvRMSE (%)	SI (%)
Reconnaissance	No Wind	0.73	22.42	87.68	84.78
Reconnaissance	40 x 60	0.76	32.51	92.05	86.14
Design	50 x 50	0.78	33.55	106.17	100.73

C) Wave Energy Period

		R^2	NB (%)	CvRMSE (%)	SI (%)
Reconnaissance	No Wind	0.23	30.55	40.79	27.03
Reconnaissance	40 x 60	0.31	23.96	36.51	27.57
Design	50 x 50	0.64	12.13	18.54	14.02

D) Spectral Width

		R^2	NB (%)	CvRMSE (%)	SI (%)
Design	50 x 50	0.37	-2.87	27.65	27.50

E) Direction

		R^2	NB (%)	CvRMSE (%)	SI (%)
Design	50 x 50	0.28	111.2	56.47	56.35

F) Directionality Coefficient

		R^2	NB (%)	CvRMSE (%)	SI (%)
Design	50 x 50	0.28	36.15	48.28	32.01

8.6.3 IEC Errors

Figure 8.24 shows the systematic and random errors for the reconnaissance class assessment. From this figure it can be observed that while the constant wind is able to provide the best systematic error and comparable random error for the wave energy period, it results in the highest error for both the wave height and power. Alternatively, using no wind provides the best estimate for the wave height and the wave power, but the highest error for the energy period. This appears at odds to the statistical assessment of the models, where the varying wind provides the highest R^2 value, and the lowest error and scatter index, however, the systematic error is a measure of the bias which results in the no wind case providing the lower error. Both models show similar random errors with the model with no wind having marginally lower error values.

When examining the impact of the wind resolution on the design class assessment, Figure 8.25, it was observed that the errors are all very similar. This supports all previous observations that the design class assessment was not sensitive to the wind resolution.

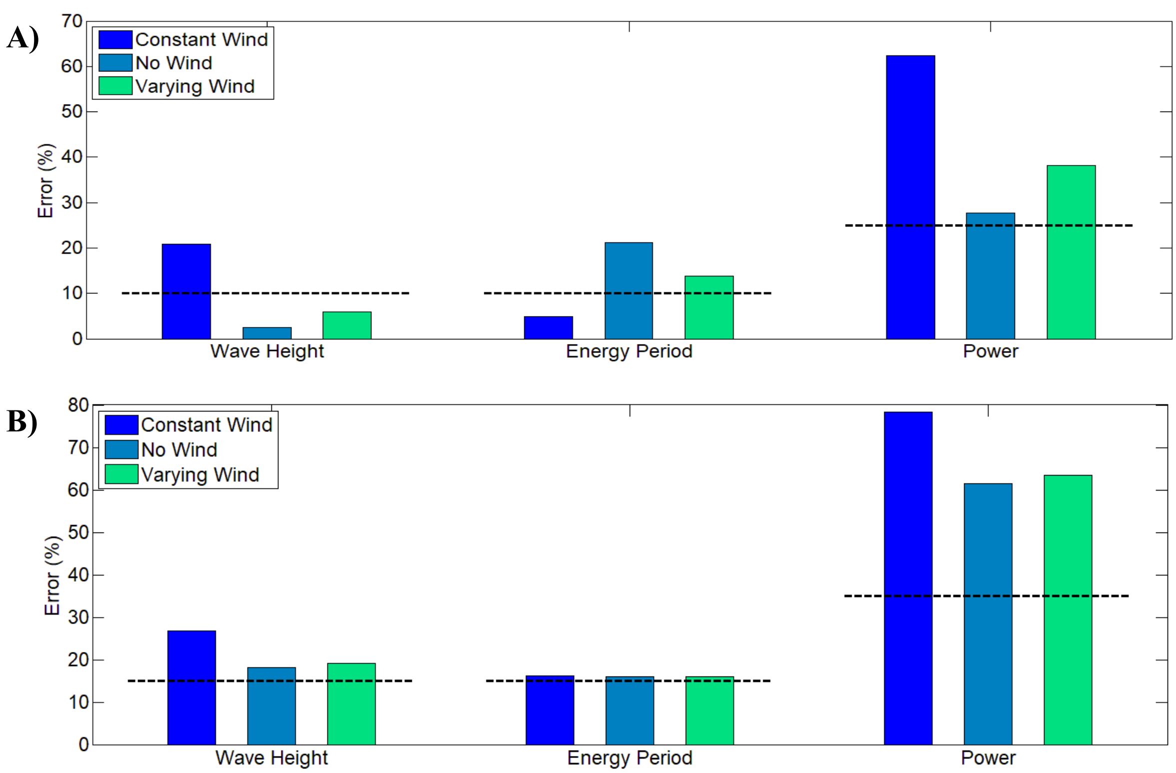

Figure 8.24 – Systematic and Random Errors for the Reconnaissance Class Wind Resolution A) Systematic Errors; and B) Random Errors

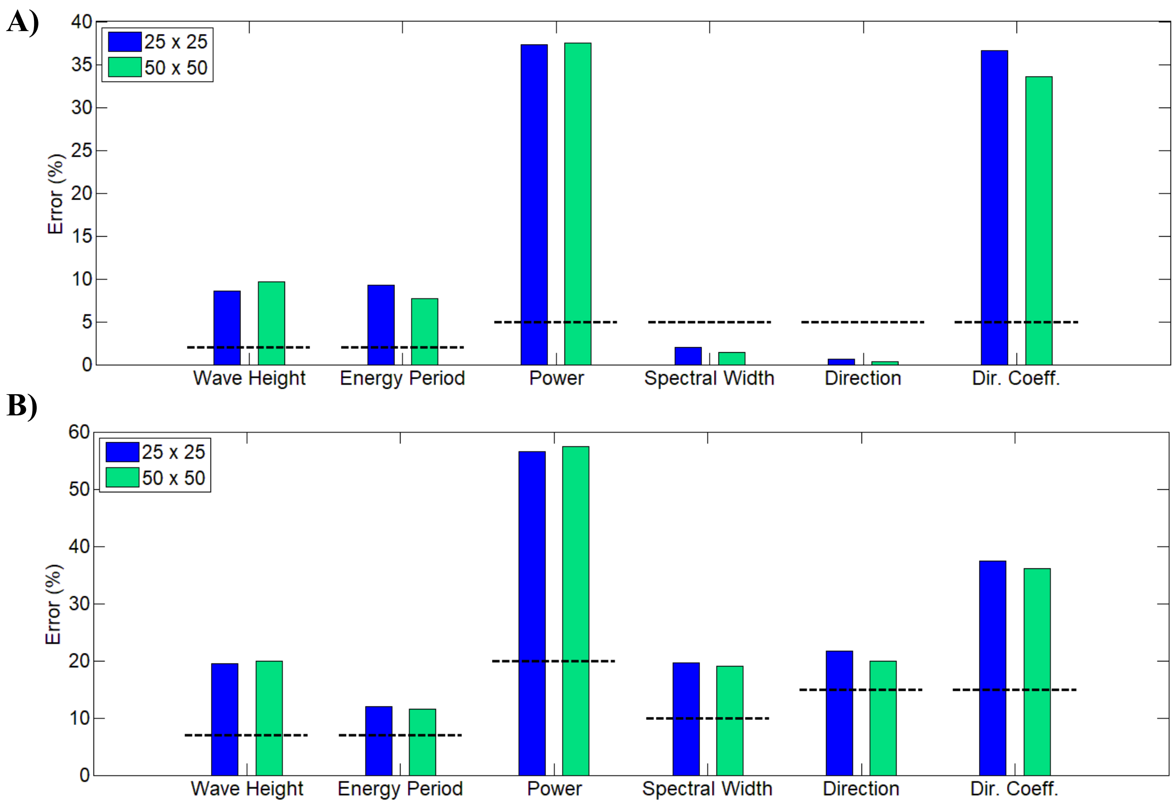

Figure 8.25 – Systematic and Random Errors for the Design Class Wind Resolution A) Systematic Errors; and B) Random Errors (Direction Error is in Deg.)

8.6.4 Model Sensitivity

This section shows the sensitivity of the modeled wave height and power to changes in the wind resolution. In Table 8.23 both models were considered sensitive to changes in the wind resolution based on the IEC-TS recommendation. While this observation is supported for the reconnaissance class assessment, where large variation in the statistics and IEC errors were observed it is not supported for the design class assessment. Similar to observations made about the sensitivity of the mesh resolution, this appears to be a result of the low sensitivity threshold. When using the newly recommended characterization criteria, the design class assessment was not found to be sensitive to the wind resolution for the wave power, though it still was for the wave height.

Table 8.23 - Sensitivity of Model to Direction Resolution for the Reconnaissance and Design Class Assessments with Respect to the Baseline Model for A) IEC TS Recommendation; and B) New Recommendation

		No Wind	Variable
Reconnaissance	Wave Height	A) Sensitive B) Sensitive	A) Sensitive B) Sensitive
	Power	A) Sensitive B) Sensitive	A) Sensitive B) Sensitive
		50 x 50m	
Design	Wave Height	A) Sensitive B) Sensitive	
	Power	A) Sensitive B) Not Sensitive	

8.7 Characterization of Sensitivity

This section examines the characterization of the model sensitivity as per the IEC-TS recommendations. The purpose of this is to determine the advantages and disadvantages of this method and to propose a new methodology that improves upon these. To do this examination a single case from each class of assessment was used as a test.

The original IEC-TS sensitivity characterization was conducted using three random sample time periods for each significant wave state (defined as wave states with a relative frequency of occurrence greater than 0.1%). This was compared to the newly proposed method which instead uses every value within the significant wave states, and an additional test method which only used one random sample time period for each significant wave state. Both randomized samples were completed three times to assess the -range of sensitivity values that could be obtained

8.7.1 Reconnaissance Case Study

For the reconnaissance class assessment, the model selected for this case study was the 2,500 m mesh resolution, as it was determined that the model was sensitive to the wave power but was sensitive to the wave height only by a small margin.

The results of this case study are shown in Figure 8.26, they indicate that a large spread of values can be obtained depending on the points randomly selected from each wave state. In the case of the wave power the model was found to always be sensitive to this change in resolution, though not necessarily by a large factor. In the case of the wave height the model sensitivity ranged from sensitive to not sensitive even when using the same number of random sample points. When you consider the actual average error instead of the number of bins with errors above the threshold the range of values obtained is smaller.

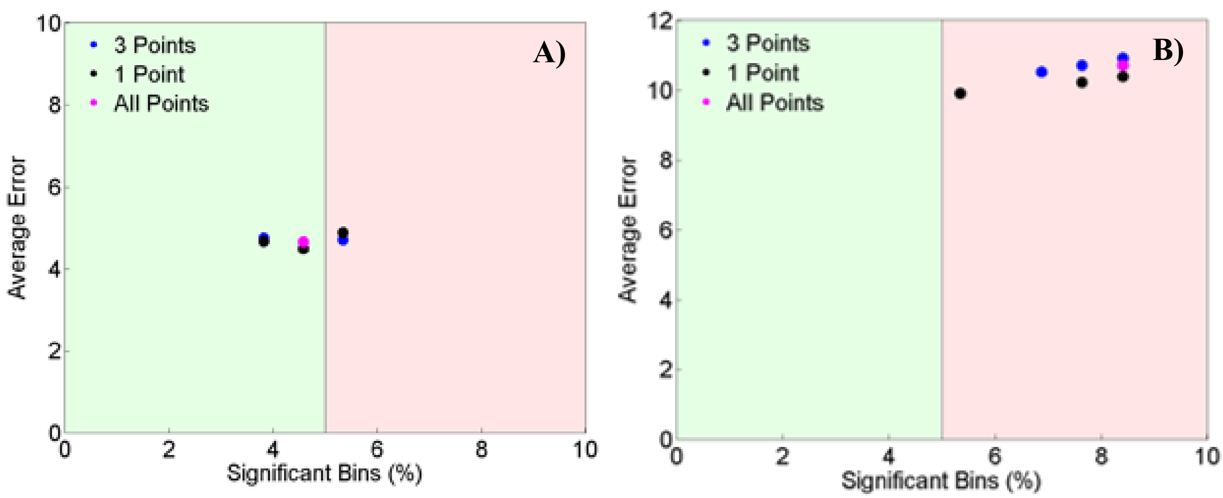

Figure 8.26 – Percentage of Significant Bins VS the Average Error for A) Wave Height; and B) Wave Power for the Reconnaissance Class Assessment

When comparing the observations made from this characterization of sensitivity to the baseline statistics obtained previously, there is a noticeable difference in the bias, scatter index and error in the wave power when comparing the baseline model to the 2,500m mesh resolution model. Therefore, the characterization of the wave power as sensitive is reasonable. However, for the wave height the difference in the model statistics is less pronounced, which makes characterizing the sensitivity of the model more difficult.

8.7.2 Feasibility Case Study

For the feasibility class assessment, the case study selected was the wave breaking physical processes, this was selected as both the wave height and wave power were deemed to be sensitive to the exclusion of this process. The results of the analysis, shown in Figure 8.27, show that in all test cases the wave power would be considered sensitive, but that the wave height ranged from completely not sensitive to sensitive. The wave height sensitivity also highlights the potential issue of classifying something as simply sensitive or not sensitive as it does not account for the potential percentages that can be calculated (in this case the number of wave states was 99, therefore having 2 bins considered sensitive resulted in a percentage of 2.02% which would be considered sensitive). Similar to the reconnaissance class assessment case study a range of values was found which means that the sensitivity of the model may be classified through a fortunate or unfortunate selection of random points and may not be representative of the actual model sensitivity.

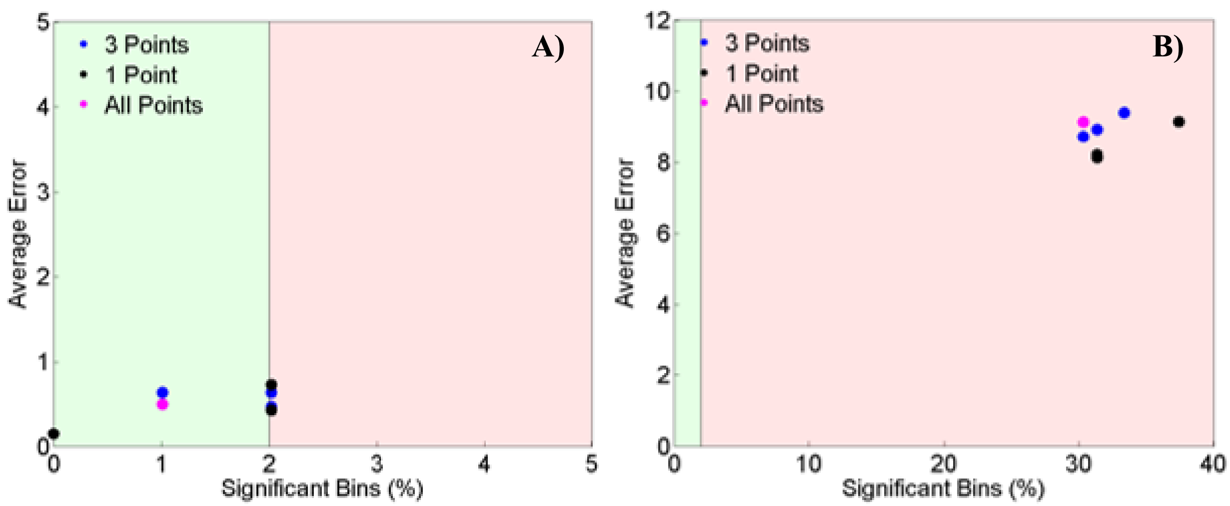

Figure 8.27 - Percentage of Significant Bins VS the Average Error for A) Wave Height; and B) Wave Power for the Feasibility Class Assessment

For the feasibility class assessment, the required threshold percentage difference was decreased from that used for the reconnaissance class, and the maximum percentage of significant wave states was also decreased. Meaning that the characterization of the sensitivity maybe deeming that parameters and processes are sensitive to changes, even if this is not supported through statistics or observation. When examining the statistics there is minimal difference between the different statistical parameters (within 1% of the baseline statistics) for the wave heights. Therefore, the characterization of almost half the randomized test cases as sensitive may be an indication that the thresholds for sensitivity are too stringent.

8.7.3 Design Case Study

For the design class assessment, the characterization of the wind resolution was selected as a case study. This parameter was selected as statistically the wind resolution did not appear to have a significant impact on the resource assessment, but it was deemed to be sensitive for both wave height and power. The results of this analysis are shown in Figure 8.28, from this figure it was observed that the model was significantly more sensitive to the wave height than the wave power. Though it should be noted that in both cases no tests were considered to be not sensitive. This is due to the fact that a single bin containing a sensitive value would result in the percentage of bins containing a sensitive value to be over the threshold of 1%, due to the fact that there are only 90 wave states.

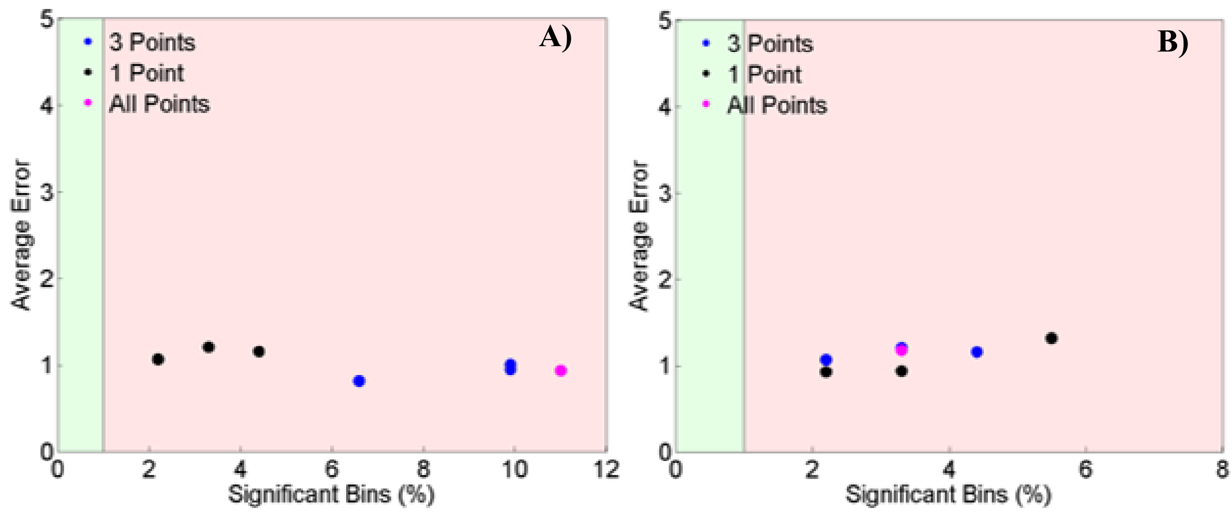

Figure 8.28 - Percentage of Significant Bins VS the Average Error for A) Wave Height; and B) Wave Power for the Design Class Assessment

When examining the baseline statistics for the wind resolution it was found that the statistical parameters were within 1% of each other. This indicates that the threshold for sensitivity is too stringent, as none of the tests indicated that this parameter was not sensitive.

8.7.4 Alternative Characterization of Sensitivity

To objectively characterize the model sensitivity, without relying on a random selection of points within a wave state, an alternative method of calculating the number of significant bins and a new sensitivity threshold is being proposed.

The alternative method proposed recommends using the average percentage difference based on the selection of all points within wave states with a relative frequency of occurrence greater than 0.1%. The dimensions of the bins should be no larger than 0.5m and 1s for the wave height and energy period, respectively. The sensitivity of the model shall be determined using the existing recommended threshold for the percentage differences; however, the condition of insensitivity is recommended to be held constant at 5%. Additionally, it is recommended that there is a buffer around this threshold indicating a partial sensitivity. This would require the user to examine the parameter further to justify its exclusion from the model, or to classify its sensitivity. This buffer would also remove the limitation of values which fall just above or below the 5% threshold due to the number of wave states being considered. When considering the previous case studies for all three classes of assessment using this new method, shown in Figure 8.29, it was observed that reconnaissance class assessment is considered to be partially sensitive for the wave height and sensitive for the wave power. For the feasibility class assessment, the model was not sensitive for the wave height, but was sensitive for the wave power, while for the design class assessment it was considered sensitive for the wave height but not for the wave power.

The value in a standardized method such as this is that it does not rely on a small selection of randomized points which may be subject to cherry-picking and may lead to inconsistent results.

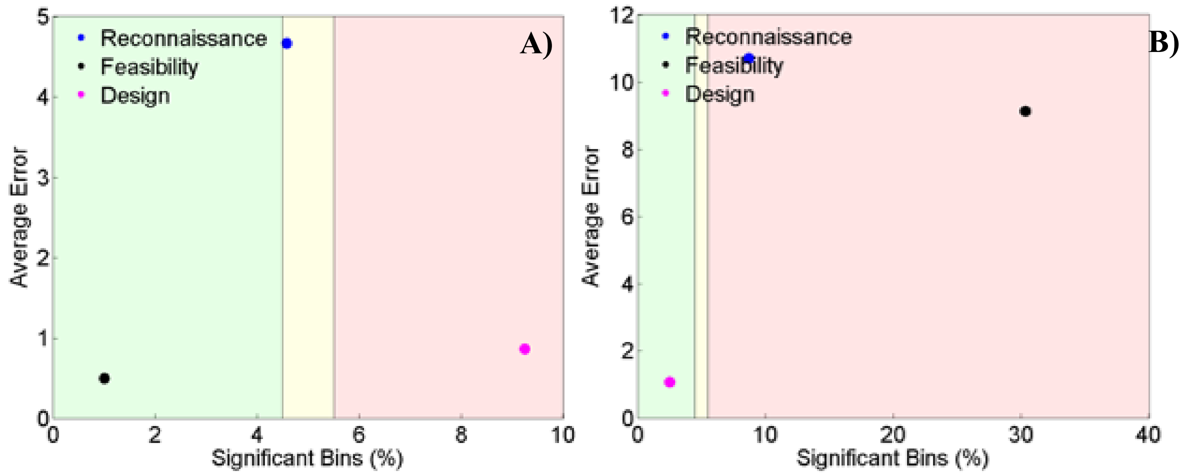

Figure 8.29 – Alternative Characterization of Sensitivity

8.8 Uncertainty and Climatic Variability

This section examines the uncertainty of the model, which includes the measurement uncertainty, the model uncertainty, and the long-term uncertainty. The measurement uncertainty is beyond the scope of this thesis The long-term uncertainty, will be considered in terms of the climatic variability which is the variation in the wave conditions due to natural or anthropogenic sources.

8.8.1 Model Uncertainty

The IEC-TS requires the modelling uncertainty describe all uncertainties associated with the wave model outputs. Currently, the TS stipulates that the calculation of the uncertainty in the resource assessment is highly complex and there are currently not enough definitive procedures for them to prescribe a specific method. As such when examining the IEC-TS it is not possible to test and validate their method of choice for model uncertainty. At this point in time the user should select the method of calculating uncertainty that they are most familiar with.

8.8.2 Climatic Variability

The IEC-TS recommends that a hindcast of 10-years be considered due to natural climatic variations such as the North Atlantic Oscillation (NAO), or the Pacific Decadal Oscillation (PDO). These oscillations are periodic and can result in changes to the wave climate which need to be considered when assessing the wave resource at a location. This 10-year hindcast period came from an examination of locations primarily impacted by the NAO; therefore, the validity of this hindcast period was examined to see if it was applicable to locations impacted by other climatic oscillations.

This assessment was conducted for the reconnaissance class assessment for a 15-year time period from 2000 to 2014, unfortunately it was not possible to examine the impact of a 20-year period due to the availability of wave and wind data for forcing the numerical model.

The first assessment was to examine the moving averages of the wave height and power at the Beverley Buoy location, as shown in Figure 8.30. The moving average was based on a window x-years backwards and x-years forward, centered on the current year. From this figure it was observed that the annual and even 2-year moving average result in significant variation in the modeled parameters. This indicates that using such a short duration would result in an over or underestimation of the wave climate. When looking at the 5- and 7-year estimates less variation can be seen; however, there is still a range of 0.5m and 0.4m in the wave height, respectively, which translates to a range of approximately 18kw/m and 1kW/m, respectively for the wave power. Finally, when considering the 10- and 12-year moving averages this is reduced to 0.24m and 0.07m, respectively for the wave height, and approximately 8kW/m and 3kW/m, respectively for the wave power.

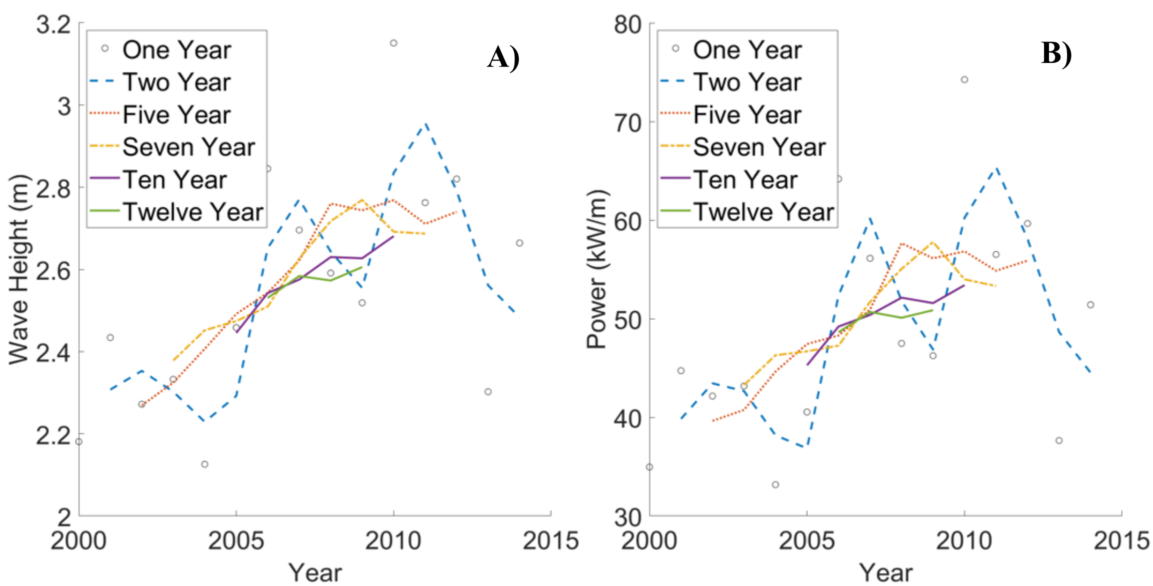

Figure 8.30 – Annual, 2-Year, 5-Year, 7-Year, 10-Year, and 12-Year Moving Averages for A) Wave Height; and B) Wave Power

The range of wave heights and power for the assessment period is better illustrated through Figure 8.31, which shows the range of values obtained for each moving average time period, and which also includes the 15-year average. From this it can be seen that there is a lower value within the 10-year averaging period that results in it having a larger range of values indicating that there is still some potential variability in the values with this hindcast period. However, it does appear that it is not necessary to use a 15-year hindcast period as the 12-year moving averages are quite close in value.

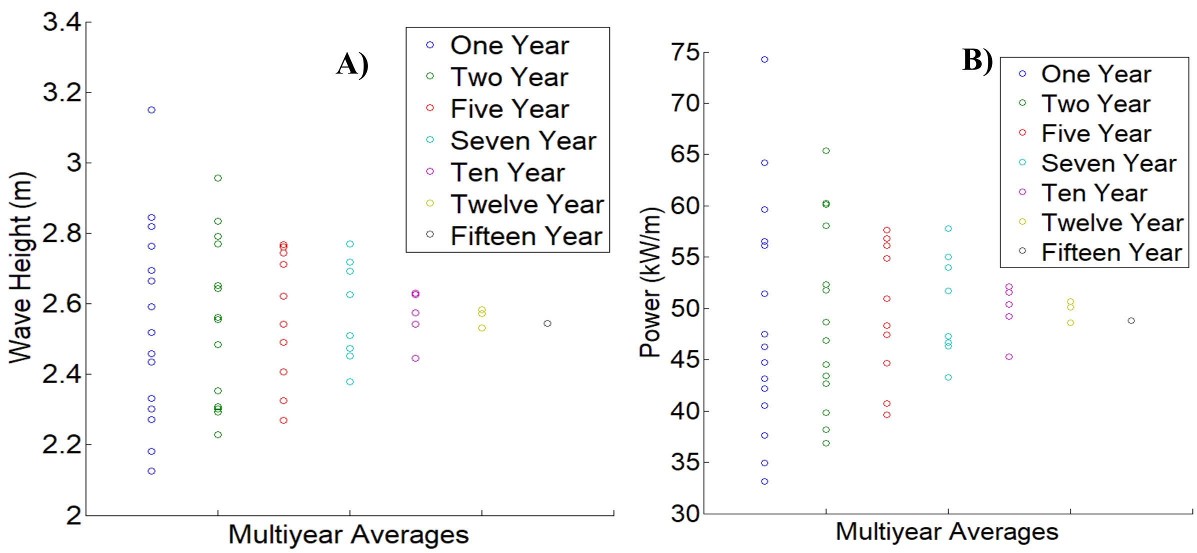

Figure 8.31 – Range of Averages for A) Wave Height; and B) Wave Power

8.9 Validation Criteria

The purpose of model validation within the IEC-TS is to determine the model error in a manner which shows the accuracy of the model in a manner that might be of interest to WEC developers. This involves the calculation of the systematic and random errors within the model with respect to the frequency of the individual wave states and the wave power of that state. This intends to give the wave states that occur most frequently and those with the highest wave power the largest weighting on the model error.

As noted in the current research and that performed by Ramos and Ringwood [2016] and Ramos *et al.,* [2016] the systematic and random error thresholds proposed by the IEC-TS where not always achieved by the numerical model, despite it having comparable statistical errors to previously published research. This could be an indication that the existing accuracy of most wave resource models is not acceptable as per the IEC-TS; however, it is much more likely that the means of calculating the validation errors needs improvements, or that the current thresholds need to be increased to reflect a reasonable standard for wave models. This section examines another method of calculating the error, factors within the IEC-TS which impact the calculation of this error, and a recommendation for the new thresholds.

8.9.1 Validation Calculation

The existing method of calculating the systematic and random errors resulted in significant error values, especially for the wave power. The principle behind the error calculation was to give more weight to the errors occurring for the most frequent and highest power wave states, which would be the ones that WEC developers would be most interested. In developing a new method for completing the validation it was important to keep that in consideration.

8.9.1.1 Proposed Validation Method

The IEC-TS uses the arithmetic mean within its method of calculating the systematic and random errors. The first modified method proposed here recommends instead the use of the geometric mean.

The arithmetic mean is the result of adding up all numbers in a data set and dividing the resultant by the total number of data points. The geometric mean is calculated by multiplying the numbers in the dataset and then taking the n^{th} root. The use of the geometric mean has a significant dampening effect on outliers, which would give a more accurate representation of the error within each wave state. Figure 8.32 shows a comparison between the calculated systematic and random errors. The reconnaissance class assessment baseline model is shown as an example. This assessment was conducted for all classes of assessment.

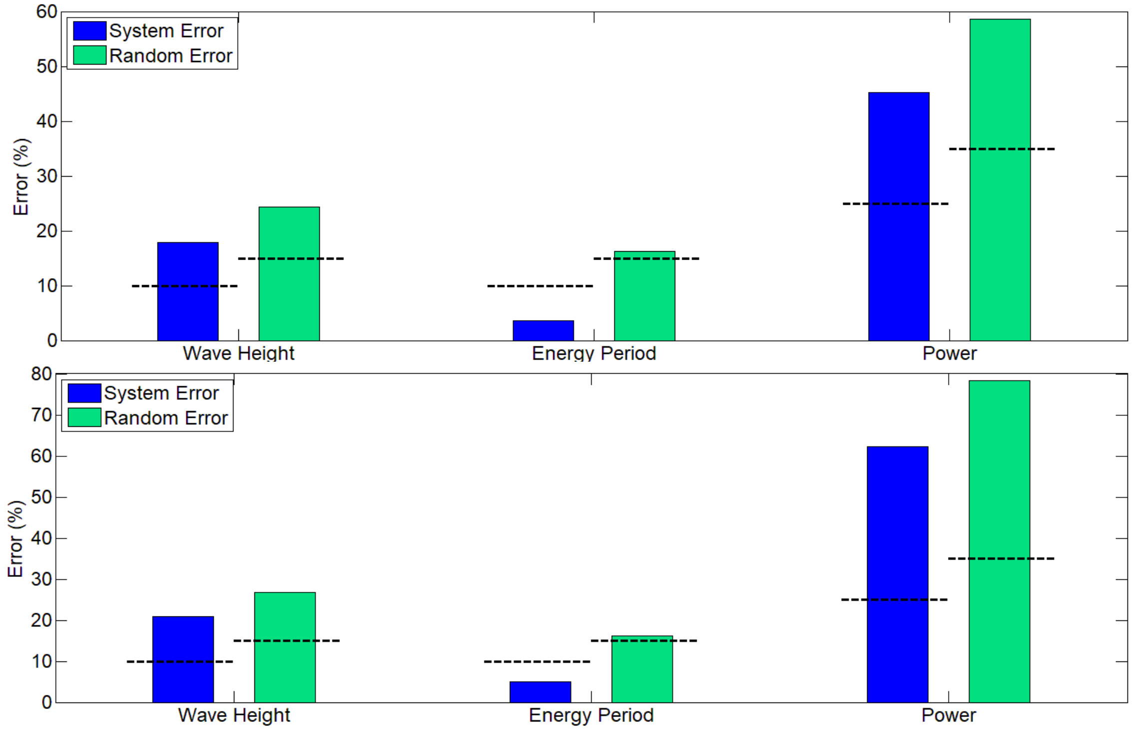

Figure 8.32 - Systematic and Random Error for Geometric and Arithmetic Calculations

The results of the geometric analysis seemed to indicate that for parameters such as the wave power, which has a wide range of potential values, the use of the geometric mean and standard deviation have a significant impact on reducing the model error. However, for parameters that have a smaller range of potential values (such as the spectral width) the geometric systematic error has the risk of compounding the error. It should be noted that even with this change the wave power is still over the recommended threshold in Figure 8.32, but by a more reasonable margin. It is therefore also recommended that these thresholds be increased to reflect the expected and reasonable accuracy of the numerical models.

8.9.2 Bivariate Distribution

The IEC-TS prescribed validation criteria require the calculation of the bivariate distribution based on the wave height and the energy period. They require that the bivariate distribution have wave heights bins of no more than 0.5m and the energy period bins to have a range of no more than 1s. To ensure that the data points are not correlated the user is also required to not include consecutive data points within a single wave state should they occur within six hours of each other, and to not include wave states with insufficient data points.

It has been established by other authors that the selection of the bin size in the bivariate distribution can have a significant impact on the appearance of the local climate. However, this impact and the impact of the data threshold on the calculation of the error within the model has not been examined. This section seeks to examines the impact that their factors may have on the validation of the numerical model. For this assessment all tests were completed using the design class assessment model.

8.9.2.1 Minimum Data Separation

The IEC-TS includes the condition of ensuring data points within the same wave state due not occur within 6 hours of each other. The intent was to remove any chance of data correlation within the error for waves that are within the same storm system. The minimum gap suggested by the IEC-TS was six hours. Additional time periods that were also examined in this section were three hours and nine hours. The use of no separation period was also considered. A summary of the validation coverage for these different tests is shown in Table 8.24. From this table it was observed that even the six-hour separation required by the IEC-TS resulted in the removal of a significant amount of data points for use in the validation based on the criteria of having at least five data points per wave state. In all cases the minimum data coverage criteria is met.

Table 8.24 – Validation Coverage for Different Minimum Separations

	No Gap	**3Hr Gap**	**6Hr Gap**	**9Hr Gap**
Coverage (%)	98.71	97.62	96.53	95.43
Data Points	8281	4471	3061	2524

When considering the systematic and random errors for these different separation tests, shown in in Figure 8.33, it was observed that the separation between the data points has little impact on the systematic error; however, it did have an impact on the random error with the error increasing as the separation gap increased. This could be an indication of correlation within the data; however the error continues to increase past the suggested six hour minimum separation period. This implies that if the increase is due to data correlation, then it would be necessary to increase the minimum separation period past 6 hours. It is more likely however, that the data is being impacted by the reduced pool of data points.

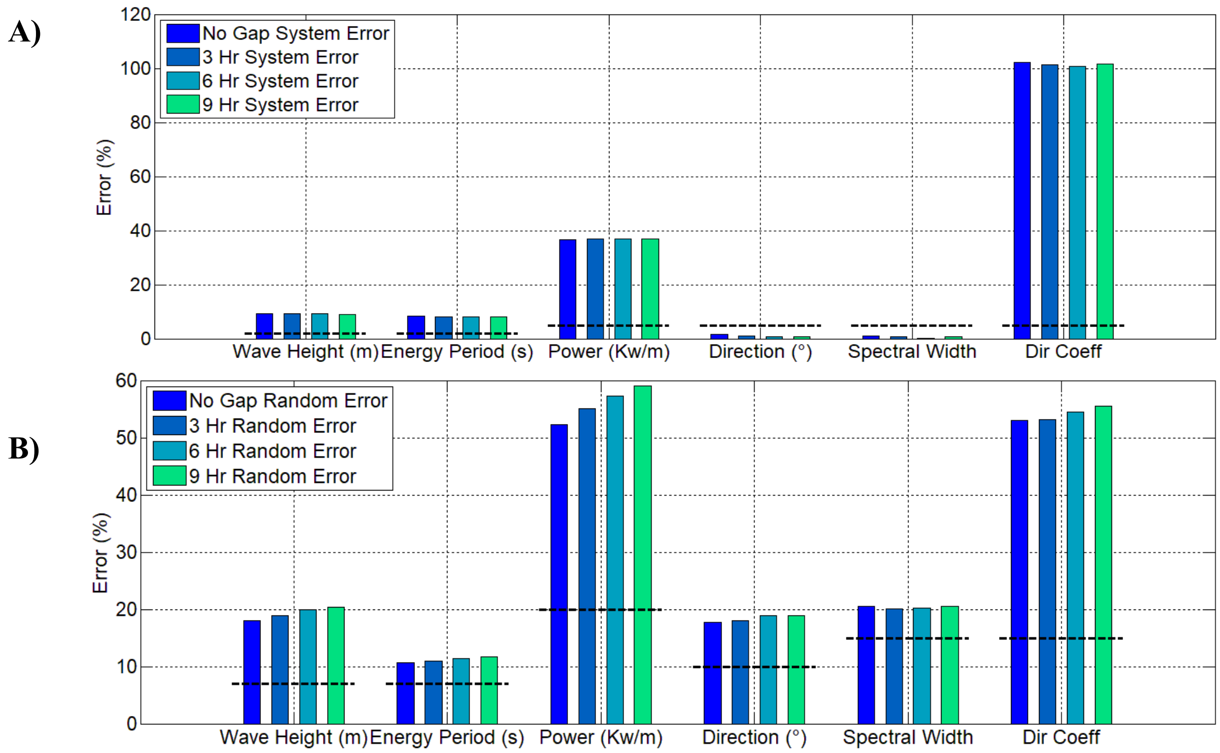

Figure 8.33 - Systematic and Random Errors for the Different Validation Separation Gaps A) Systematic Errors; and B) Random Errors (Direction Error is in Deg.)

8.9.2.2 Minimum Number of Data points

When conducting model validation, the IEC-TS requires a minimum number of validation points within a wave state. Should this criterion not be met the wave state will not be used for the validation which impacts the coverage of the validation data. This criterion is dependent on the class of assessment being considered. In the case of the design class assessment the minimum number of data points is required to be at least five. The impact this minimum threshold has on the systematic and random errors was examined by increasing and decreasing the number of required data points. A summary of the validation coverage for these different tests is shown in Table 8.25. From this table it was observed that changing the number of required data points did not have a large impact on the number of validation points, but it was sufficient to push the coverage below the minimum requirement of 95% when requiring seven points.

Table 8.25 – Validation Coverage for Different Minimum Data Representation

	1 Point	3 Points	5 Points	7 Points
Coverage (%)	100	97.96	96.53	94.08
Validation Points	3228	3132	3061	3037

When considering the systematic and random errors, shown in Figure 8.34, it was observed that this criterion had an impact on both the systematic and random errors. When using every data point available for the error it was noted that the systematic and random errors were lower, with the error increasing as the required number of points increased. While this was not expected as the errors were weighted by the proportional frequency of occurrence, it is believed that increasing the number of wave states resulted in lower weights for the more frequent wave states with higher wave powers. This brings into question the purpose of removing lower frequency of occurrence wave states from the validation criteria as it simply puts more weight onto the remaining bins.

A) B)

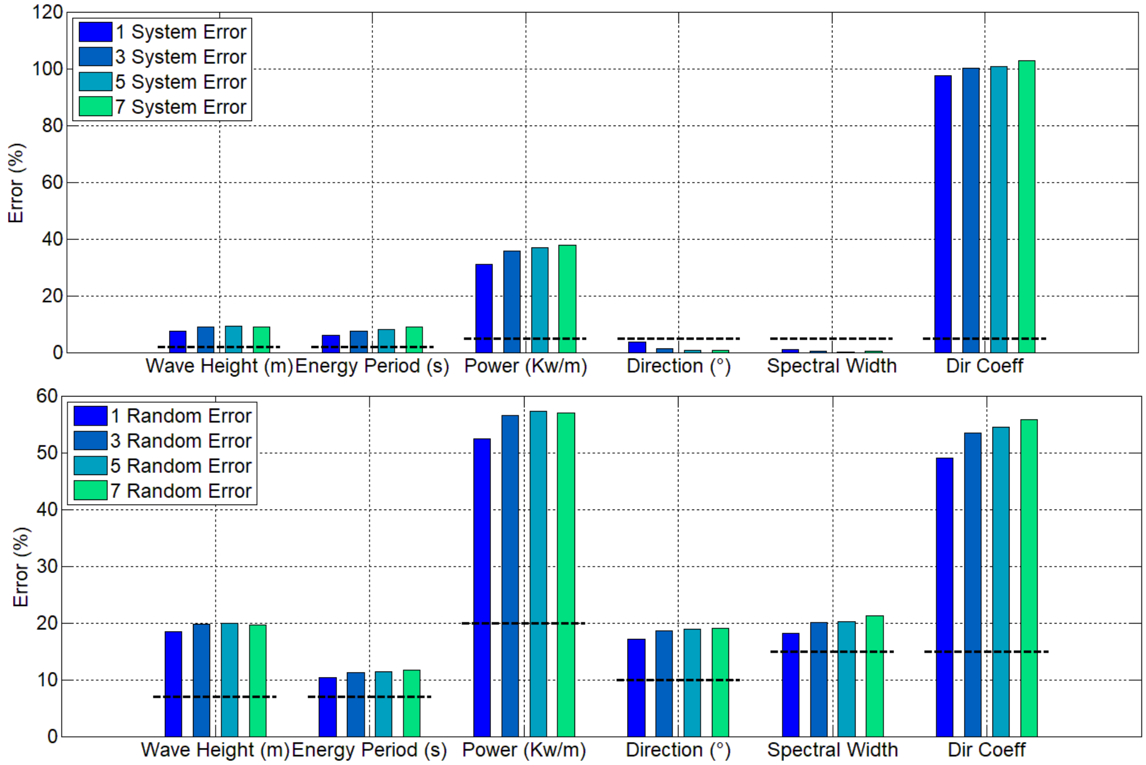

Figure 8.34 - Systematic and Random Errors for the Minimum Validation Points per Bin A) Systematic Errors; and B) Random Errors (Direction Error is in Deg.)

8.9.2.3 Validation Duration

The IEC-TS stipulates that a selection of data points from across the year must be included in the validation calculation to ensure that there is no seasonal bias with the model and error. It was noted that the IEC-TS does not explicitly state a validation during or that the entire year must be considered when conducting the validation analysis. To examine the impact of smaller sets of data throughout the year the validation analysis was conducted using a smaller selection of data consisting of six-month data sets which consider these seasons:

- Summer and winter
- Fall and winter
- All seasons

A summary of the validation coverage for these different tests is shown in Table 8.26 and were compared against the full-year validation period. In the cases of the data only covering two seasons the validation coverage criteria were not met. This requirement was only met when considering the 6-month seasonal data set and the full year period.

Table 8.26 – Validation Coverage for Different Time Periods

	6 Months	6 Months	6 Months	12 Months
Time Period	July – Sept 2013, Jan – Mar 2014	Nov 2013 – April 2014	July - Aug 2013, Oct – Nov 2013, Feb – March 2014	May 2013 – April 2014
Coverage (%)	93.60	92.57	95.93	96.53

When considering the systematic and random errors for the different validation periods it becomes very clear that the selected time period has an impact on the calculated errors. For the systematic error it was apparent that the summer/ winter had the lowest error overall, with the full year typically having the next lowest data range. This is not surprising as the summer months tended to have the lower wave height and power events, meaning that the error would be typically lower. Periods that had a larger amount of fall and winter values tended to show higher error as the model was less accurate during these high wave and wave power events. The full year period appears to be a good balance between the other periods, having influence from the lower energy summer months and the more active winter months.

When considering the random error, it appeared that the 6-month all-season period gave the highest values with the rest of the test periods being relatively similar. This could be due to the small time periods selected which have wildly different values resulting in a higher standard deviation. Both the systematic and random errors support the use of a full years' worth of data being used for the validation as it will be less subject to the seasonality.

A)

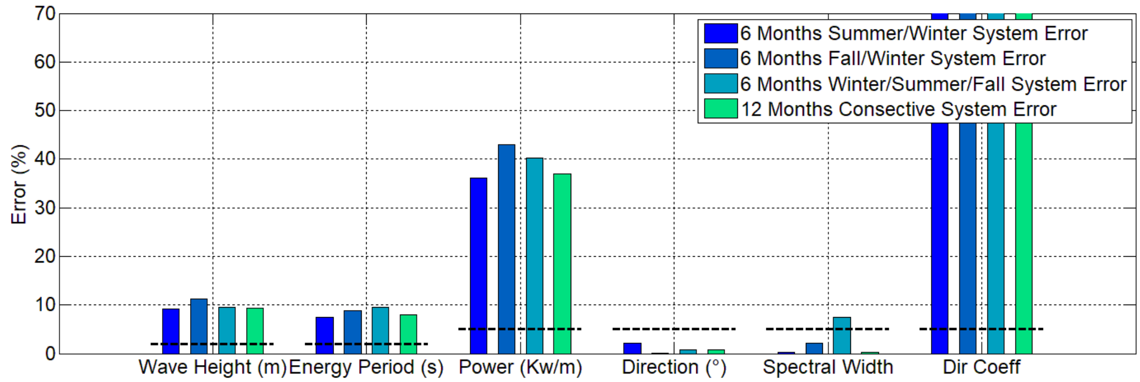

B)

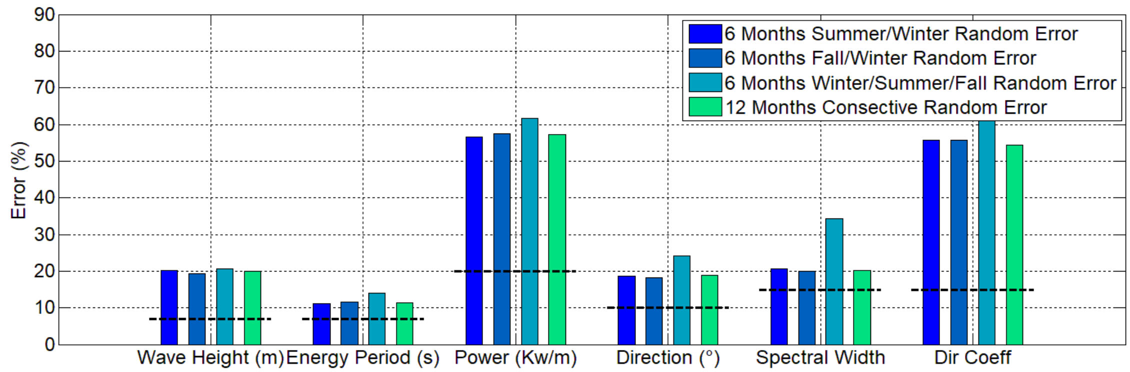

Figure 8.35 - Systematic and Random Errors for the Validation Data Record Periods A) Systematic Errors; and B) Random Errors (Direction Error is in Deg.)

8.9.2.4 Wave State Bin Size

The final assessment completed for the bivariate distribution was an analysis of the wave state bin sizes for both wave height and energy period to assess the impact this would have on the IEC-TS validation. The IEC-TS requires that the bins should be no larger than 1s for the energy period and no larger than 0.5m for the wave height. This criterion was tested by increasing and decreasing the bin sizes as shown in Table 8.27.

When examining Table 8.27 it was clear that increasing the bin size beyond the recommended maximum results in less wave states but a higher coverage value. When decreasing the number of bins, the opposite is true, all cases with a lowered wave height resulted in the validation coverage not being met.

Table 8.27 – Validation Coverage for Different Wave State Bin Sizes

Wave Height Bin	0.5m	0.25m	0.5m	0.25m	1m	0.5m	1m
Energy Period Bin	**1s**	**1s**	**0.5s**	**0.5s**	**1s**	**2s**	**2s**
Number of Validation Wave States	63	110	108	178	43	42	26
Coverage (%)	96.53	94.32	94.53	92.16	97.72	97.59	98.65

Figure 8.36 shows the impact of increasing the bin sizes relative to the recommended bin size. From here it was observed that there was an impact on the systematic and random errors, though no clear trend could be determined.

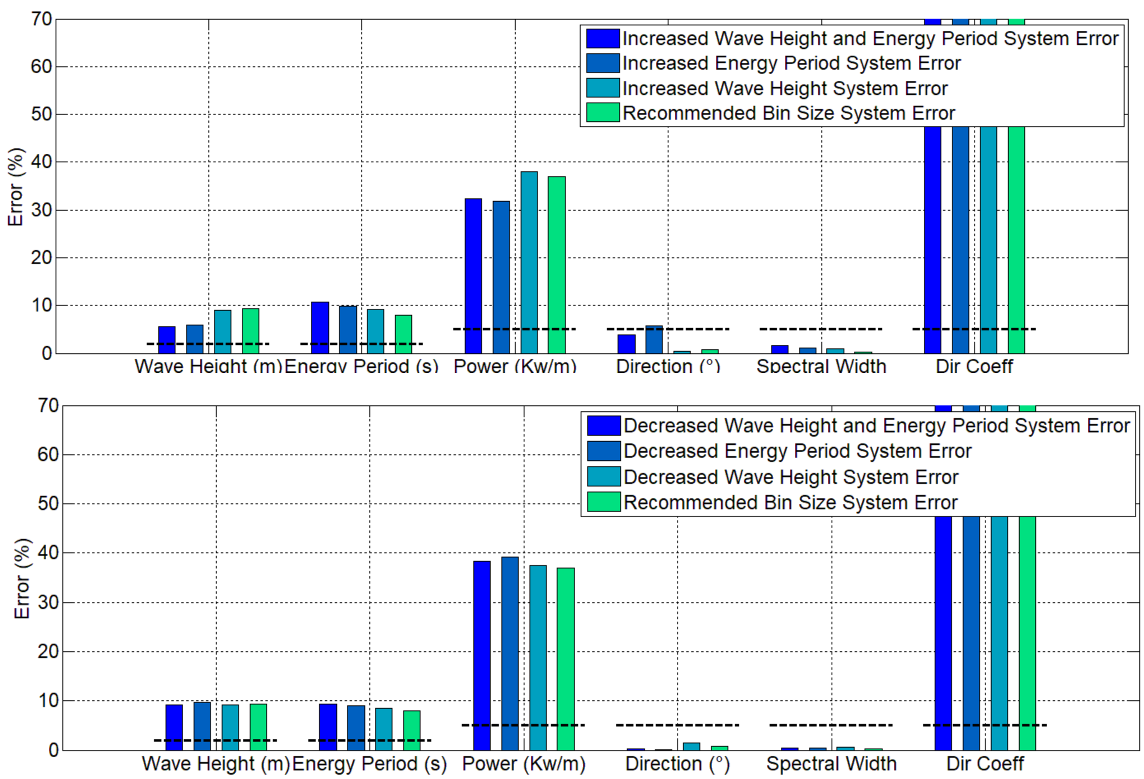

Figure 8.36 - Systematic and Random Errors for the Validation Data Increasing Wave State Bin Sizes A) Systematic Errors; and B) Random Errors (Direction Error is in Deg.)

When considering a decrease in the bin size, as shown in Figure 8.37, slightly less variation in the systematic and random error was observed. This did appear to have a bit more of an observable trend with the recommended bin sizing generally providing lower systematic errors, but the highest random errors, and decreased energy period bin size having the highest systematic errors.

From all of these tests it appears that decreasing the bin size did not have a significant impact on the error but increases to the bin sizes did. Therefore, the use of the recommended values provided by the IEC-TS as a maximum should not have a large impact on the errors. Though as stated previously, all tests done using a wave height smaller than the IEC-TS recommended maximum did result in the coverage criteria not being met.

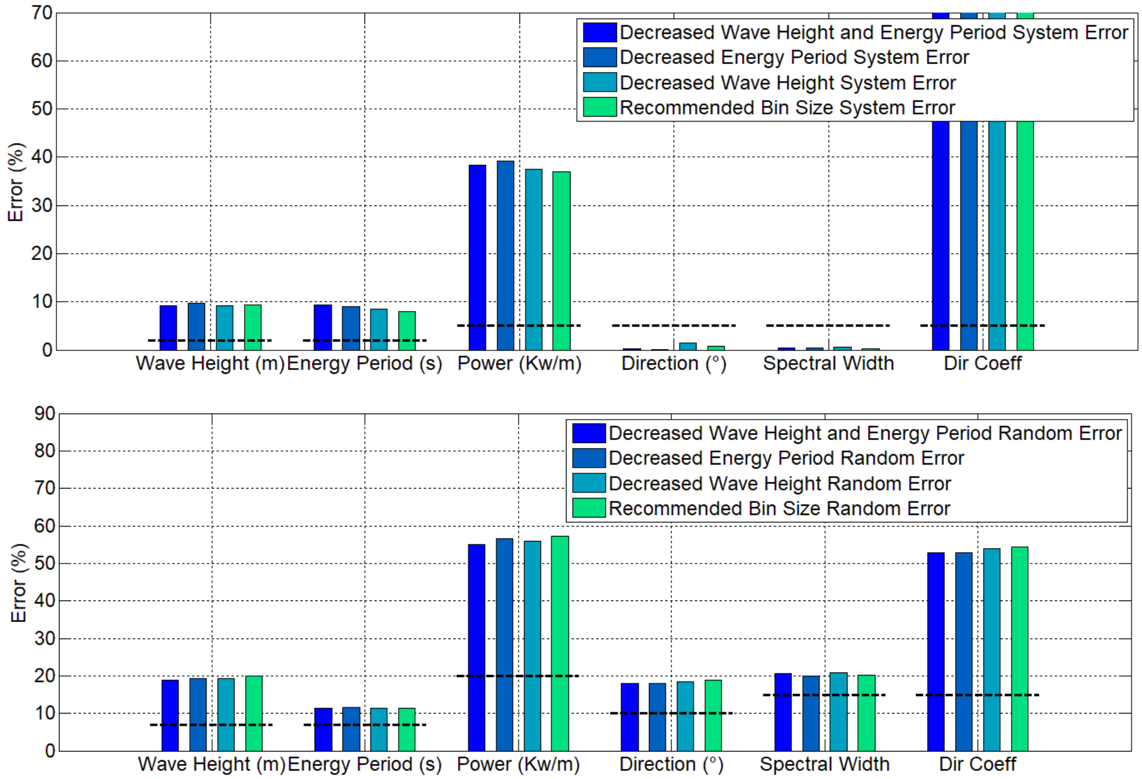

Figure 8.37 - Systematic and Random Errors for the Validation Data Decreasing Wave State Bin Sizes A) Systematic Errors; and B) Random Errors (Direction Error is in Deg.)

8.10 Discussion

This chapter examined a number of aspects key to this project, namely the sensitivity of the model to the specifications of the IEC-TS, the model sensitivity criteria, the model validation, and the long-term uncertainty. In doing this, it aims to establish a scientific basis for the IEC-TS and to provide recommendations for improvements and revisions of future iterations of the specification. It should be noted that many of the conclusions and recommendations provided within this chapter may be site specific, highlighting the need for this analysis to be conducted in different locations and environments.

The validation and sensitivity analysis of the SWAN models were completed based on the recommendations provided by the IEC-TS using a one-year period from 2013-2014 with comparisons against the Beverley wave Buoy (deployed by the West Coast Wave Initiative) located off the coast of Vancouver Island. The validation and sensitivity analysis were completed using the recommended set of six wave parameters: wave height, wave energy period, omni-directional wave power, spectral width, wave direction, and directionality coefficient (only the first three were used for the reconnaissance class assessment). This section outlines the observations and conclusions made through this assessment.

8.10.1 Sensitivity Criteria

During this study, it was observed that the main downfall of the IEC-TS method for determining sensitivity was that it could result in a wide range of errors within a single wave state. It was observed through multiple case studies that it was not possible to consistently predict the accuracy of the model based on a randomized selection from each wave state. This means that the randomized selection is not necessarily a good indication of whether the resource assessment is sensitive to specific parameters.

This was addressed by proposing a modification to the IEC-TS method for determining sensitivity. It is recommended that the error proposed by the IEC-TS be calculated for every data point occurring in wave states with a percentage frequency of occurrence greater than 0.1% and that the threshold for significance be maintained at 5% for all classes of assessment. Additionally, it is recommended that a 1% buffer zone be placed around this threshold (4.5%-5.5%) to indicate values which are very close to the threshold and may require further examination. The benefits of these changes are that it results in a consistent assessment of the sensitivity, which is not reliant on the selection of random data points and is not as subject to the impact of outliers. As the stipulation that this calculation only be done for wave states with a frequency of occurrence greater than 0.1% there no risk of wave states with a single data point impacting the percentage of significant bins.

8.10.2 Sensitivity Analysis and Validation

The sensitivity analysis and validation examined the model with respect to six different model parameters for the different classes of assessment. The sensitivity of the model to different processes and resolutions was characterized based on the sensitivity criteria described in the previous section, as well as model statistics and time-histories. The characterization of the model sensitivity is considered based on the results of the new recommendation provided and not the recommendation outlined in the IEC-TS.

Unfortunately, there were several factors which could not be assessed during the sensitivity analysis due to data availability, such as bathymetric resolution, different sources for wind data, and for boundary wave forcing. Further studies are necessary to determine the impact of these parameters on the resource assessment.

8.10.2.1 Model Processes

The sensitivity analysis began by investigating the impact of key model processes on both the reconnaissance and feasibility class assessments. This analysis was not completed for the design class assessment as the general observations were consistent between the other two classes. When examining these processes, it was observed that the inclusion/exclusion of the different physical processes only had a significant impact in the case of the whitecapping process for the reconnaissance class assessment. However, the feasibility class assessment was found to be sensitive to all the tested wave processes for the wave power.

The whitecapping parameter is required by the TS for all classes of assessment as are the bottom friction, triad interactions, and wave breaking parameters for the feasibility and design class, and it is recommended that this criterion be kept. However, the sensitivity of the model to the depth-induced wave breaking and triad wave interactions were minimal for the reconnaissance class assessment, and it may not be required that they be considered for the assessment. Based on the observations of the model domain it appears that these two parameters only had an impact in very shallow water depths, and therefore would not need to be considered for resource assessments at moderate or deep depths.

8.10.2.2 Mesh Resolution

The sensitivity of the modeled resource assessment to the mesh resolution was examined for all classes of assessment. When examining the sensitivity of the model based on the three classes of assessment, it was apparent that the model was most impacted by the large resolution changes in the reconnaissance class assessment and was least impacted by the small resolution changes in the design class assessment.

When considering the reconnaissance class assessment, the model was only considered sensitive to decreases in the mesh resolution from 1,500m to 2,500m. While for the feasibility class assessment the model was sensitive to all changes in resolution. When examining the statistics and validation criteria for this class of assessment, it was not found that the 100m resolution model performed better than the models at 300m or 500m resolution, and in many cases, it appears to have performed worse. This could be due to the fact that the spectral resolution and bathymetry were not changed to account for the higher mesh resolution. However, from these observations it does appear that the range of mesh resolutions provided for both the reconnaissance and feasibility classes are sufficient. Finally, for the design class assessment the model was not considered sensitive to changes in resolution. This may indicate that for the design class it is not necessary to require a resolution of 50m, which has a significant computational cost, as a resolution of 100m preformed comparably.

8.10.2.3 Boundary Conditions

The impact of the type of boundary condition on the resource assessment was considered for both the reconnaissance and feasibility class assessment. This was done by using both spectral and parametric boundary forcing.

In the case of the reconnaissance, the model was sensitive to changes in the type of boundary condition selected, though the differences in the modeled resource were predominantly observed in the spring and summer months for the wave height and power. For the validation criteria it appeared that the selection of boundary condition had the largest impact on the wave power. Based on these observations it would be recommended that the spectral boundary condition should be used when possible.

For the feasibility class assessment, the model was also found to be sensitive to the selection of boundary condition. In this case it was determined that the use of the parametric boundary condition introduced significant error into the resource assessment, therefore it is recommended that spectral boundary conditions be used at this class of assessment as per the IEC-TS recommendations.

8.10.2.4 Spectral Resolution

The impact of the directional and frequency resolution was examined for all classes of assessment by increasing and decreasing the resolution. The sensitivity of the models was assessed based on both the sensitivity relative to the baseline model, and in terms of incremental increases in model resolution.

8.10.2.4.1 Directional Resolution

For the reconnaissance class assessment, the models did not appear to be sensitive to changes in the directional resolution with respect to the baseline model up until resolutions of 72 and 120 bins. When comparing the increasing resolutions incrementally the model did not appear to be sensitive to any changes in the directional resolution. This indicates that the recommended resolution of 24 bins would be sufficient, as increasing the resolution up to 72 or 120 bins would result in a significant increase in the computational cost for what is intended to be a quick and easy assessment of the wave resource.

For the feasibility class assessment, the model was observed to be sensitive to decreases in the directional resolution down to 24 bins but was found to be sensitive to the wave power when increasing the bins to 72 and both the wave power and height when increasing it to 120 bins relative to the baseline model bin resolution. When considering incremental increases in bin resolution it was found to be sensitive to nothing except for the 24-bin resolution. This would indicate that the minimum required resolution for the bins should be no lower than 36 bins for this class of assessment. This has been accounted for the latest iteration of the IEC-TS.

Finally, for the design class assessment the model was determined to be sensitive to decreases in the directional resolution but was not found to be sensitive to increases in the resolution. However, when examining the statistics, it did not appear that there was any benefit to increasing beyond the recommended resolution of 48 bins, except for the directionality coefficient. In addition, it was noted that even decreasing the directional resolution down to 36 bins only introduced error into the model direction and directionality coefficient, and in fact performed equally as the higher resolution model in all but these parameters. This indicates that lowering the minimum requirement to 36 bins may be suitable as it has a small impact on the model parameters.

8.10.2.4.2 Frequency Resolution

For the reconnaissance class assessment, it was observed that the model was more sensitive to the frequency resolution than the directional resolution. It was observed that increasing the frequency bin resolution up to 41 had a small impact on the model, but increasing the resolution beyond this point impacted the model more heavily when compared to the baseline resolution. However, as with the directional resolution, the model was not sensitive to incremental increases in the resolution. Based on these observations there may be benefits to increasing the minimum required resolution; however, this would result in a significant increase in the computational cost which defies the intent and purpose of a reconnaissance class assessment.

For the feasibility class assessment, the model was not found to be sensitive to increases in the frequency resolution for most increments, with only the change between 41 to 57 bins being sensitive. This was surprising as there was a statistical decrease in the accuracy when going down to 25 bins which was more pronounced. However, this may indicate that this change is still within reasonable bounds for the feasibility class assessment. This indicates that the minimum frequency resolution can be kept at 25 frequency bins, but that the model can be improved with some computational cost by increasing the resolution up to 41 or 57 bins.

Finally, for the design class assessment it was observed that the model was sensitive to decreases in the resolution down to 25 frequency bins. Decreasing the resolution down to 25 bins resulted in a marked decrease in the accuracy in the wave height, power, and direction, though it did result in marginal improvements for other parameters. However, it appears that the minimum resolution for the frequency resolution at the design class should be increased to 41 bins despite the increase in the computational cost as the accuracy of this model is intended to be high.

8.10.2.5 Wind Resolution

The final assessment completed as a part of this sensitivity analysis was an examination of the impact of wind resolution on both the reconnaissance class and design class assessments. For the reconnaissance class assessment, the model was tested using a spatially constant wind, a variable wind and with no wind at all. It was noted that the model was quite sensitive to the wind resolution, with the constant wind tending to overestimate the wave height and power but providing a better estimate of the energy period. Using no wind found the opposite, with the most accurate wave height and power, but the worst estimate of the energy period. This assessment was deemed to be site specific as the impact that the wind has on the modeled resource is dependent on the spatial variability of the wind and its magnitude. However, it is suggested that the minimum recommended resolution be increased as the current recommendation is quite large and may result in a lack of accuracy.

In the case of the design class assessment the wind resolution was doubled to determine what impact this might have on the resource assessment. When examining the statistics and time-histories it was determined that this increase in wind resolution had a minimal impact on the modeled resource. Though when looking at the model sensitivity it did appear to be sensitive to changes for the wave height. Despite this it was decided that the IEC-TS could decrease the resolution of the wind within minimal impact. Similar to the reconnaissance class assessment this is site-specific, other locations may find more sensitivity to changes in the wind resolution.

8.10.3 Validation Criteria

The existing validation criteria tends to overestimate the level of error present in the resource assessment when compared to more traditional statistical methods of determining the level of error using the R^2, bias etc. This overestimation is especially pronounced when considering the wave power.

The intent of this validation method (as described in more detail in Chapter 3) is to estimate the level of error within the wave states that are of most concern for a wave resource assessment i.e., those with the most power and the highest frequency. Thus, by weighting the error by the frequency and the power it is possible to give more weight to the errors of these relevant wave states. However, as observed in this study and that of Ringwood, these errors are not necessarily reflective of the model performance especially for the wave power.

The large error observed for the wave power is believed to be the result of the fact that the largest errors in the modeled wave power tend to occur with the highest wave power events. This is compounded by the validation methodology putting more weight on these higher power wave states which results in unrealistic errors.

To maintain the intent of the validation method, it is recommended that minimal changes be made to the procedure. The only recommended changes are to require the use of the geometric mean and standard deviation as opposed to the arithmetic mean and standard deviation for all parameters except for the spectral width. The main recommendation is that this validation parameter should not be used as the only method of validation, and the other main statistical parameters should also be considered. Additionally, it is recommended that more testing of the proposed validation thresholds be tested to ensure that they are reflective of the level of accuracy and effort required for each class of assessment.

9 Wave Energy Resource Assessment

To assess the wave climate and the energy resource across this region a 10-year resource assessment (2005 to 2014) was conducted for all three classes of assessment. This allowed the result of the resource assessments to be compared with observations made by previous studies in the region, and for comparisons to be made between the different classes of assessment.

This chapter shows results from these resource assessments, making sure to provide all the figures and information required for reporting by the IEC-TS. In addition to this it shows the full resource assessment, including average power, wave height, and energy period, across the model domain, the seasonal and long-term trends observed at the Beverley Buoy site, and the wave climate obtained at the Beverley Buoy site.

9.1 Comparison with Measurements

The section looks at the differences between the modeled wave climate and wave spectra with those obtained by the wave buoy(s). The wave spectra were obtained at three locations from the numerical model, this was used to calculate the wave parameters to compare with the measured wave climate from the Beverley Buoy, the Environment Canada buoy at La Perouse and the NOAA buoy at Neah Bay. Additionally, a direct comparison was made between the wave spectra measured by the Beverley Buoy and the numerical model. This comparison, Figure 9.1, was completed for January 14th, 2014.

Figure 9.1 shows that the wave spectra generated by SWAN were not able to capture the fluctuations in the energy density across all of the frequencies and directions. This is likely due to the lower resolution of the model for all classes of assessment when compared to the measured spectra obtained by the wave buoy.

The wave spectrum for the reconnaissance class assessment was only able to capture the lower frequency energy peak observed in the measured wave spectrum, while the spectra from the feasibility and design class assessments were capable of capturing the higher frequency energy. However, even though there were able to capture the higher frequency energy range, they still exhibited a single peak energy spectrum, while the buoy measured a multi–peak spectrum (showing one high energy peak at approximately 0.075Hz and two smaller peaks at approximately 0.1Hz and 0.125Hz).

In the case of the energy direction, it was found that the numerical models all tended to over predict the spread of the energy across the directions. The reconnaissance and feasibility models do indicate that the peak wave energy is coming from the same direction as seen in the measured spectrum; however, the design class assessment indicates that the peak wave energy is coming from 285° as opposed to 270°. Similar to the spectrum frequency the wider spread could be a result of the model resolution.

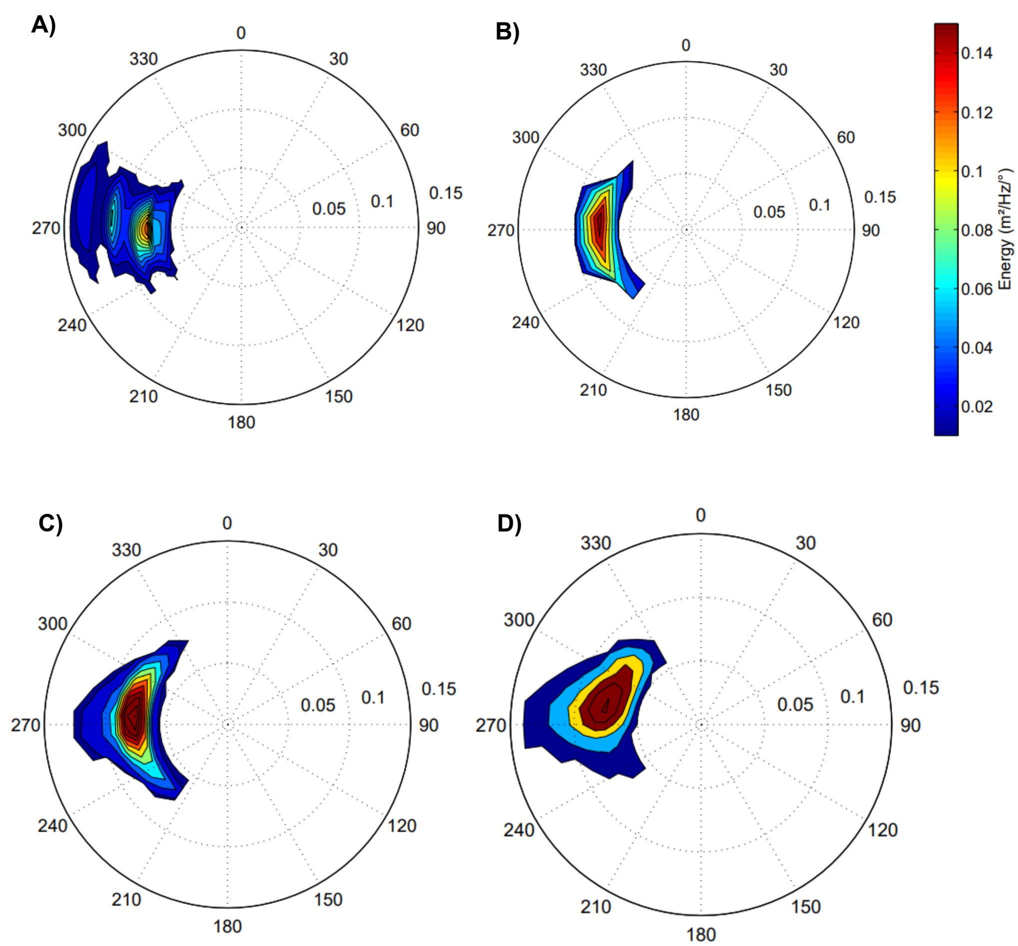

Figure 9.1 – Measured and Modeled Wave Spectra for January 14th for the A) Beverley Buoy; B) Reconnaissance Stage; C) Feasibility Stage; and C) Design Stage

The comparison between the measured and modeled wave parameters is shown in Figure 9.2 for January 2014. This shorter period is used so that the differences between the modeled and measured parameters can be seen clearly. The comparisons were made at the main validation site (Beverley Buoy), as well as at La Perouse and Neah Bay. Both the La Perouse and Neah Bay buoys were not omni-directional buoys, therefore there were a limited number of parameters available at these sites. Additionally, it should be noted that the comparison for the design class assessment could only be done for the Beverley Buoy due to the domain size.

Beginning with the comparison at the Beverley Buoy site, it can be seen that the modeled wave height, omni–directional power, and energy period show marked improvement when comparing the reconnaissance class assessment to the feasibility or design class assessments. From these time–histories the reconnaissance class assessment tends to over predict the storm events for both the wave height and power. However, when comparing the design class assessment to the feasibility class assessment there is very little difference in the wave parameters, except for the spectral width and the directionality coefficient. For less energetic periods the reconnaissance model varied in its ability to predict conditions, while the feasibility and design assessments were more reliable in their prediction.

The buoys available at Neah Bay and La Perouse were not omni–directional and so only a limited number of wave parameters were available for comparison. Therefore, only the wave height is shown here. Similar to the Beverley site, the reconnaissance class assessment tends to overestimate the wave height during storm events, while the feasibility assessment was better able to capture the wave heights for both locations. This indicates that the trends observed at the Beverley site are similar to those observed throughout the model domain.

The use of a constant wind field for the reconnaissance class assessment is likely to blame for the over predictions during storm events as the high-wind speeds would be applied over the entire model domain resulting in increased wave generation.

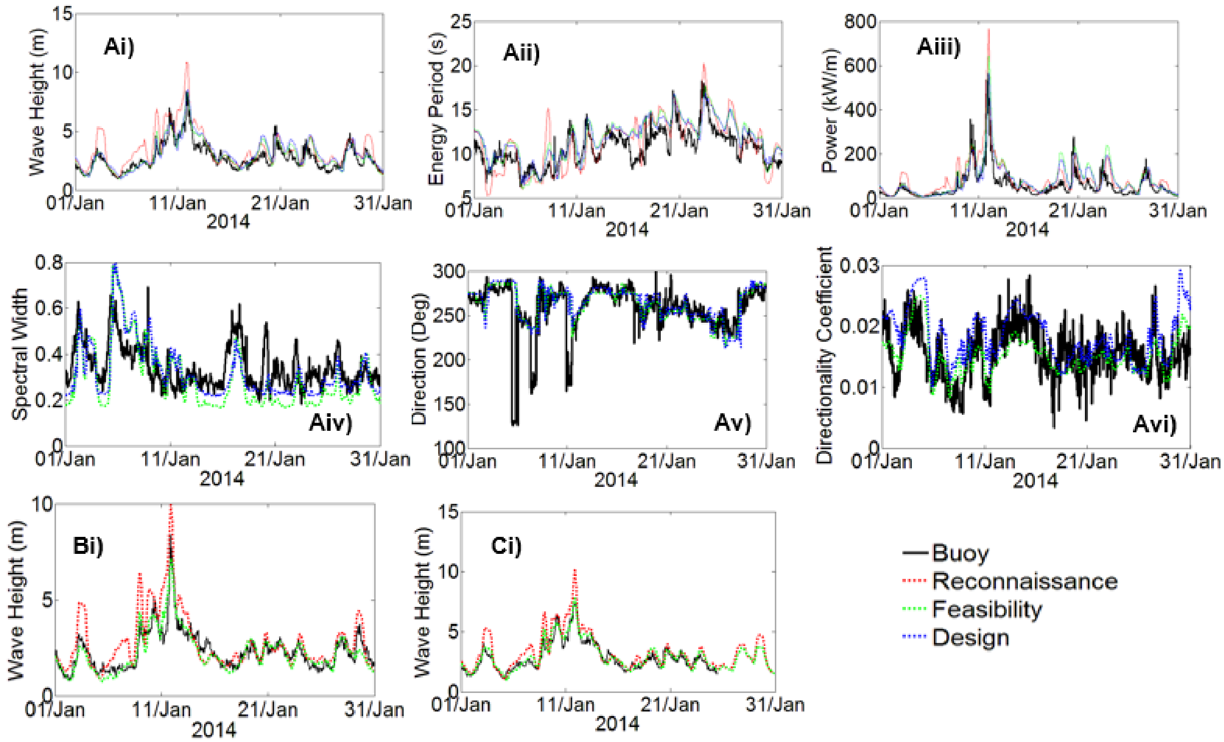

Figure 9.2 – Measured and Modeled Time–Series for January 2014 for A) Beverley: i) Wave Height; ii) Energy Period; iii) Wave Power; iv) Spectral Width, v) Direction, and vi) Directionality Coefficient; B) Neah Bay: i) Wave Height; and, C) La Perouse: i) Wave Height

9.2 Domain Variation

This section compares modeled wave parameters across the entire model domain for all classes of assessment. This is represented in different ways throughout the section, including sample results at a specific time, seasonal results averaged over the 10-year period, and the averaged results over the entire 10-year period.

A sample of the model output from January 14th, 2014, is shown in Figure 9.3, where the model wave height can be seen for all three resource assessments. When considering the model output for this time step, the impact of the localized bathymetry is apparent. Distinct increases in the wave height can be seen nearshore at the Beverley buoy site due to the presence of a shelf.

When examining the model output for this time step the impact of the localized bathymetry is apparent, as distinct increases in the wave height can be seen nearshore at the Beverley site due to the presence of a shelf. There is variety between the wave heights shown by the different modeled resource assessments, both in its magnitude and distribution.

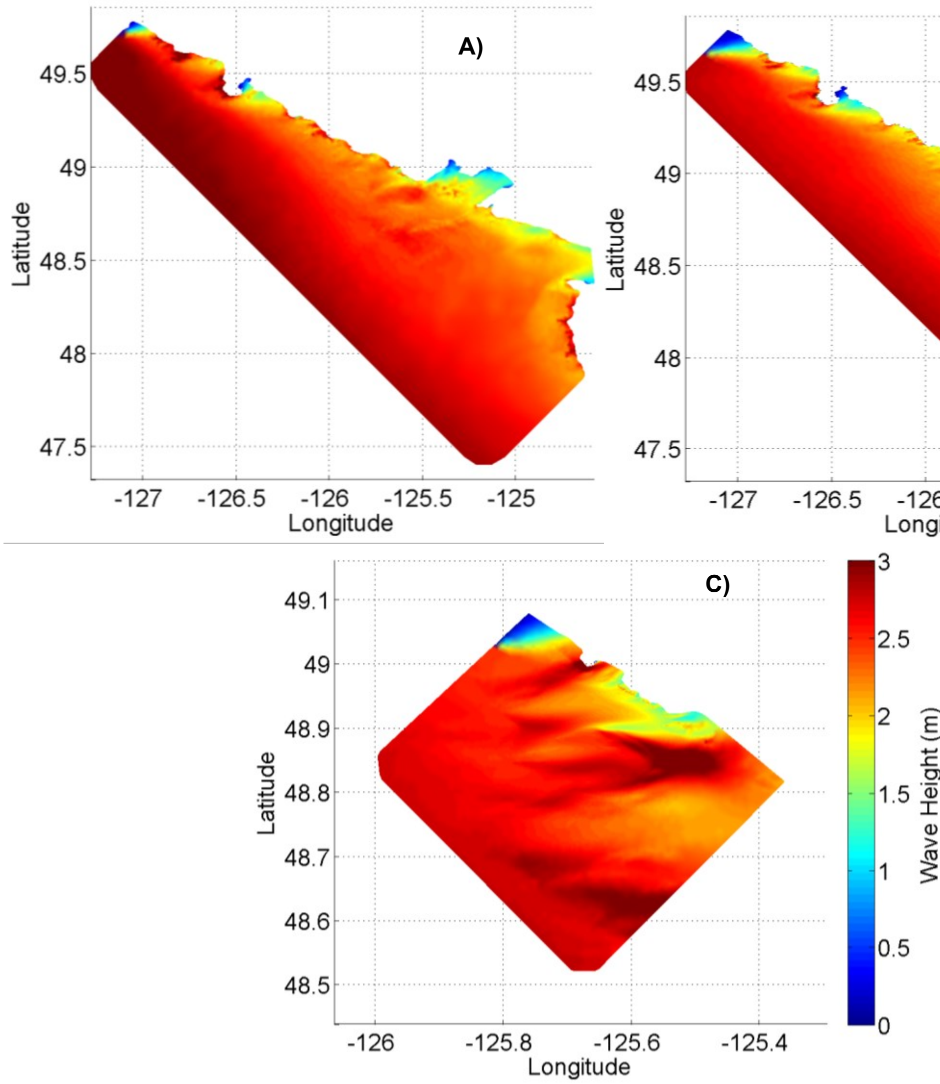

Figure 9.3 – Modeled Wave Height (m) for January 14th, 2014 00:00 for the A) Reconnaissance Stage; B) Feasibility Stage; and C) Design Stage

Figure 9.4 shows the shows the mean wave energy transport across the domain for the study period of 2005-2014 based on the models three-hour time resolution. It was observed from this figure that the reconnaissance class assessment shows high wave energy transport along the border, and particularly in the north-western region of the domain. This contrasts with the feasibility class assessment which shows a more consistent energy transport in the deeper regions of the model.

Nearshore, particularly around the Beverley buoy site there is significant variation in the energy transport due to the impact of the localized bathymetry. This is particularly notable in the design class assessment.

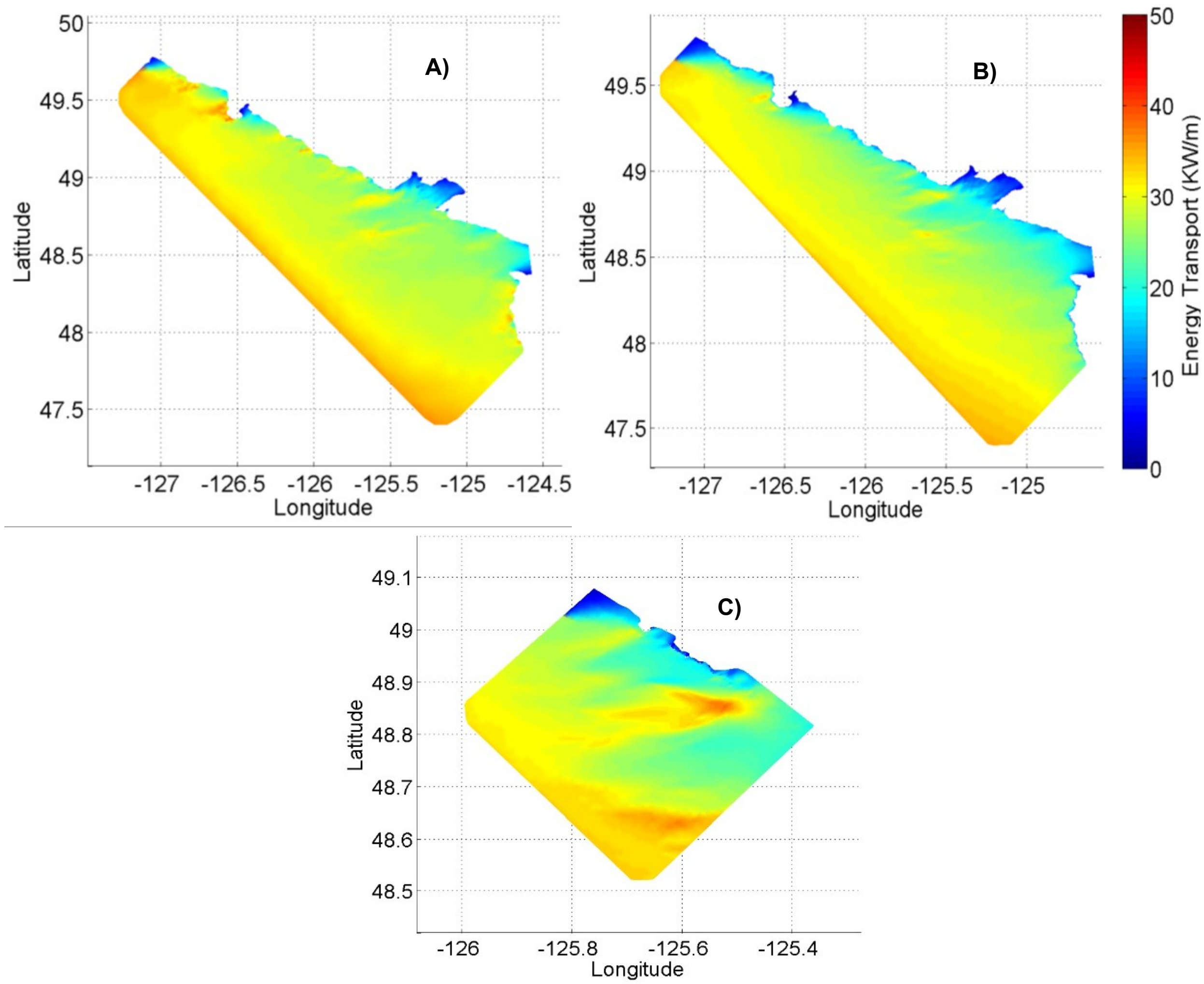

Figure 9.4 – Mean Wave Energy Transport for A) Reconnaissance Stage; B) Feasibility Stage; and C) Design Stage from 2005 – 2014

A comparison was made between the mean wave energy transports observed at the Beverley buoy site with that obtained by Robertson *et al.* [2014a] at the Amphitrite Bank site. For the reconnaissance class assessment, the mean wave energy transport was determined to be 29.88kW/m, while for the feasibility class resource assessment it was 28.00kW/m, and 31.00kW/m for the design class resource assessment. Robertson *et al.* [2014a] predicted a value of 34.5kW/m at this location which compares reasonably well with the modeled results, though it was noted that all classes of assessment had lower values. When compared to the observations made by Cornett and Zhang [2008], the model compares less favorably at the Beverley location as they observed an annual energy transport of 49.00kW/m.

An additional comparison was made between the current study and the previous research at a shallow water location, this location was selected to be similarly situation that that used by Robertson *et al.* [2014a]. At this location the reconnaissance class assessment was determined to have a mean energy transport of 34.17kW/m, the feasibility class assessment had 18.16kW/m, and the design class assessment had a mean energy transport of 17.46kW/m. The high variability in wave energy that occurred in the shallow water made it difficult to compare the models at this location, this resulted in the feasibility and design models have values significantly lower than the 27.8kW/m obtained by Robertson *et al.* [2014a], and the 25.53kW/m obtained by Cornett and Zhang [2008].

A comparison between the monthly variability across the seasons is shown in Figure 9.5 for the wave energy transport. The remainder of the monthly plots can be found in Appendix A. This figure shows a strong seasonal trend in the energy transport. This is denoted be very low energy transport in the summer, and high energy transport during the winter. This is important to note as it means that any devices deployed in this region will need be able to withstand the high energy events occurring during the winter. Additionally, it would be difficult to optimize the WEC to be able to capture energy under such varied conditions.

When comparing between the different classes of assessment it appears that the reconnaissance class assessment depicts higher wave energy transport in the north-western region of the domain during the winter months, while the feasibility class assessment shows a more even distribution in the deeper water. All three models show minimal energy transport during the summer.

When comparing the values between the different classes of assessment it appears that the reconnaissance class assessment depicts higher wave energy transport in the northern region of the domain, while the feasibility class assessment shows higher transport in the center and southern region of the domain. All three models show minimal energy transport in August.

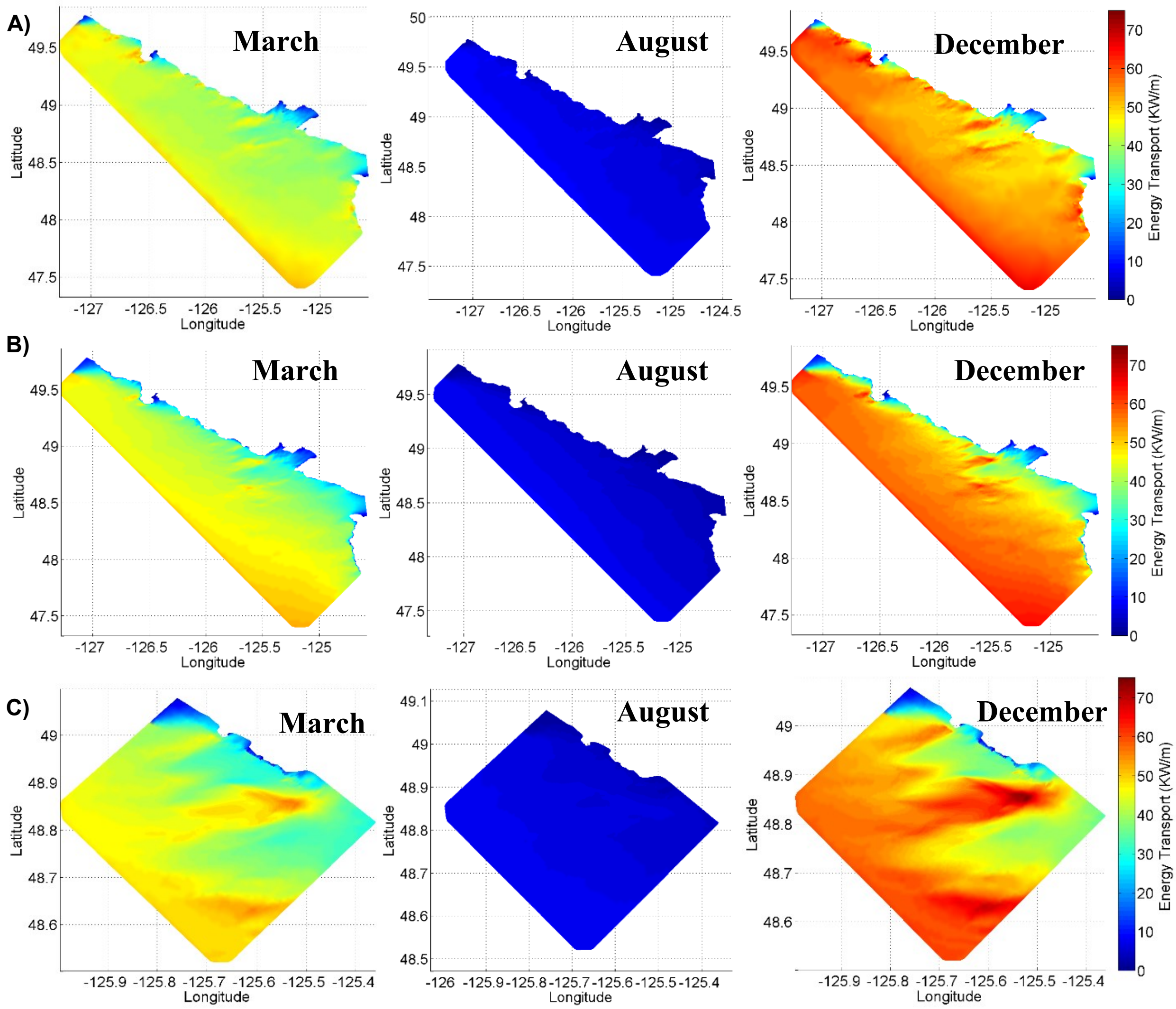

Figure 9.5 – Monthly Variability of the Wave Energy Transport for A) Reconnaissance Stage; B) Feasibility Stage; and C) Design Stage from 2005 – 2014

Additional parameters that were examined across the domain include the mean significant wave height, the mean wave energy period (taken as 0.9 times the peak period[1] as per Cornett and Zhang [2008]), and the direction of energy transport. The mean values across the domain are shown in Figure 9.6, Figure 9.8, and Figure 9.10, respectively, while the monthly variability is shown in Figure 9.7, Figure 9.9, and Figure 9.11.

[1] The value of 0.9 is an approximate fit from the JONSWAP distribution to field data and is based on combined wind and swell waves. The value can differ when considering wind-dominated waves or swell-dominated waves.

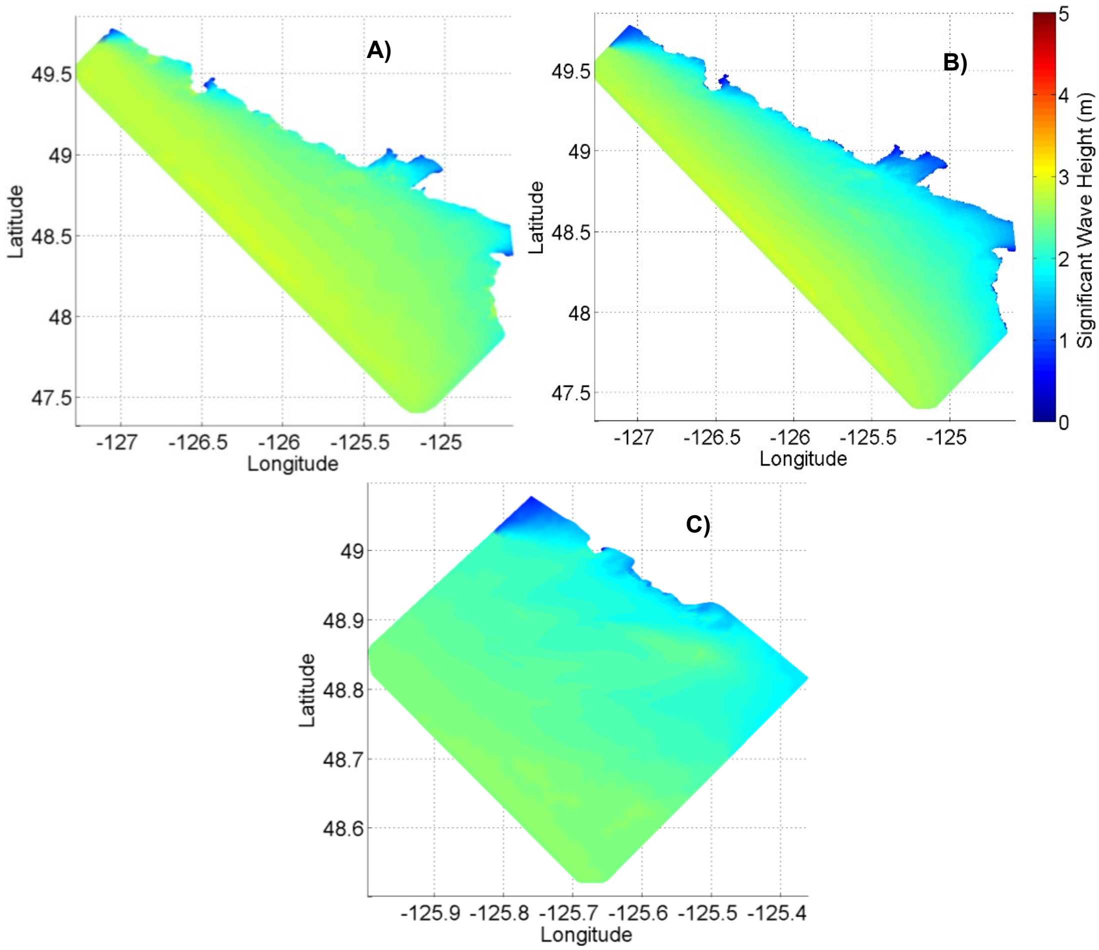

Figure 9.6 – Mean Significant Wave Height for A) Reconnaissance Stage; B) Feasibility Stage; and C) Design Stage from 2005 – 2014

The mean significant wave height, Figure 9.6, shows similar trends to those observed for the wave energy transport, with the wave height decreasing as it approaches the shoreline, and a slight increase in wave height at the Beverley buoy site due to the shelf, the similarity in trends is expected as energy transport is proportional to the wave height squared. However, unlike with the wave energy transport there is no significant amount of variation in wave height as it approaches nearshore.

The results show that the reconnaissance class assessment presents higher wave heights across the domain and especially along the north–western border when compared to the feasibility class assessment, however, the feasibility and design class assessments have very similar results.

A comparison between the monthly variability across the seasons is shown in Figure 9.7 for the wave height. The remainder of the monthly plots can be found in Appendix A. Similar to the wave energy transport, the wave heights are largest in the winter, with minimal wave reaching the nearshore region at summer. For this parameter the reconnaissance class assessment tends to predict higher wave heights throughout the domain, while the feasibility and design class assessments result in similar estimations.

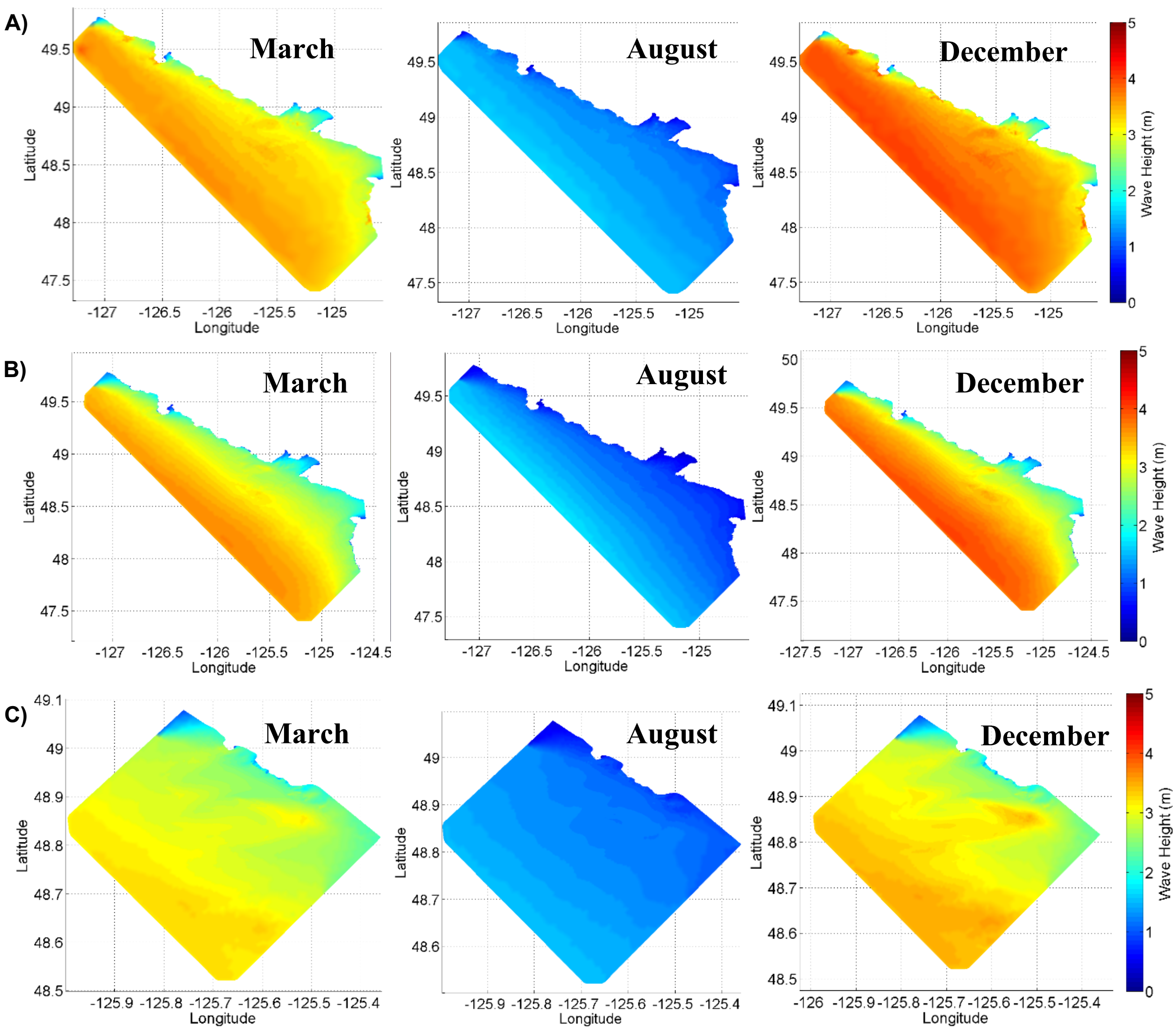

Figure 9.7 – Monthly Variability of Wave Height for A) Reconnaissance Stage; B) Feasibility Stage; and C) Design Stage from 2005 – 2014

Larger differences between the three assessment classes were observed for the wave energy period, Figure 9.8. The reconnaissance class assessment has relatively constant mean modeled energy periods throughout the domain, while both the feasibility and design class assessments show higher energy periods nearshore, and lower energy periods at the offshore boundary. For the design class assessment, the variation in the energy period is greatest, this model shows lower energy periods than in either of the other two classes of assessment.

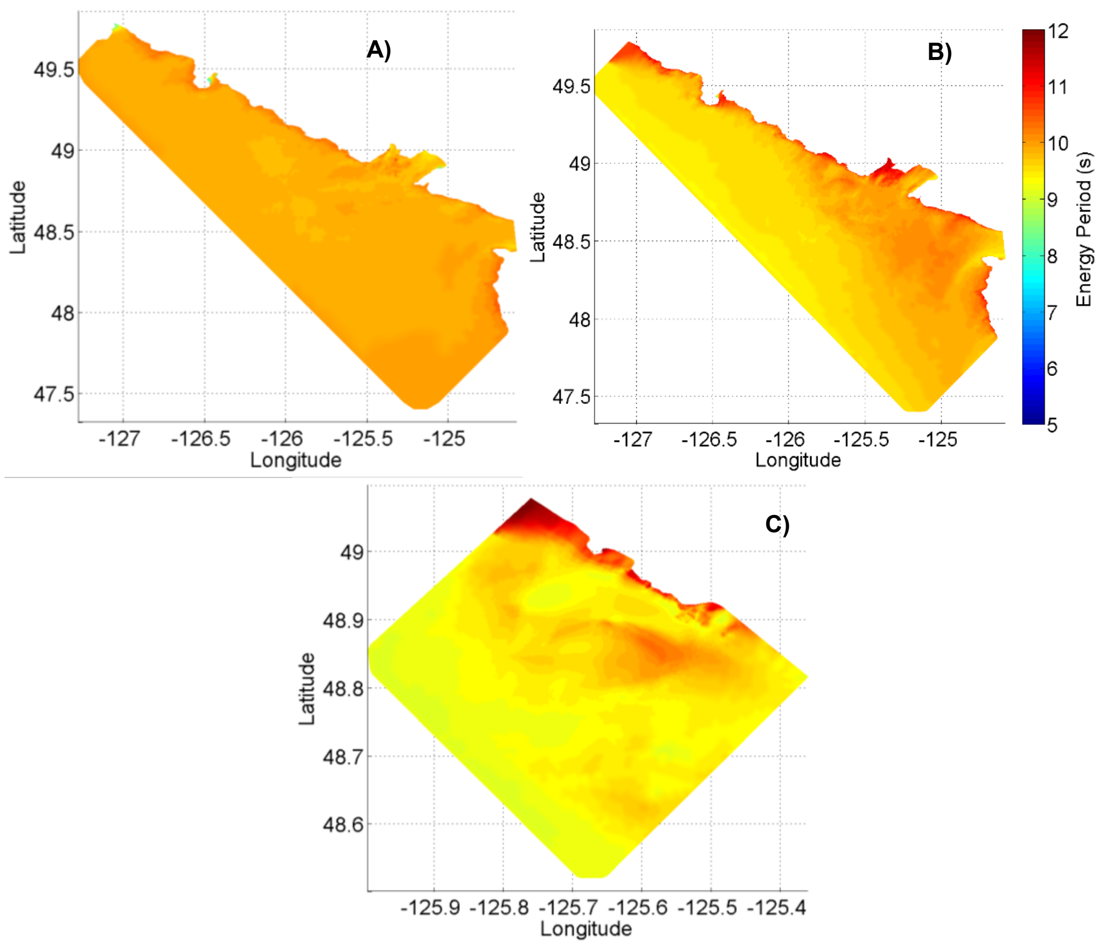

Figure 9.8 – Mean Wave Energy Period for A) Reconnaissance Stage; B) Feasibility Stage; and C) Design Stage from 2005 – 2014

A comparison between the monthly variability across the seasons is shown in Figure 9.9 for the energy period. In general, these figures show that there are lower energy periods during the summer months, than for the winter or spring. This seasonal variability is especially notable in the feasibility and design class assessments. For these two resource assessment the offshore regions show low energy periods, while the nearshore region show significantly higher values. For the reconnaissance class assessment, the energy period is more consistent across the domain and the stark increase in the energy period is not seen along the shoreline. During the winter months there is less of a difference between the three classes of assessment, though the design class assessment does tend to have slightly lower energy period in all seasons.

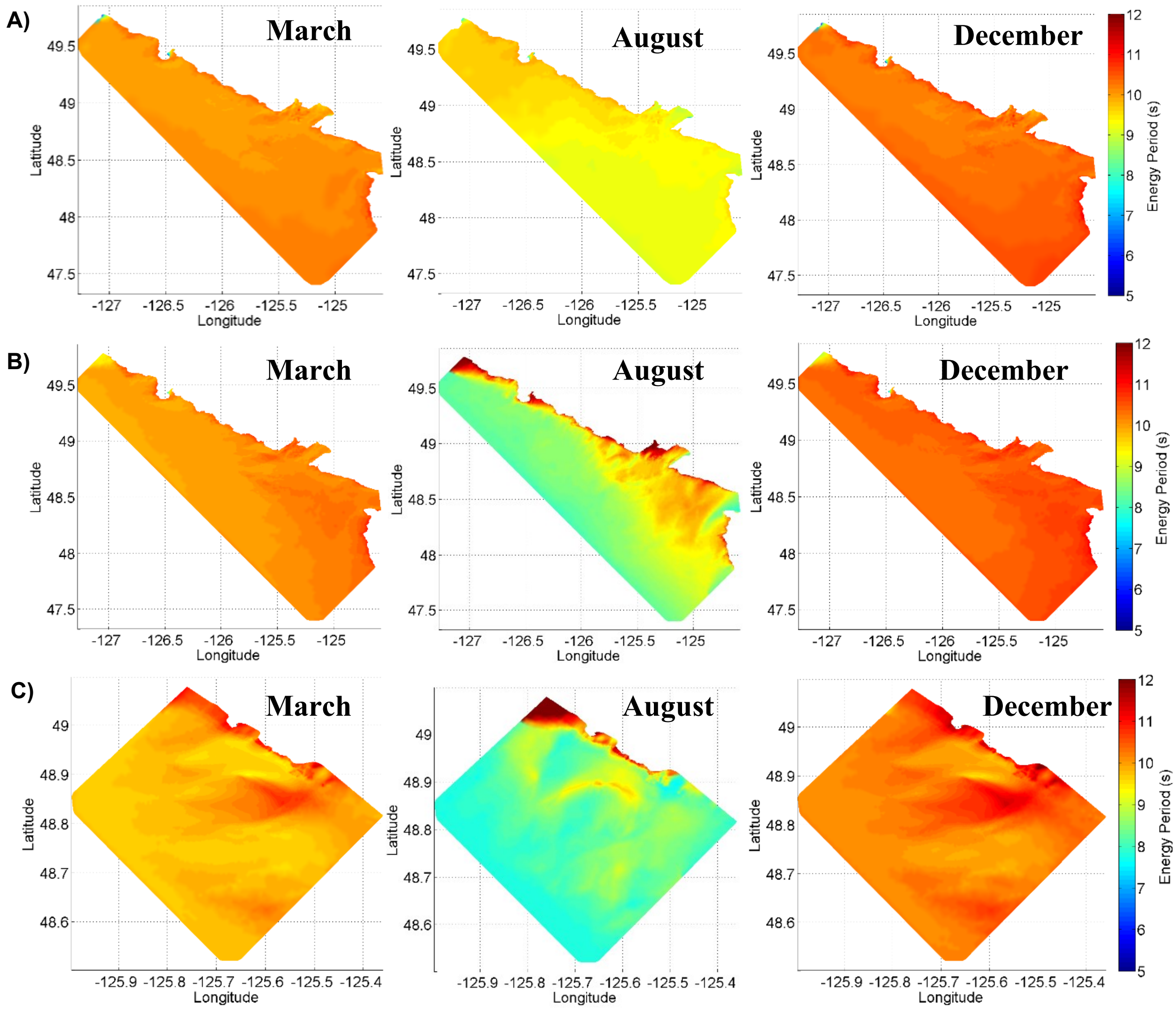

Figure 9.9 – **Monthly Variability of Energy Period for A) Reconnaissance Stage; B) Feasibility Stage; and C) Design Stage from 2005 – 2014**

The final parameter that was examined was the modeled wave direction. The mean wave direction, Figure 9.10, shows that the three resource assessments have relatively consistent model directions throughout the domain, and when compared to each other. Additionally, when looking at the monthly variability of the wave direction, Figure 9.11, there is only a slight difference in the direction across the months and across the models. From this it appears that the dominant wave direction is from the west and southwest.

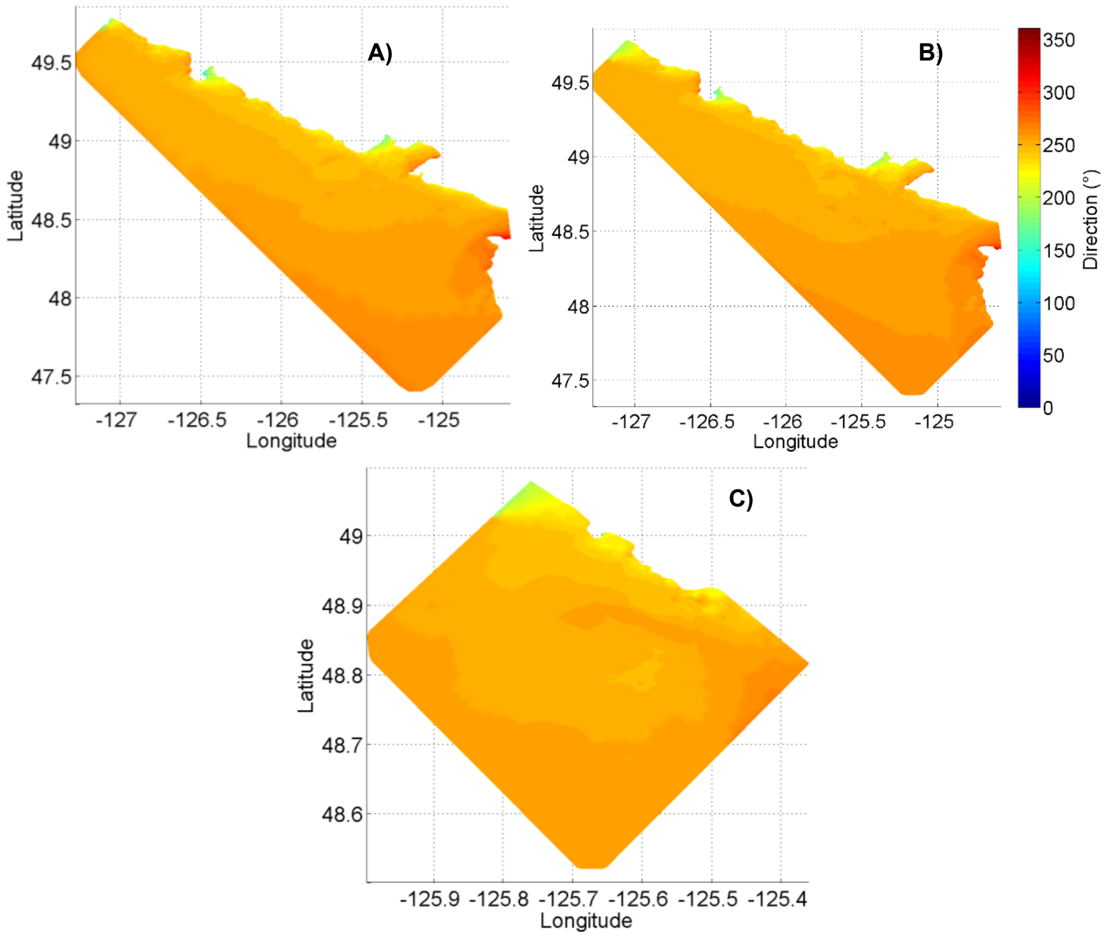

Figure 9.10 – Mean Wave Direction A) Reconnaissance Stage; B) Feasibility Stage; and C) Design Stage from 2005 – 2014 (North is 0°)

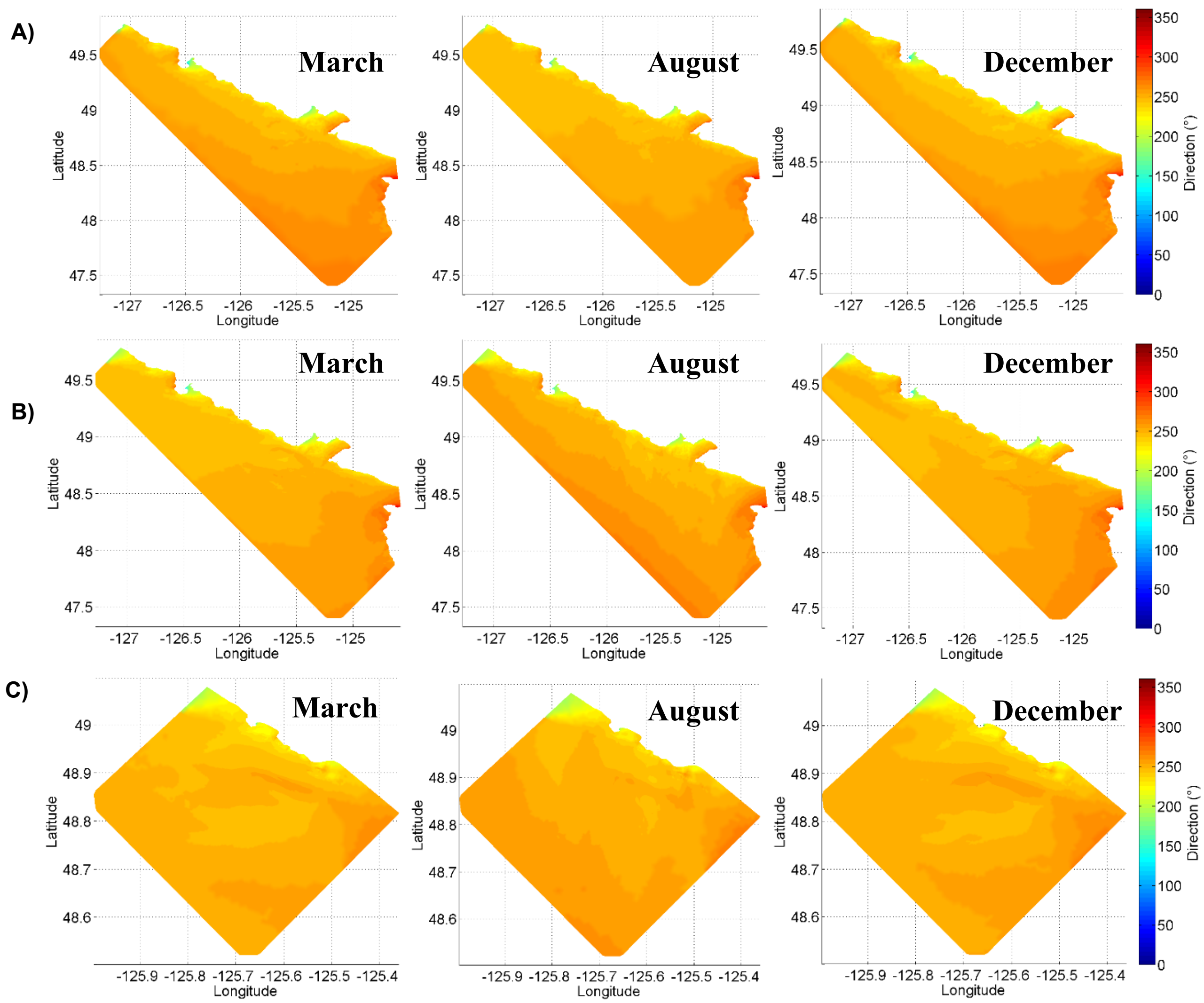

Figure 9.11 – Monthly Variability of Direction for A) Reconnaissance Stage; B) Feasibility Stage; and C) Design Stage from 2005 – 2014 (North is 0°)

9.3 Temporal Variation

This section compares the temporal variations of the modeled wave parameters at the Beverley buoy site for the 2005-2014 time period. This analysis can be used to examine seasonal variations at the site of interest, and to determine if there are long-term significant variations in the wave climate.

Monthly temporal variations in the omni-directional wave power can be seen in Figure 9.12 for the three classes of assessment. When examining this figure, a clear seasonal variation in the power available at the Beverley site is observed throughout the year. This seasonal variation shows that the potential wave energy at the site is highest from the late fall to early spring, and lowest in the summer. This agrees with the observations made when examining the entire model domain. Additionally, this figure shows that the reconnaissance class assessment has the tendency to estimate higher wave powers than both the feasibility and design class assessments, who provide similar estimations. The increased estimate in wave power is likely a result of the boundary and wind conditions. Unfortunately, it was not possible to compare the modeled and measured wave power at this site, as the buoy measurements were not consistently obtained over a long period of time.

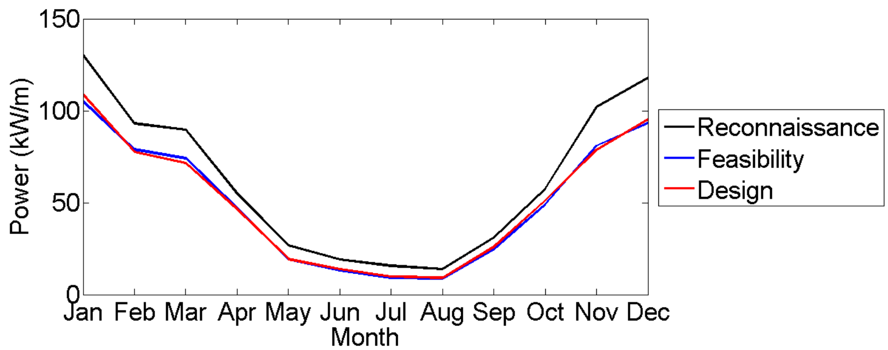

Figure 9.12 – Monthly Temporal Variation of the Wave Power at Beverly Buoy from 2005–2014

When examining the other wave characteristics required for consideration by the IEC-TS, Figure 9.13, a similar seasonal trend was observed for the wave height. Smaller seasonal trends were also observed in the wave energy period (most notably for the design class assessment), and in the spectral width. The seasonality of the data does seem to be tied slightly to class of assessment in some cases, with some showing stronger trends than others. These figures are supported by the domain wide monthly observations where it was observed that the wave power, height, and energy period had seasonal trends indicating lower values during the summer months, while the seasonal trend is less evident for the direction. The difference between the feasibility and the design class assessment is likely a result of differences in the boundary condition definition, which used different locations and methods for their development.

As the IEC-TS also requires the presentation of the maximum directionally resolved wave power, this was also included in this 8.13, despite not being one of the validation parameters. It was normalized based on the directional bin size, similar to the directionality coefficient.

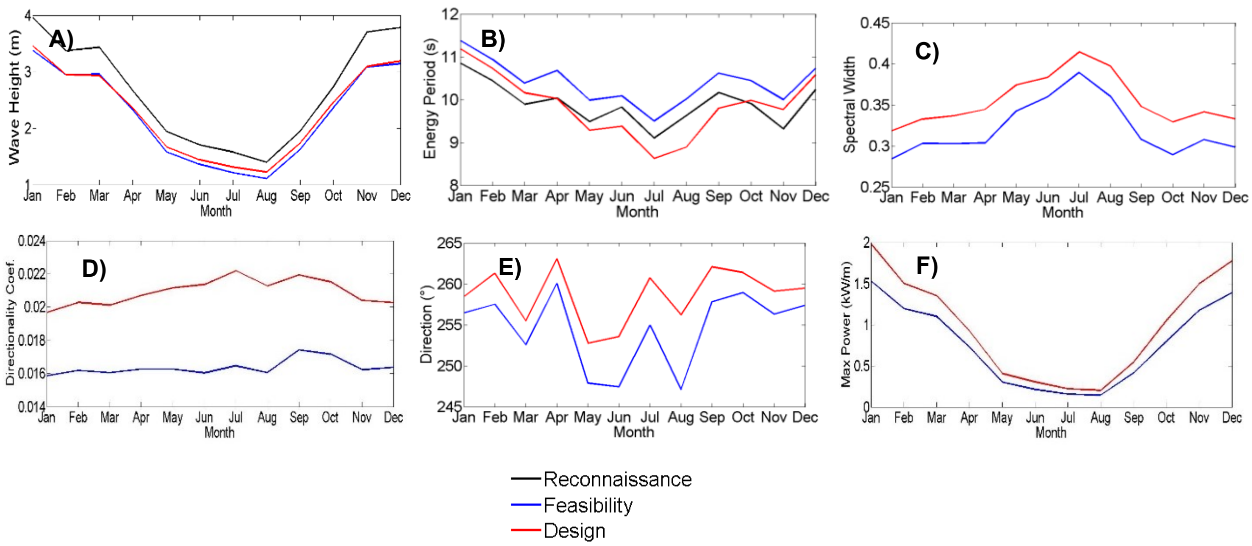

Figure 9.13 – Monthly Temporal Variation in A) Wave Height; B) Energy Period; C) Spectral Width; D) Directionality Coefficient; E) Wave Energy Direction; and F) Maximum Directionally Resolved Wave Power from 2005–2014

The yearly temporal variation of the IEC-TS parameters is shown in Figure 9.14. This variation was used to determine if there were any long-term trends associated with the wave climate. When examining the parameters there does not appear to be any trends in the data, though there is evidence of years with exceptionally high wave activity, such as in 2010, and years with much lower wave activity such as 2013. This data supports the need for long hindcast periods as using a shorter period would have resulted in skewed wave heights and powers. As there is no long-term trend visible in the data the mean values obtained over this ten year period can be taken as representative of the wave climate for the future development of WEC.

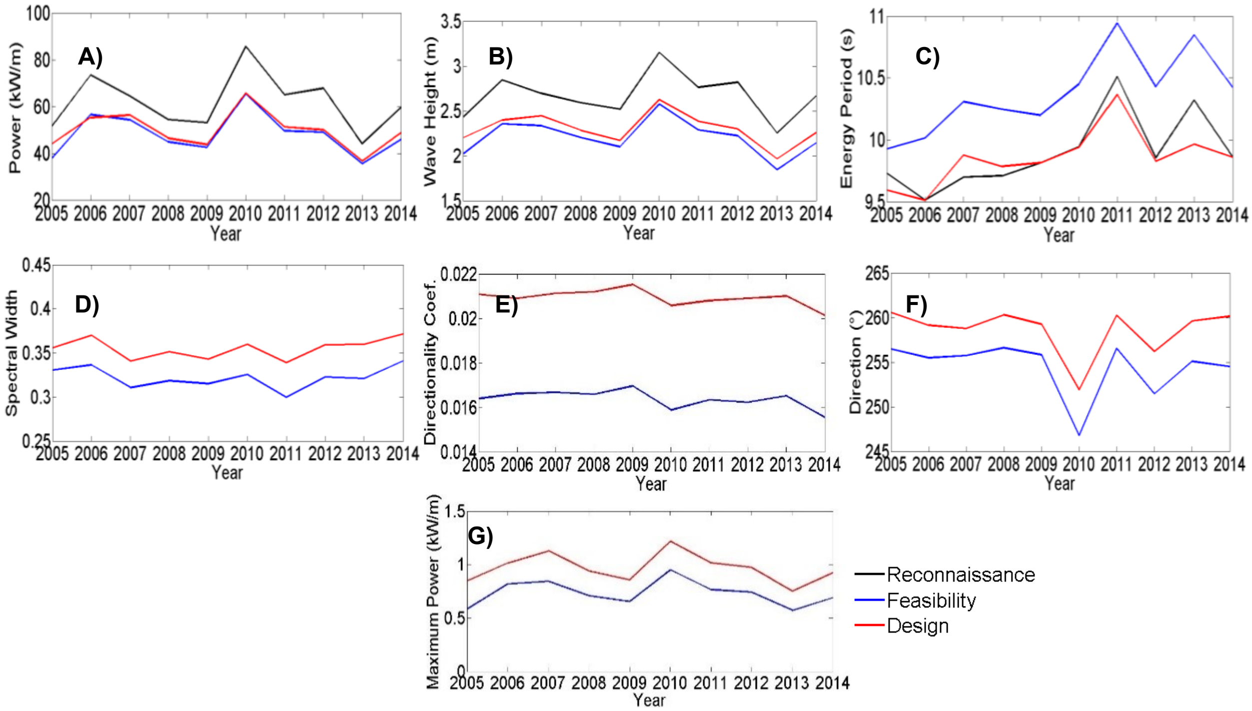

Figure 9.14 – Yearly Temporal Variation of the Wave Energy Parameters at the Beverly Buoy A) Wave Power; B) Wave Height; C) Energy Period; D) Spectral Width; E) Directionality Coefficient; F) Wave Energy Direction; and G) Directionally Resolved Maximum Wave Power from 2005–2013

The next set of figures shows the annual variation in the mean monthly wave parameters, Figure 9.15. Similar to Figure 9.14, the intent of these figures was to determine if there were any notable yearly trends in the wave parameters. This figure supports the observations that there are no significant long-term trends, however it does show that on a yearly basis there is significant seasonal variation in some of the wave parameters, for example the wave power and height during the winter months.

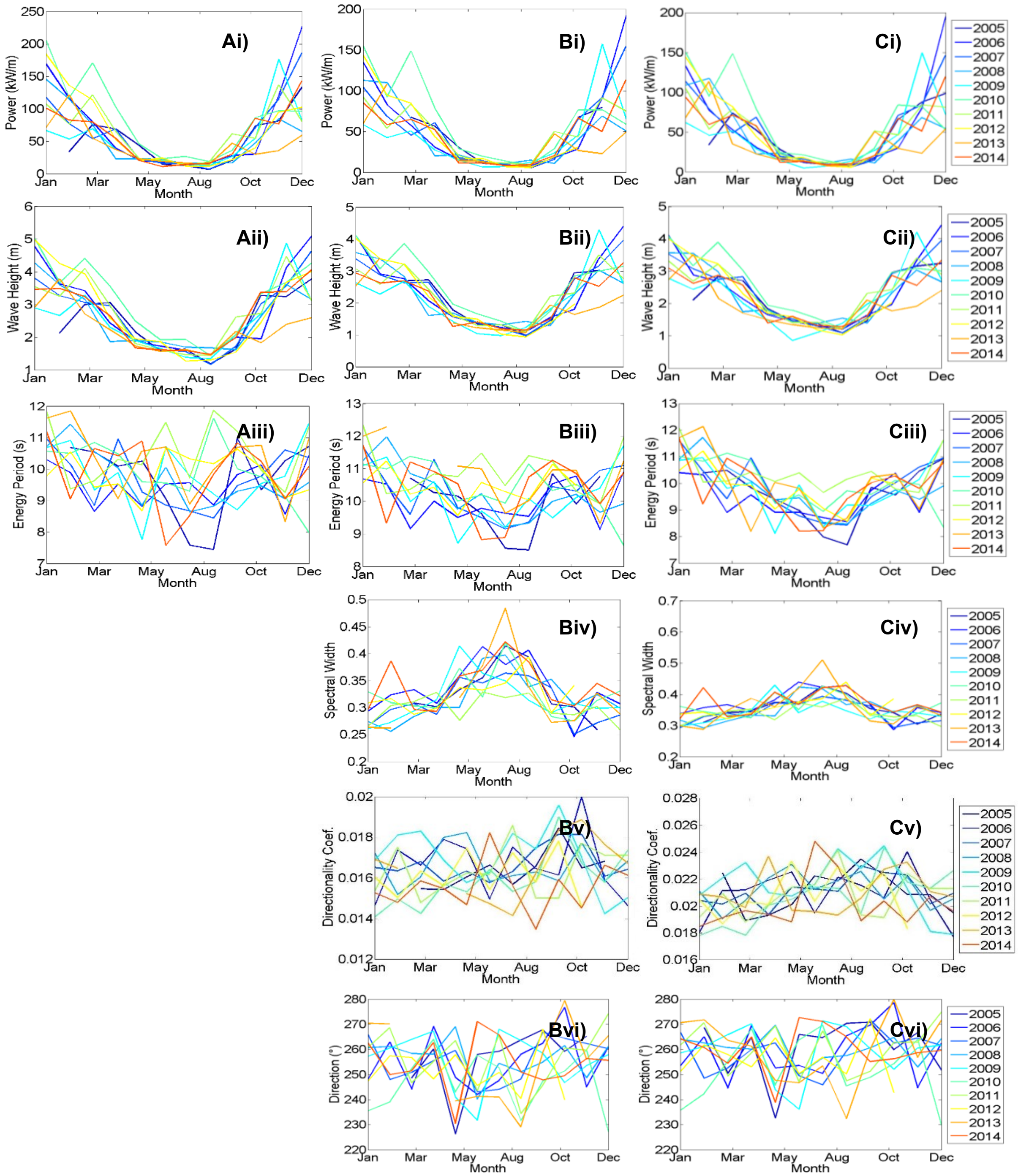

Figure 9.15 – Annual Variation of the Monthly Mean Values from 2005 to 2014 at the Beverley Buoy for a) Reconnaissance; b) Feasibility; and c) Design Stages for i) Wave Power; ii) Wave Height; iii) Energy Period; iv) Spectral Width; v) Directionality Coefficient; and vi) Wave Energy Direction

The cumulative distribution curves for the wave height, power, and energy period are shown in Figure 9.16 to Figure 9.18 for all three classes of assessment. Figure 9.16 shows the modeled wave power, where it was observed that the summer months had a steeper curve than the winter months, indicating a lower percentage of higher wave power. The annual curve fits in decently between the more active winter months and the calmer summer months and is similar to the spring and fall cumulative percentage curves. When comparing the different classes of assessment, it was noted that the reconnaissance class assessment did have higher potential wave power than the feasibility and design class assessments. Very similar observations were made for the cumulative distribution curves of the wave heights as well, shown in Figure 9.17.

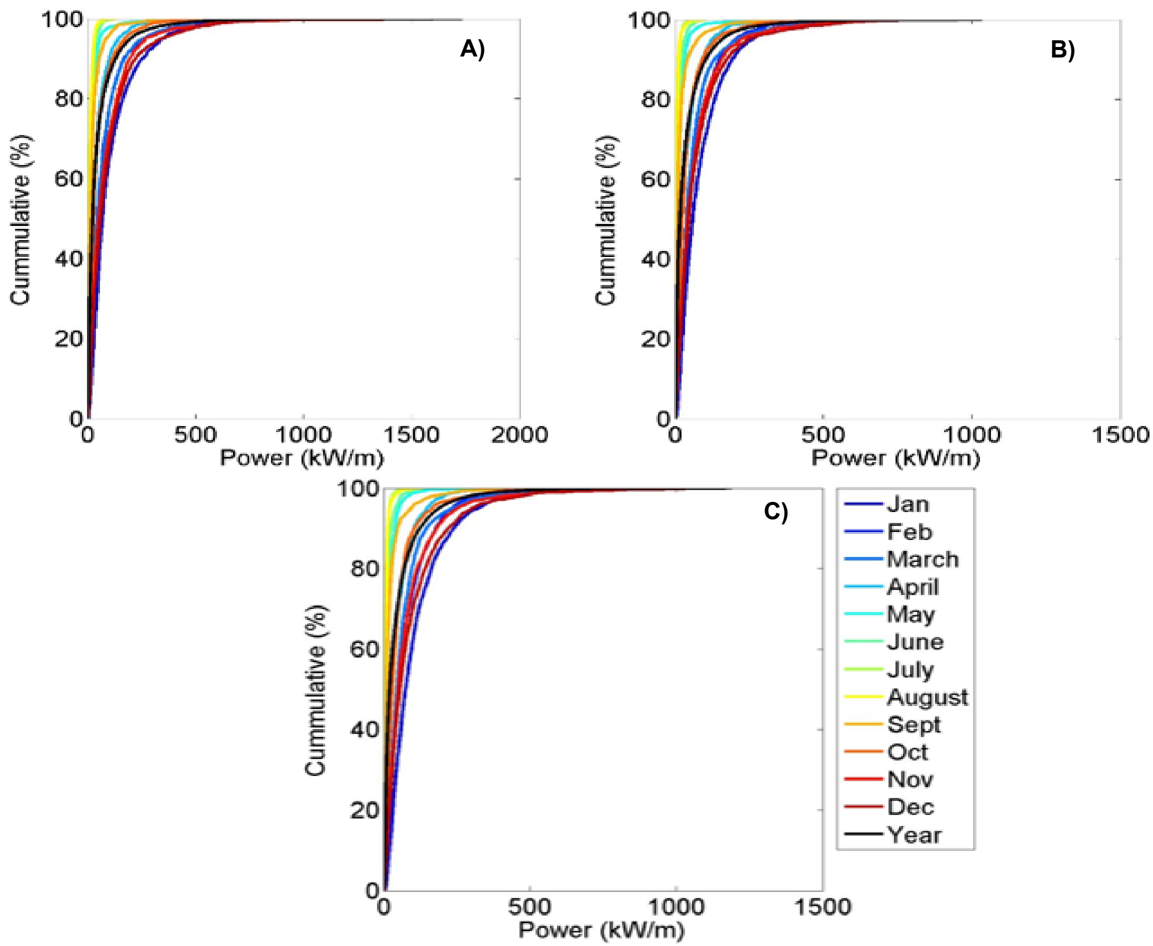

Figure 9.16 – Cumulative Distribution Curves for the Wave Power at the Beverley Buoy for A) Reconnaissance Stage; B) Feasibility Stage; and C) Design Stage from 2005 – 2014

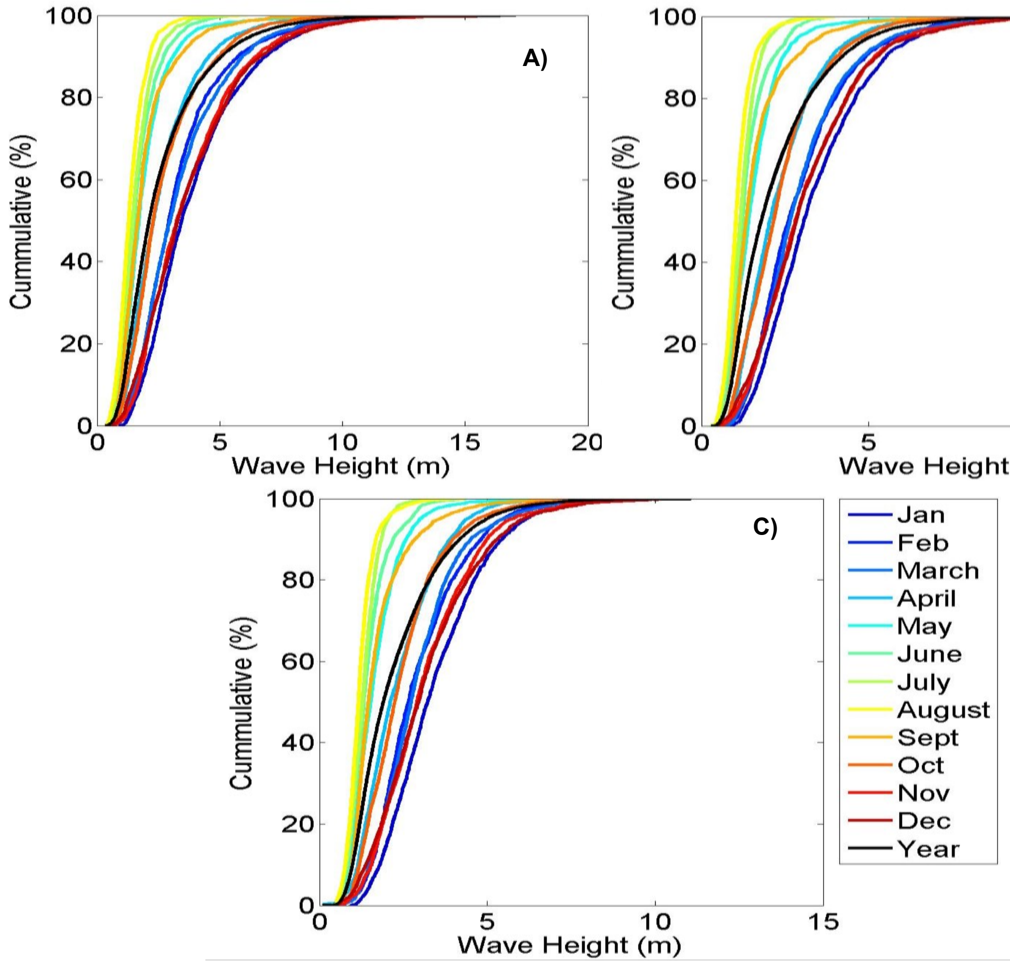

Figure 9.17 – Cumulative Distribution Curves for the Wave Height at the Beverley Buoy for A) Reconnaissance Stage; B) Feasibility Stage; and C) Design Stage from 2005 – 2014

Finally, the cumulative distribution of the energy period is shown for all classes of assessment in Figure 9.18. For the reconnaissance class assessment, the monthly and annual curves are very similar for all of seasons, and no distinct trends were observed. Greater distinction between the curves was noted for the feasibility class assessment, where the summer months seemed to have lower values, however the lines are still grouped close together and there is not a significant seasonal difference. This changes for the design class assessment which shows distinction between the different cumulative curves with a seasonal trend of lower energy periods in the summer and higher periods in the winter months.

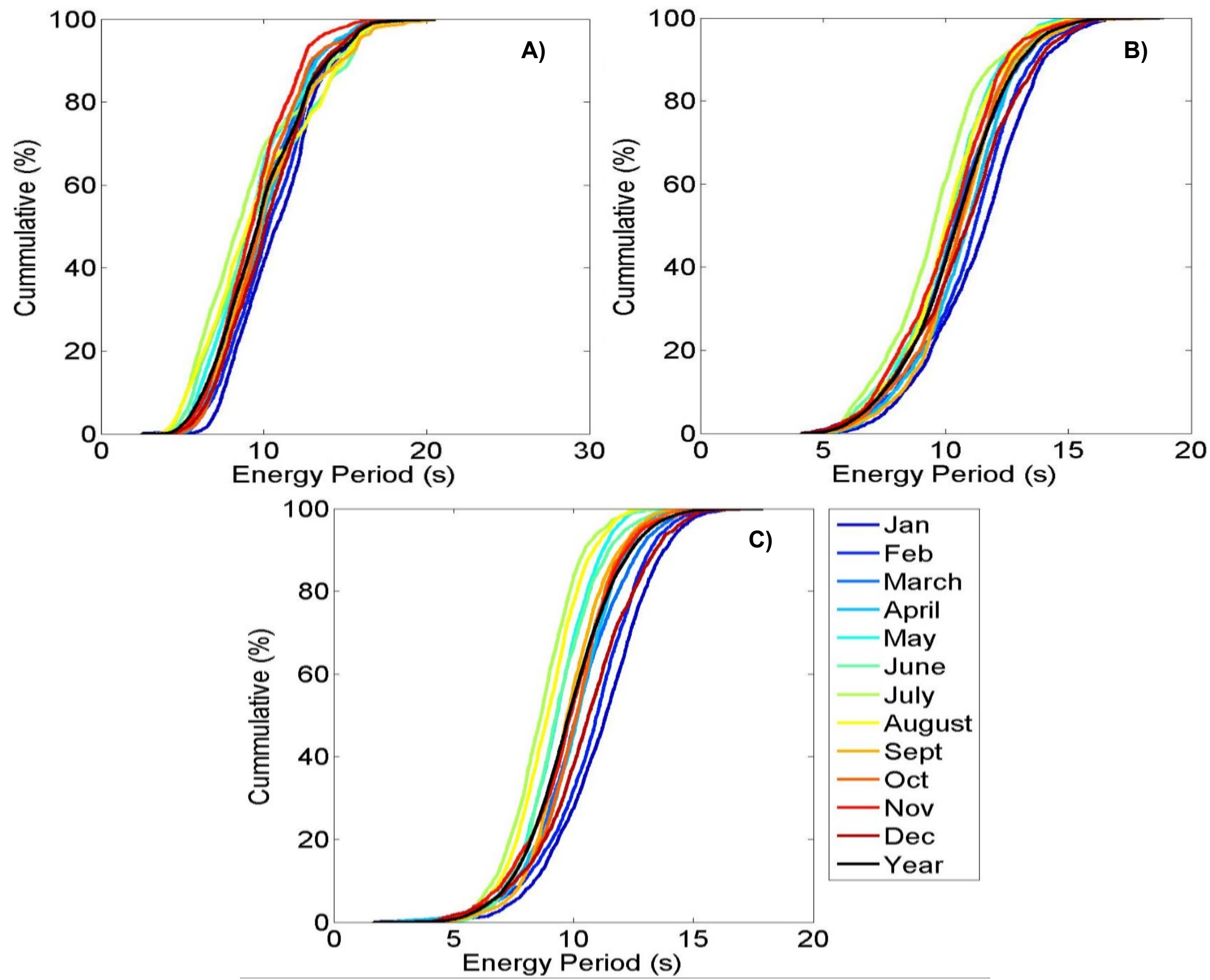

Figure 9.18 – Cumulative Distribution Curves for the Wave Energy Period at the Beverley Buoy for A) Reconnaissance Stage; B) Feasibility Stage; and C) Design Stage from 2005 – 2014

9.4 Wave Climate

The wave climate can be described in several manners, such as through a bivariate distribution or a wave rose. Bivariate distributions of the wave height and the wave energy period are tools that technology developers can used to determine which sea states contribute the most to the annual energy for a specific site of interest. Whereas wave roses show the directions that the wave energy predominantly travels in. Both are shown in this section as per the requirements of the IEC-TS.

Figure 9.19 shows the bivariate distribution at the Beverley site for all three classes of assessment. The bivariate distribution discretizes the wave heights in 0.5m bins, with wave energy periods discretized into 1s bins. The number of hours per year that the wave state occurs is included within each bin, while the percentage of the total wave power for each bin is indicated by the bin colour. Despite all three figures representing the climate at the Beverley site, there is significant variation in the distribution that occurs based on the class of assessment.

For the reconnaissance class assessment, the available wave power is distributed over a large range of wave energy periods and heights, with the most commonly occurring wave climate having a wave height between 1 and 1.5m, and an energy period between 9 and 10s, which occurs for approximately 298 hours per year. This differs from the sea state with the most power, which occurs between a wave height of 6.5 and 7m, and an energy period of 7 to 8s, occurring only 52 hours per year.

In the case of the feasibility and design class assessments, both show a more compact distribution with distinct high energy zones. Additionally, the shape of these two distributions is more similar to each other and what has been seen in literature. For the feasibility class assessment, the highest wave power occurs between a wave height of 2.5 and 3m with an energy period between 11 and 12s, representing a total of 2.5% of the total available annual wave power, and occurring for approximately 187 hours a year. While the design class assessment has the highest wave power occur at a wave height of 2.5 to 3m and an energy period of 10 to 11s, representing 2.7% of the available annual wave power and occurring 227 hours per year. When compared to the bivariate distributions obtained by Robertson *et al*. [2014] for a nearby site it can be seen that the plots compare favorably for the feasibility and design class assessment. In Robertson's study the sea state with the highest available annual wave power has a wave height of 2.75m and an energy period of 9.5s, occurring 346 hours per year. While this does have a higher rate of occurrence than that seen for either class, it does correspond to similar wave heights and energy periods.

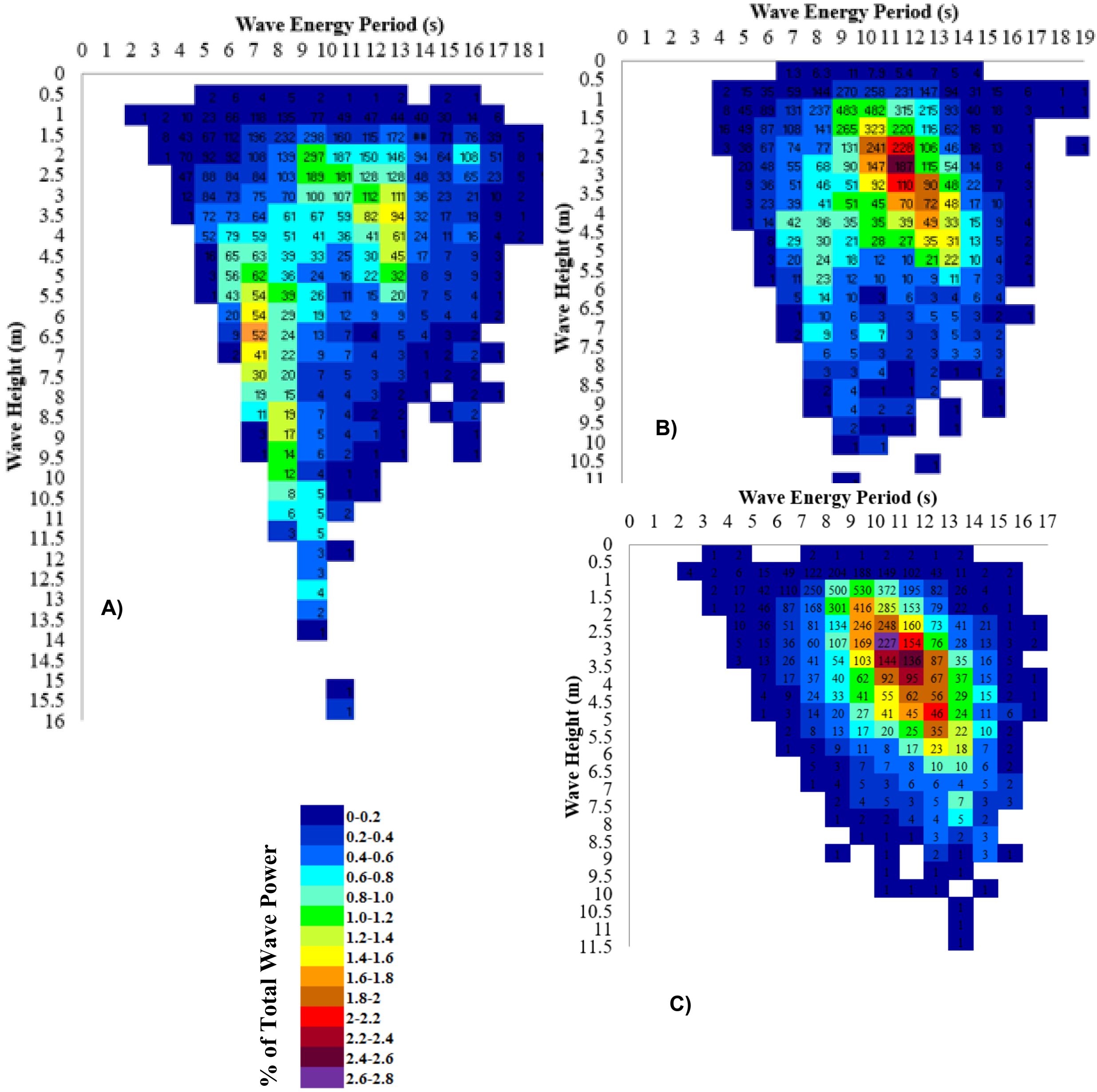

Figure 9.19 – Bivariate Distribution Showing the Probability and Power Distribution for A) Reconnaissance, B) Feasibility; and C) Design Stage. Numbers Indicate the Number of Hours per Year, While Contour Indicates the Percentage of Wave Power in Each Sea State

The most commonly occurring wave state for the feasibility and design class assessments have wave heights of 1 to 1.5m and energy periods of 9 to 10s occurring for 483 hours a year at the feasibility class assessment; and wave heights of 1 to 1.5m and energy periods of 9 to 10s occurring for 530 hours per year for the design class assessment. Again, this compares relatively favorably to the observations of Robertson *et al.* [2014a] who found that the most commonly occurring wave state was 1.75m with a wave period of 8.25s which occurred for 516 hours.

Figure 9.20 shows the wave power rose at the Beverley site for all three classes of assessment. These plots show the wave direction and its percentage of occurrence, as well as the wave power for each of the different directions. From this figure it was determined that the waves tend to come from the west or southwestern direction, which is also the direction of the highest percentage of wave power. Due to the directional resolution of the reconnaissance class assessment waves from a wider range of directions are grouped together, giving them a higher rate of occurrence. It can also be noted from this figure that while the reconnaissance and feasibility class assessments have the wave power coming predominantly from the same direction, the design class assessment has the power coming from a slightly more westerly direction, this is likely a result of the different boundary conditions and increased directional resolution.

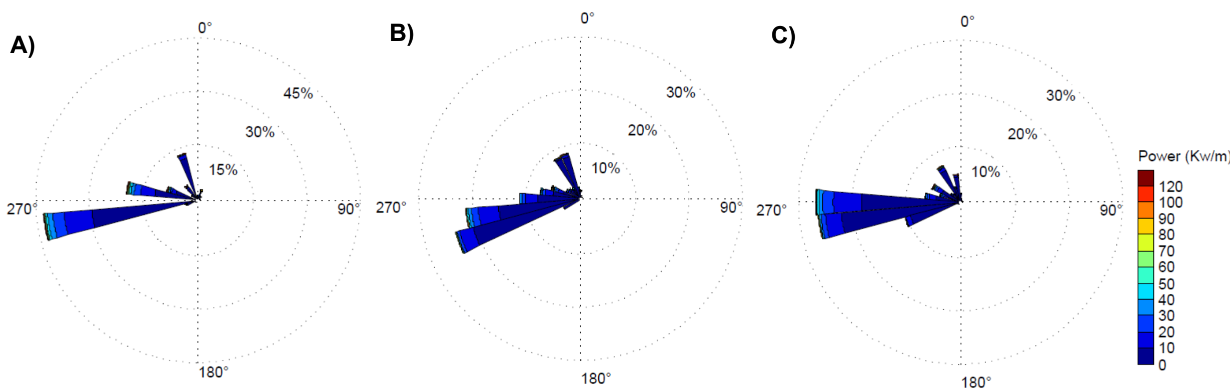

Figure 9.20 – Wave Roses for A) Reconnaissance, B) Feasibility; and C) Design Stage

9.5 Discussion

To assess the wave climate in western Canada and to compare the wave energy resource for all three classes of assessment a 10-year wave energy resource assessment (2005-2014) was conducted based on the recommendations and requirements of the IEC-TS.

When comparing the modeled wave parameters at the three validation sites with those obtained in the field it was noted that the reconnaissance class assessment tended to overestimate the wave resource and climate; while both the feasibility and design class assessments appeared to provide more accurate estimations. However, it should be noted that while the reconnaissance and feasibility class assessments were validated at three locations only the Beverley Buoy could be used to validate the design class assessment due to the model domain size. Additionally, both Neah Bay and La Perouse could only be used for the validation of the wave height as they were not omni-directional wave buoys. These observations are in line with the expectations set out by the IEC-TS which indicate that the reconnaissance class assessment would be less accurate than both the feasibility and design class assessments.

It was also noted during this study, that while the modeled wave parameters were reasonably comparable to the measured parameters, there were large discrepancies in terms of the actual wave spectra. It was noted that the modeled wave spectra did not accurately represent the multi-nodal nature of the measured wave spectra and typically represented the energy as a single large energy peak instead. As the IEC-TS does not require the researchers to present the individual wave spectra this representation of the wave energy is not considered to be a concern for developers.

9.6 Domain Variation

The average and monthly wave height, power, energy period, and wave direction were examined for all three classes of assessment across the entire domain. The observations made for the average wave parameters were compared with those obtained in previous studies to determine how the current research compares with the observations of those done within the region.

The average wave energy transport was compared at both the Beverley site and a nearshore location to the observations made by Robertson *et al. [*2014a]. It was noted from this comparison that the current model compared relatively favourably with the observations provided by Robertson *et al.* at the Beverley site, but less favourably at the nearshore location. This is considered to be a result of the high variability of the wave energy transport within the nearshore zone which makes it difficult to compare between models. When compared to the model completed by Cornett and Zhang [2008], the model does not compare as favourably at the Beverley location, while agreeing slightly better at the shallow water location. Visually, the trends observed within the current model appear to be consistent with the observations seen in both the results provided Robertson *et al.* [2014a] and Cornett and Zhang [2008].

When examining the monthly variability of the four different parameters, it was noted that both the wave height and wave power show strong seasonal trends, with the wave climate being very active in the late fall and winter, and extremely calm in the summer months. This trend was also noted for the energy period, which showed high periods throughout the entire domain in the winter, with lower energy periods offshore during the summer months (and throughout the entire domain for the reconnaissance class assessment). The wave direction did not appear to show significant seasonal variation. This type of seasonal trend appears to be very common both within the study region and at other sites across the globe (Robertson, Hiles, & Buckham, Canada, 2014a; Liberti, Carillo, & Sannino, 2013; Ramos & Ringwood, 2016). This may indicate that the IEC-TS should require the assessment and reporting of the seasonal variation across the domain, as well as the seasonal variation of the entire assessment period, as opposed to just the annual variation of the monthly mean values. Seasonality of the wave energy can be a concern for wave energy converters and the amount of accessible power, as the devices are intended to work within a specified range of conditions which may be exceeded in the winter months and not met in the summer. This may mean that while the potential available energy within a region may be high, the amount of power that can be extracted may be much lower.

9.7 Temporal Variation

The temporal variation at the Beverley site was examined for all three classes of assessment to examine the seasonal variation in the wave climate and to examine if the site displays any long-term trends.

The monthly average temporal resolution at the Beverley site shows similar seasonal variation as noted across the model domain, with the wave height and wave power (both omni-directional and maximum) being more active in the winter and much calmer in the summer months. The wave energy period does show some seasonal variation, though this difference is more marked for the design class assessment than for the feasibility or reconnaissance assessments, while for the spectral width the seasonal variation is more pronounced at the feasibility class than the design class. Both the directionality coefficient and the direction do not show any real seasonal trends.

The yearly average temporal resolutions do not indicate any long-term trends within the wave climate, which indicate that the 10-year assessment period should be a good indicator of the future wave energy resource.

9.8 Wave Climate

The wave climate is represented in terms of the bivariate distribution of the wave energy over the different wave states, and through wave roses, which were examined for all three classes of assessment.

The main observations from the bivariate distributions were that the reconnaissance class assessment is not suitable for use in development as the available wave energy was distributed over a large range of wave states and did not accurately represent the real system. The feasibility and design classes showed much more realistic distributions which showed that the most active wave states were not the most frequent, which agrees with the findings of Robertson *et al.* Both wave states had the highest wave power occurring between wave heights of 2.5 and 3 with the energy period being between 11-12s for the feasibility class and 10-11s for the design class assessment. This agrees favourably with the observations made by Robertson *et al.* for the same location.

The wave roses show the impact that the directional bin size has on the representation of the wave energy. In the case of the reconnaissance class assessment, almost 45% of the wave energy is coming from a direction of approximately 260°, while at the feasibility this is split into two different wave energies coming from 255° and 265° both accounting for less than 25% of the energy. Surprisingly, for the design class assessment the most wave energy is coming from approximately 273° with slightly less coming from approximately 266° which indicates that this model has a slightly more westerly direction of energy transport. In all cases the wave energy came predominantly from a westerly direction, with smaller amounts of energy also coming from the north-west.

9.9 Resource Class Comparison

This final section compares the difference wave energy assessment classes and evaluates their performance based on the expectations of the IEC-TS. Based on the observations made during the 10-year resource assessment it became clear that the reconnaissance assessment provided the least accurate estimations of the wave climate and resource, this agrees with the expectations of the IEC-TS which indicated that the reconnaissance class assessment was intended as a quick method of determining the resource in a region with some accuracy. However, when comparing the differences between the feasibility and design class assessments in terms of accuracy and computational cost, the benefits of having two different stages is not as evident. When examining the wave height and the power, both classes of assessment provide nearly identical values, and the only significant variation between these two classes occurs for the spectral width and the directionality coefficient. When examining the wave climate both classes show similar zones of high energy, and both had the same most frequent wave states. However, this slight change in resource assessment comes at a significant computational cost with the design class model taking almost 3 times the duration to run as the feasibility class assessment.

10 Guidance and Recommendations for the IEC Specification

This section contains guidance on the application of the IEC for future users and recommendations and comments on the requirements and methodologies prescribed within the IEC-TS.

10.1 User Guidance

The user guidance is intended to help aide users of the IEC-TS in selecting parameters and resolutions appropriate for the stage of assessment under consideration based on the observations made during this study. It should be noted that the recommendations may be site specific and so best judgement must be used when conducting a resource assessment.

10.1.1 Guidance for the Reconnaissance Stage Assessment

10.1.1.1 Model Resolution

It was found when running the model that using the larger wind resolution suggested by the IEC-TS did introduce more error into the wave height and power estimations, better results were obtained using the wind resolution from the feasibility stage level. For locations with highly spatially variable winds this even more important as the lower resolution requirement may result in the over or under prediction of these variables.

For the model spectral resolution, it was found that the accuracy of the model increased as the directional resolution increased, while the for the frequency bin the increase in accuracy was minimal once a resolution of 57 bins was reached. Increasing either of these two parameters resulted in a large increase in computational cost and so it is suggested that lower values are used for this stage of assessment.

10.1.1.2 Boundary Conditions

The reconnaissance stage assessment can use either parametric boundary conditions (defined by the wave height, energy period, and direction) or spectral boundary conditions. If available, the spectral boundary conditions allow for a more realistic representation of the wave conditions and will provide more accurate and reliable results at no additional computational cost. If this is not available, then a good understanding of the spectral wave shape in the study domain is necessary as the selection of the spectral shape can result in a wide range of model errors.

10.1.1.3 Physical Processes

The reconnaissance stage assessment requires the consideration of wind-wave growth, whitecapping, quadruplet and triad wave interactions, diffraction, and refraction. It considers the use of wave breaking and bottom friction to be acceptable but not required. The parameters requiring consideration must be included in the numerical model unless it is shown through sensitivity analysis that it does not impact the wave energy resource.

Based on the observations made during the sensitivity analysis it was found that the resource assessment was not sensitive to the depth-induced wave breaking or triad interactions at a study site in 45m water depth. The exclusions of these parameters resulted in a slight time reduction of the numerical model which may be valuable for larger domains. In the case of the triad interactions a sensitivity analysis would be required to prove that the model is not sensitive to this parameter in the location of interest.

In the case of the bottom friction, the model was found to be sensitive to this process for all three validation parameters. It is therefore recommended that this process be considered in the numerical model.

10.1.1.4 General Observations

It was noted when completing the sensitivity analysis that the computational time-step used by the model did not have a significant impact on the resource assessment but had a significant impact on the computational cost of the model. The maximum frequency included in the numerical model had a slightly larger impact on the results and should be optimized for the study site of interest.

10.1.2 Guidance for the Feasibility Stage Assessment

10.1.2.1 Model Resolution

When looking at the spectral resolution of the model, it was found that there was slight sensitivity to the number of frequency bins used in the model, mostly in terms of the wave power. It is recommended that between 41 and 57 bins be used as they had relatively good accuracy for lower computational costs. In terms of the directional resolution a minimum of 36 bins should be required as lower values introduced a large amount of error. However, increasing the resolution beyond this value did not result in significantly large improvements while resulting in much longer computational times.

10.1.2.2 Physical Processes

The feasibility stage assessment requires that all physical processes be included in the model. These parameters must be included in the numerical model unless it is shown through sensitivity analysis that it does not impact the wave energy resource.

It was found when running the sensitivity analysis that the resource assessment was not sensitive to triad wave interactions for the site of interest located at 45m water depths. Due to the relatively large decrease in the models computational cost when excluding this parameters it is suggested that a sensitivity analysis is carried out as per the TS instructions to determine if they are required.

10.1.2.3 General Observations

It was noted when completing the sensitivity analysis that the computational time-step used by the model did not have a significant impact on the resource assessment but had a significant impact on the computational cost of the model. The maximum frequency included in the numerical model had a slightly larger impact on the results and should be optimized for the study site of interest.

10.1.3 Guidance for the Design Stage Assessment

The sensitivity of the model to the physical processes required by the TS was not examined for the design stage of assessment as the observations between the reconnaissance and feasibility stage assessments were very similar.

10.1.3.1 Model Resolution

The modeled wave resource assessment did not appear to be very sensitive to either the mesh resolution or the wind resolution which were both tested at lower resolutions than required by the

TS. However, it should be noted that improved bathymetry may result in better estimations for a finer mesh resolution.

For the models spectral resolution there was an increase in the model accuracy and reliability as the number of bins increased. However, due to the relatively large increase in computational cost it is suggested that the minimum requirements provided by the TS be utilized.

10.1.3.2 General Observations

It was noted when completing the sensitivity analysis that the computational time-step used by the model did not have a significant impact on the resource assessment but had a significant impact on the computational cost of the model.

10.1.4 Guidance for the Model Validation

When testing the validation criteria provided by the TS it was noted that the omni-directional wave power always had significantly higher errors than recommended which may indicate that this threshold used for this parameter may need modification.

To properly complete the model validation, it is recommended that a full year of consecutive data be used as this was found to have a large impact on the coverage criteria and potentially on the error values calculated.

11 Conclusions and Future Work

11.1 Conclusions

The research conducted in this study sought to appraise and validate the IEC-TC-114 technical specification for wave energy resource assessment in terms of its mythologies, requirements, and sources of error. This assessment was conducted through the pilot application of the IEC-TS to a project site located on the west coast of Vancouver Island in British Columbia. The objectives of this research were to (1) establish a firm scientific rational for the technical specification, (2) suggest improvements for future iterations of the TS, (3) conduct a sensitivity analysis to determine sources or error and uncertainty within the specification, (4) develop a user guidance , and (5) to complete an assessment of the wave energy resource for all three classes of assessment at the pilot project site.

It was observed during this study that the IEC-TS could be applied to the assessment of wave energy with reasonable computational effort. Additionally, the IEC-TS is overall relatively easy to understand and apply, with the only exception to this being the validation procedure which lacks clarity. However, it was noted that in many cases the IEC-TS would not provide defined requirements, but only recommendations which would allow researchers to potentially disregard the recommendations provided within. While this is likely due to the fact that different sites may have different requirements, it does call into question the need for a standard if it is not going to have strict requirements to ensure that all resource assessments are completed using state of the art knowledge and procedures.

The sensitivity analysis carried out in Chapter 8 was used to identify the main sources of error and uncertainty within the IEC-TS and to determine if the recommendations within the TS were adequate. The main observations from this sensitivity analysis were:

1. The wave resource is highly sensitive to the whitecapping energy dissipation process but is not sensitive to triad wave-wave interactions which indicates that triads may not be required for consideration in the wave energy resource assessment. Similarly, the reconnaissance class assessment was not sensitive to depth-induced wave breaking.

2. The prescribed range of acceptable mesh resolutions is considered sufficient for the reconnaissance and feasibility class assessment. However, no change in the resource assessment was observed at the design class, indicating that a larger resolution could be used at lower computational cost.
3. The spectral boundary conditions provided better resource assessments for the reconnaissance and feasibility class assessments, indicating that it should be used whenever possible.
4. The updated recommended directional resolutions provide accurate wave resource assessments at reasonable computational costs. Decreasing below these resolutions were found to introduce more error, while increasing resulted in more accurate assessments between significant increases in the computational cost.
5. The baseline frequency resolution provided accurate wave resource assessments at reasonable computational costs. The feasibility class assessment could be kept at the IEC-TS recommended resolution with only a slight decrease in accuracy. However, the design class assessment showed a marked decrease in accuracy when using the IEC-TS recommended resolution.
6. The wind resolution must be dependent on the site-specific wind conditions as this will dictate how best to capture the wind variability with the mesh.

Included in Chapter 8 are recommendations to improve future versions of the IEC-TS based on observations made through the sensitivity analysis. This included a new recommendation on the method of calculating the model's sensitivity to different parameters.

An assessment of the wave energy resource along the western coast of Vancouver Island was performed in Chapter 9. This resource assessment was found to compare favourably to others performed within the same region, with mean energy transports ranging from 28kW/m to 31 kW/m at the Beverley site. However, a strong seasonal bias was observed at the site which means that the average power is not necessarily an indication of the actual available power. Due to this it is suggested that the IEC-TS require the reporting of the seasonal variation across the domain, and at the site of interest. The modeled wave climate was also found to compare favourably with previous research at the site for both the feasibility and design class assessments. When comparing the different resource assessments and their objectives within the IEC-TS it was clear that the reconnaissance class assessment fulfilled its role as a quick and easy method of determining areas of high energy. The feasibility and design class assessments were able to provide more accurate and realistic estimations of the wave resource; however, both models provided very similar resource assessments leading to the question of whether it is necessary to have both stages of assessments within the IEC-TS or whether it is possible to combine their requirements into one assessment class, reducing the amount of computational effort.

11.2 Recommendations for Future Work

The observations made through the sensitivity analysis and resource assessment are site-specific. Further research still needs to be performed to ensure that these observations are consistent at other research sites and using other numerical models. Additionally, due to restrictions on the availability of data, there were certain parameters that could not be assessed. As a result, it is recommended that the following topics be examined in the future:

1. The sensitivity of the model results to the bathymetric resolution; due to the unavailability of additional bathymetric sources for the design assessment it was not possible to determine the impact that finer resolution bathymetry might have on the results.
2. Comparisons between additional data sources for the wind and boundary conditions were not addressed within this research. Comparisons between different global wave models have been made in other research, but their impact on the calculation of the wave energy resource has not been assessed.

The final test of the IEC-TS is its applicability to real-world applications. While pilot projects such as this are useful for determining the restrictions in modelling the wave energy resource it is necessary to work with technology developers to ensure that the proposed deliverables and the accuracy is suitable to their needs.

12 References

Alves, J., & Banner, M. (2003). Performance of a Saturation-Based Dissipation-Rate Source Term in Modelling the Fetch-Limited Evolution of Wind Waves. *j. Phys. Oceanography*, 33, 1274-1298.

Battjes, J. A., & Janssen, J. (1978). Energy Loss and Set-up Due to Breaking of Random Waves. *Proc. 16th Int. Conf. Coastal Engineering* (pp. 569-587). ASCE.

Beji, S., & Battjes, J. A. (1993). Experimental Investiagion of Wave Propagation over a Bar. *Coastal Engineering*, 19: 151-162.

Beya, I., Buckham, B., & Robertson, B. (2021). Impact of Tidal Currents and Model Fidelity on Wave Energy Resource Assessments. *Renewable Energy*, 176, pp. 50-66.

Buckham, B. (2013). The West Coast Wave Initiative - A Strategic Approach to Wave Energy Development. *Presented at the Marine Renewables Canada Annual Conference.* Ottawa, Canada.

Carballo, R., Sanchez, M., Ramos, V., & Castro, A. (2014). A Tool for Combined WEC-Site Selection Throughout a Coastal Region: Rias Baixas, NW Spain. *Applied Energy*, 135: 11-19.

Carter, R. W. (2005). *Wave Energy Converters and a Submerged Horizontal Plate.* University of Hawai'i.

CHC-Canadian Hydraulics Centre. (2011). *Blue Kenue Reference Manual.* Ottawa, Canada: National Research Council.

Clement, A., McCullen, P., Falcao, A., Fiorentino, A., Gardner, F., Hammarlund, K., . . . Thorpe, T. (2002). Wave Energy in Europe: Current Status and Perspectivees. *Renewable and Sustainable Energy Revies*, Vol. 6, pp. 405-431.

Cornett, A., & Zhang, J. (2008). *Nearshore Wave Energy Resources, Western Vancouver Island, B.C.* Ottawa, Canada: Canadian Hydraulics Centre, National Research Council of Canada.

Drew, B., Plummer, A. R., & Sahinkaya, M. N. (2009). A Review of Wave Energy Converter Technology. *Proceedings IMechE Part A: J. Power and Energy*, (pp. Vol. 223, pp. 887-902).

Dykes, J. D., Hsu, Y. L., & Rogers, W. E. (2003). SWAN Evaluation in the Northern Gulf of Mexico. *7th International Workshop on Wave Hindcasting and Forecasting.* Banff, Alberta, Canada.

Eldeberkey, Y. (1996). *Nonlinear Transformation of Wave Spectra in the Nearshore Zone.* Ph.D. Thesis, Delft University of Technology, Department of Civil Engineering, The Netherlands.

Eldeberky, Y., & Battjes, J. (1995). Parameterization of Triad Interactions in Wave Energy models. *Proc. Coastal Dynamics Conf. '95*, (pp. 140-). Gdansk, Poland.

Elderberky, Y., & Battjes, J. A. (1995). Parameterization of Triand Interactions in Wave Energy Model. *Proc. Coastal Dynamics Conf '95*, (pp. 140-148). Gdansk, Polan.

EMEC. (n.d.). *Pelamis Wave Power*. Retrieved from EMEC Orkney: The European Marine Energy Centre LTD: http://www.emec.org.uk/about-us/wave-clients/pelamis-wave-power/

Ente Vasco De La Energia. (2013, July 24). *Jornada de Puertas Abiertas en la Planta de Energía de las Olas de Mutriku*. Retrieved from http://www.eve.eus/Noticias/Jornada-de-puertas-abiertas-en-la-planta-de-energi.aspx?lang=en-GB

Environment Canada. (n.d.). Retrieved from http://www.meds-sdmm.dfo-mpo.gc.ca/isdm-gdsi/waves-vagues/search-recherche/list-liste/data-donnees-eng.asp?medsid=C46206

Falcão, A. F. (2010). Wave Energy Utlization: A Review of the Technologies. *Renewable and Sustainable Energy Reviews*, Vol. 14, pp. 899-918.

Falnes, J. (2007). A Review of Wave-Energy Extraction. *Marine Structures*, Vol. 20, pp. 185-201.

Folley, M., Elsaesser, B., & Whittaker, T. (2009). Analysis of the Wave Energy Resource at the European Marine Energy Centre. *Coasts, Marine Structures and Breakwaters.* Edinburgh.

García-Medina, G., Yang, Z., Wu, W.-C., & Wang, T. (2021). Wave Resource Characterization at Regional and Nearshore Scales for the U.S. Alaska Coast based on a 32-Year High-Resolution Hindcast. *Renewable Energy*, 170 pp 595-612.

Gray, A., Dickens, B., Bruce, T., Ashton, I., & Johanning, L. (2017). Reliability and O & M Sensitivity Analysis as a Consequence of Site Specific Characteristics for Wave Energy Converters. *Ocean Engineering*, 141: 493-511.

Guillou, N. (2017). Modelling Effects of Tidal Currens on Waves at a Tidal Stream Energy Site. *Renewable Energy*, 114: 180-190.

Hagerman, G., & Bedard, R. (2003). *Guidelines for Preliminary Estimation of Power Production by Offshore Wave Energy Conversion Devices.* EPRI.

Harris, R. E., Johanning, L., & Wolfram, J. (2004). Mooring Systems for Wave Energy Converters: A Review of Design Issues and Choices. *Proceedings of World Renewable Energy Congress VII.* Denver, USA.

Hasselmann, K. (1974). On the Spectral Dissipation of Ocean Waves Due to Whitecapping. *Bound. -layer Meteor.*, 6(1-2): 107-127.

Hasselmann, K., Barnett, T. P., Bouws, E., Carlson, H., Cartwright, D. E., Enke, K., . . . Walden, H. (1973). Measurement of Wind-Wave Growth and Swell Decay During the Joint North Sea Wave Project (JONSWAP). *Dtsch. Hydrogr. Z. Suppl.*, 12: A8.

Hasselmann, S., Hasselmann, K., Allender, J. H., & Barnett, T. P. (1985). Computations and Parameterizations of the Nonlinear Energy Transfer in a Gravity Wave Spectrum. Part II: Parameterizations of the Nonlinear Transfer for Application in Wave Models. *Journal of Physical Oceanography*, 15(11): 1378-1391.

Hiles, C., Bickham, B., Wild, P., & Robertson, B. (2013). Ocean Renewable Wave Energy Resources Near Hot Springs Cove, Canada. *Renewable Energy*, 23.

Holmberg, P., Andersson, M., Bolund, B., & Strandanger, K. (2011). *Wave Power - Surveillance Study of the Development.* Elforsk.

Huckerby, J. A., Jeffery, H., & Moran, B. (2011). *An International Vision for Ocean Energy*. Retrieved from Ocean Energy Systems Implementing Agreement: http://www.oceanrenewable.com/wp-content/uploads/2011/05/oes_vision_brochure_2011.pdf

IEC. (2014). *Wave Energy Resource Assessment and Characterization.* IEC/TS 62600-101.

Ivanova, I. A., Bernhoff, H., Agren, O., & Leijon, M. (2005). Simulated Generator for Wave Energy Extraction in Deep Water. *Ocean Engineering*, Vol. 32, pp. 1664-1678.

Jones, C., Magalen, J., & Roberts, J. (2014). *Wave Energy Converter (WEC) Array Effects on Wave, Current, and Sediment Circulation: Monterey Bay, CA.* Albuquerque, New Mexico: Sandia National Laboratories.

Kim, C. -K., Toft, J. E., Papenfus, M., Verutes, G., Guerry, A. D., Ruckelshaus, M. H., . . . Polasky, S. (2012). Catching the Right Wave: Evaluating Wave Energy Resources and Potential Compatibility with Existing Marine and Coastal Uses. *PLOS-one*, 7(11) e47598.

Komen, G. J., Cavaleri , L., Donelan, M., Hasselmann, K., Hasselmann , S., & Janssen, P. (1994). *Dynamics and Modelling of OCean Waves.* Cambridge Univeristy Press.

Lenee-Bluhm, P., Paasch, R., & Tuba Ozkan-Haller, H. (2011). Characterizing the Wave Energy Resource of the US Pacific Northwest. *Renewable Energy*, 2106-2119.

Liang, B., Shao, Z., Wu, Y., Shi, H., & Liu, Z. (2017). Numerical Study to Estimate the Wave Energy Under Wave-Current Interaction in the Qingdao Coast, China. *Renewable Energy*, 101: 845-855.

Liberti, L., Carillo, A., & Sannino, G. (2013). Wave Energy Resource Assessment in the Mediterranean, the Italian Perspective. *Renewable Energy*, 938-949.

Lokuliyana, R., Folley, M., Gunawardance, S., & Wickramanayake, P. (2020). Sri Lankan Wave Energy Resource Assessment and Characterisation based on IEC Standards. *Renewable Energy*, Vol 162, pp. 1255-1272.

Mackay, E., & Hassan, G. L. (2012). 8.03 Resource Assessment for Wave Energy. In A. Sayigh, *Comprehensive Renewable Energy, Volume 8.* Elsevier.

Madsen, P. A., & Sorensen, O. R. (1993). Bound Waves and Triad Interactions in Shallow Water. *Ocean Engineering*, 20(4): 359-388.

McCormick, M. E. (1978). Wind-Wave Power Available to a Wave Energy Converter Array. *Ocean Engineering*, Vol. 5, pp. 67-74.

Mei, C. C. (1983). *The Applied Dynamics of Ocean Surface Waves.* New York: Wiley.

Miles, J. W. (1957). On the Generation of Surface Waves by Shear Flows. *Journal of Fluid Mechanics*, 3: 185-204.

National Oceanic and Atmospheric Administation. (n.d.). Retrieved from ftp://polar.ncep.noaa.gov/pub/history/waves

NOAA. (n.d.). Retrieved from Available http://www.ndbc.noaa.gov/station_history.php?station=46087

NOAA. (n.d.). Retrieved from ftp://polar.ncep.noaa.gov/pub/history/waves

Phillips, O. M. (1957). On the Generation of Waves by Turbulent Wind. *Journal of Fluid Mechanics*, 2: 417-445.

Piche, S., Cornett, A., Baker, S., & Nistor, I. (2015). Appraisal of the IEC Technical Specification for Assessment of Wave Energy Resources. *Proc. 2015 Int. Conf. on Ocean, Offshore and Artic Eng.* St Johns, Canada.

Piche, S., Cornett, A., Baker, S., & Nistor, I. (2015). Validation of the IEC Technical Specification for Wave Energy Resource Assessment. *European Wave and Tidal Energy Conf.* Nantes, France.

Ramos, V., & Ringwood, J. (2016). Exploring the Utility and Effectiveness of the IEC (International Electrotechnical Commission) Wave Energy Resource Assesment and Characterisation Standard: A Case Study. *Energy*, (107) 668-682.

Ramos, V., Carballo, R., & Ringwood, J. V. (2016). Assessing the Utility and Effectiveness of the IEC Standards for Wave Energy Resource Characterisation. In G. Soares, *Progress in Renewable Energies Offshore* (pp. ISBN 978-1-138-62627-0). London: Taylor & Francis Group.

Robertson, B. B., Hiles, C. E., & Buckham, B. J. (2014a). Characterizing the Near Shore Wave Energy Resource on the West Coast of Vancouver Island, Canada. *Renewable Energy*, 665-678.

Robertson, B. B., Hiles, C. E., Luzko, E., & Buckham, B. J. (2014b). Quantifying the Wave Energy Resource and Farm Siting Opportunities for Western Canada. *ICOE.* Halifax, Canada.

Saruwatari, A., Ingram, D. M., & Cradden, L. (2013). Wave-Current Interaction Effects on Marine Energy Converters. *Ocean Engineering*, 73: 106-118.

Smith, H. C.; Haverson, D.; Smith , G. H.; Cornish, C. S.; Baldock, D.;. (2011). *Assessment of the Wave and Current Resource at the Wave Hub Site.* Tech. Rep. University of Exeter: Marine Energy Matters.

Stopa, J. E., Filipot, J.-F., Li, N., Cheung, K. F., Chen, Y. -L., & Vega, L. (2013). Wave Energy Resources along the Hawaiian Island Chain. *Renewable Energy*, 305-321.

SWAN t. (2013a). *SWAN Technical Manual.* Netherlands: Delft University of Technology.

SWAN t. (2013b). *SWAN User Manual.* The Netherlands: Delft University of Technology.

Szabó, L., Oprea, C., Festilã, C., & Dulf, E. (2008). Study on a Wave Energy Based Power System. *Proceedings of the 2008 International Conference on Electrical Machines*, (p. ID 1199).

Tethys. (2017, May 16). *Mutriku Wave Power Plant*. Retrieved from https://tethys.pnnl.gov/annex-iv-sites/mutriku-wave-power-plant

Thomson, R. (1981). *Oceanography of the British Columbia Coast.* Department of Fisheries and Oceans.

Tolman , H. L. (2014). *User Manual and System Documentation of WAVEWATCH III Version 4.18.* Technical Note 31: NOAA/NWS/NCEP/MMAB.

U.S National Renewable Energy Laboratory (NREL). (2009). *Ocean Energy Technology Overview.* U.S. Department of Energy Federal Energy Management Program.

Van Der Westhuysen, A. J. (2007a). *Advances in the Spectral Modelling of Wind Waves in the Nearshore.* Ph.D. Thesis, Delft University of Technology, Department of Civil Engineering, The Netherlands.

Van der Westhuysen, A. J., Zijlema, M., & Battjes, J. A. (2007b). Nonlinear Saturation-Based Whitecapping Dissipation in SWAn for Deep and Shallow wAter. *Coastal Engineering*, 54: 151-170.

Van Vledder, G., & Akpinar, A. (2015). Wave Model Predictions in the Black Sea: Sensitivity to Wind Fields. *Applied Ocean Research*, 53: 161-178.

Venugopal, V., Nemalidinne, R., & Vogler, A. (2017). Numerical Modelling of Wave Energy Resources and Assessment of Wave Energy Extraction by Large Scale Wave Farms. *Ocean and Coastal Management*, 147: 34-48.

Wave Dragon. (2009, March 15). *Protorype Testing in Denmark*. Retrieved from http://www.wavedragon.co.uk/2009/03/15/prototype-testing-in-denmark/

Whitham, G. B. (1974). *Linear and Nonlinear Waves.* New York: Wiley.

Xu, X., Robertson, B., & Buckham, B. (2020). A Techno-Economic Approach to Wave Energy Resource Assessment and Development Site Identification. *Applied Energy*, 260.

Yan, L. (1987). *An Improved Wind Input Source Term for Third Generation Ocean Wave Modelling.* De Bilt, The Netherlands: WR-NO 87-8.

Yang, Z., Neary, V., Wang, T., Gunawan, B., Dallman, A., & Wu, W.-C. (2017). A Wave Model Test Bed Study for Wave Energy Resource Characterization. *Renewable Energy*, 114: 132-144.

13 Appendix A

13.1 Reconnaissance Class Monthly Parameters

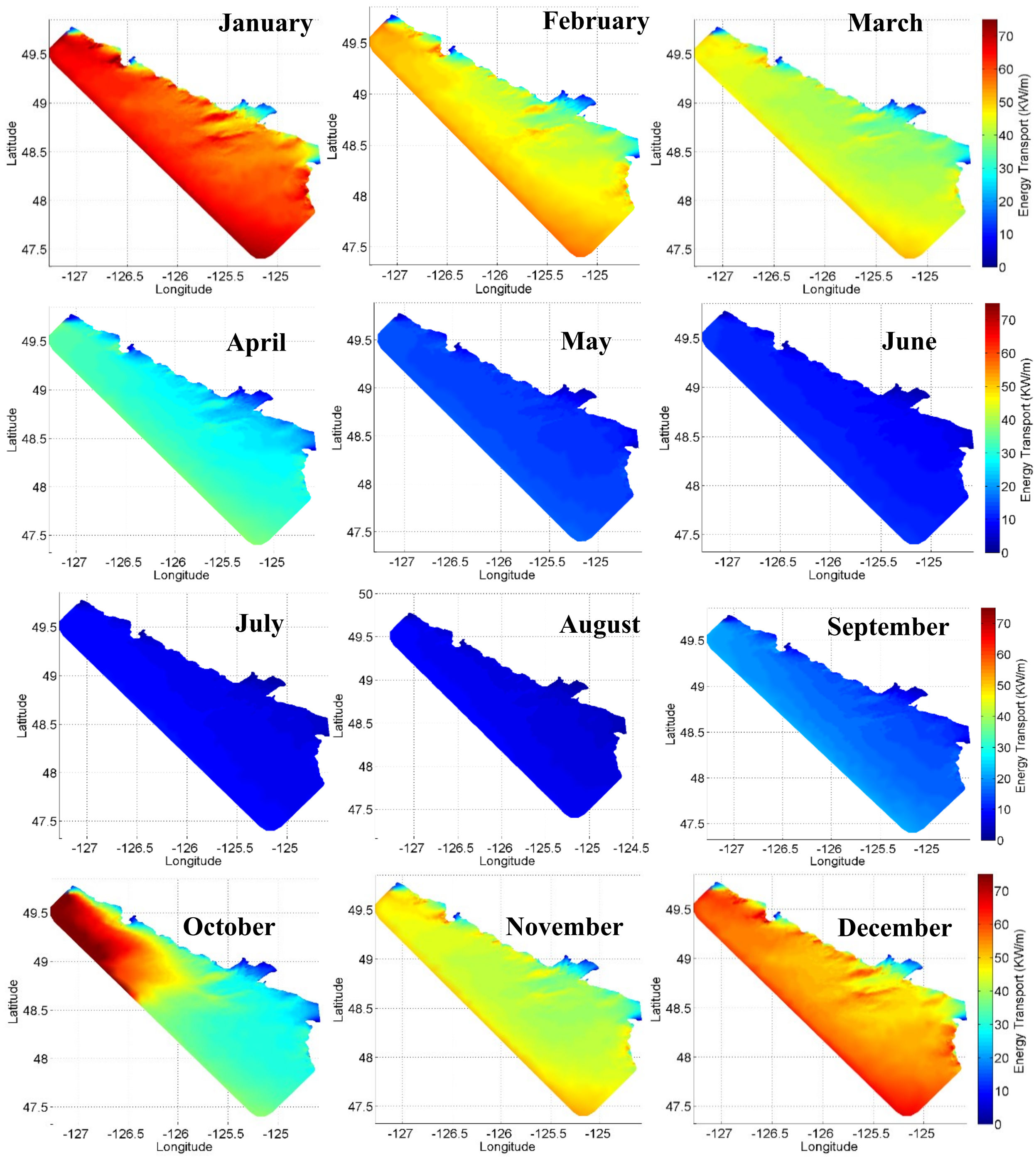

Figure 13.1 – Reconnaissance Class Assessment Monthly Wave Energy Transport

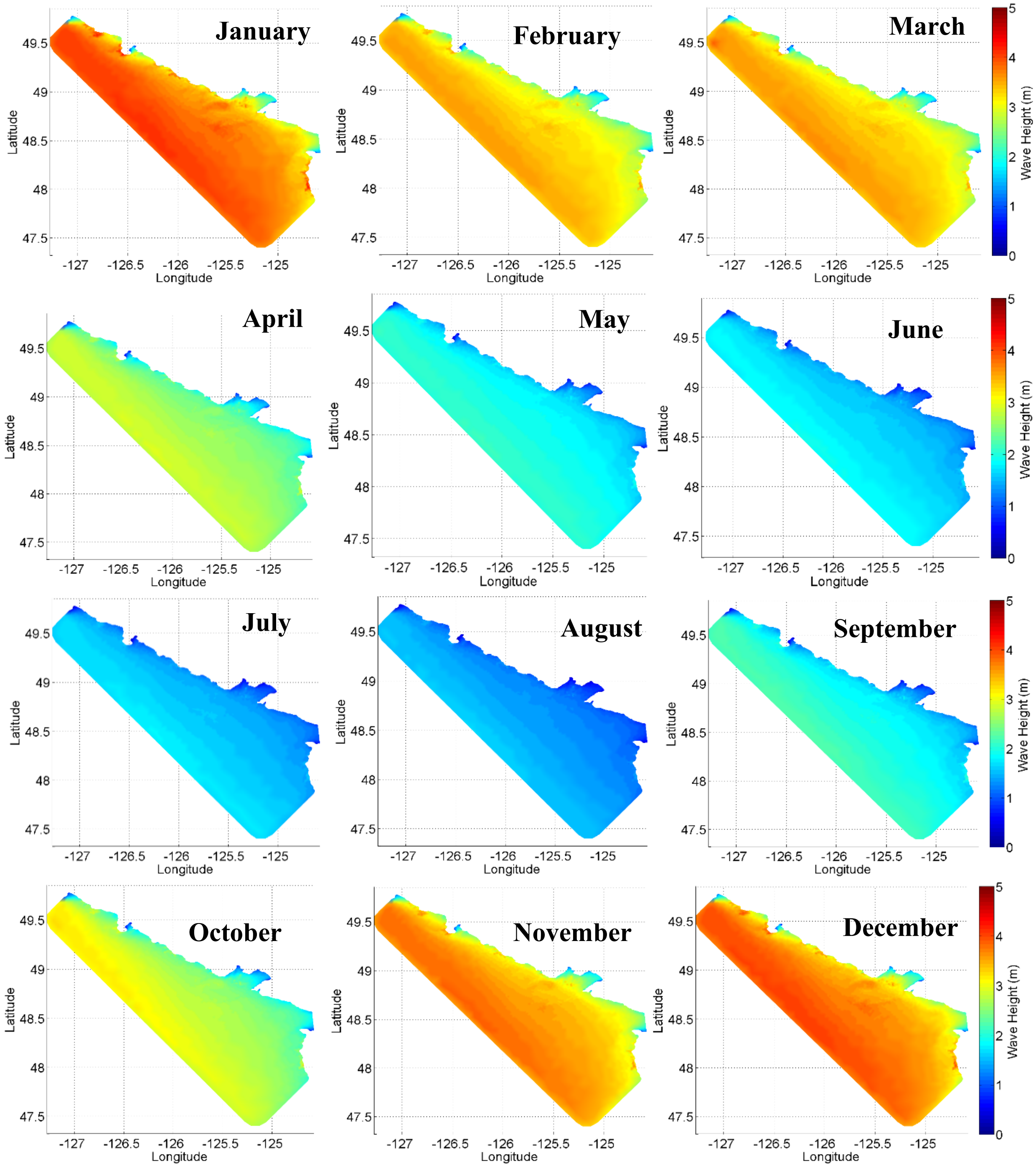

Figure 13.2 – Reconnaissance Class Assessment Monthly Wave Height

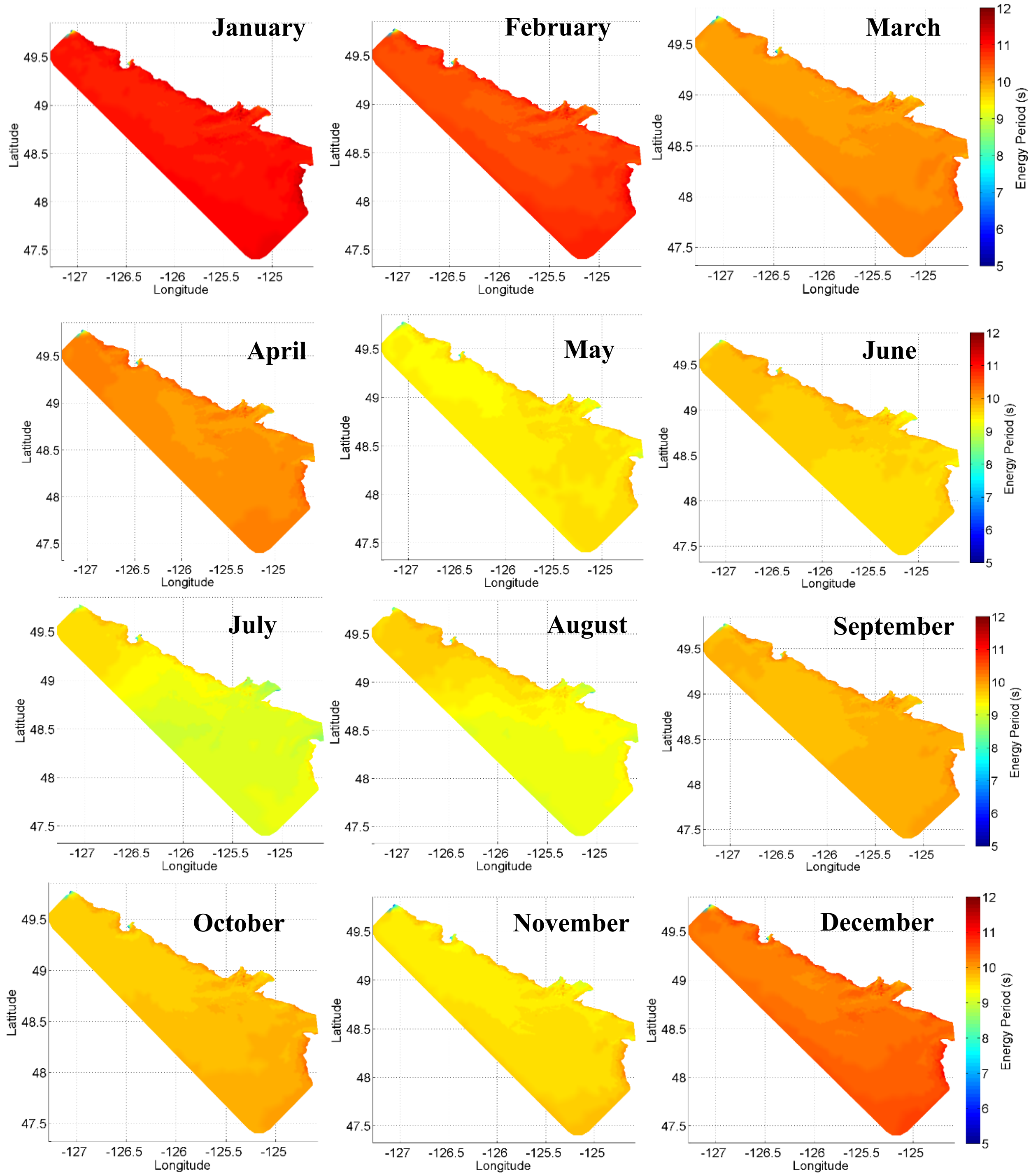

Figure 13.3 – Reconnaissance Class Assessment Monthly Wave Energy Period

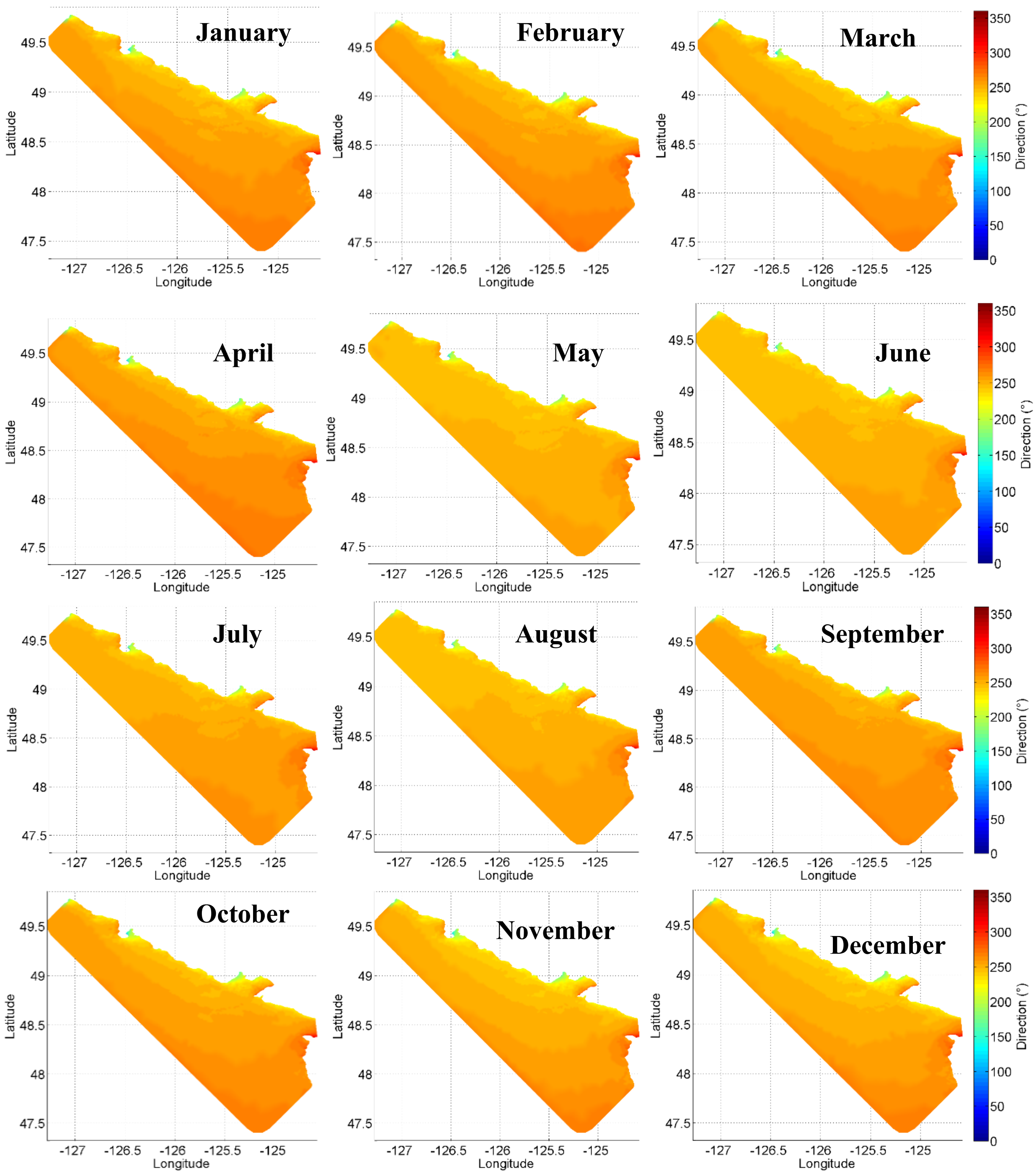

Figure 13.4 – Reconnaissance Class Assessment Monthly Wave Direction

13.2 Feasibility Class Monthly Parameters

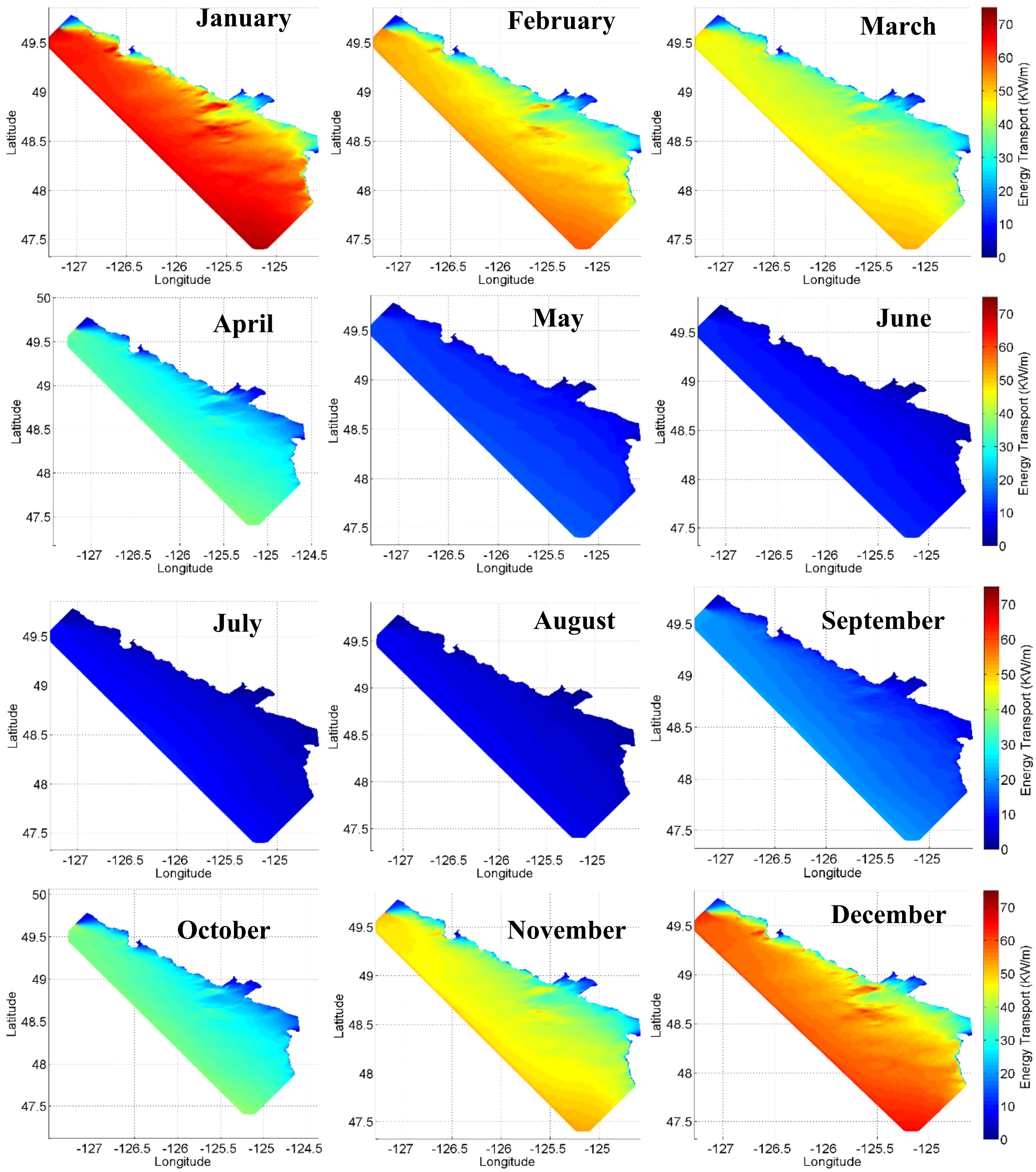

Figure 13.5 – Feasibility Class Assessment Monthly Wave Energy Transport

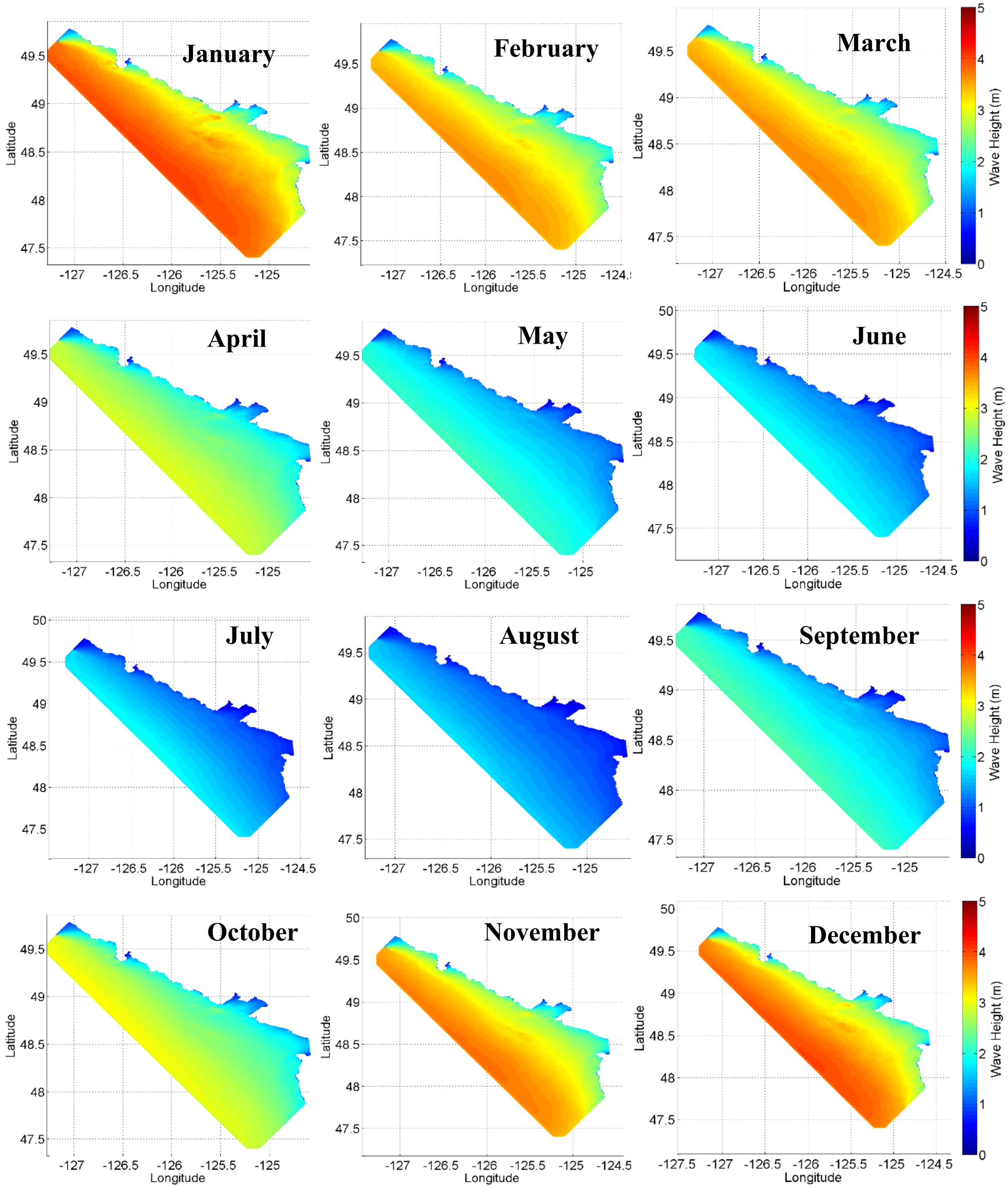

Figure 13.6 – Feasibility Class Assessment Monthly Wave Height

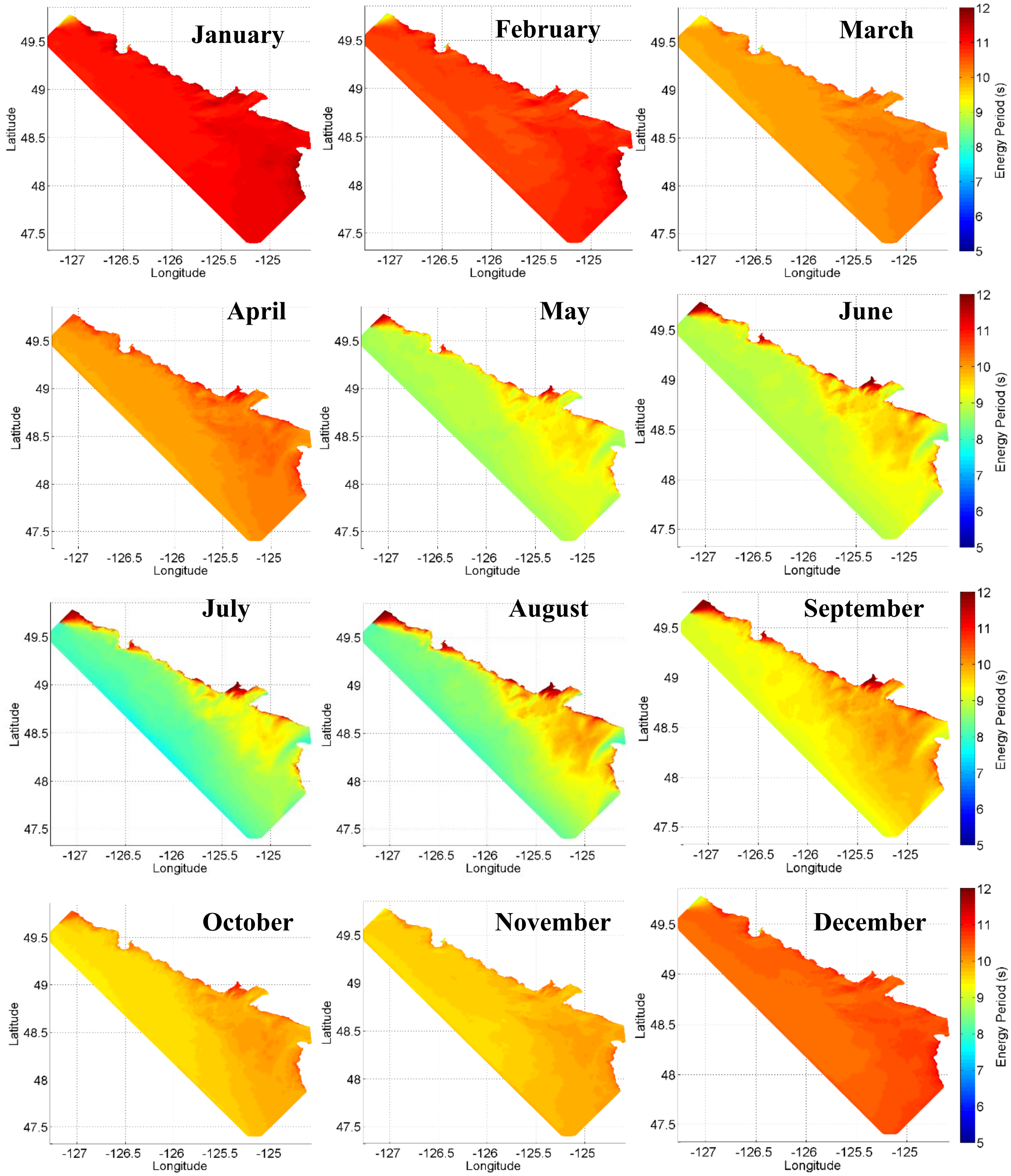

Figure 13.7 – Feasibility Class Assessment Monthly Wave Energy Period

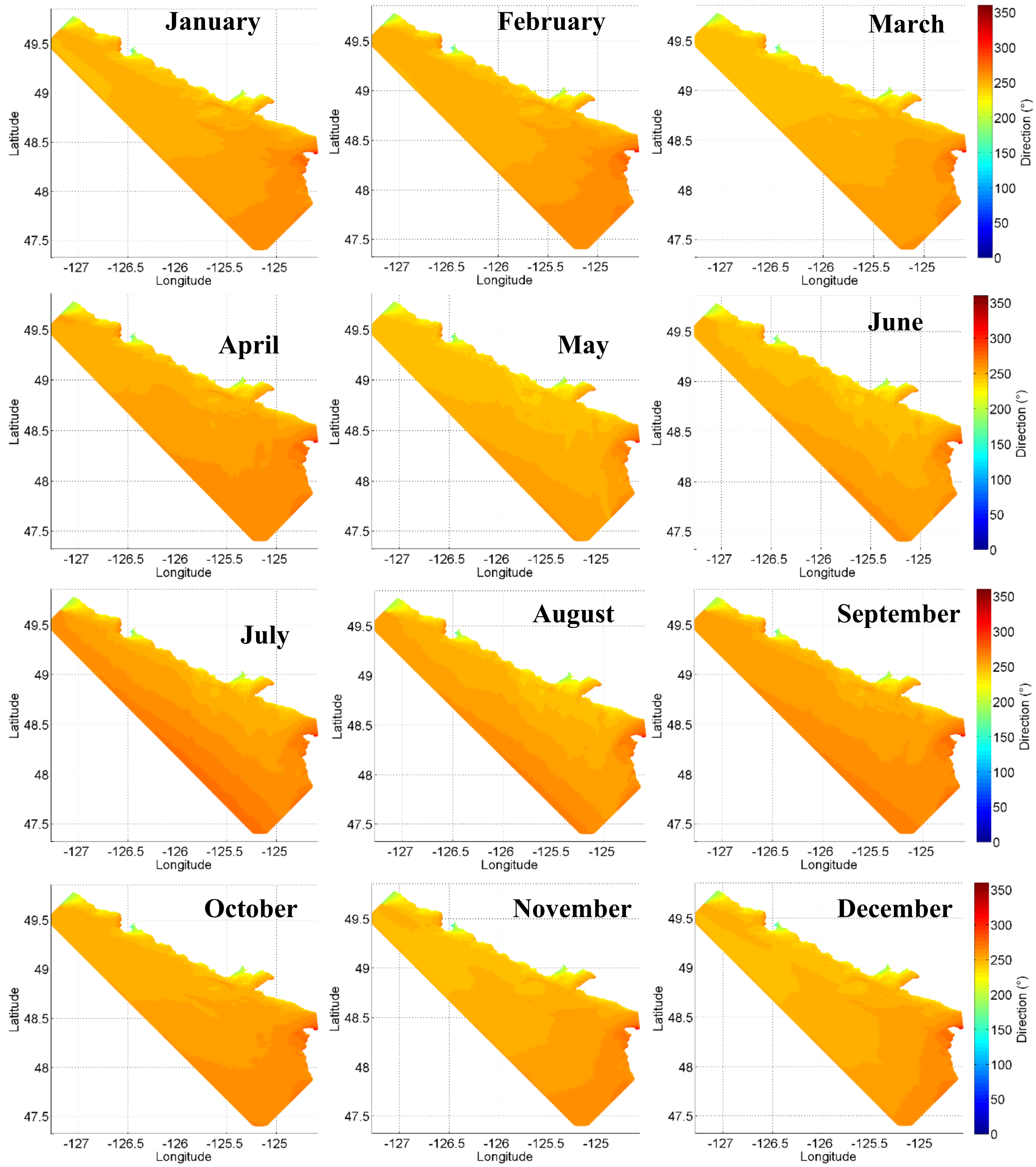

Figure 13.8 – Feasibility Class Assessment Monthly Wave Direction

13.3 Design Class Monthly Parameters

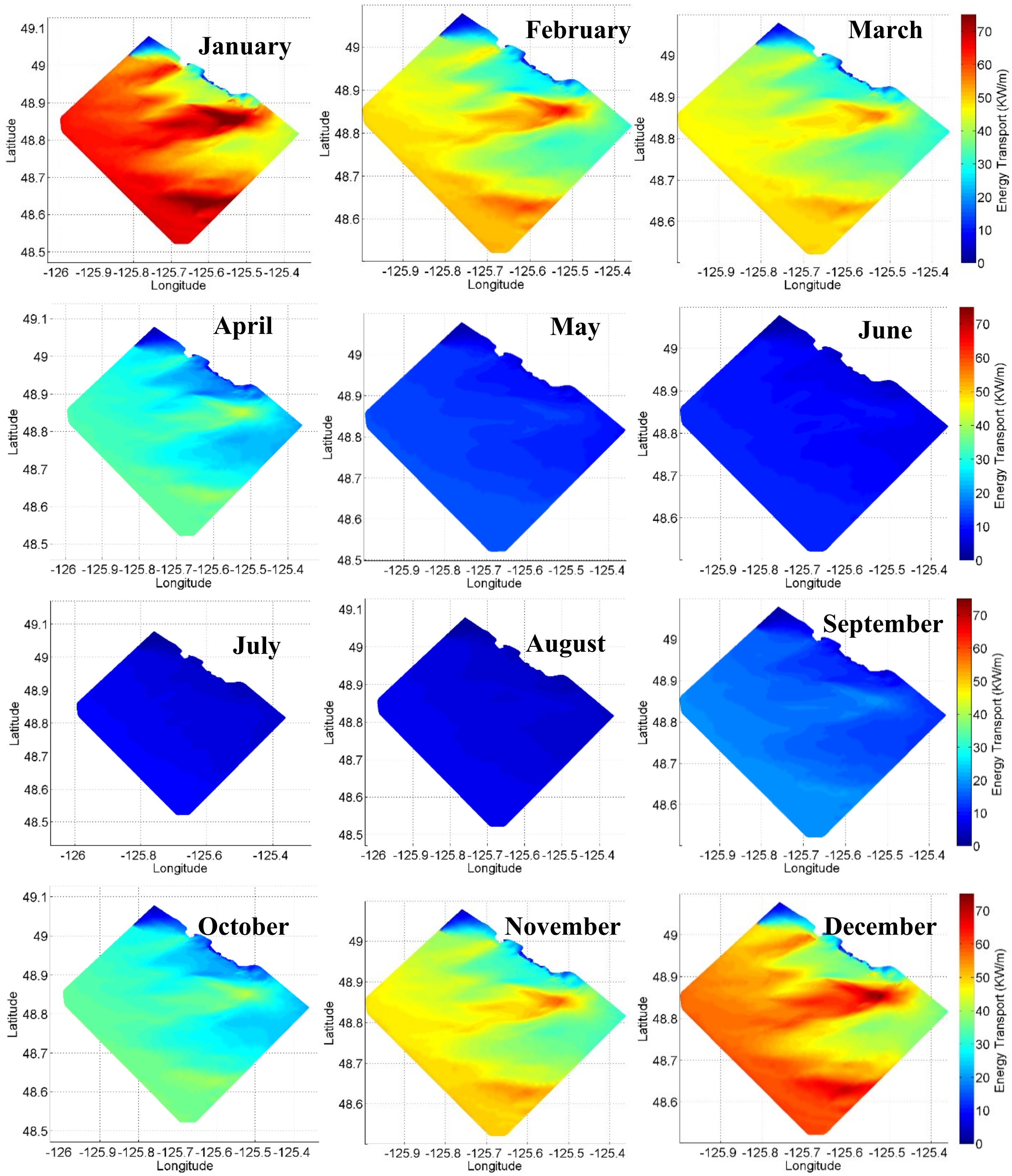

Figure 13.9 – Design Class Assessment Monthly Wave Energy Transport

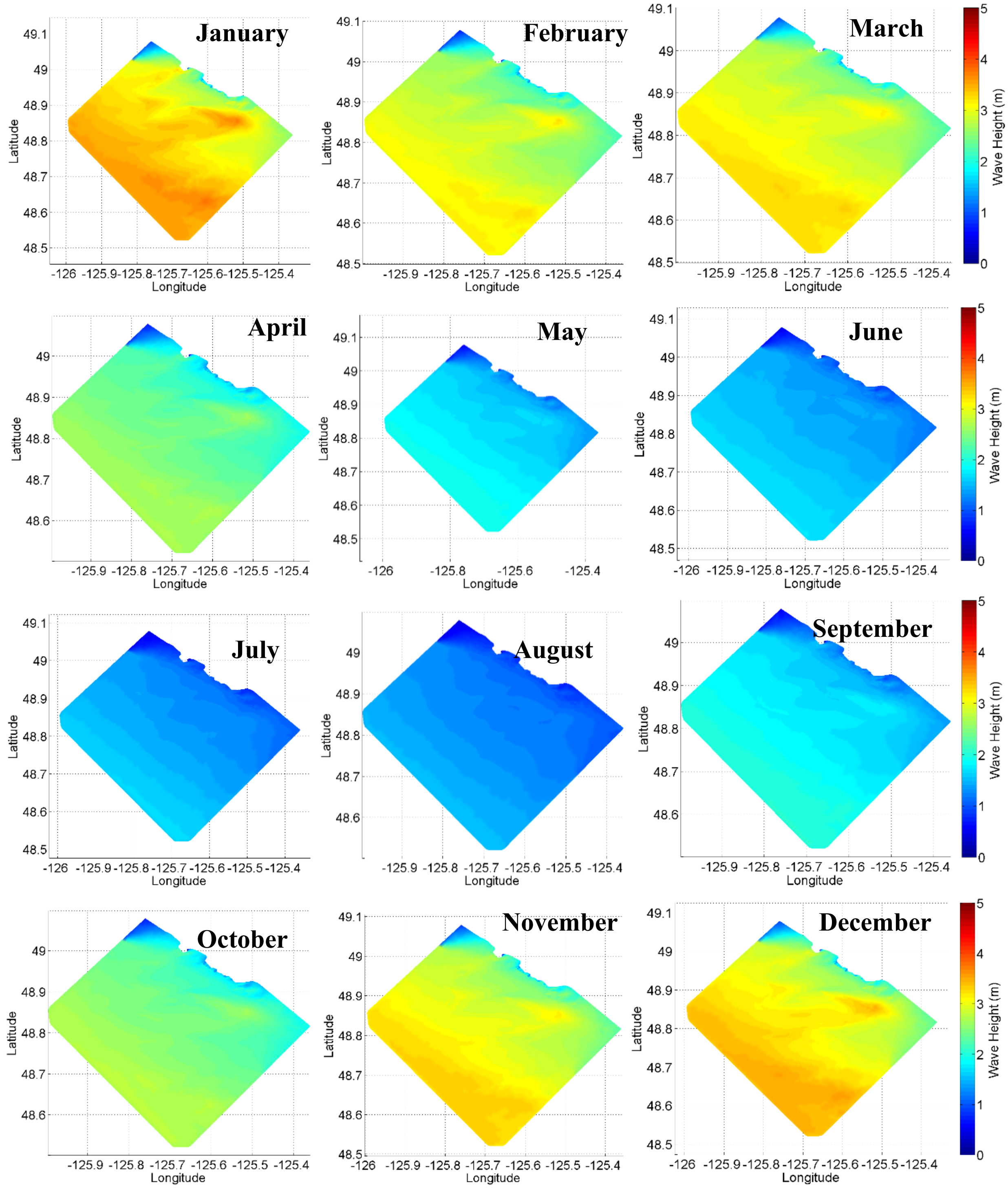

Figure 13.10 – Design Class Assessment Monthly Wave Height

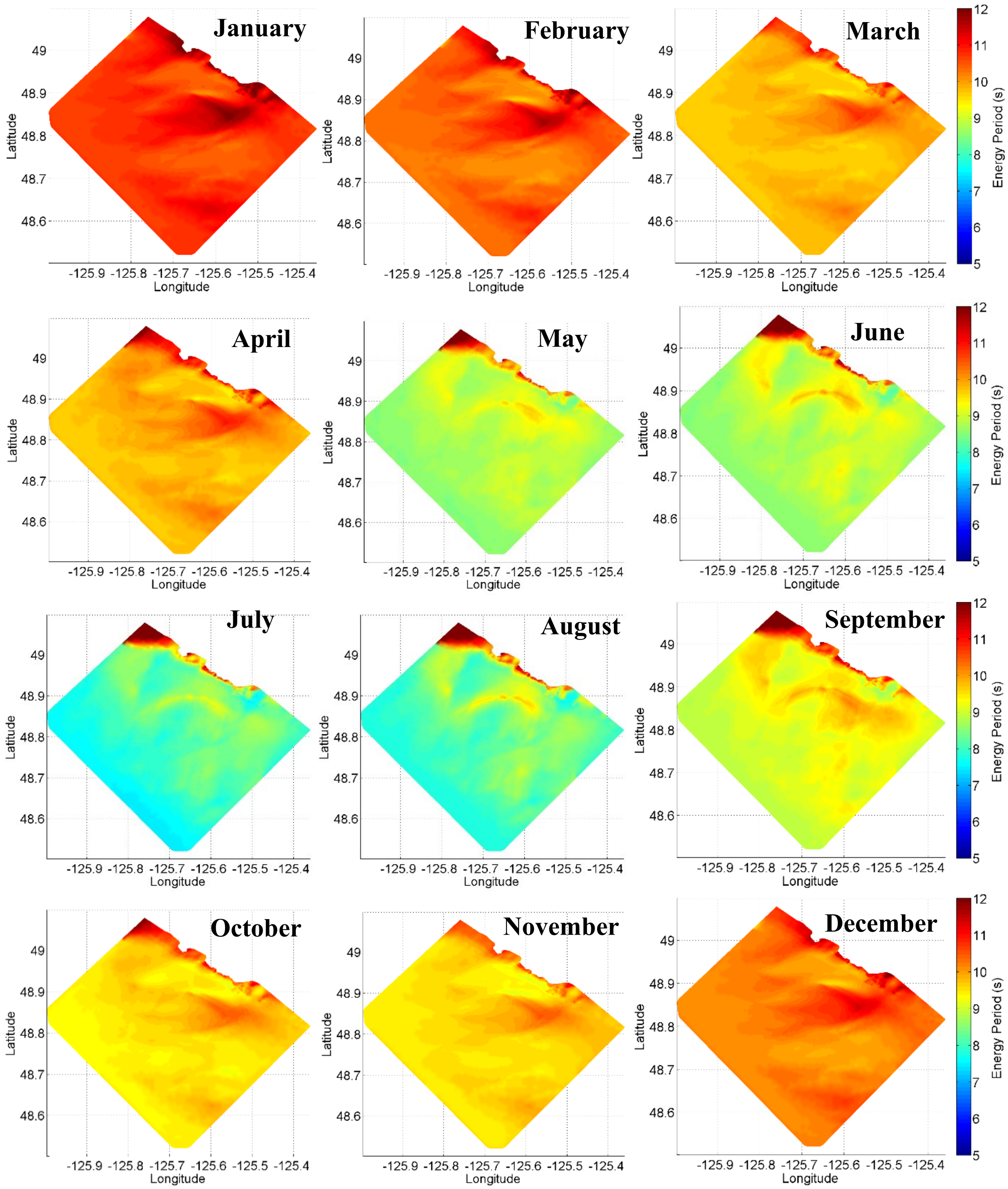

Figure 13.11 – Design Class Assessment Monthly Wave Energy Period

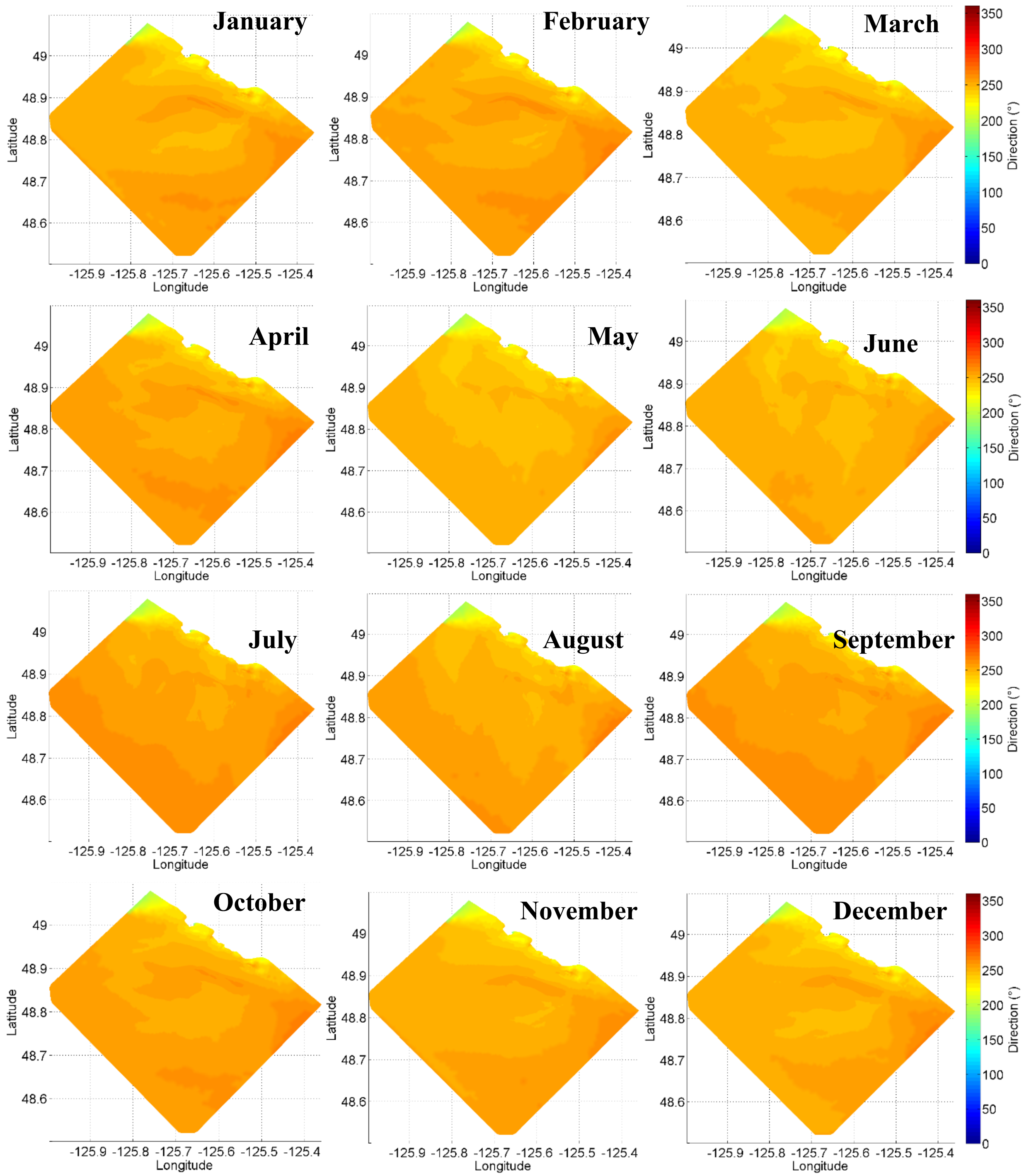

Figure 13.12 – Design Class Assessment Monthly Wave Direction

13.4 Bivariate Distributions

Wave Energy Period (s) / **Wave Height (m)**

Wave Height (m)	0–1	1–2	2–3	3–4	4–5	5–6	6–7	7–8	8–9	9–10	10–11	11–12	12–13	13–14	14–15	15–16	16–17	17–18	18–19	19–20	20–21	%
0.5	0.00	0.00	0.00	0.00	0.00	0.02	0.07	0.05	0.06	0.02	0.01	0.01	0.02	0.00	0.03	0.01	0.00	0.00	0.00	0.00	0.00	0.29
1	0.00	0.00	0.01	0.02	0.11	0.27	0.75	1.34	1.54	0.88	0.57	0.54	0.50	0.45	0.34	0.16	0.07	0.01	0.00	0.00	0.00	7.58
1.5	0.00	0.00	0.00	0.09	0.49	0.77	1.28	2.23	2.64	3.40	1.82	1.32	1.97	1.37	0.81	0.86	0.45	0.06	0.09	0.01	0.00	19.66
2	0.00	0.00	0.00	0.01	0.79	1.05	1.05	1.23	1.59	3.39	2.13	1.71	1.67	1.08	0.73	1.23	0.58	0.09	0.12	0.06	0.05	18.57
2.5	0.00	0.00	0.00	0.00	0.54	1.01	0.95	0.96	1.17	2.16	2.07	1.46	1.47	0.54	0.38	0.75	0.27	0.05	0.06	0.02	0.02	13.88
3	0.00	0.00	0.00	0.00	0.14	0.96	0.84	0.86	0.79	1.14	1.22	1.28	1.26	0.42	0.27	0.24	0.11	0.02	0.01	0.01	0.00	9.56
3.5	0.00	0.00	0.00	0.00	0.01	0.82	0.83	0.73	0.70	0.77	0.67	0.93	1.08	0.36	0.19	0.22	0.10	0.01	0.01	0.01	0.00	7.45
4	0.00	0.00	0.00	0.00	0.00	0.59	0.90	0.68	0.58	0.47	0.41	0.47	0.69	0.27	0.13	0.18	0.05	0.02	0.01	0.00	0.00	5.43
4.5	0.00	0.00	0.00	0.00	0.00	0.18	0.74	0.71	0.45	0.38	0.28	0.34	0.51	0.20	0.08	0.11	0.03	0.00	0.00	0.00	0.00	4.03
5	0.00	0.00	0.00	0.00	0.00	0.03	0.63	0.70	0.41	0.27	0.18	0.26	0.37	0.09	0.10	0.10	0.03	0.00	0.00	0.00	0.00	3.18
5.5	0.00	0.00	0.00	0.00	0.00	0.01	0.49	0.62	0.45	0.29	0.12	0.17	0.23	0.08	0.06	0.05	0.01	0.00	0.00	0.00	0.00	2.59
6	0.00	0.00	0.00	0.00	0.00	0.00	0.23	0.62	0.33	0.21	0.14	0.10	0.10	0.06	0.04	0.05	0.02	0.00	0.00	0.00	0.00	1.91
6.5	0.00	0.00	0.00	0.00	0.00	0.00	0.10	0.59	0.27	0.15	0.08	0.04	0.06	0.05	0.03	0.02	0.00	0.00	0.00	0.00	0.00	1.39
7	0.00	0.00	0.00	0.00	0.00	0.00	0.02	0.46	0.25	0.10	0.08	0.04	0.04	0.01	0.02	0.03	0.01	0.00	0.00	0.00	0.00	1.07
7.5	0.00	0.00	0.00	0.00	0.00	0.00	0.00	0.34	0.23	0.08	0.06	0.04	0.03	0.01	0.02	0.02	0.00	0.00	0.00	0.00	0.00	0.83
8	0.00	0.00	0.00	0.00	0.00	0.00	0.00	0.22	0.17	0.05	0.05	0.04	0.02	0.01	0.00	0.02	0.01	0.00	0.00	0.00	0.00	0.59
8.5	0.00	0.00	0.00	0.00	0.00	0.00	0.00	0.13	0.22	0.08	0.05	0.02	0.02	0.00	0.01	0.02	0.00	0.00	0.00	0.00	0.00	0.54
9	0.00	0.00	0.00	0.00	0.00	0.00	0.00	0.03	0.19	0.06	0.04	0.01	0.01	0.00	0.00	0.01	0.00	0.00	0.00	0.00	0.00	0.36
9.5	0.00	0.00	0.00	0.00	0.00	0.00	0.00	0.01	0.16	0.07	0.03	0.01	0.01	0.00	0.00	0.01	0.00	0.00	0.00	0.00	0.00	0.29
10	0.00	0.00	0.00	0.00	0.00	0.00	0.00	0.00	0.13	0.04	0.01	0.01	0.00	0.00	0.00	0.00	0.00	0.00	0.00	0.00	0.00	0.19
10.5	0.00	0.00	0.00	0.00	0.00	0.00	0.00	0.00	0.09	0.06	0.01	0.01	0.00	0.00	0.00	0.00	0.00	0.00	0.00	0.00	0.00	0.18
11	0.00	0.00	0.00	0.00	0.00	0.00	0.00	0.00	0.07	0.06	0.02	0.00	0.00	0.00	0.00	0.00	0.00	0.00	0.00	0.00	0.00	0.16
11.5	0.00	0.00	0.00	0.00	0.00	0.00	0.00	0.00	0.03	0.06	0.00	0.00	0.00	0.00	0.00	0.00	0.00	0.00	0.00	0.00	0.00	0.10
12	0.00	0.00	0.00	0.00	0.00	0.00	0.00	0.00	0.00	0.03	0.01	0.00	0.00	0.00	0.00	0.00	0.00	0.00	0.00	0.00	0.00	0.05
12.5	0.00	0.00	0.00	0.00	0.00	0.00	0.00	0.00	0.00	0.03	0.00	0.00	0.00	0.00	0.00	0.00	0.00	0.00	0.00	0.00	0.00	0.03
13	0.00	0.00	0.00	0.00	0.00	0.00	0.00	0.00	0.00	0.05	0.00	0.00	0.00	0.00	0.00	0.00	0.00	0.00	0.00	0.00	0.00	0.05
13.5	0.00	0.00	0.00	0.00	0.00	0.00	0.00	0.00	0.00	0.02	0.00	0.00	0.00	0.00	0.00	0.00	0.00	0.00	0.00	0.00	0.00	0.02
14	0.00	0.00	0.00	0.00	0.00	0.00	0.00	0.00	0.00	0.01	0.00	0.00	0.00	0.00	0.00	0.00	0.00	0.00	0.00	0.00	0.00	0.01
14.5	0.00	0.00	0.00	0.00	0.00	0.00	0.00	0.00	0.00	0.00	0.00	0.00	0.00	0.00	0.00	0.00	0.00	0.00	0.00	0.00	0.00	0.00
15	0.00	0.00	0.00	0.00	0.00	0.00	0.00	0.00	0.00	0.00	0.00	0.00	0.00	0.00	0.00	0.00	0.00	0.00	0.00	0.00	0.00	0.00
15.5	0.00	0.00	0.00	0.00	0.00	0.00	0.00	0.00	0.00	0.00	0.01	0.00	0.00	0.00	0.00	0.00	0.00	0.00	0.00	0.00	0.00	0.01
16	0.00	0.00	0.00	0.00	0.00	0.00	0.00	0.00	0.00	0.00	0.01	0.00	0.00	0.00	0.00	0.00	0.00	0.00	0.00	0.00	0.00	0.01
%	0.00	0.00	0.01	0.12	2.09	5.71	8.87	12.52	12.52	14.34	10.09	8.83	10.06	5.01	3.24	4.08	1.74	0.27	0.30	0.10	0.08	100.00

Figure 13.13 – Bivariate Distribution Showing the Frequency of Occurrence for the Reconnaissance Class Assessment

Wave Energy Period (s)

Wave Height (m)	0–1	1–2	2–3	3–4	4–5	5–6	6–7	7–8	8–9	9–10	10–11	11–12	12–13	13–14	14–15	15–16	16–17	17–18	18–19	%
0–0.5	0.00	0.00	0.00	0.00	0.00	0.00	0.00	0.01	0.07	0.13	0.09	0.06	0.08	0.06	0.05	0.00	0.00	0.00	0.00	0.56
0.5–1	0.00	0.00	0.00	0.00	0.03	0.17	0.39	0.67	1.65	3.08	2.94	2.64	1.68	1.07	0.35	0.17	0.07	0.01	0.01	14.92
1–1.5	0.00	0.00	0.00	0.00	0.09	0.52	1.02	1.49	2.70	5.52	5.50	3.60	2.46	1.06	0.45	0.20	0.03	0.01	0.01	24.64
1.5–2	0.00	0.00	0.00	0.00	0.18	0.56	0.99	1.23	1.61	3.02	3.68	2.51	1.32	0.71	0.19	0.12	0.01	0.00	0.00	16.13
2–2.5	0.00	0.00	0.00	0.00	0.03	0.43	0.76	0.84	0.88	1.50	2.76	2.61	1.21	0.52	0.18	0.14	0.01	0.00	0.01	11.90
2.5–3	0.00	0.00	0.00	0.00	0.00	0.23	0.55	0.63	0.77	1.03	1.67	2.13	1.32	0.62	0.16	0.09	0.04	0.00	0.00	9.24
3–3.5	0.00	0.00	0.00	0.00	0.00	0.10	0.41	0.58	0.52	0.59	1.05	1.26	1.03	0.55	0.25	0.08	0.03	0.00	0.00	6.46
3.5–4	0.00	0.00	0.00	0.00	0.00	0.03	0.27	0.44	0.47	0.58	0.51	0.80	0.82	0.55	0.19	0.11	0.01	0.00	0.00	4.79
4–4.5	0.00	0.00	0.00	0.00	0.00	0.01	0.16	0.48	0.42	0.40	0.40	0.44	0.56	0.37	0.17	0.10	0.05	0.00	0.00	3.56
4.5–5	0.00	0.00	0.00	0.00	0.00	0.00	0.09	0.34	0.35	0.24	0.31	0.31	0.40	0.36	0.14	0.05	0.02	0.00	0.00	2.61
5–5.5	0.00	0.00	0.00	0.00	0.00	0.00	0.04	0.22	0.27	0.20	0.14	0.11	0.24	0.25	0.12	0.05	0.02	0.00	0.00	1.67
5.5–6	0.00	0.00	0.00	0.00	0.00	0.00	0.01	0.12	0.27	0.14	0.11	0.11	0.10	0.13	0.08	0.03	0.01	0.00	0.00	1.12
6–6.5	0.00	0.00	0.00	0.00	0.00	0.00	0.00	0.06	0.16	0.11	0.04	0.07	0.04	0.05	0.07	0.04	0.00	0.00	0.00	0.64
6.5–7	0.00	0.00	0.00	0.00	0.00	0.00	0.00	0.01	0.12	0.07	0.04	0.04	0.06	0.05	0.04	0.02	0.01	0.00	0.00	0.46
7–7.5	0.00	0.00	0.00	0.00	0.00	0.00	0.00	0.02	0.10	0.06	0.08	0.04	0.04	0.05	0.03	0.02	0.00	0.00	0.00	0.45
7.5–8	0.00	0.00	0.00	0.00	0.00	0.00	0.00	0.00	0.07	0.05	0.03	0.03	0.03	0.04	0.04	0.03	0.00	0.00	0.00	0.32
8–8.5	0.00	0.00	0.00	0.00	0.00	0.00	0.00	0.00	0.03	0.04	0.04	0.01	0.02	0.01	0.01	0.02	0.00	0.00	0.00	0.19
8.5–9	0.00	0.00	0.00	0.00	0.00	0.00	0.00	0.00	0.02	0.04	0.01	0.01	0.02	0.00	0.00	0.01	0.00	0.00	0.00	0.11
9–9.5	0.00	0.00	0.00	0.00	0.00	0.00	0.00	0.00	0.01	0.04	0.02	0.02	0.00	0.01	0.00	0.01	0.00	0.00	0.00	0.11
9.5–10	0.00	0.00	0.00	0.00	0.00	0.00	0.00	0.00	0.00	0.02	0.01	0.01	0.00	0.01	0.00	0.00	0.00	0.00	0.00	0.05
10–10.5	0.00	0.00	0.00	0.00	0.00	0.00	0.00	0.00	0.00	0.01	0.01	0.00	0.00	0.00	0.00	0.00	0.00	0.00	0.00	0.03
10.5–11	0.00	0.00	0.00	0.00	0.00	0.00	0.00	0.00	0.00	0.00	0.00	0.00	0.01	0.00	0.00	0.00	0.00	0.00	0.00	0.01
11–11.5	0.00	0.00	0.00	0.00	0.00	0.00	0.00	0.00	0.00	0.01	0.00	0.00	0.00	0.00	0.00	0.00	0.00	0.00	0.00	0.01
%	0.00	0.00	0.00	0.00	0.33	2.05	4.68	7.16	10.48	16.88	19.47	16.81	11.43	6.47	2.53	1.31	0.33	0.04	0.04	100.00

Figure 13.14 – Bivariate Distribution Showing the Frequency of Occurrence for the Feasibility Class Assessment

Wave Energy Period (s)

Wave Height (m)	0–1	1–2	2–3	3–4	4–5	5–6	6–7	7–8	8–9	9–10	10–11	11–12	12–13	13–14	14–15	15–16	16–17	17–18	%
0–0.5	0.00	0.00	0.00	0.01	0.02	0.00	0.00	0.02	0.01	0.01	0.03	0.02	0.01	0.02	0.00	0.00	0.00	0.00	0.18
0.5–1	0.00	0.00	0.05	0.02	0.06	0.17	0.56	1.40	2.33	2.14	1.70	1.16	0.49	0.13	0.02	0.02	0.00	0.00	10.26
1–1.5	0.00	0.00	0.00	0.02	0.20	0.48	1.25	2.86	5.71	6.05	4.25	2.23	0.94	0.30	0.05	0.01	0.00	0.00	24.33
1.5–2	0.00	0.00	0.00	0.01	0.13	0.52	0.99	1.92	3.44	4.75	3.25	1.75	0.90	0.25	0.07	0.01	0.00	0.00	18.00
2–2.5	0.00	0.00	0.00	0.00	0.12	0.41	0.59	0.93	1.53	2.81	2.83	1.83	0.83	0.47	0.23	0.01	0.01	0.00	12.59
2.5–3	0.00	0.00	0.00	0.00	0.06	0.17	0.41	0.68	1.22	1.93	2.59	1.76	0.87	0.32	0.14	0.04	0.02	0.00	10.21
3–3.5	0.00	0.00	0.00	0.00	0.04	0.15	0.29	0.47	0.62	1.18	1.64	1.56	1.00	0.40	0.19	0.05	0.00	0.00	7.58
3.5–4	0.00	0.00	0.00	0.00	0.00	0.08	0.19	0.43	0.46	0.71	1.05	1.09	0.77	0.42	0.17	0.02	0.01	0.00	5.41
4–4.5	0.00	0.00	0.00	0.00	0.00	0.05	0.11	0.27	0.38	0.47	0.63	0.71	0.64	0.33	0.17	0.03	0.01	0.00	3.79
4.5–5	0.00	0.00	0.00	0.00	0.00	0.01	0.04	0.16	0.23	0.31	0.47	0.52	0.53	0.27	0.12	0.07	0.01	0.00	2.73
5–5.5	0.00	0.00	0.00	0.00	0.00	0.00	0.03	0.09	0.14	0.20	0.22	0.28	0.40	0.25	0.12	0.02	0.00	0.00	1.76
5.5–6	0.00	0.00	0.00	0.00	0.00	0.00	0.01	0.05	0.10	0.12	0.09	0.19	0.26	0.20	0.08	0.03	0.00	0.00	1.14
6–6.5	0.00	0.00	0.00	0.00	0.00	0.00	0.00	0.05	0.04	0.08	0.08	0.09	0.12	0.11	0.06	0.02	0.00	0.00	0.65
6.5–7	0.00	0.00	0.00	0.00	0.00	0.00	0.00	0.01	0.04	0.05	0.04	0.07	0.07	0.05	0.06	0.02	0.00	0.00	0.41
7–7.5	0.00	0.00	0.00	0.00	0.00	0.00	0.00	0.00	0.03	0.05	0.05	0.04	0.05	0.08	0.03	0.04	0.00	0.00	0.37
7.5–8	0.00	0.00	0.00	0.00	0.00	0.00	0.00	0.00	0.01	0.02	0.02	0.04	0.05	0.06	0.03	0.00	0.00	0.00	0.24
8–8.5	0.00	0.00	0.00	0.00	0.00	0.00	0.00	0.00	0.00	0.01	0.01	0.01	0.04	0.02	0.04	0.01	0.00	0.00	0.14
8.5–9	0.00	0.00	0.00	0.00	0.00	0.00	0.00	0.00	0.01	0.00	0.01	0.00	0.02	0.01	0.03	0.01	0.00	0.00	0.09
9–9.5	0.00	0.00	0.00	0.00	0.00	0.00	0.00	0.00	0.00	0.00	0.01	0.00	0.01	0.01	0.00	0.00	0.00	0.00	0.03
9.5–10	0.00	0.00	0.00	0.00	0.00	0.00	0.00	0.00	0.00	0.00	0.01	0.01	0.01	0.00	0.01	0.00	0.00	0.00	0.04
10–10.5	0.00	0.00	0.00	0.00	0.00	0.00	0.00	0.00	0.00	0.00	0.00	0.00	0.00	0.01	0.00	0.00	0.00	0.00	0.01
10.5–11	0.00	0.00	0.00	0.00	0.00	0.00	0.00	0.00	0.00	0.00	0.00	0.00	0.00	0.01	0.00	0.00	0.00	0.00	0.01
11–11.5	0.00	0.00	0.00	0.00	0.00	0.00	0.00	0.00	0.00	0.00	0.00	0.00	0.00	0.01	0.00	0.00	0.00	0.00	0.01
%	0.00	0.00	0.05	0.06	0.63	2.03	4.47	9.35	16.31	20.90	18.99	13.35	7.99	3.72	1.62	0.42	0.09	0.01	100.00

Figure 13.15 – Bivariate Distribution Showing the Frequency of Occurrence for the Design Class Assessment

14 Appendix B

14.1 Reconnaissance Class Sample Sea States

Figure 14.1 - Sample Sea States Selected for Reconnaissance Sensitivity Assessment for Physical Processes A) Wave Breaking; B) Bottom Friction; C) Triad; D) Whitecapping

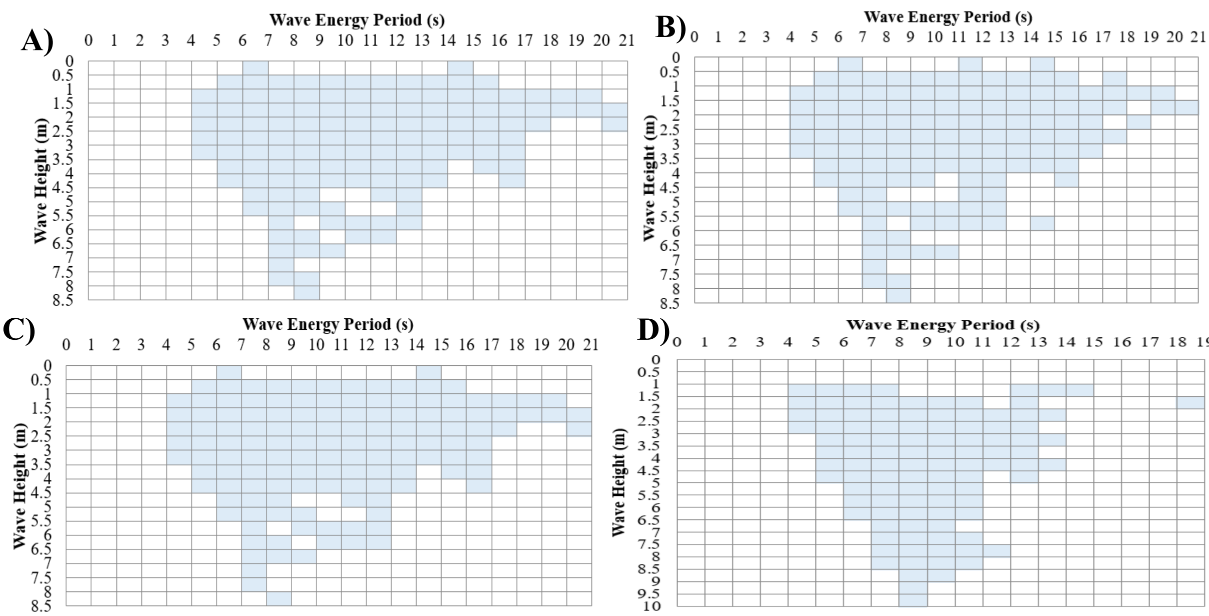

Figure 14.2 -- Sample Sea States Selected for Reconnaissance Sensitivity Assessment for the Mesh Resolution A) 1,000m; B) 2,500m; and C) 4,000m

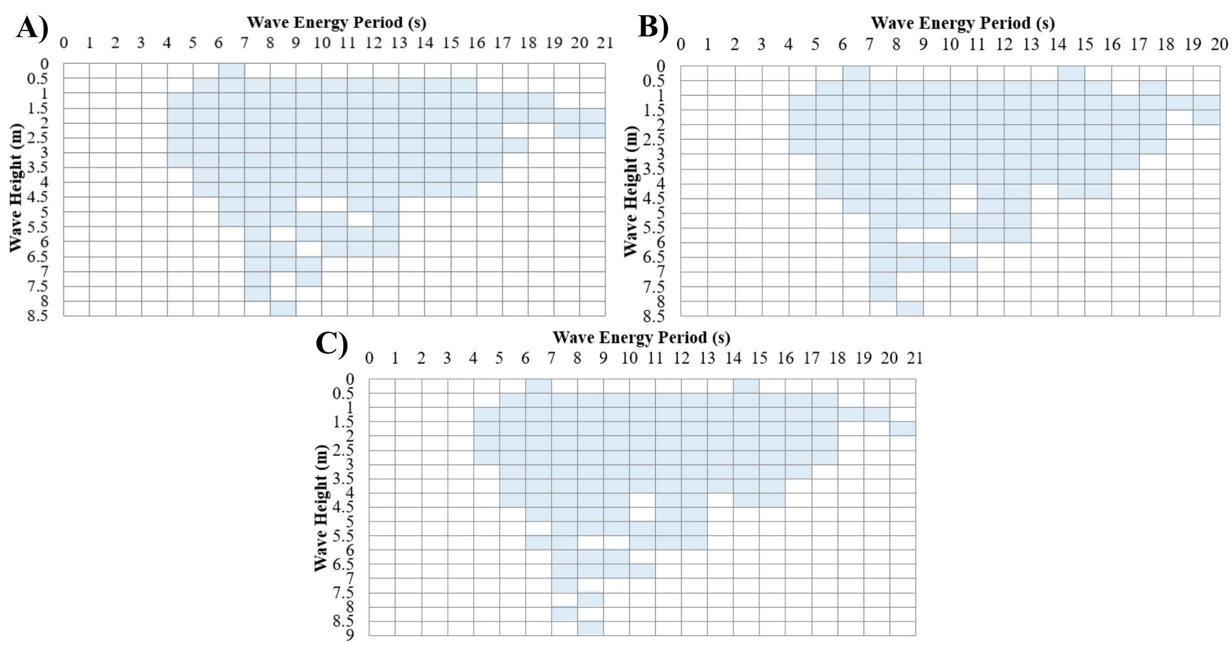

Figure 14.3 – Sample Sea States Selected for Reconnaissance Sensitivity Assessment for the Spectral Boundary Condition

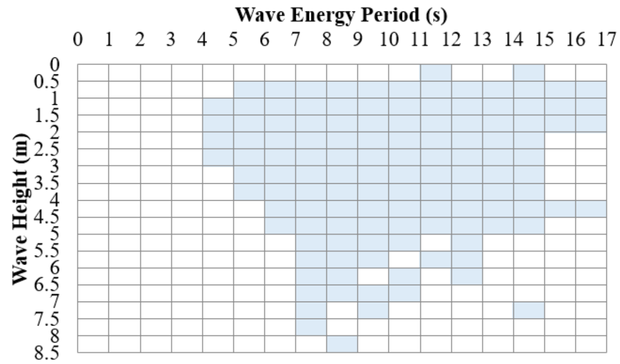

Figure 14.4 – Sample Sea States Selected for Reconnaissance Sensitivity Assessment for the Frequency Resolution A) 41 bins; B) 57 bins; C) 73 Bins; and D) 89 Bins

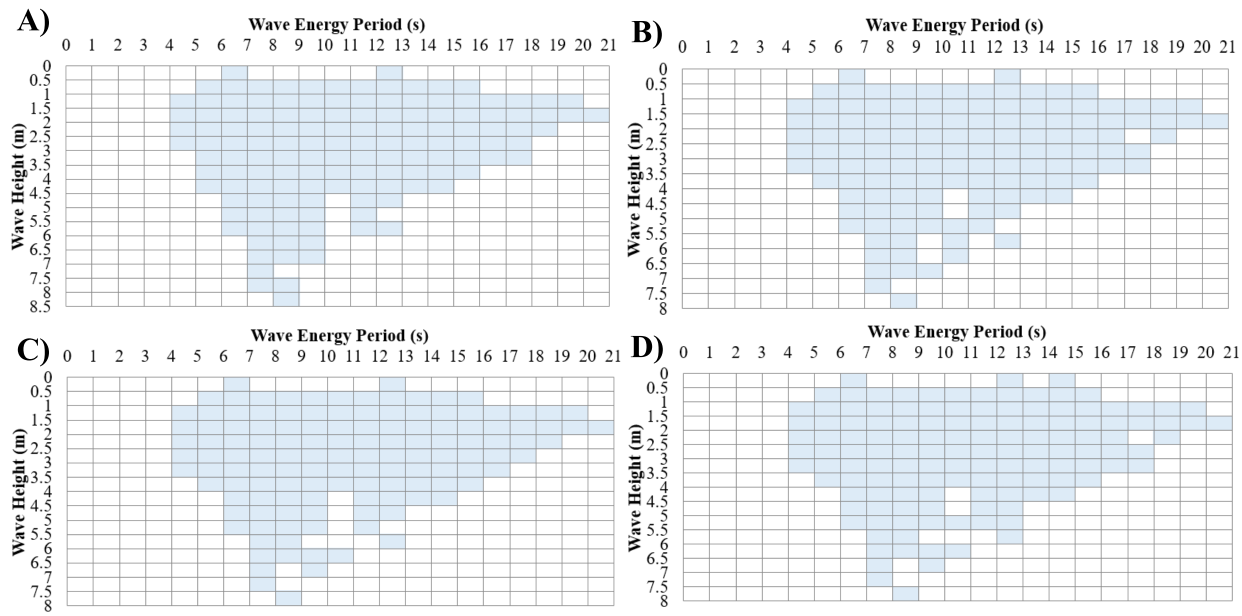

Figure 14.5 – Sample Sea States Selected for Reconnaissance Sensitivity Assessment for the Directional Resolution A) 36 bins; B) 48 bins; C) 72 Bins; and D) 120 Bins

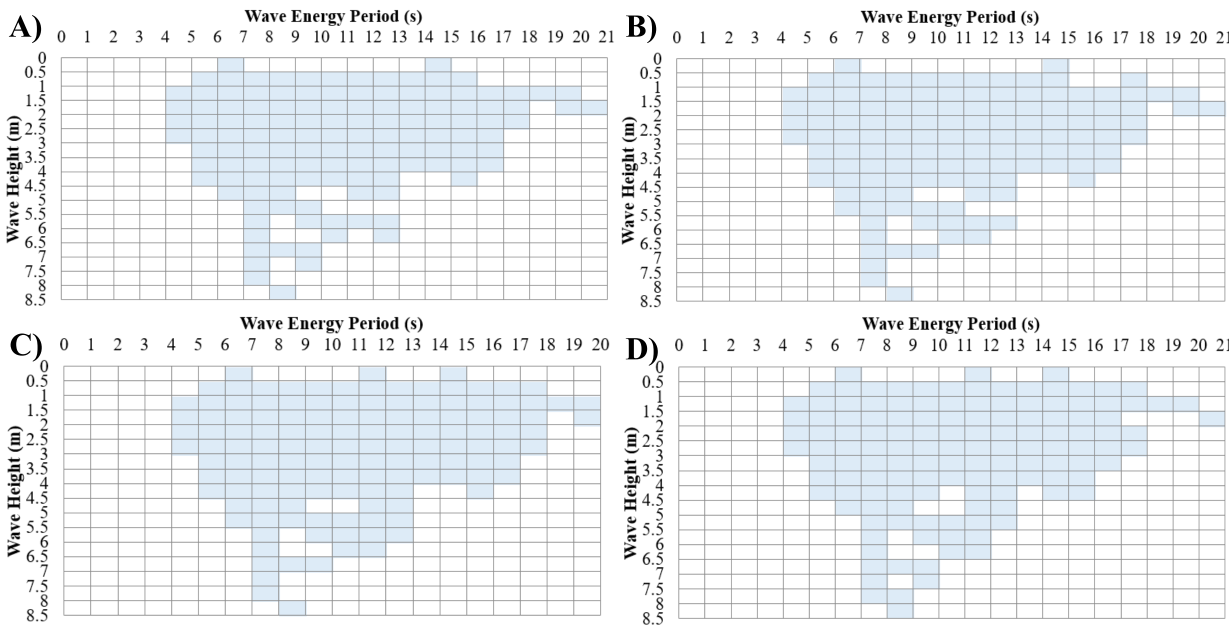

Figure 14.6 – Sample Sea States Selected for Reconnaissance Sensitivity Assessment for the Wind Resolution A) No Wind; and B) Varying Wind

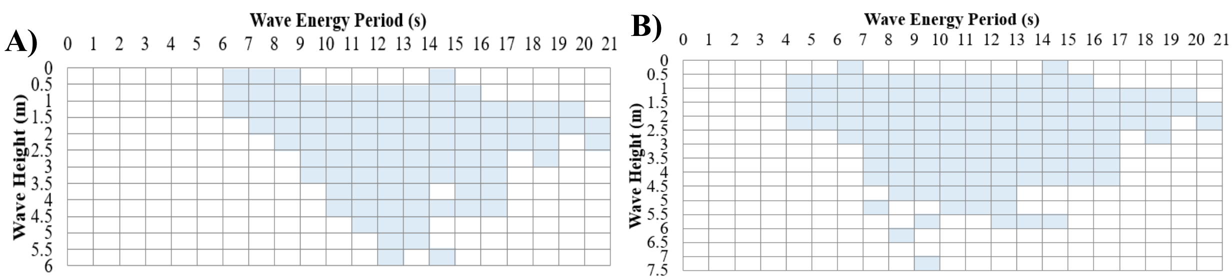

14.2 Feasibility Class Sample Sea States

Figure 14.7 – Sample Sea States Selected for Reconnaissance Sensitivity Assessment for Physical Processes A) Wave Breaking; B) Bottom Friction; C) Triad; D) Whitecapping

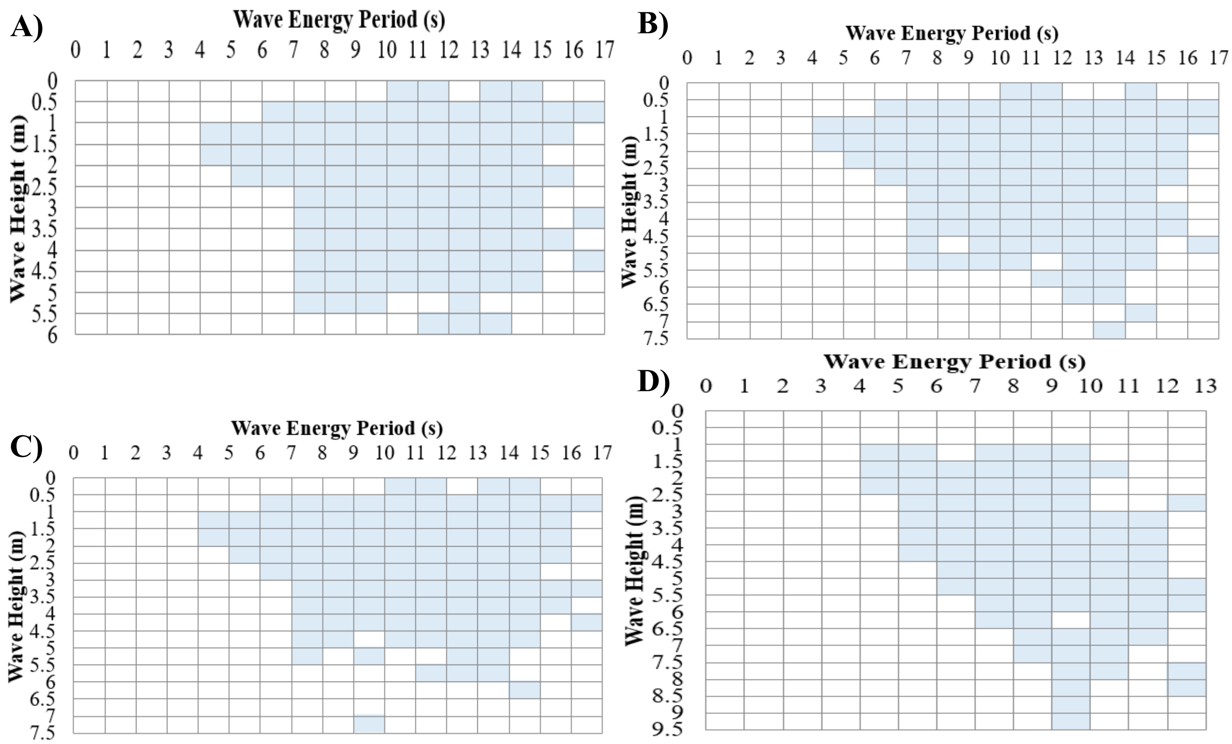

Figure 14.8 - Sample Sea States Selected for Feasibility Sensitivity Assessment for the Mesh Resolution A) 100m; and B) 300m

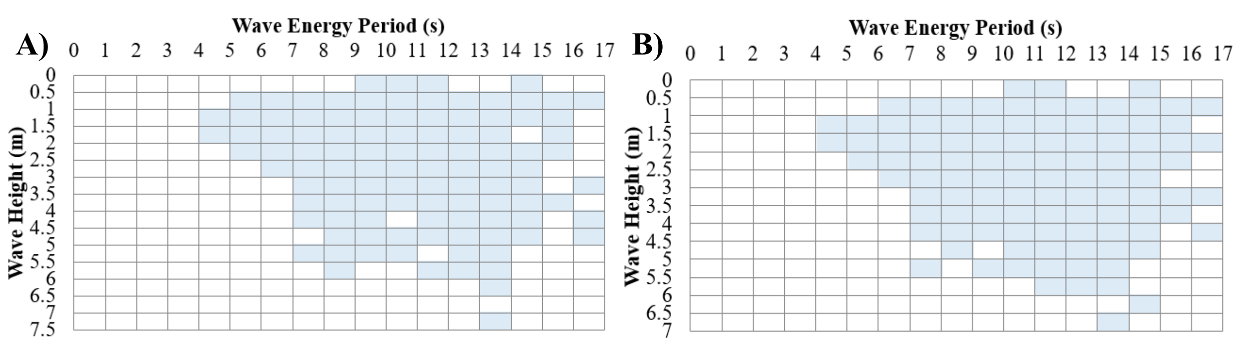

Figure 14.9 – Sample Sea States Selected for Feasibility Sensitivity Assessment for the Parametric Boundary Condition

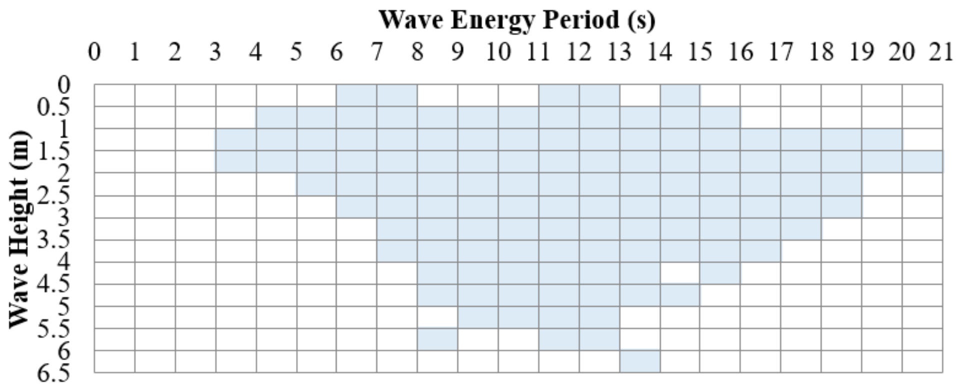

Figure 14.10 – Sample Sea States Selected for Feasibility Sensitivity Assessment for the Frequency Resolution A) 25 bins; B) 57 bins; C) 73 Bins; and D) 89 Bins

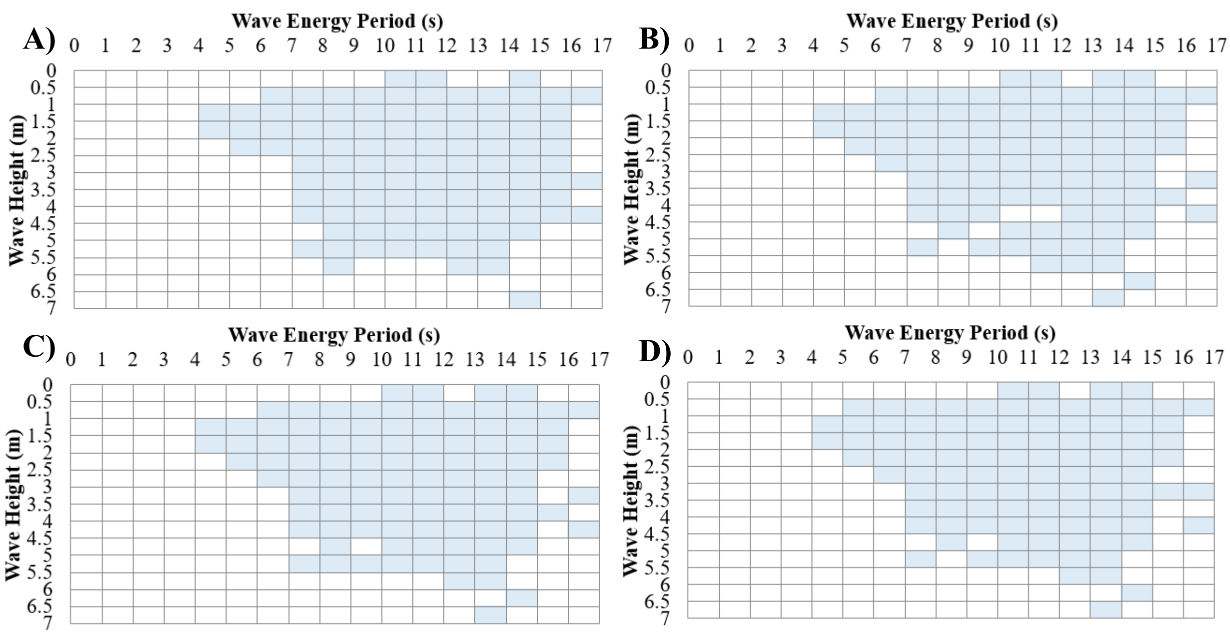

Figure 14.11 – Sample Sea States Selected for Feasibility Sensitivity Assessment for the Directional Resolution A) 24 bins; B) 48 bins; C) 72 Bins; and D) 120 Bins

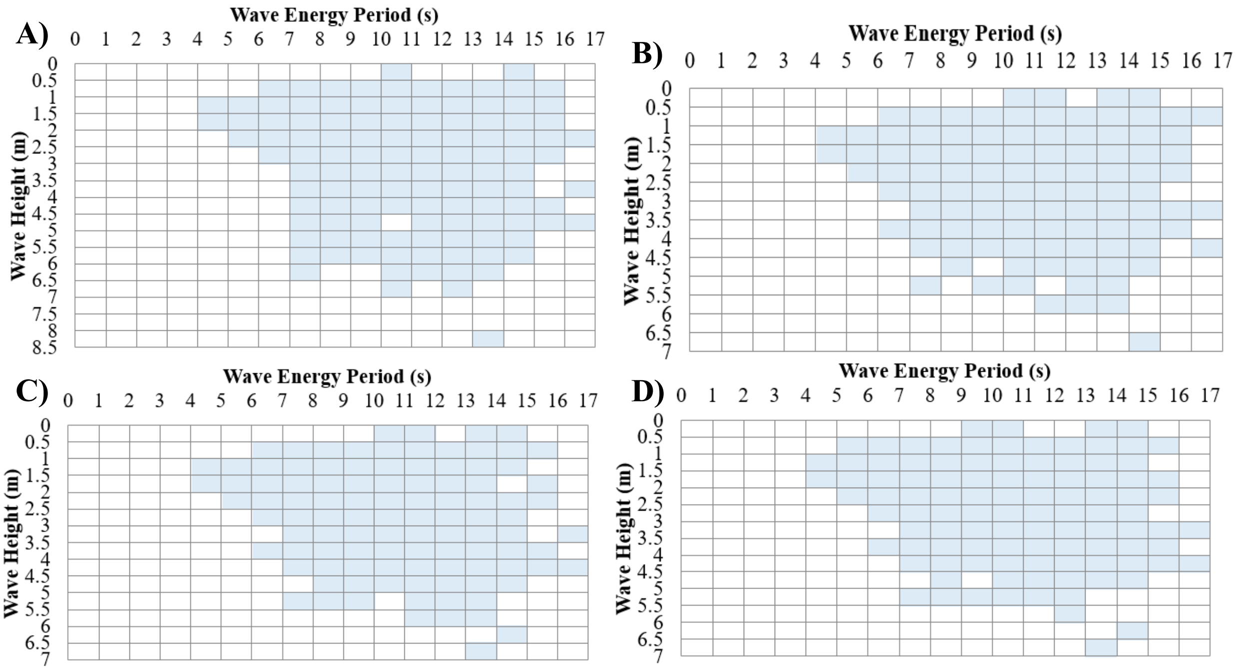

14.3 Design Class Sample Sea States

Figure 14.12 - Sample Sea States Selected for Design Sensitivity Assessment for the 100m Mesh Resolution

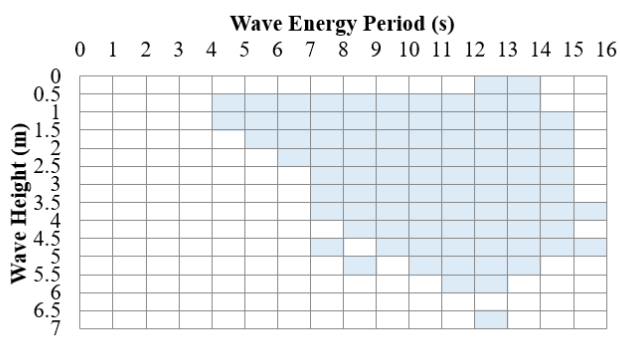

Figure 14.13 – Sample Sea States Selected for Design Sensitivity Assessment for the Frequency Resolution A) 25 bins; and B) 57 bins

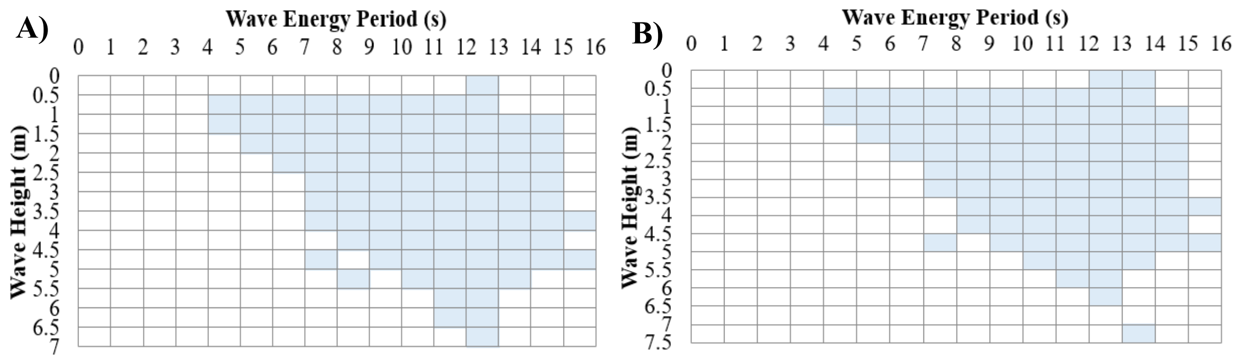

Figure 14.14 – Sample Sea States Selected for Design Sensitivity Assessment for the Directional Resolution A) 36 bins; and B) 72 bins

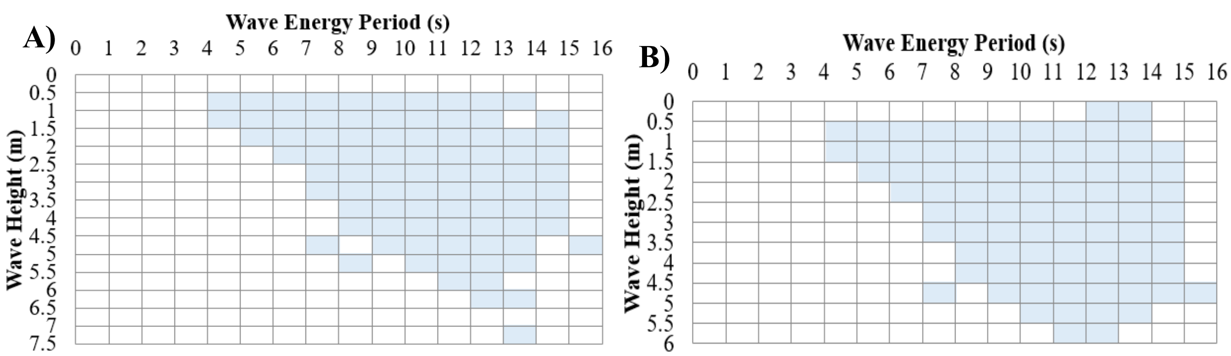

Figure 14.15 - Sample Sea States Selected for Design Sensitivity Assessment for the 50m Wind Resolution